# LABORATORY INVESTIGATION OF DIRECT MEASUREMENT OF ICE WATER CONTENT, ICE SURFACE AREA, AND EFFECTIVE RADIUS OF ICE CRYSTALS USING A LASER-DIFFRACTION INSTRUMENT

**FINAL REPORT**

December 28, 1995

NASA AMES RESEARCH CENTER
(Contract NAS2-14261)

H. Gerber[1], P.J. DeMott[2], D.C. Rogers[2]

[1] Gerber Scientific Inc., 1643 Bentana Way, Reston, VA 22090
[2] Colorado State University, Ft. Collins, CO 80523

# LABORATORY INVESTIGATION OF DIRECT MEASUREMENT OF ICE WATER CONTENT, ICE SURFACE AREA, AND EFFECTIVE RADIUS OF ICE CRYSTALS USING A LASER-DIFFRACTION INSTRUMENT

**FINAL REPORT**

December 28, 1995

NASA AMES RESEARCH CENTER
(Contract NAS2-14261)

H. Gerber[1], P.J. DeMott[2], D.C. Rogers[2]

[1] Gerber Scientific Inc., 1643 Bentana Way, Reston, VA 22090
[2] Colorado State University, Ft. Collins, CO 80523

## Table of Contents


| | Pg. |
|---|---|
| Title Page | 1 |
| Table of Contents | 2 |
| Summary | 3 |
| 1. Introduction | 4 |
| 2.Theory | 5 |
| 3. Experiment | 8 |
| 3.1 Instrumentation | 8 |
| 3.2 Experimental Procedure | 10 |
| 3.3 Measurements | 11 |
| 4. Analysis | 17 |
| 4.1 Strategy | 17 |
| 4.2 Ice-Crystal Orientation | 18 |
| 4.3 IWC and PSA of Ice Crystals | 19 |
| 4.4 Effective Radius of Ice Crystals | 21 |
| 4.5 Resolution Limit | 23 |
| 5. Conclusions | 24 |
| 6. References | 25 |
| 7. Acknowledgements | 26 |
| Appendix A - Experimental Notes | 27 |
| Appendix B - CSU Dynamic Cloud Chamber Measurements for all Experiments | 35 |
| Appendix C - Raw Data Produced by the PVM for all Experiments | 54 |
| Appendix D - Analyzed Data | 73 |
| Form 298 | 142 |

## SUMMARY

The aircraft microphysics probe, PVM-100A, designed for measuring liquid water content (LWC), droplet surface area (PSA), and droplet effective radius (Re) of liquid water clouds, was tested in the Colorado State University dynamic cloud chamber to establish its ability to measure related parameters consisting of ice water content (IWC), PSA, and Re in ice clouds. The PVM response was compared to other means of measuring those ice-cloud parameters in the chamber that included using FSSP-100 and 230-X 1-D (Particle Measuring Systems Inc.) optical probes for ice-crystal concentrations, a film-loop microscope for ice-crystal habits and dimensions, and an in-situ microscope for determining ice-crystal orientation. Intercomparisons were made for ice clouds generated in the CSU chamber containing ice crystals ranging in size from about 10 um to 150 um diameter, and ice crystals with plate, columnar, dendritic, and spherical shapes.

It was not possible to determine conclusively from the intercomparisons that the PVM accurately measures IWC, PSA, and Re of ice crystals, because heat from the PVM evaporated in part the crystals in its vicinity in the chamber thus affecting its measurements. Similarities in the operating principle of the FSSP and PVM, and a comparison between Re measured by both instruments, suggest, however, that the PVM can make those measurements. The resolution limit of the PVM for IWC measurements was found to be on the order of 0.001 $g/m^3$. Algorithms for correcting IWC measured by FSSP and PVM were developed.

## 1. Introduction

The purpose of this work is to quantify the operation of the Particulate Volume Monitor, Model PVM-100A, in clouds that consist of ice crystals. While this probe (termed PVM in the following), designed for aircraft use, was shown to produce accurate measurements of liquid water content (LWC), particle surface area (PSA), and effective radius (Re) in clouds containing liquid water and droplets with sizes ranging over about 3 um to 50 um diameter (Gerber, 1993; Gerber et al., 1994), its response to particles of irregular shape, such as ice crystals, is unknown. If such a quantification for ice crystals is possible, then the PVM could become a useful tool for studying the smaller ice crystals in cirrus clouds and con-trails, because it has measurement advantages including a large optical sample volume, and data sampling rates of up to 2 KHz.

The PVM can be classed as a "laser diffraction instrument", in that it uses a collimated laser beam that irradiates suspended particles that scatter light into a narrow forward cone. The scattered light consists primarily of light diffracted by the particles, as can be shown for the PVM and spherical particles by comparing predictions of Fraunhofer diffraction theory and Mie theory (Gerber, 1991). There is ample evidence that spherical particles as well as particles of irregular shape diffract light proportionally to their projected geometric area (Hodkinson and Greenleaves, 1963; Hodkinson, 1966; Born and Wolf, 1980; Bohren and Huffman, 1983). A motivation for the present work is that the PVM may not respond in that fashion for non-spherical particles, because non-linear spatial filters is used in the PVM to weight the forward scattered light in such a manner that particle area and volume are obtained. This filter may cause the expected proportionality of the diffracted light to the projected area of irregular particles to be partially lost. Thus in this work we test the following hypothesis: 1) The PVM measures the projected area, the projected area to the 3/2 power (volume) of ice crystals, and Re of ice crystals. A second hypothesis is also tested: 2) The PVM can estimate values of ice water content (IWC) as small as about 0.001 g/m$^3$, which is an amount found in diffuse atmospheric ice clouds (e.g., Liou, 1992.)

The method for testing the behavior of the PVM is to expose it to ice crystals of known shape and size. This is done in the Dynamic Cloud Chamber (DCC) located at Colorado State University in Ft. Collins, CO. This chamber has the capability of forming ice clouds similar to those found in the atmosphere, is large enough to contain the PVM, and includes a variety of other instrumentation used to characterize the ice crystals (DeMott, 1988, 1990; DeMott and Rogers, 1990). Given that the sub-freezing temperature and ice-nuclei content can be controlled in the DCC, means that crystals with different sizes and habits can be generated (e.g., see Magono and Lee, 1966.) The following sections include a theoretical discussion relating diffracted light of ice crystals to IWC, PSA, and Re; a description of the experiments run with the PVM in the DCC, and data collected; an analysis of the data; and a final section that draws conclusions on the validity of the two hypotheses.

## 2. Theory

We start with the definitions of LWC, PSA, and Re for a cloud with spherical water droplets of radius r (see Fig.1):

$$LWC\,(g/m^3) = \frac{4\pi\rho}{3}\sum_r r^3 n(r) \qquad (1)$$

$$PSA\,(cm^2/m^3) = 4\pi\sum_r r^2 n(r) \qquad (2)$$

$$Re\,(cm) = \frac{\sum_r r^3 n(r)}{\sum_r r^2 n(r)} = 3\rho_w \frac{LWC}{PSA} \qquad (3)$$

here $\rho_w$ is the droplet density, and n(r) is the droplet size distribution.

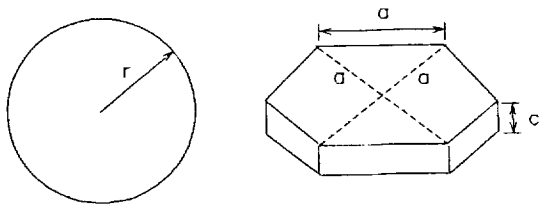


Fig. 1 - Spherical droplet and hexagonal ice crystal.

In developing expressions analogous to Eqs. (1)-(3) for ice crystals, we use as an example a solid and symmetrical hexagonal ice crystal shown in Fig. 1, for which the length of a facet on the basal plane is a, and the thickness is c. It is obvious that the determination of IWC, PSA, and Re for such an ice crystal with a laser-diffraction-type optical instrument must include a discussion about the orientation in space of the crystal with respect to the axis of the instrument's laser beam. We know from atmospheric measurements that ice crystals are sometimes oriented (Platt et al., 1978). However, it is though that in most situations the crystals are not strongly oriented; although, the degree of orientation is usually an unknown. We make the assumption here that the ice crystals are randomly oriented in space, so that the

crystals will also be randomly oriented with respect to the laser beam in the PVM. Evidence of ice crystal orientation for crystals generated in the DCC is given in ***Section 4.2.***

The volume V of the crystal in Fig. 1 is given by (Takano and Liou, 1995) as

$$V = 3\sqrt{3}a^2 c/2 \qquad (4)$$

which can be converted to IWC my multiplication with the density of ice ($\rho_i \approx 0.917$ g/cm$^3$).

They also give

$$G = 3a^2[\sqrt{3} + 4(c/2a)]/4 \qquad (5)$$

as the geometric projected area of the randomly oriented hexagonal crystal, where the total surface area, PSA, of the crystal is given by 4G.

In keeping with the form of Eq. (3), a *sphere-equivalent Re* for hexagonal ice crystals, such as in Fig. 1, is defined by

$$Re = 3\rho_i \frac{\sum_{a,c} IWC}{\sum_{a,c} PSA} = 2.75 \frac{\sum_{a,c} (\sqrt{3}ac/2)\, n(a,c)}{\sum_{a,c} (\sqrt{3}a + 2c)\, n(a,c)} \qquad (6)$$

where the summations must be done over the hexagonal ice-crystal size distribution, n(a,c), that depends on both a and c. This definition of Re is consistent with the use of Re from the standpoint that the denominator is proportional to the total area concentration of randomly oriented crystals affecting the scattering properties of the incident radiation, and that the numerator is proportional to the total ice volume concentration affecting the absorption of radiation. It would be expected that isometric solid hexagon crystals will produce values of Re that are most consistent with Re for spheres of the equal volume and area, while hexagonal crystals with significantly different values of a and c will differ from Re for spheres, because of differences in their scattering cross sections. Small crystals with characteristic dimensions close to or smaller than the first Mie peak would show the largest differences.

For monodisperse hexagonal ice crystals Eq. (6) is simply

$$Re = 1.5 \frac{\sqrt{3}ac}{\sqrt{3}a + 2c} \qquad (7)$$

If the PVM operates properly as a diffraction-only instrument it should be able to measure G in Eq. (5) and the denominator of Re in Eq. (6) correctly for randomly oriented crystals (barring non-linear filter effects.) However, the same is not true for the ice volume V in Eq. (4) and the numerator in Eq. (6), because a diffraction instrument that is capable of measuring volume $\propto r^3$ for a sphere, measures volume $\propto G^{3/2}$ for a randomly oriented particle of irregular shape. The latter *diffraction volume*, $V_d$, is defined by

$$V_d = 4\pi^{-1/2} G^{3/2}/3 \qquad (8)$$

$V_d$ is larger than the true value of the ice volume V of the crystal, so that the PVM will overestimate IWC as well as the sphere-equivalent Re of the hexagonal ice crystals. It is thus necessary to apply a correction factor to the IWC and Re measured by the PVM. This factor, C, is given for solid hexagonal crystals by

$$C = \frac{V}{V_d} = \frac{3\sqrt{\pi}\,(c/a)}{[3\sqrt{3} + 2(c/a)]^{3/2}} \qquad (9)$$

The value of C given by Eq. (9) is shown in Fig. 2 as a function of the dimensions c and a of hexagonal as well as other shapes of randomly oriented ice crystals. Figure 2 suggests that for a range of c/a typical of atmospheric hexagonal ice crystals the PVM should overestimate IWC and Re by a factor of between about 1.25 to 2.

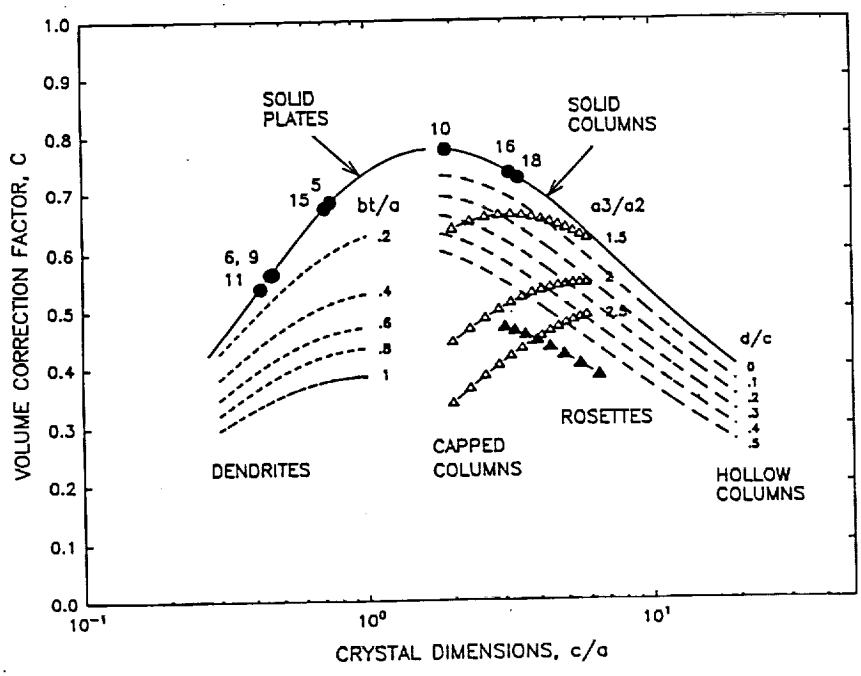


Fig. 2 - Volume correction factor for a diffraction instrument for randomly oriented ice crystals. Details given in text.

The foregoing illustrates a set of equations developed for IWC, PSA, and Re for solid, symmetrical, and randomly oriented hexagonal ice crystals measured by a diffraction instrument. Atmospheric ice crystals are often more complex than the simple crystals discussed so far. Such complex crystals can include dendrites, capped columns, and bullet rosettes, which can also have various degrees of hollowness. Takano and Liou (1995) give expressions for V and S for models of these more complex randomly oriented crystals, so that equations similar to the preceding can be derived for IWC, PSA, and Re. Calculated values of C for these other crystals are shown in Fig. 2. The parameters bt/a for dendrites, a3/a2 for capped columns, and d/c for hollow columns shown in Fig. 2 are defined in Takano and Liou (1995); the "shadowing factor", s, is applied to all three crystal types; and the crystal dimension ratio c/a for capped columns is defined here as $(l_1+l_2+l_3)/a$. The numbered data points are described in **Section 4.4.**

This analysis shows that, if the PVM is not adversely affected by the non-linearity of its spatial filters, it should overestimate IWC as well as Re, while giving the proper value of the projected geometric area of ice crystals. The work by Takano and Liou (1995) provides the mechanism by which these overestimates can be corrected, if the habit and orientation of the ice crystals are known.

## 3. Experiment

### *3.1 Instrumentation*

The instrumentation used for testing the PVM-100A is located at the Colorado State University Cloud and Aerosol Simulation Laboratory. All tests are conducted using the Dynamic Cloud Chamber (DCC) located at that laboratory, with most other instruments placed on or inside the DCC. The DCC and equipment used in the tests are summarized in Table 1.

Table 1 - Instrumentation used for testing at the CSU Cloud and Aerosol Simulation Laboratory the response of the PVM to ice crystals.

| Instrument | Description |
|---|---|
| 1. Dynamic Cloud Chamber | 1.2 $m^3$ pressure vessel with air-expanding and cooling capabilities, with vents and windows for probes and aerosol and gas injection.<br>Range of Operation:<br>Temperature +40C to -55C<br>Pressure 90 kpa to 50 kpa<br>RH 0.1% to >100%<br>Vertical Velocity 0.2 m/s to 20 m/s |

| | |
|---|---|
| 2. Thermocouples (Type-E) | inside wall and air temperature of DCC |
| 3. Strain Gauge | pressure inside DCC |
| 4. G.E. and E.G.&G. hygrometer | optical dew-point hygrometers for RH measurement in DCC |
| 5. TSI Nucleus Counter (3020) | ice and condensation nucleus concentration |
| 6. Film-Loop Microscope | continuous horizontal 16 mm film loop near bottom of DCC on which ice crystals sediment and are observed with a microscope/CCD video and recording system |
| 7. In-Situ Microscope | long-focal length microscope (Infinity, K2) for in-situ observation of crystals in DCC, observed with CCD video and recording system |
| 8. FSSP-100 | Forward-Scattering Spectrometer probe (PMS), particle spectra from 2 um - 47 um diameter |
| 9. 230-X Probe | 1-D Spectrometer (PMS), particle spectra from 20 um - 300 um diameter |
| 10. PVM-100A | Particulate Volume Monitor (GSI), LWC, PSA, Re; size sensitivity 3 um - 50 um (100% points), 2 um - 70 um (50% points) |
| 11. Laser | diode laser (680 nm) used to observe backscatter and scintillation from crystals |

The locations of the optical instruments in the cylindrical DCC are as follows: the film-loop microscope is near the base plate of the DCC; the FSSP-100 is located about 1/5 up the outside wall of the DCC, sample air is drawn from the chamber at a low rate; the 230-X is located below the bottom plate of the chamber, sample air is drawn from the chamber; the in-situ microspcope is mounted in and about 1/5 up the chamber wall; and the PVM is located for most tests in the chamber so that the focal point of the in-situ microscope is positioned just above the cylindrical aperature of the PVM, see Fig. 3. The PVM is further positioned so that the opening of its cylindrical aperture and sensitive volume is horizontal to permit unobstructed sedimentation of the crystals. For some of the tests the PVM is moved more towards the center of the DCC. The exposed metal shell of PVM is thermally insulated with light-weight closed-cell styro-foam in order that heat exchange between it and the chamber environment is kept at a minimum.

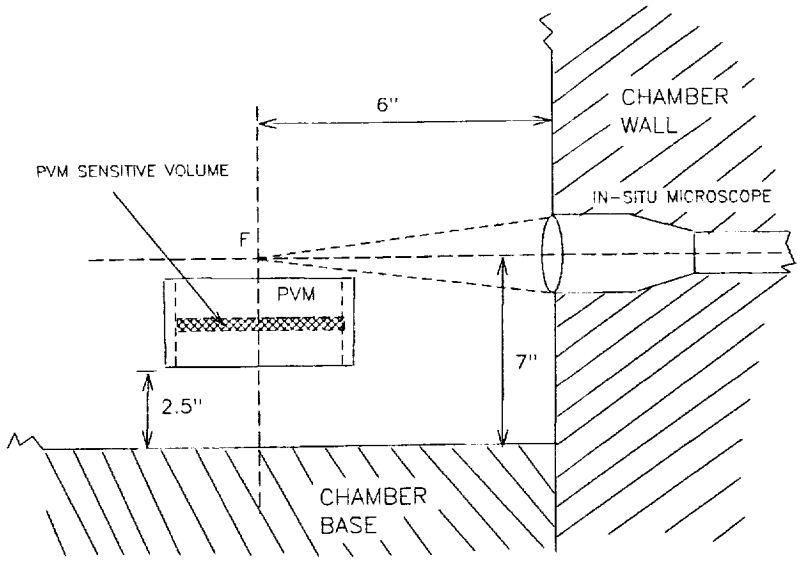


Fig. 3 - Location of PVM inside the Dynamic Cloud Chamber (DCC) with respect to the focal point F of the in-situ microscope.

### *3.2 Experimental Procedure*

The goal for generating ice crystals in the DCC is to create ideally monodisperse ice crystals varying in size and habit for different experiments, in order that the evaluation procedures for the optical instrument would be less time consuming. It is desired to generate crystals ranging in size from about 10-um to 200-um diameter, and, at the minimum, to generate crystal habits consisting of plates, dendrites, columns, and spheres. The experimental procedure used in attempting to meet this goal is summarized as follows:

The chamber pressure and temperature is reduced by computer control at a constant rate, simulating a moist adiabatic ascent of about 5 m/s. Given that the air in the DCC originally contains room moisture, a cloud forms when the dew point is reached. Upon reaching a target sub-freezing temperature, chosen from temperature/ice-crystal habit relationships (e.g., Magono and Lee, 1966), the temperature of the supercooled cloud is kept constant. Ice nuclei of a given concentration are then injected into the chamber to nucleate water vapor and supercooled water to form a totally glaciated cloud consisting only of ice crystals. The size of the resulting ice crystals is roughly proportional to the number of injected ice nuclei, as well as the dew point of the air prior to condensation. An attempt is made to operate all instruments in the chamber during each entire experiment; however, a detailed analysis of the data is only done here for intervals of time following total

glaciation of the cloud.

### *3.3 Measurements*

Eighteen experiments in the DCC were run over a period of two weeks. The experiment # is identified as PVM#, and each interval #, lasting 60 sec, for which a detailed analysis is done on the glaciated cloud is given by I#. The experiments are summarized in Table 2.

Table 2 - Summary of experiments run in the CSU Dynamic Cloud Chamber

| Exp. No. PVM# | Interval No. I# | Detailed Ice-Crystal Analysis | Comments |
|---|---|---|---|
| 1 | | no | no seeding |
| 2 | | no | no film loop |
| 3 | | no | marginal LWC and xls |
| 4 | | no | marginal LWC and xls |
| 5 | 1, 2, 3 | yes | hex plates with some dendritic structure, up to about 60-um diameter. -10C |
| 6 | 4 | yes | hex plates to about 150-um, -10C |
| 7 | | no | no film loop |
| 8 | | no | no film loop, stobe and in-situ microscope properly operating |
| 9 | 5, 6 | yes | hex plates to about 50 um, -18 C; add aspirator to base of PVM |
| 10 | 7 | yes | columns to about 50 um , -6 C |
| 11 | 8, 9 | yes | mostly hex plates < 20-um, -23.5 C |
| 12 | 10, 11 | yes | hex plates with dendritic features, to 100 um, -15.5 C |
| 13 | | no | overseeded, columns and plates, -10 C |
| 14 | | no | no film loop |
| 15 | 12 | yes | hex plates to 80 um, -12 C; move PVM towards center of DCC |
| 16 | 13 | yes | columns to 40 um, -7 C |
| 17 | 14, 15 | yes | spherical poly-crystals about 10 um, -30 C |
| 18 | 16, 17, 18 | yes | mostly columns, - 33 C |

Detailed notes describing each experiment are given in Appendix A. The raw time-dependent data consisting of temperature, pressure, RH, and FSSP and 1-D probe outputs measured in the DCC are illustrated for one experiment in Fig. 4; Appendix B shows this data for all experiments. Figure 5 shows the raw data output by the PVM for the same experiment; Appendix C shows the PVM ouput for all the experiments.

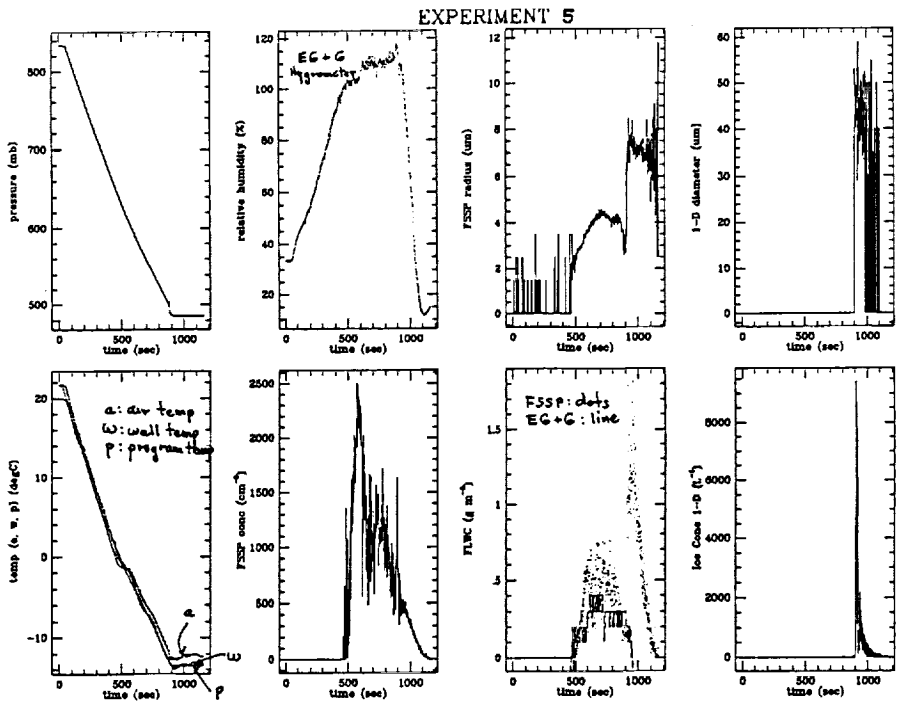


Fig. 4 - Pressure, temperature, RH, and FSSP and I-D probe data measured as a function of time during Experiment PVM5.

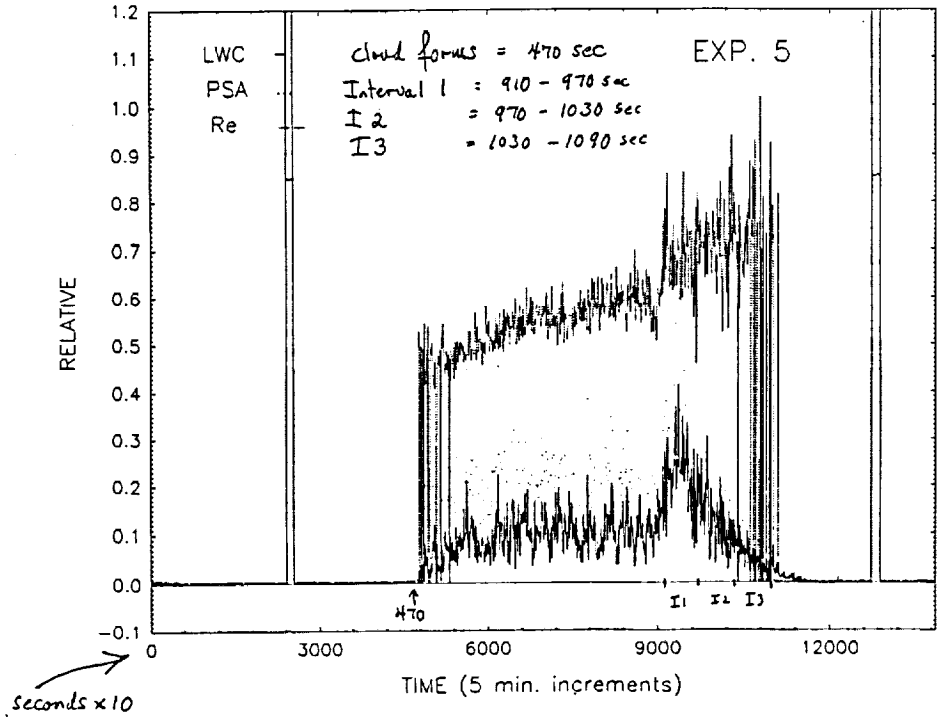


Fig. 5 - PVM measurements of IWC, PSA, and Re during Exp. PVM 5. The scale of the vertical axis gives IWC (g/m$^3$), Re/10 (um), and is relative for PSA. Intervals I1-I3 for which detailed ice crystal analyses are done are shown.

Figure 6 shows examples of images of ice crystals collected with the film-loop microscope and the in-situ microscope. Continuous video recordings by both systems were made during all tests. The distribution of a and c dimensions of crystals were determined by manually measuring large numbers of images on the film-loop video. The in-situ microscope images were used to determine the orientation of the crystals as they sediment just above the open cavity of the PVM. Crystals of single habits were generated as expected; however, they were not monodisperse.

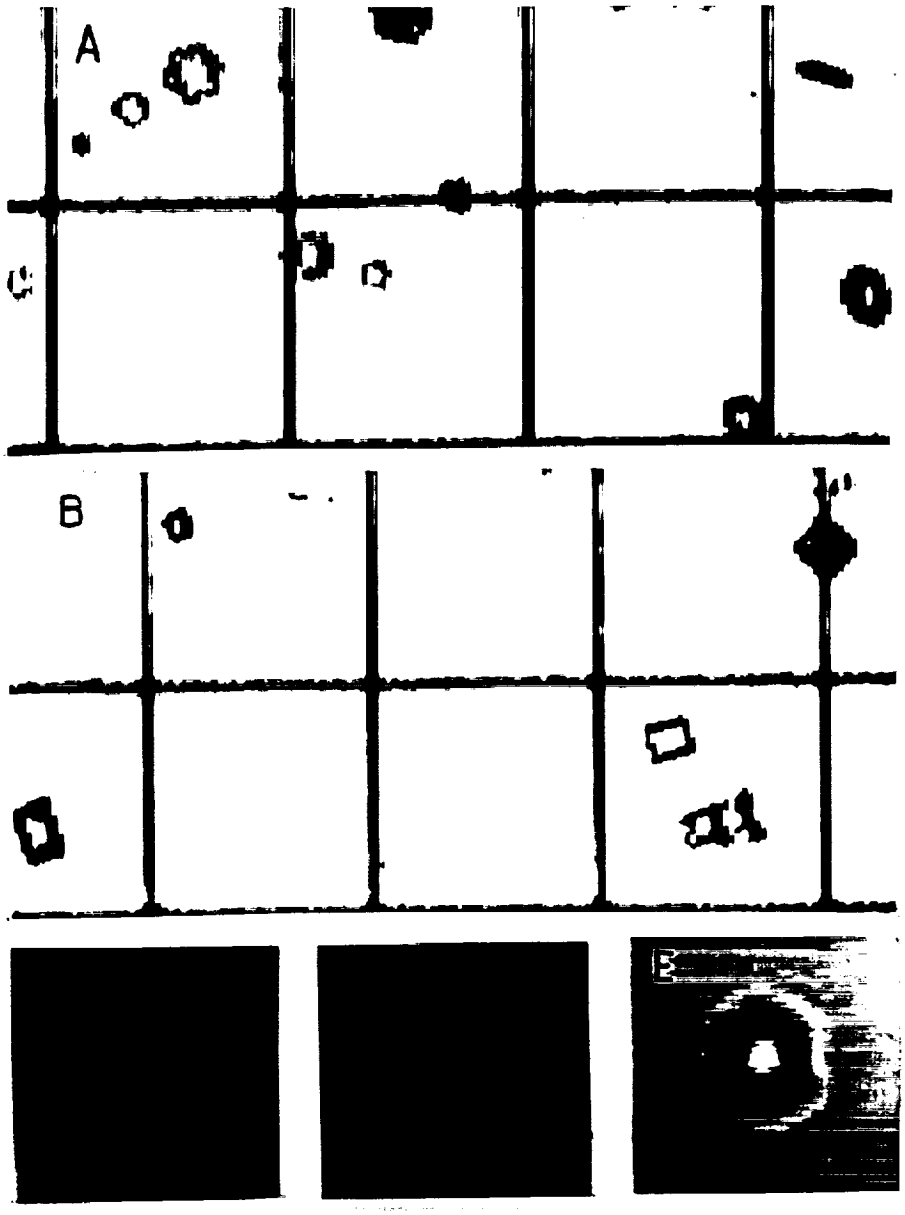


Figure 6 - Examples of video images collected with the film-loop microscope (A, Exp. PVM9; B, PVM16), and with the in-situ microscope (C, PVM7; D, PVM8; E, PVM8). The grid spacing in A, B is 200 um; the scale in C,D,E is estimated from the 50-um crystal diameter in C.

The raw data for the optical probes, FSSP, 1-D, and PVM, are reduced and assigned new variable names as defined in Table 3. Figures 7 - 13 illustrate the nature of the reduced data for experiment PVM5. Appendix D gives similar sets of graphical data for all the experiments for which a detailed analysis was done on the

Table 3 - Definitions of variables used in the description of the reduced data shown in Figs. 6 - 12, and in Appendix D.

| | |
|---|---|
| PVMWC: | PVM100-A 10 Hz liquid or ice water content. |
| PVMWC5s: | Running 5s average of PVMWC. |
| TOTWC: | Total calculated liquid and/or ice water content. |
| FVIDIWC: | FSSP ice water content computed by combining the video film loop size distribution, mass versus size relations from Redder and Fukuta (1989), and 5s average FSSP concentration. |
| 1DVIDIWC: | 230X (1D probe) ice water content computed by combining the video film loop size distribution, mass versus size relations and 5s average 1D concentration |
| GELWC: | liquid water content estimated from the heated-inlet dewpoint hygrometer. |
| FRFIWC: | FSSP ice water content computed using the empirical formulas of Redder and Fukuta and 5s average FSSP size distribution to represent major axis dimension. |
| FCORIWC: | FSSP ice water content computed as for FRFIWC, but outside the regime of the Redder and Fukuta formulas. Ice volume was based on the observed ice crystal shape and an assumed ice density $\rho_I = 0.7$ g m$^{-3}$. |
| 1DCORIWC: | 1D ice water content computed outside the regime of the Redder and Fukuta formulas, based on explicit shape of ice crystals and an assumed ice density $\rho_I = 0.7$ g m$^{-3}$. |
| PVMPSA: | PVM100-A particle surface area (PSA) channel. |
| PVMPSA5s: | Running 5s average of PVMPSA. |
| TOTPSA: | Total calculated PSA. |
| FVIDPSA: | FSSP PSA calculated based on the video film loop size distribution. |
| 1DVIDPSA: | 1D PSA calculated based on the video film loop size distribution. |
| FRFPSA: | FSSP PSA calculated using the FSSP size distribution to represent major axis dimension and Redder and Fukuta axial relationships. |
| 1DRFPSA: | 1D PSA calculated using the 1D size distribution to represent major axis dimension and Redder and Fukuta axial relationships. |
| PVMREFF: | PVM100-A effective radius. |
| FSPHREFF: | FSSP effective radius calculated assuming the particles are measured as spheres. |
| 1DSPHREFF: | 1D effective radius calculated assuming the particles are measured as spheres. |
| TOTREFF: | Total calculated effective radius using TOTWC and TOTPSA. |
| I##: | 60 s interval number (##) of particular interest during which only ice crystals were present and video size distributions were measured. |

glaciated cloud in the DCC. All sets, except for experiments 11, 17, 18 contain the relative distributions of a and c for the crystals measured manually from the film loop; the exceptions are due to the small size of the crystals which sediment inefficiently onto the film. In these three cases, FSSP data was used for establishing ice crystal sizes. The reduced-data variables in Figs. 7 - 13 are defined and discussed further in the next section.

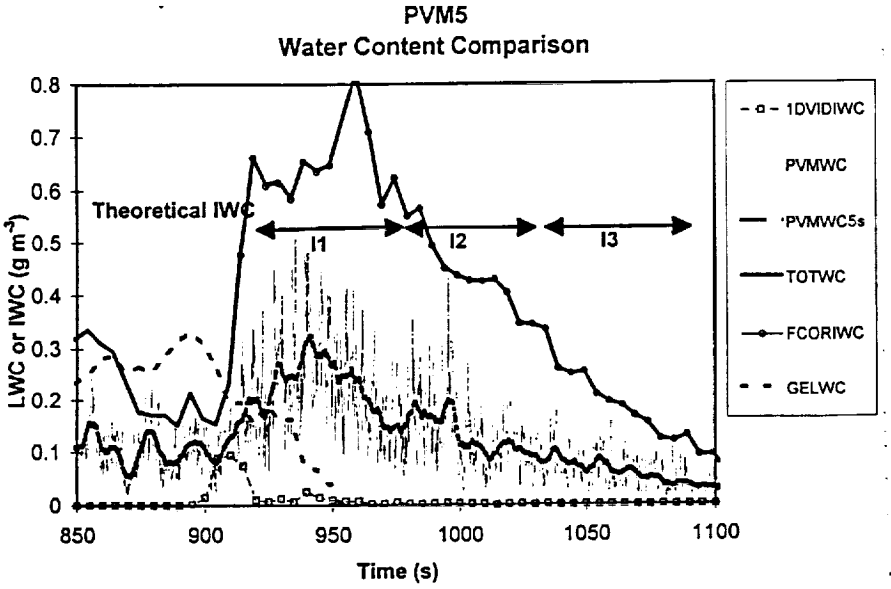


Fig. 7 - Comparison of LWC and IWC calculated and measured by FSSP, 1-D, and PVM for exp. PVM5.

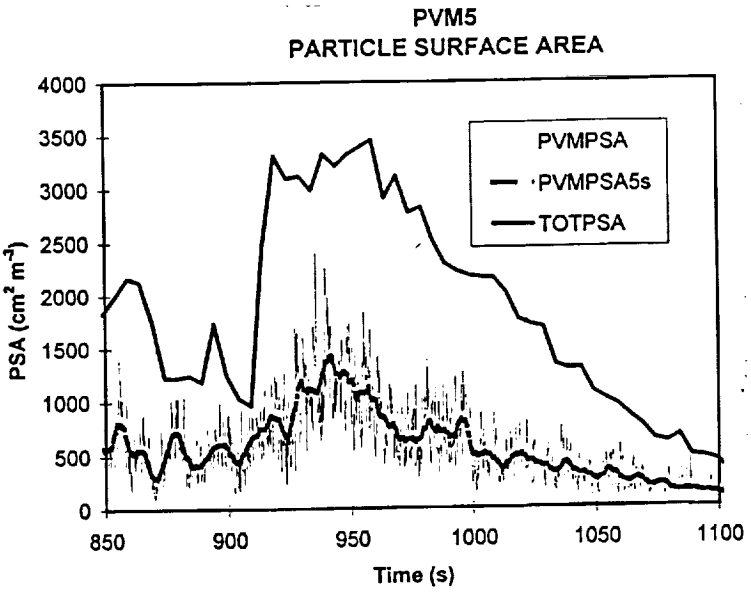


Fig. 8 - Comparison of measured and calculated PSA.

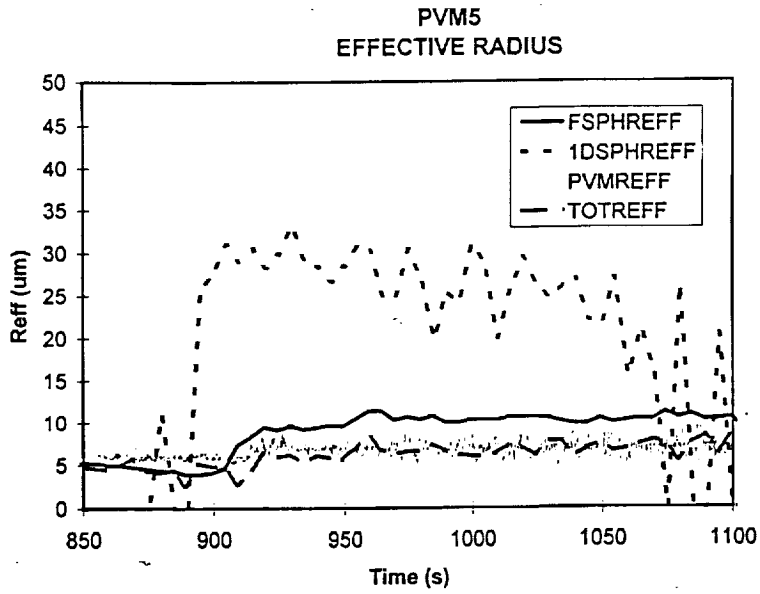


Fig. 9 - Comparison of Re measured with FSSP, 1-D and PVM.

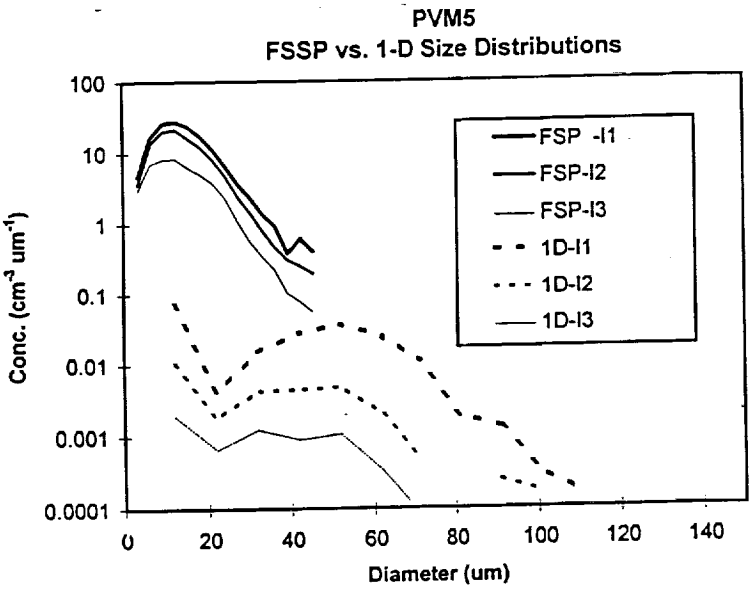


Fig. 10 - FSSP and 1-D ice crystal size distributions.

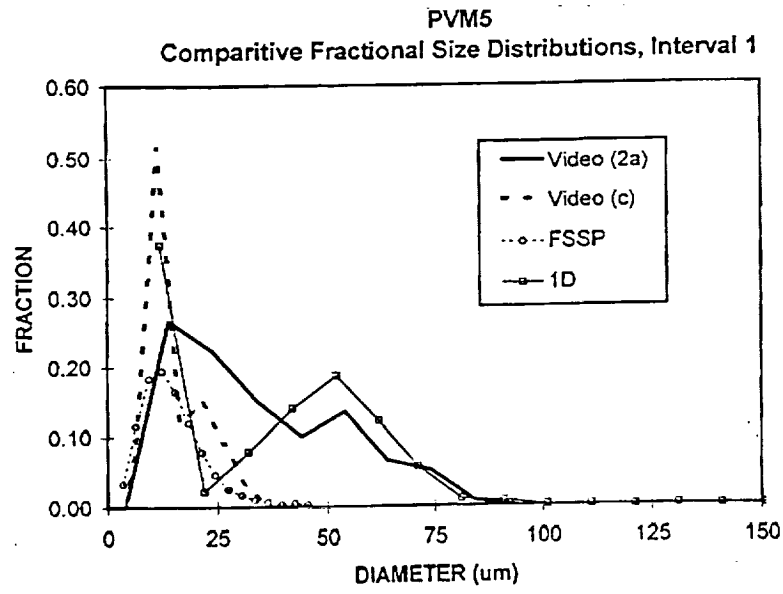


Fig. 11 - Relative size distributions of a and c crystal axes determined from film-loop video, FSSP and 1-D.

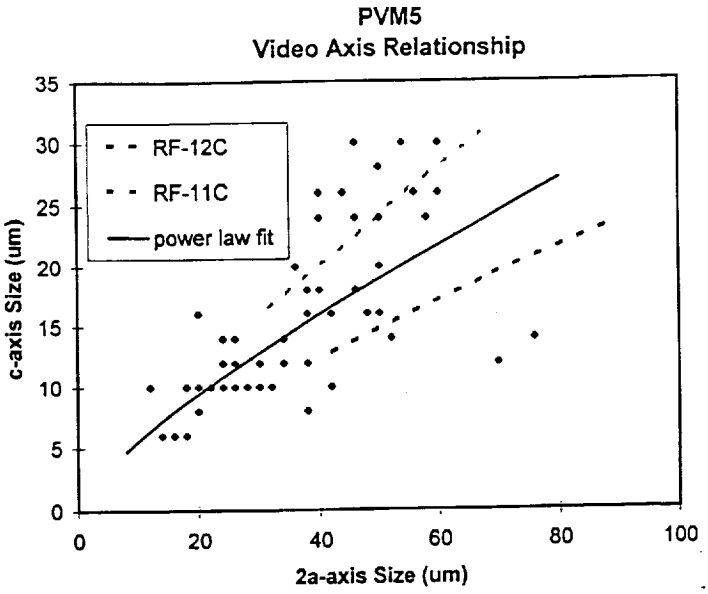


Fig. 12 - Film-loop video measurements of crystal dimensions a and c, and the predictions of the Redder-Fukuta (1989) realtionship for two temperatures.

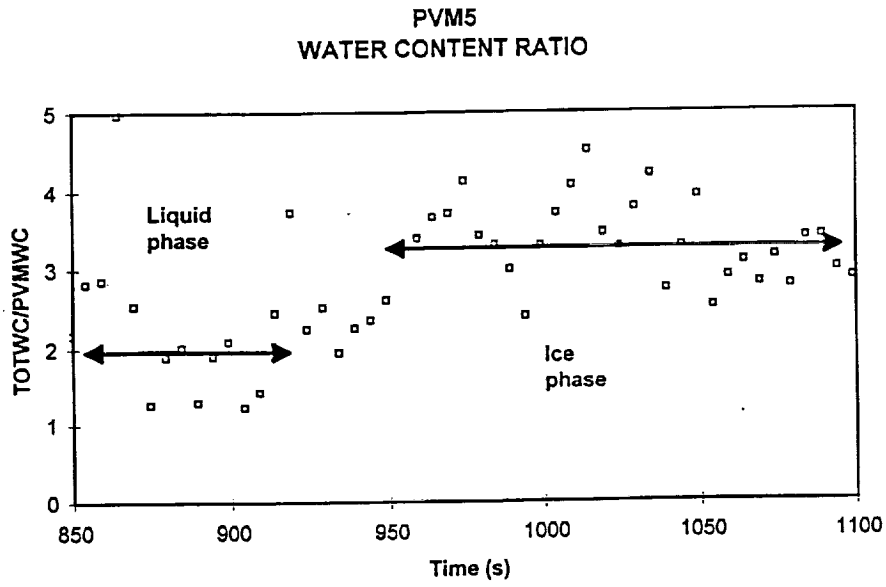


Fig. 13 - The ratio of total LWC and IWC to PVM LWC and IWC.

## 4. Analysis

### *4.1 Strategy*

The requirement for comparing PVM outputs to measured values in the DCC of IWC, PSA, and Re for ice crystals can be addressed in various ways, given that four other optical systems, FSSP, 230-X, in-situ microscope, and film-loop microscope, are used in the DCC to collect size and concentration information on the ice crystals. None of the systems is judged to be able to produce by itself accurate values of IWC,

etc., for comparison with the PVM: The FSSP and 230-X probes respond to the non-spherical ice crystals in an unknown fashion, the film-loop microscope gives only relative values of ice-crystal concentration, and the very small sample volume of the in-situ microscope results in insufficient data for concentration measurements.

It was decided that the most suitable role of the instruments for determining IWC, PSA, and Re of the crystals was to use the film-loop microscope to establish, by manual measurements of the ice crystal dimensions on the film-loop video, the relative size distribution of the ice crystals, and to use the total ice crystal concentrations measured by FSSP and 230-X probes to make these relative distributions absolute. If the crystals were smaller than about 42-um diameter, then only the FSSP concentrations was applied, and when the crystals size distributions extended above that size, the FSSP and the 230-X concentrations were both applied. This procedure is illustrated in Fig. 11 where the relative size distribution of the crystal dimensions a and c, as measured on the film-loop video, is shown for Experiment PVM5; and Fig. 10 illustrates the FSSP and 230-X concentrations that are applied to the relative spectra in Fig. 11.

The procedure to obtain IWC from the ice crystal sizedistributions is to apply empirical algorithms (Redder and Fukuta, 1989) that relate ice crystal dimensions to ice crystal mass. This is done for all experiments except for PVM11, PVM17, and PCM18 for which the crystals were too small to efficiently sediment onto the film loop (see Table 3.) For those three experiments the FSSP size distribution data is used instead; this is felt to give reasonable results, because the crystals in those three experiments are either nearly isometric or spherical. IWC values determined in the preceding ways are labeled TOTWC in the reduced data (see Fig. 7, and Appendix D.)

PSA is also determined by relying on the relative size distribution of the ice crystal dimensions measured on the film loop multiplied by total FSSP and 230-X concentrations. PSA is calculated by applying the relationship for PSA = 4 x G given by Takano and Liou (1995) for randomly oriented ice crystals, see Eq. (5). PSA values determined in this manner are labeled PSATOT in the reduced data (e.g., see Fig. 8.)

Re is determined by using Eq. (6) with TOTWC and TOTPSA. Re values determined in this fashion are labeled TOTREFF in the reduced data (e.g., see Fig. 9.)

### *4.2 Ice-Crystal Orientation*

The treatment in the preceding section requires the assumption that ice crystals produced in the DCC are oriented randomly in space. While an absolute statement can not be made about the orientation of all the crystals, the following evidence is presented that suggests random orientation: 1) The in-situ microscope showed ice crystals sedimenting with their longer axis at various angles with respect to the horizontal (e.g., see Fig. 6.), 2) ice crystals sedimented onto the film-loop with their axes at various angles with respect to the horizontal surface of the film (this includes plates some of which land on edge that permits a measure of the c dimension), and 3)

the back-scattered light from the diode laser projected into the ice cloud showed strong scintillation suggesting the presence of tumbling ice crystals.

### *4.3 IWC and PSA of Ice Crystals*

Analyzed data consisting of measured values of IWC and PSA are summarized in Table 4 (see Table 3 for definition of variable names.) Table 4 shows that not all experiments produced analyzed data, as also indicated in Table 2. The criteria for choosing to analyze an experiment's data depended largely on the proper operation of the film-loop microscope, which did not function occasionally. Overseeding or underseeding with ice nuclei also caused non-analysis of the experiment.

A typical result in comparing IWC (defined as PVMWC) measured by the PVM with TOTWC (see Section 4.1) is shown in Figs. 7 and 13 for Experiment PVM5. PVMWC is substantially less than TOTWC. The maximum TOTWC agrees reasonably well in Fig. 7 with the theoretical IWC calculated by differencing the appropriate vapor mixing ratios in the chamber. This suggests that the PVM was underestimating IWC for some reason; whereas, it should have been overestimating IWC according to the arguments presented in the theory section. The underestimate is also evident in the liquid cloud as Fig. 13 shows. Figure 14 summarizes the comparison between PVMWC and TOTWC. Except for some columnar crystals of low IWC, the trend in the underestimate of IWC by the PVM is consistent for all experiments.

We concluded that the PVM underestimated both IWC and LWC during the experiments, because we were unable to eliminate entirely heat conduction from the PVM during the experiments. This caused water droplets as well as ice crystals to evaporate in the vicinity of the PVM as the chamber was cooled. The diode laser confirmed this behavior, because the backscattered light from ice crystal clouds showed a minimum area located just above the circular opening of the PVM during the experiments. This evaporative effect was not complete, as shown by the existence of some backscatter just above the PVM, as well as by the outputs from the PVM; however, the exact nature of the evaporation remained unknown. It appeared that the cylindrical annulus of the PVM acted as a warm chimney, despite careful insulation of the metal PVM probe with styrofoam. This effect became apparent early in the course of the two-week experiment. In an attempt to counteract the heating in the annulus a low-speed suction fan was constructed and attached to the bottom opening of the annulus to draw the crystals more rapidly past the PVM heat sources. This was done starting experiment PVM9. The results were largely unchanged. A final attempt to deal with this problen was done starting experiment PVM15 when the PVM was moved closer to the middle of the DCC, and it was raised above the chamber floor to a height of 9". The latter modification gave the best comparisons between PVMWC and TOTWC, especially for experiments PVM17 and PVM18. This improvement may, however, have been due to the slowed evaporation, because of the low ice vapor pressures existing at the cold temperatures used in those experiments.

Table 4 - Summary of analyzed data for IWC, PSA, and Re of ice crystals measured with FSSP, 230-X, and PVM probes and calculated from film-loop microscope ice-crystal size measurements as a function of the 60-s interval for the given experiments. See Table 3 for definitions of quantities listed.

| Interval | Expt. | FSPHREFF | 1DSPHREFF | TOTREFF | PVMREFF | TOTWC | PVMWC | TOTPSA | PVMPSA |
|---|---|---|---|---|---|---|---|---|---|
| I1 | 5 | 10.08 | 26.01 | 6.42 | 6.91 | 0.637 | 0.225 | 3077.08 | 979.36 |
| I2 | 5 | 10.33 | 23.06 | 6.75 | 6.96 | 0.398 | 0.127 | 1895.64 | 537.28 |
| I3 | 5 | 10.40 | 20.80 | 7.28 | 7.20 | 0.157 | 0.056 | 739.47 | 231.92 |
| I4 | 6 | 17.77 | 33.97 | 10.93 | 8.95 | 0.082 | 0.052 | 236.45 | 195.35 |
| I5 | 9 | 16.74 | 24.69 | 8.25 | 8.67 | 0.158 | 0.094 | 577.16 | 326.90 |
| I6 | 9 | 16.58 | 24.28 | 8.22 | 9.24 | 0.083 | 0.037 | 302.50 | 126.29 |
| I7 | 10 | 11.94 | 32.65 | 12.98 | 10.41 | 0.079 | 0.038 | 184.14 | 115.77 |
| I8 | 11 | 4.79 | 22.73 | 3.09 | 5.73 | 0.089 | 0.031 | 862.76 | 171.65 |
| I9 | 11 | 8.05 | 14.25 | 4.95 | 6.33 | 0.099 | 0.026 | 598.47 | 127.62 |
| I10 | 12 | 16.07 | 31.91 | 9.03 | 8.65 | 0.219 | 0.143 | 731.41 | 508.89 |
| I11 | 12 | 17.51 | 30.37 | 9.37 | 9.27 | 0.090 | 0.063 | 288.01 | 224.19 |
| I12 | 15 | 15.28 | 38.74 | 6.16 | 9.67 | 0.050 | 0.036 | 248.15 | 137.02 |
| I13 | 16 | 11.92 | 15.86 | 10.08 | 10.03 | 0.015 | 0.023 | 48.16 | 72.18 |
| I14 | 17 | 8.58 | 15.78 | 7.88 | 8.08 | 0.045 | 0.033 | 172.69 | 124.02 |
| I15 | 17 | 9.25 | 15.94 | 8.55 | 9.10 | 0.026 | 0.020 | 96.45 | 66.61 |
| I16 | 18 | 10.54 | 17.06 | 7.69 | 9.47 | 0.012 | 0.019 | 62.04 | 61.35 |
| I17 | 18 | 10.88 | 20.46 | 7.71 | 8.96 | 0.011 | 0.017 | 54.33 | 57.33 |
| I18 | 18 | 10.75 | 22.09 | 7.74 | 9.45 | 0.011 | 0.014 | 53.77 | 44.09 |

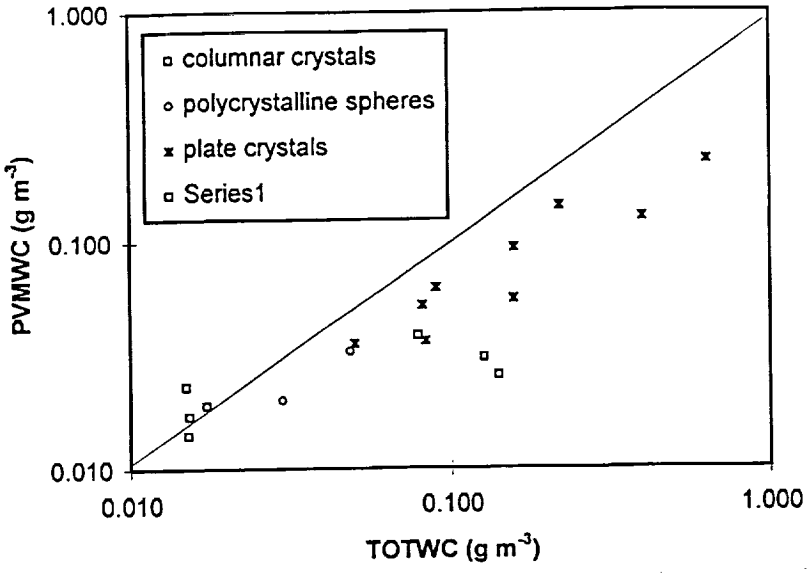


Fig. 14 - Comparison of IWC measured by the PVM (PVMWC) and determined from film-loop crystal measurements (TOTWC, see Section 4.1.) for the experiments listed in Table 4.

The same evaporative effect caused by the PVM is evident in the comparisons between PVMPSA and TOTPSA, as illustrated in Fig. 8. The evaporation could be related to inhomogenous or homogenous mixing, or a combination of the two. In the event that the first possibility holds, then the value of Re measured by the PVM may have remained unchanged, as will be discussed in the next section.

### *4.4 Effective Radius of Ice Crystals*

Table 4 lists the four measurements of effective radius, Re, of the ice crystals that were made in the cloud chamber during the experiments: FSHREFF (FSSP-100), IDSPHREFF (230-X), PVMREFF (PVM-100A), and TOTREFF (film-loop microscope and total ice crystal concentrations from PMS probes.) Re for the FSSP and the 230-X is calculated by assuming spherical particle shape.

Figure 15 compares Re measured with all the above probes except the 230-X, which gave Re values that were obviously too large, because most of the ice crystals had sizes smaller than the 42-um lower detection limit assigned to this probe. The top part of Fig. 15 shows the data as listed in Table 4, with the PVM giving apparent excellent agreement with the TOTREFF values, and the FSSP giving values that are

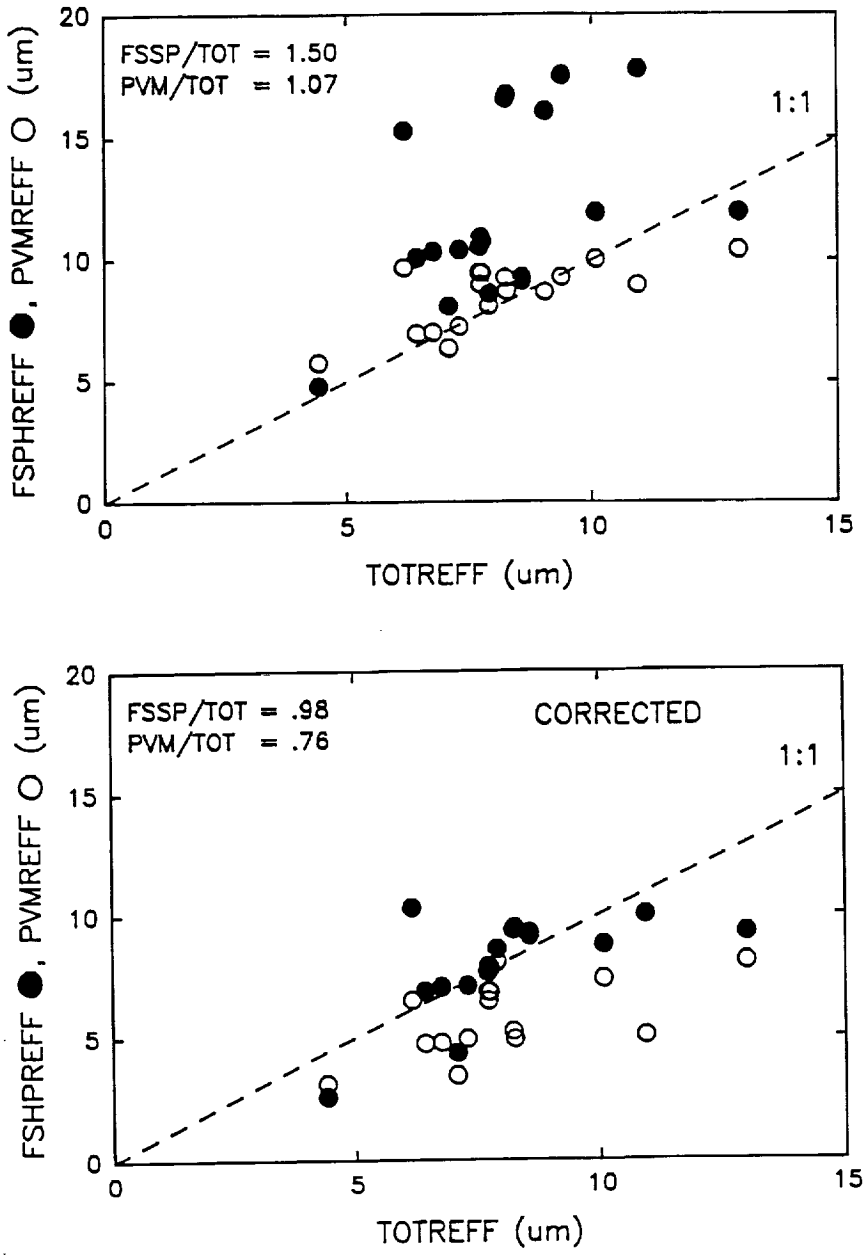


Fig. 15 - Comparison of effective radius (REFF) measurements of ice crystals made with PVM and FSSP vs film-loop microscope measurements. The corrected plot applies Eq. (9).

mostly too large. The bottom "corrected" part of Fig. 15 gives the Re values for the PVM and FSSP listed in Table 4 adjusted by the correction factor C given by Eq. (9) for which average measured values of c and a are used for all experiments except PVM12. The crystals were assumed to be solid hexagons, and the shadowing factor was not applied. These values of C are shown in Fig. 2. Applying C results in the PVM underestimating TOTREFF in the bottom part of Fig. 15, while the FSSP shows good agreement on the average with TOTREFF, as indicated by the average ratio of FSHPREFF/TOTREFF = 0.98. The spread in the data point may be less if the contributions to the actual values of Re from the larger crystals measured by the 230-

X, present in some of the experiments, are included.

*We conclude that the good agreement between PVMREFF and TOTREFF in the top part of Fig. 15 is fortuitous, and that the corrected portion of Fig. 15 shows the more likely relationship between these Re measurements.* This result further suggests that the FSSP appears to behave primarily as a "laser diffraction" instrument for which corrections for randomly oriented ice crystals similar to those given by Eq. (9) can be applied. The evaporation effect caused by the PVM must have been at least in part related to a homogenous mixing process, because the values of Re were not conserved as shown by the lower portion of Fig. 15.

### 4.5 Resolution Limit

The resolution limit of the PVM for measuring IWC was determined by observing the performance of the instrument during a period in an experiment when the ice crystal concentration was very small. Near the end of Experiment PVM18 such a period occured and is show in Fig. 16.

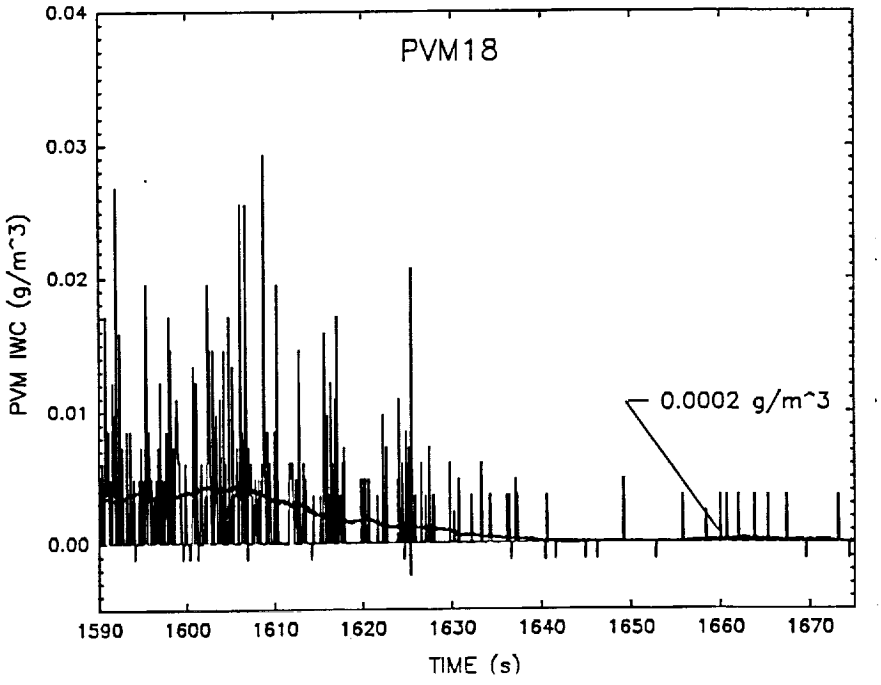


Fig. 16 - IWC measured by the PVM during Experiment PVM18.

Figure 16 shows that the PVM is capable of detecting IWC values on the order of 0.001 g/m$^3$. The spikes indicate the passage through the instrument's laser beam of individual ice crystals. The nature of the operating principle of the PVM is such that

individual spikes do not indicate accurate IWC values; however, a sufficiently long average of the spikes over time results in meaningful IWC values.

## 5. Conclusions

1) We were unable to demonstrate conclusively that the non-linear spatial filters used in the PVM to weight scattered light do not prevent the PVM from measuring the projected area, the projected area to the 2/3 power, and the effective radius Re of ice crystals generated in the CSU cloud chamber, because the residual heat conducted from the probe evaporated a portion of the crystals near it, and affected the measurements. However, the FSSP measurements made on the same crystals, where heating was not a problem, suggest indirectly that the PVM should be able to make those measurements.

2) After correcting the FSSP measurements to convert "diffraction volume" to ice crystal volume, this probe gave values of Re in best agreement with the Re established by manual sizing of the ice crystal various shapes and sizes sedimented onto the film-loop microscope located in the chamber. This suggests that FSSP measurements are useful for Re measurements when crystal sizes fall into its range of operation, and that scattered-light dependencies as a function of scattering angle other than those proportional to crystal size$^2$ and size$^3$, which the FSSP and also the PVM have, do not affect strongly the estimate of Re.

3) The measured resolution limit of the PVM for IWC of ice crystals is on the order of 0.001 g/m$^3$. This limit depends on the noise environment in which the probe is used.

4) A "sphere-equivalent" Re of the ice crystals can be defined for laser-diffraction instruments such as the PVM and FSSP when the "diffraction volume" measured by the instruments is corrected to give ice crystal volume, and the instruments measure the projected surface area of the ice crystals assumed to be randomly oriented in space. Correction factors for volume are derived and given for typical ice-crystal habits.

5) The PVM and FSSP are not stand-alone instruments for measuring IWC, PSA, and Re of ice crystals, unless approximate values of those parameters are desired. These approximate values should be determined using mean correction factors described here, and require that the majority of the crystals have sizes that fall within the instruments' range of operation that extends to about 50-um diameter. Improving the accuracy of those parameters is directly related to the application of additional information on the habit, large-size fraction, and orientation of the ambient ice crystals. Such information can be measured, for example, with replicators and the holographic instrument from Spec. Inc. It is expected that the PVM will produce useful and unique data on smaller ice crystals when used in conjunction with those other methods, because of its relatively large sampling volume and fast response time. When large and small ice crystals are found at the same time in the atmosphere, PVM

measurements should be combined with measurements from probes such as the 1-D and 2-D instruments from PMS.

## 6. References


Bohren, C.F., and D.R. Huffman, 1983: *Absorption and Scattering of Light by Small Particles.* Wiley and Sons, New York, pp. 530.

Born, M., and E. Wolf, 1980: *Principles of Optics.* Pergamon Press, New York, pp. 808.

DeMott, P.J., 1988: Comparison of the behavior of Ag-I type ice nucleating aerosols in the laboratory. *J. Weather Mod.*, **20**, 444-450.

DeMott, P.J., 1990: Exploratory studies of ice nucleation by soot aerosols. *J. Appl. Meteor.*, **29**, 1072-1079.

DeMott, P.J., and D.C. Rogers, 1990: Freezing nucleation rates of dilute solution droplets measured between -30C and -40C in laboratory simulations of natural clouds. *J. Atmos. Sci.*, **47**, 1056-1064.

Gerber, H., 1991: Direct measurement of suspended particulate volume concentration and far-infrared extinction coefficient with a laser-diffraction instrument. *Appl. Opt.*, **30**, 4824-4831.

Gerber, H., 1993: *Test of Prototype Liquid-Water-Content Meter for Aircraft Use.* Final Report, NSF Grant ATM-9207345. NASA P.R. 91344468, pp. 97.

Gerber, H., B.G. Arends, and A.S. Ackerman, 1994: New microphysics sensor for aircraft use. *Atmos. Res.*, **32**, 235-252.

Hodkinson, J.R., 1966: Particle sizing by means of the forward scattering lobe. *Appl. Opt.*, **6**, 839-844.

Hodkinson, J.R., and I. Greenleaves, 1963: Computations of light scattering and extinction by spheres according to diffraction and geometrical optics, and some comparisons with Mie theory. *J. Optical Soc. Am.*, **53**, 577-588.

Liou, K.N., 1992: *Radiation and Cloud Processes in the Atmosphere.* Oxford University Press. New York, pp. 487.

Magono, C., and C.W. Lee, 1966: Meteorological classification of small snow crystals. *J. Fac. Sci.*., Hokkaido University, **Ser. 7, No. 2,** 321-362.

Platt, C.M.R., N.L. Abshire, and G.T. McNice, 1978: Some microphysical properties of an ice cloud from lidar observation of horizontally oriented crystals. *J. Appl. Meteor.*, **17**, 1220-1224.

Redder, C.R., and N. Fukuta, 1989: Empirical equations of ice crystal growth microphysics for modeling and analysis, I. Mass and dimensions. *Atm. Res.*, **24**, 247-272.

Takano, Y., and K.N. Liou, 1995: Radiative transfer in cirrus clouds. Part III: Light scattering by irregular ice crystals. *J. Atmos. Sci.*, **52,** 818-837.

## 7. Acknowledgements

The NASA AEAP/SASS Program is thanked for making this work possible, and the NASA Ames is thanked for support under contract NAS2-14261. Appreciation is also expressed to Gerber Scientific Inc. for supporting the theoretical aspects of this work, which were beyond the scope of this experimental effort, but essential in understanding the measurements.

# APPENDIX A

## Experiment Notes

6/8/95:
PVM1

Ascent rate = 5 m $s^{-1}$
Tdew = -2°C
CCN bubbled 1 minute NaCl
Mix fan on high speed until later in test, then off
No video film loop for ice crystal habit
PMS FSSP and 1D-c not on until later in tests because reconnection of interface card was not made properly

6/9/95:
PVM2

Ascent rate = 5 m $s^{-1}$
Tdew = 5°C
CCN bubbled 3minutes NaCl
Mix fan on low speed
No video film loop for ice crystal habit
Seeded with AgI nuclei at approx. 1549(-15°C); cloud rapidly glaciated
**1D had no flow until 1551** (replacement pump not reconnected properly)
PVM had good response to ice formation

Orientation video operating. Focus set for 6.5x4.75, 200μm squares. Video review showed that off-forward-axis lighting was causing refraction through ice crystals, so that lighting is variable and details are not discernable. We should switch to forward lighting again. For the crystal sizes nucleated, could also stand a larger FOV.

6/12/95:
PVM3

Focus on orientation video reset for 6.5x8 200μm squares before camera reinstalled.
Ascent rate = 5 m $s^{-1}$
Tdew = -2°C
CCN bubbled 3minutes NaCl
Mix fan on high speed entire test
Planned to seed with AgI nuclei at approx. -10°C and halt expansion
Seeding was at 154900, ascent stopped at 154920.
Either cloud did not glaciate as much as expected, or ice did not grow sufficiently in size.
Video film loop operating this test, but record started late.

Following the continuous expansion, about 5 short rapid expansions were done to nucleate and grow more ice crystals. These temporarily cooled the air (not the walls):

| | |
|---|---|
| 1553 | 25mb (10+15 in succession) |
| 155415 | 10 mb |
| 155445 | 10 mb |
| 155615 | 10 mb |
| 155648 | 10 mb |

6/13/95:
PVM4

Focus on orientation video reset for 6.5x8 200μm squares before camera reinstalled.
Ascent rate = 5 m $s^{-1}$
Tdew = 5.5°C
CCN bubbled 3minutes NaCl
Mix fan off entire test
Both videos operating
Planned to seed with AgI nuclei (2x dilution of AgI-$NH_4I$ combustion aerosol) at approx. -10°C and halt expansion for plates only
Seeded at 153620 (-10°C air temperature)
Stop ascent at 153710 (-12°C wall temperature)

Dewpointers unbalanced flows (last 3 tests) fixed for this test and heat added to sample inlet. EG&G unit looks particularly good for LWC retrieval when cloud was present.

Test appeared competitively seeded, that is, not entirely glaciated. Excellent plate records on video film loop. No orientation video because strong lighting washed out images.

6/14/95:
PVM5

Focus on orientation video reset for 6.5x8 200μm squares before camera reinstalled.
Ascent rate = 5 m $s^{-1}$
Tdew = 5°C
CCN bubbled 3minutes NaCl
Mix fan was left on low until just after seeding
Both videos operating, strobe system readjusted for this test
Planned to seed with AgI nuclei (2x dilution of AgI-$NH_4I$ combustion aerosol) at approx. -10°C and halt expansion for plates only, heavier seeding
Cloud formation noted at 112000
Seeded at 112650 (-10°C air temperature)

Orientation video appears to indicate random crystal orientation. Excellent video film loop of plate crystals. Higher concentrations collected by film loop, in agreement with stronger 1D signal.

PVM6
Ascent rate = 5 m $s^{-1}$
Tdew = 6°C
CCN bubbled 3minutes NaCl
No mixing fan
Both videos operating
Planned to seed with AgI nuclei (2x dilution of AgI-$NH_4I$ combustion aerosol) at approx. -10°C and halt expansion for plates only, heavier seeding
Cloud formation noted at 142720
Seeded at 1436 (approx. -14°C air temperature)
Stopped expansion at 143630

Noted that slight leak through CCN bubbler system allowed some room air IN into chamber before seeding was done.

PVM7
Ascent rate = 5 m $s^{-1}$
Tdew = 4°C
CCN bubbled 3minutes NaCl
No mixing fan
Both videos operating?
Seeding planned for -14°C.
Cloud formed at ~1608, -2°C
Seeded at 161530, -16°C
Stopped ascent at 1616
Video film loop stuck in position at some point.

6/15/95:
PVM8
Planned cloud formation test only after strobe system changed to a pinhole light source.
Ascent rate = 5 m $s^{-1}$
Tdew = 8.5°C
CCN bubbled 3minutes NaCl
No mixing fan after 1030
Both videos operating
Dewpoint inlet was unheated, but did not seem to affect EG&G, so enough heating from room around sample line.
Seeded at 104350 on data system computer
Stopped ascent at 104545, ~-18°C

Excellent orientation video shoeing diffraction patterns.
No video film loop because it stuck in position

6/16/95:
PVM9
Ascent rate = 5 m $s^{-1}$
Tdew = 9°C
CCN bubbled 3minutes NaCl

No mixing fan, except on new PVM sampling system. This system consisted of a laminar flow element placed below the PVM with a fan for aspiration of the sample volume. Should provide 1-2 cm $s^{-1}$ aspiration. Voltage on the brushless fan was set to 6V this test

Both videos operating
Seeded at 101731, -18°C
Ascent stopped ~101810, T=-19.5°C

Problems this test:
1. 1D tubes not reconnected initially, so no measurements made early in cloud formed, and the pressure control oscillated to make up for the incoming air. A spike in the 1D data was caused when the 1D was finally turned on.

2. The 6V setting on the PVM aspiration fan was clearly not enough. No voltage gave LWC=0. Better LWC values were obtained with the voltage set to 12V. I suggest miving PVM higher in chamber volume and not using aspiration.

3. The video film loop was started late and it was not moving at early times during cloud, so artifacts were noted in the first few minutes of recorded data

4. The orientation video was not plugged in until well after cloud formed.

PVM10
Ascent rate = 3 m $s^{-1}$
Tdew = 9.5°C
CCN bubbled 3minutes NaCl
No mixing fan
PVM sampling fan to 12V
Both videos operating

Slight offset on initial temperature profile due to ascent profile memory problems in starting ascent.
Seeded at 113710, T=-6°C, did not glaciate cloud
Stopped ascent at -10°C
Lots of columns on film loop. One in focus on orientation film at 114045.

PVM11
Attempt to get column/sheath type crystals below -24°C
Ascent rate = 3 m $s^{-1}$
Tdew = -4°C
CCN bubbled 3minutes NaCl
No mixing fan
PVM sampling fan to 12V
Both videos operating

Dewpoint temp rose during early part of expansion, so dry air was not well mixed throughout pressure vessel initially. Cloud could be superadiabatic initially.

Cloud formed at 145747, T = -6.5°C air temp
Low concentration cloud formed (poor CCN inject?). LWC<0.05 g $m^{-3}$
FSSP switched range 0 to 1 at ~150330
Dewpoint relative humidity appears offset low this test, never registered cloud.
A few ice crystals present throughout cloud lifetime.

Video film loop stuck occasionally, more so later in experiment.
Cloud disappeared by -22°C.
Seeded anyway at 151025, -23.5°C
Stopped ascent at T=-27.6°C
~17mb pop expansion at 151240 formed all ice cloud centered at 10-12μm
13 mb more at 1515. Ice grew to 18-20μm
1D did not respond well, may have iced over inlet or very small (<30μm) crystals present.

Strobe system had problems until aobut 1512 when Brian noticed loose connections. Some good images both before and after this time.
Video film loop shows mostly columns, few plates.

6/19/95:
PVM12
Ascent rate = 5 m $s^{-1}$
Tdew = 6°C
CCN bubbled 3minutes NaCl
No mixing fan
PVM sampling fan to 12V. Not on until 104115
Both videos operating

FSSP on late (PMS switch was off) so missed first few 1Hz cloud records.
Video film loop also started recording about 30s late for ice formation.
Seeded at 104750, T=-15.5°C
stopped ascent 104850

PVM13
Ascent rate = 5 m $s^{-1}$
Tdew = 6°C
CCN bubbled 3minutes NaCl
No mixing fan
PVM sampling fan to 12V.
Both videos operating

Seeded at 115435, T=-10°C air, continued cooling to -15°C
Ice was present early at -8°C (columns)
Seeding was overseeding. Plates of all sizes and thicknesses apparent. Some were so thick that I believe they look like columns.

Note noise in data system last tow tests must be omitted in plotting data.

PVM14
Ascent rate = 5 m $s^{-1}$
Tdew = 9.5°C
CCN bubbled 3minutes NaCl
No mixing fan
PVM sampling fan to 12V.
Both videos operating
Attempt to get larger crystals

Seeded at 143910
Stopped ascent at 143940
Noted crystals formed to >150μm on 1D updates, with a mode at 70-80μm
Video film loop stuck early in experiment, so no habit data!

6/20/95:
PVM15
Repeat last test with 1 additional dilution of aerosol
Ascent rate = 5 m $s^{-1}$
Tdew = 8.5°C
CCN bubbled 3minutes NaCl
Mixing fan on high
PVM fan removed and PVM raised an additional 5 inches to sit 9 inches off chamber floor, very near to the center of the chamber.
Video film loop only this test while Brian works on strobing faster

Seeded at 143235
Film loop stuck some, so some crystal melting noted at times. Otherwise excellent images of flat and on-end plates for IWC calculation. Good test for larger crystals.

Appears that residual heating from PVM may be decreasing its LWC value compared to the hygrometer and FSSP measurements.

PVM16
Repeat last test, but seed at -7°C for columns
Ascent rate = 5 m $s^{-1}$
Tdew = 8.5°C
CCN bubbled 3minutes NaCl
Mixing fan on high
video film loop only

Seeded at 152145
Excellent test execution. Only columns noted with a final air temperature of -8.5°C
Good film loop data for both size and concentration.

6/21/95:
PVM17
Ascent rate = 5 m $s^{-1}$
Tdew = -10°C at start, warmed to -7.5°C during the experiment before falling again
CCN bubbled 3minutes NaCl
Mixing fan on high
video film loop only

Attempt to seed for columns below -24°C. Lots of ice formed before seeding. Was contamination in the air and from the CCN bubbler.

Seeded at 100320
Fan was turned off near the end because the small crystals did not appear to be efficiently captured on the film loop with the fan on high.

Excellent FSSP/PVM comparison for polycrystalline, nearly spherical, ice crystals.
Dewpoint hygrometer data not of much use at this colder temperature. Time lag and lack of secondary cooling are problems.

PVM18
Ascent rate = 5 m $s^{-1}$
Tdew = -15°C at start, warmed a little during the experiment before falling again
CCN bubbled 3minutes NaCl
Mixing fan on low speed until seeding
video film loop only

Solid cloud formed at -15°C
Seeded at 115430 (~-33°C)
Mostly columns and some morph spherical particles noted on video.

# APPENDIX B

## CSU Dynamic Cloud Chamber Measurements for all Experiments

# EXPERIMENT 1

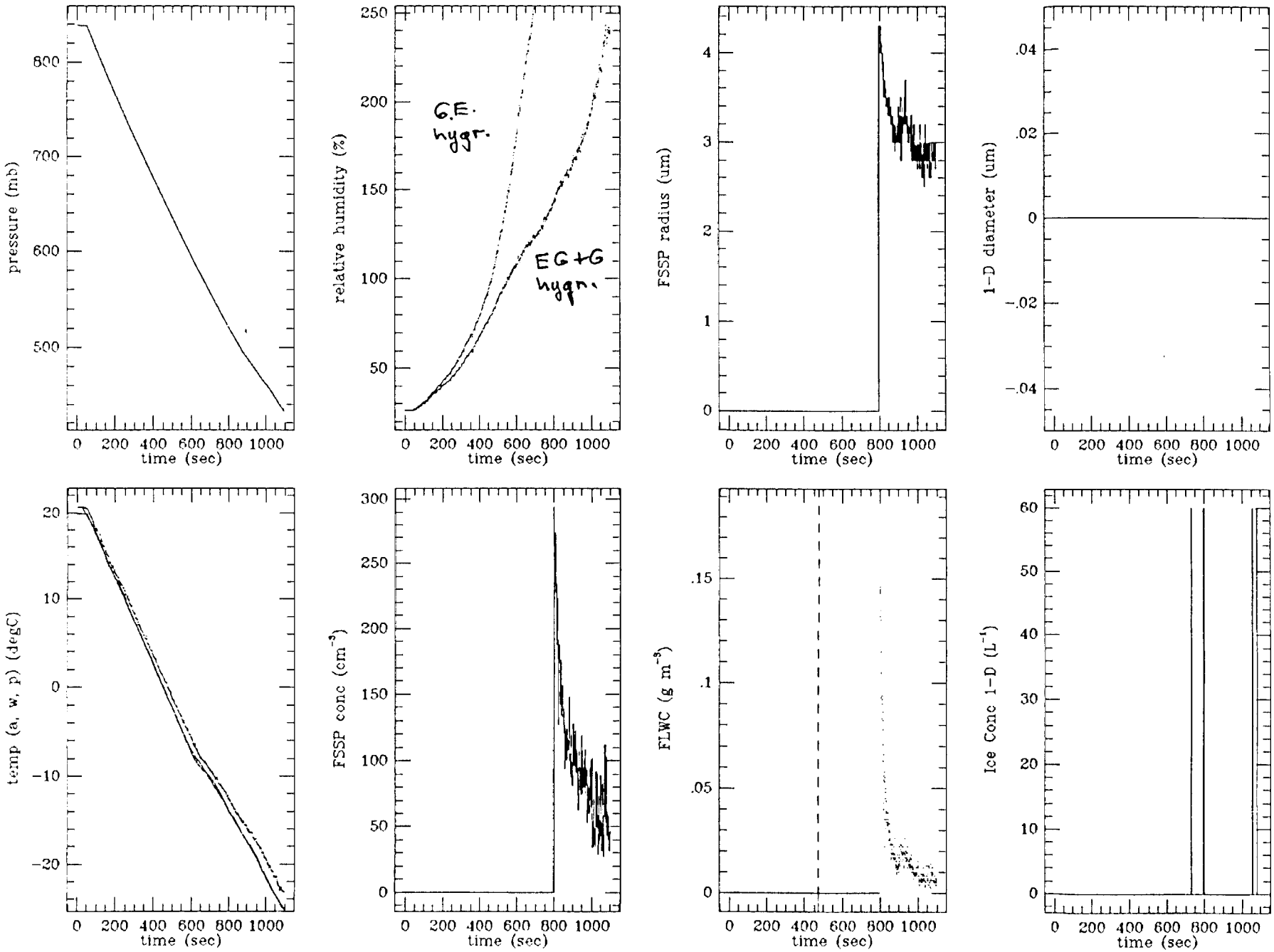

# EXPERIMENT 2

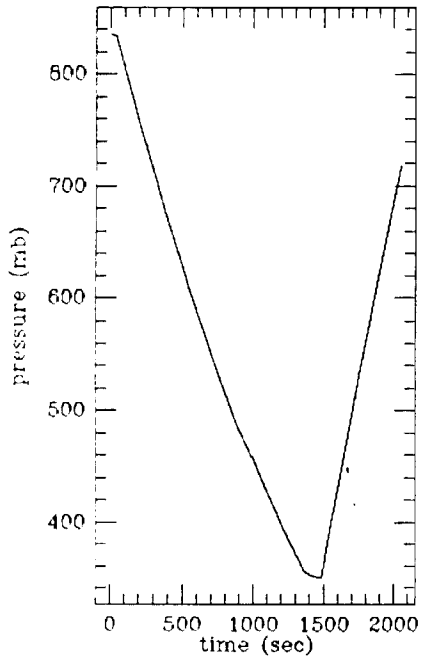


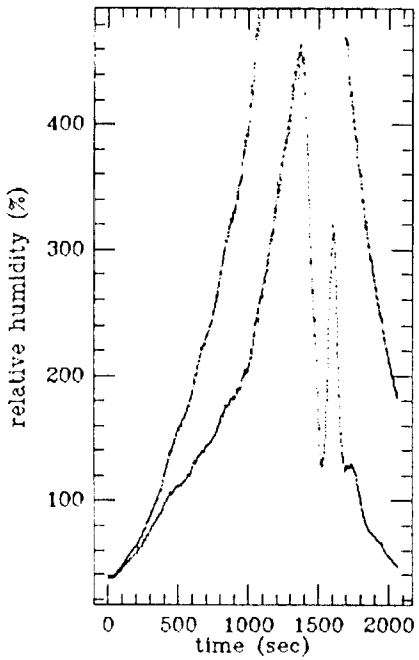


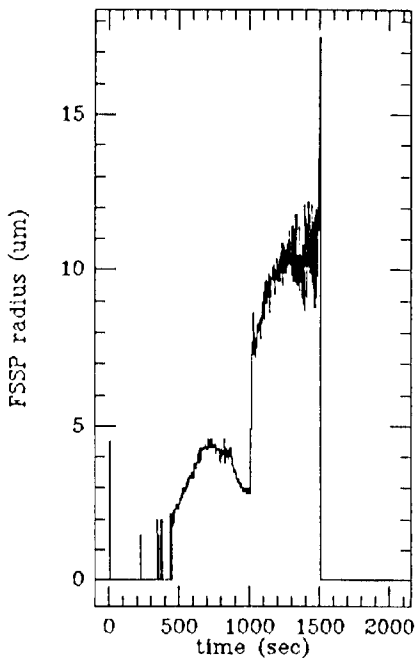


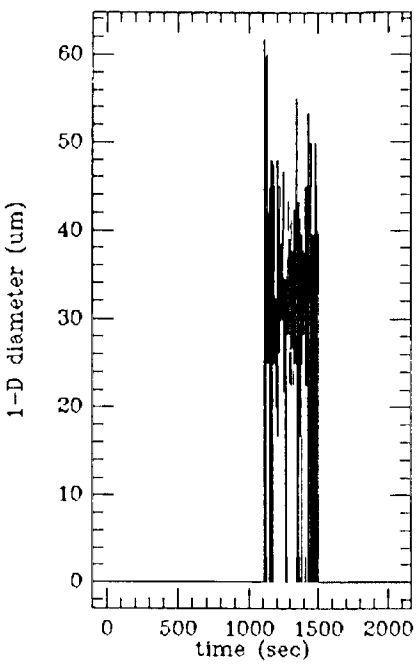


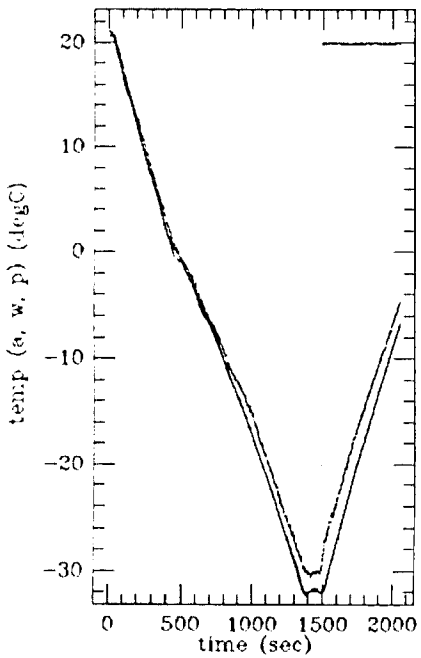


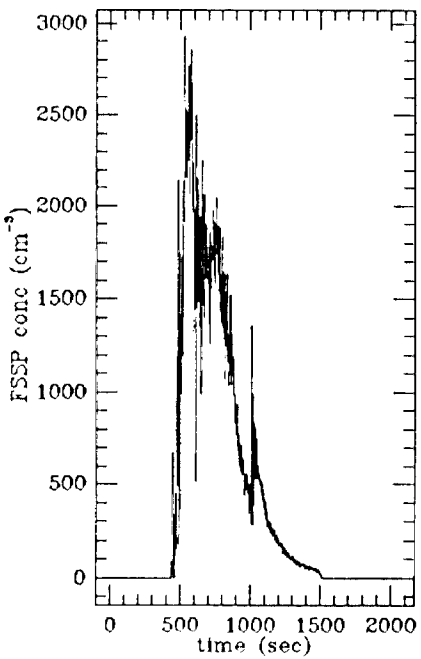


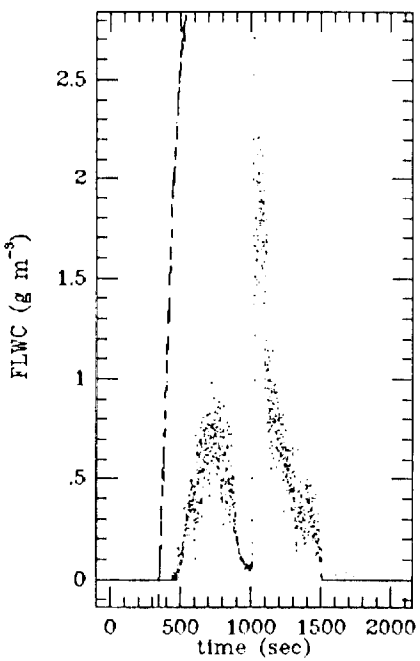


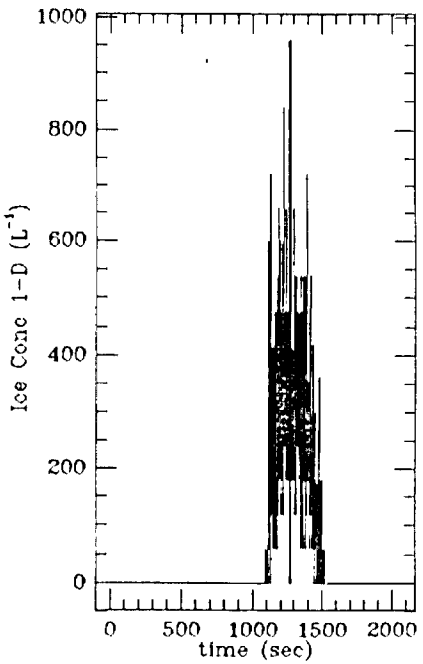

EXPERIMENT 3
pressure (mb)
temp (a, w, p) (degC)
relative humidity (%)
FSSP conc (cm⁻³)
FSSP radius (um)
FLWC (g m⁻³)
1-D diameter (um)
Ice Conc 1-D (L⁻¹)
time (sec)

# EXPERIMENT 4

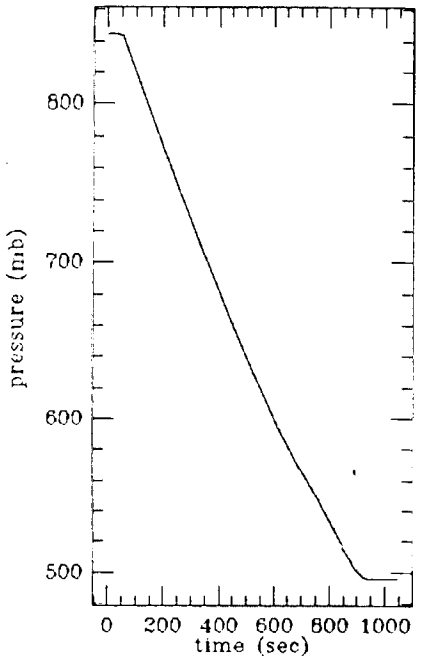


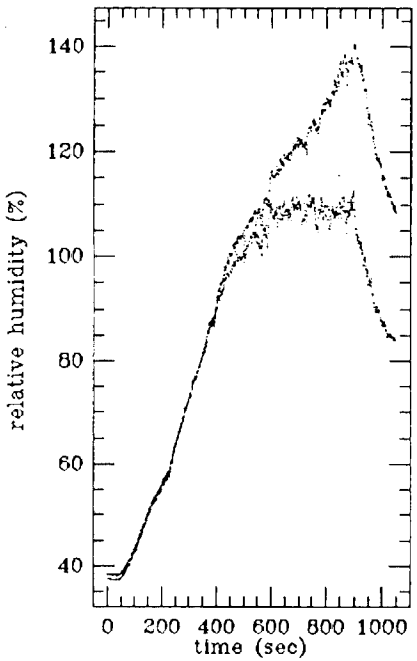


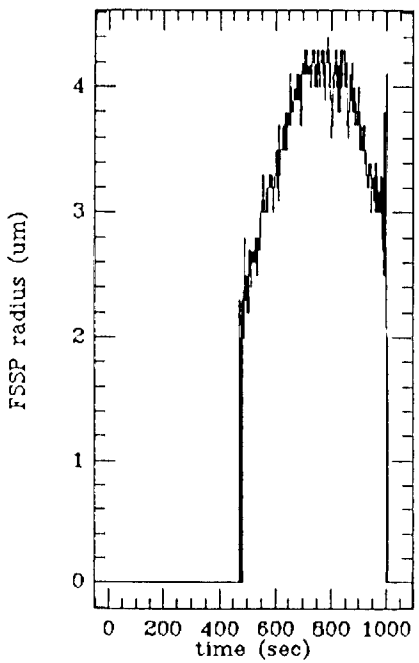


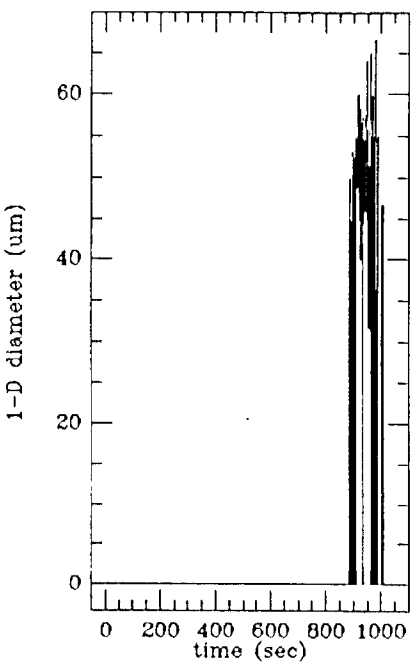


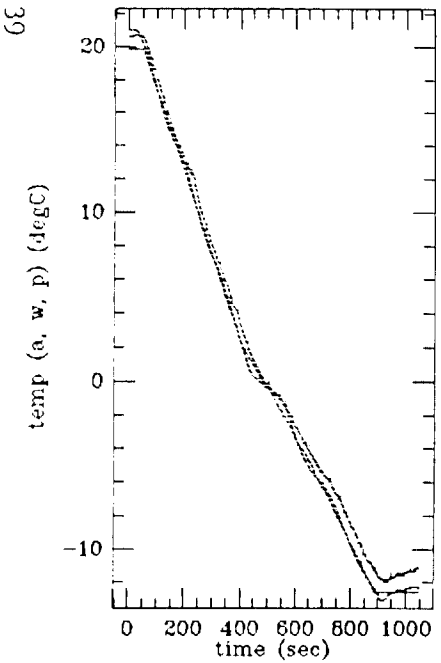


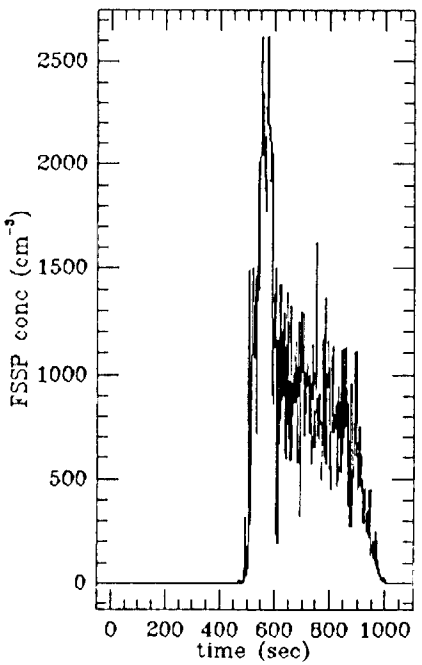


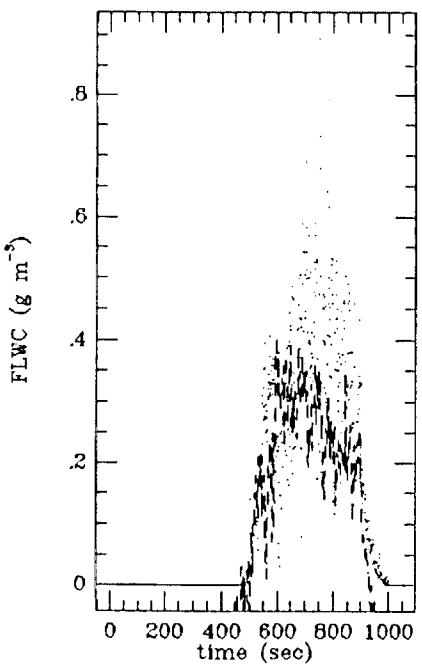


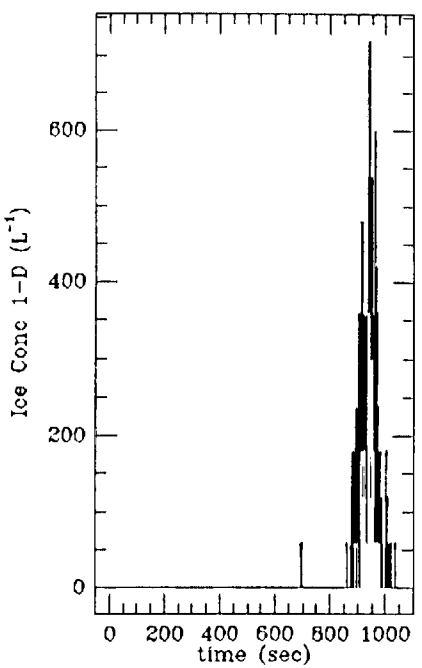

EXPERIMENT 5
pressure (mb)
relative humidity (%)
EG+G Hygrometer
temp (a, w, p) (deg C)
a: air temp
w: wall temp
p: program temp
FSSP conc (cm⁻³)
FLWC (g m⁻³)
FSSP: dots
EG+G: line
FSSP radius (um)
Ice Cone 1-D (L⁻¹)
1-D diameter (um)
time (sec)

EXPERIMENT 6
pressure (mb)
temp (a, w, p) (degC)
relative humidity (%)
FSSP conc (cm-3)
FSSP radius (um)
FLWC (g m-3)
Ice Conc 1-D (L-1)
1-D diameter (um)
time (sec)

# EXPERIMENT 7

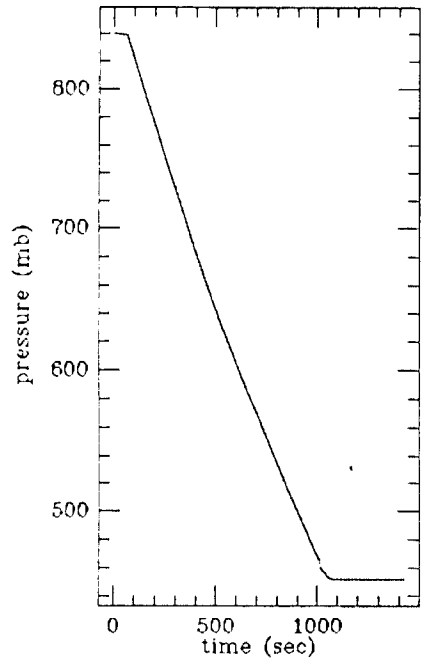


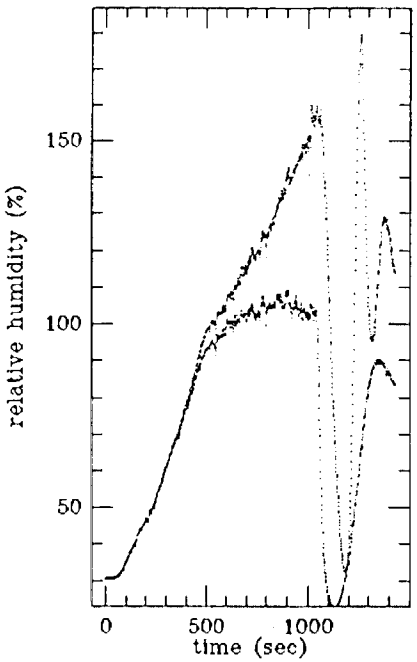


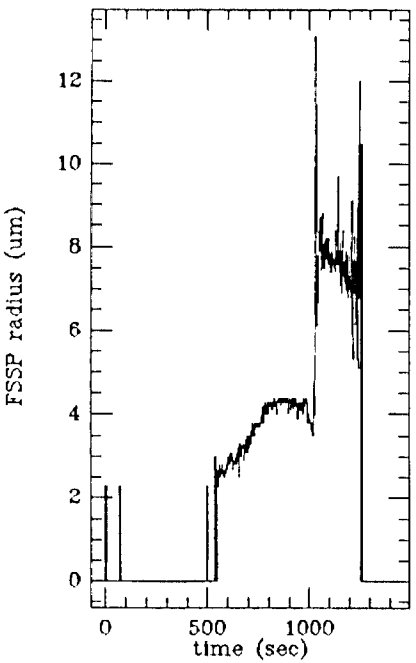


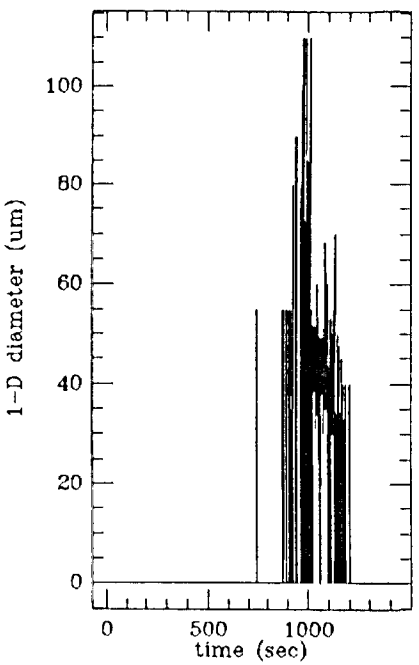


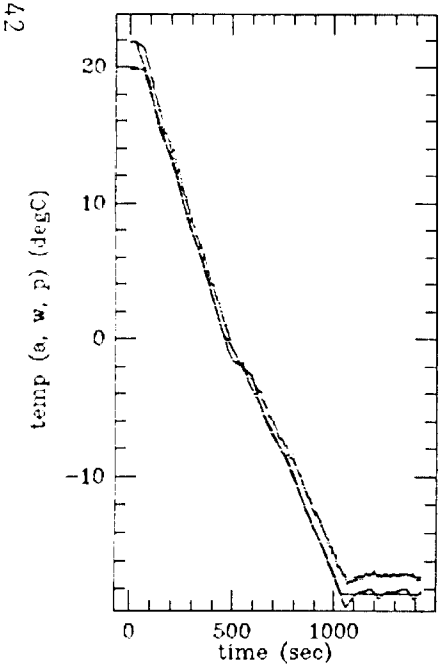


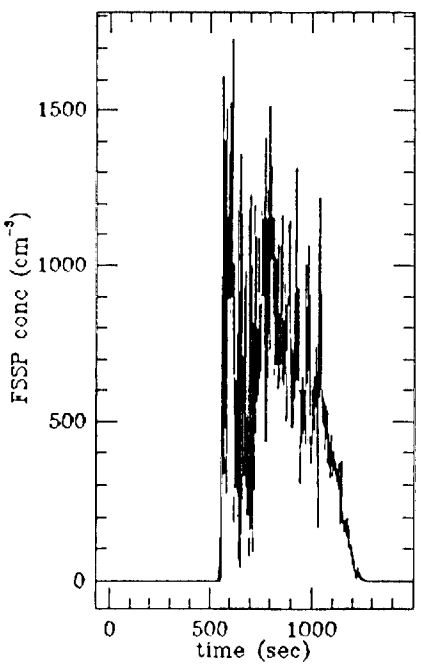


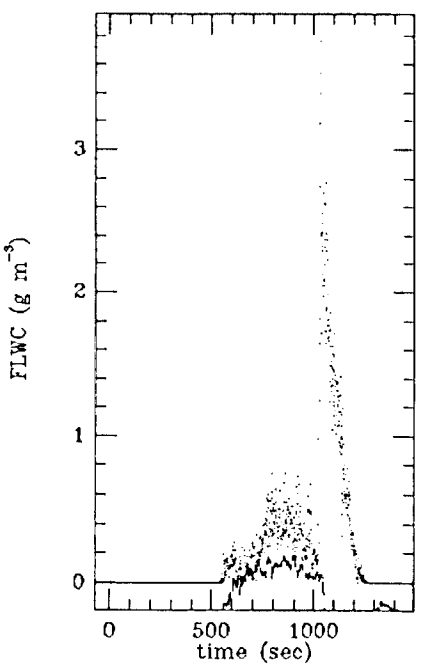


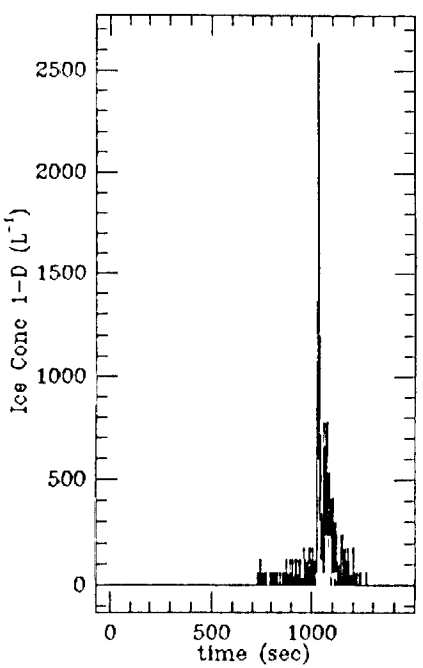

# EXPERIMENT 8

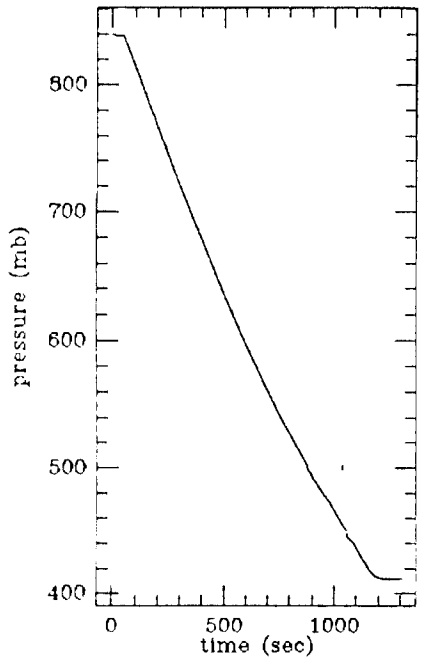


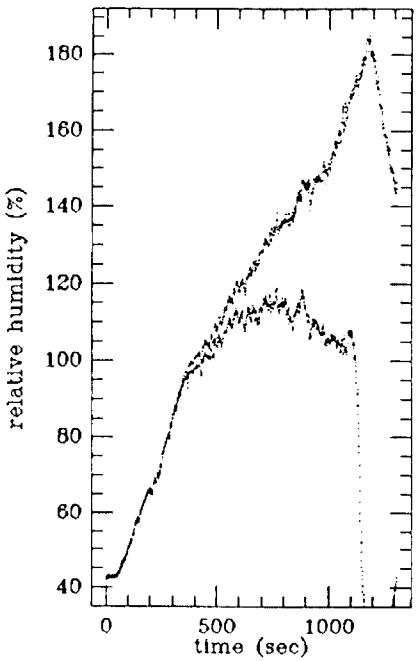


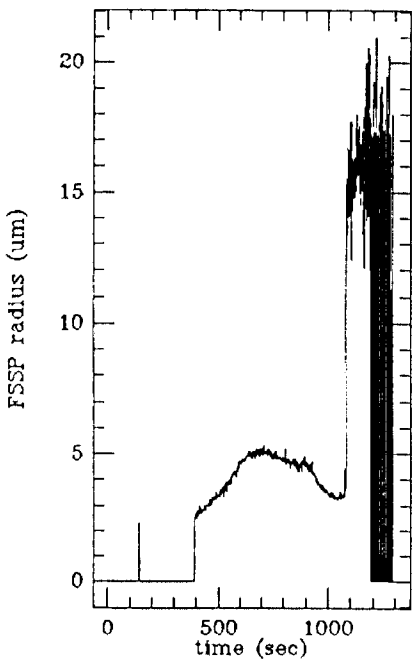


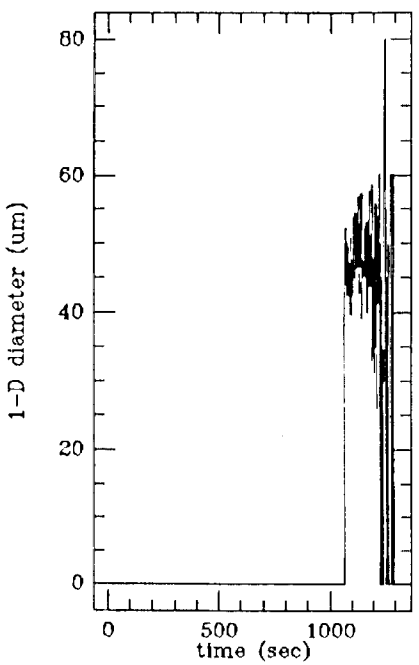


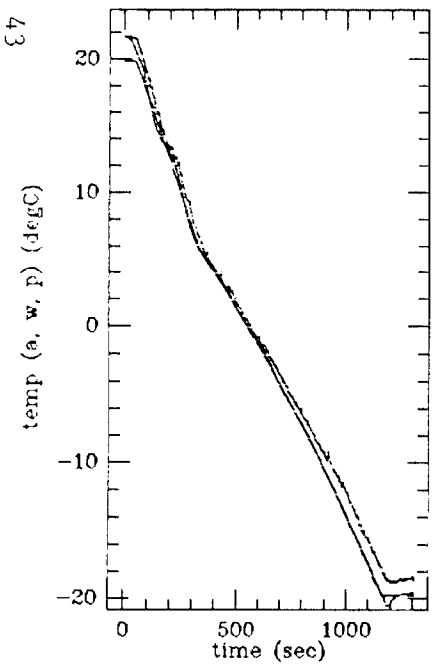


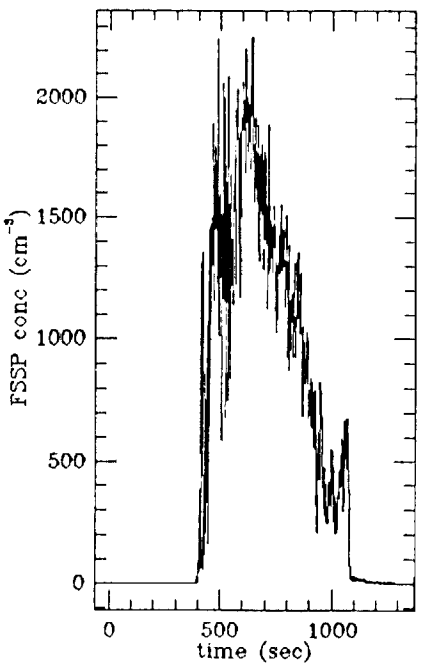


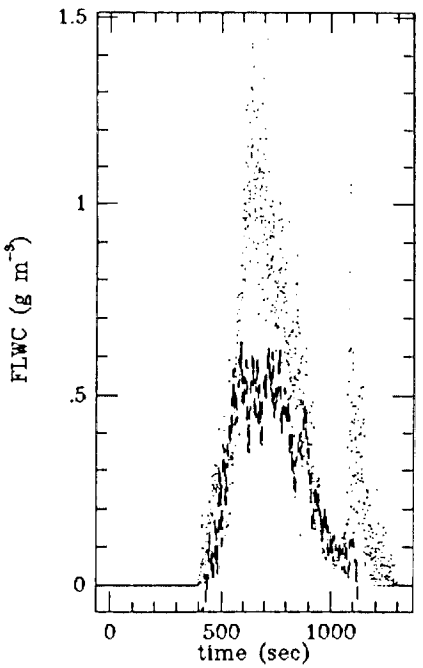


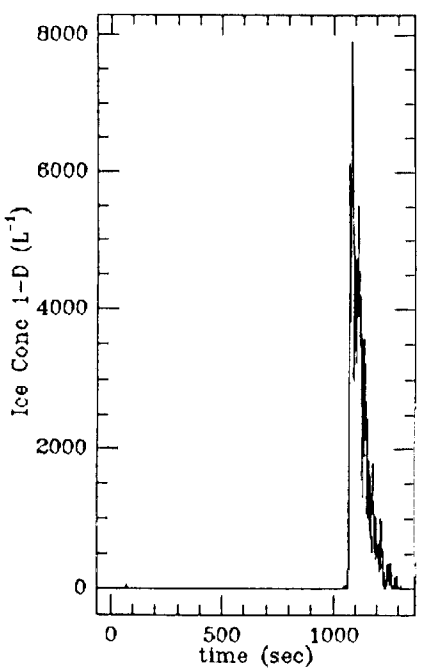

# EXPERIMENT 9

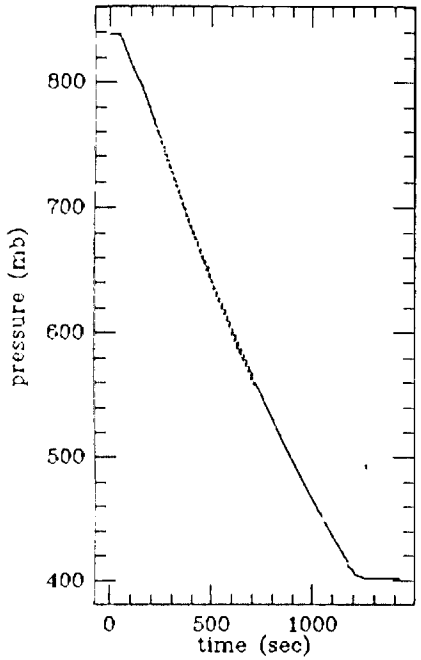


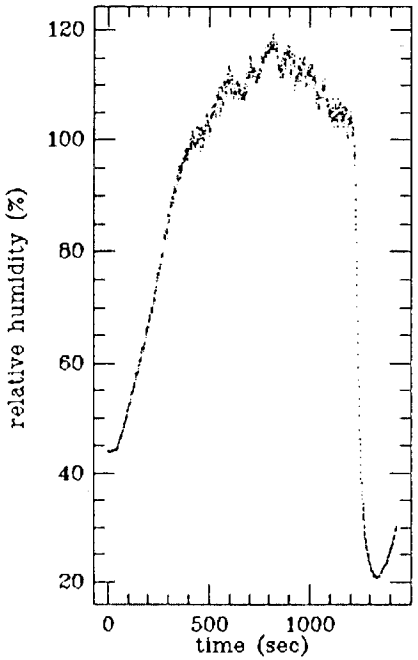


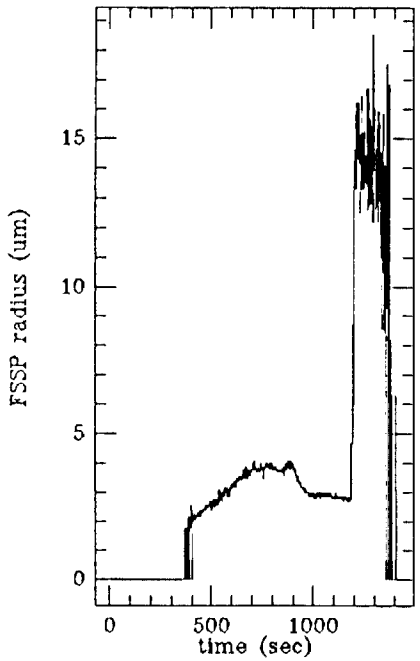


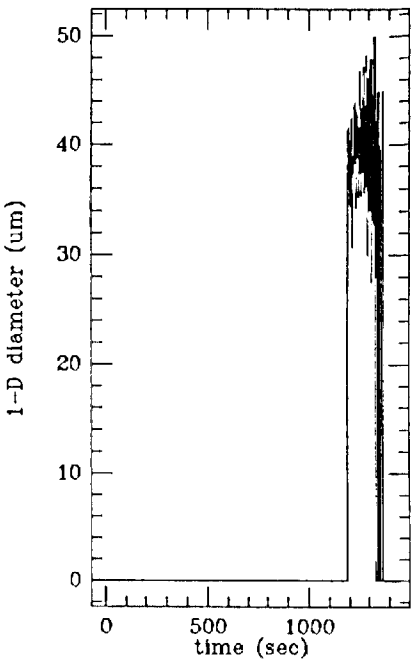


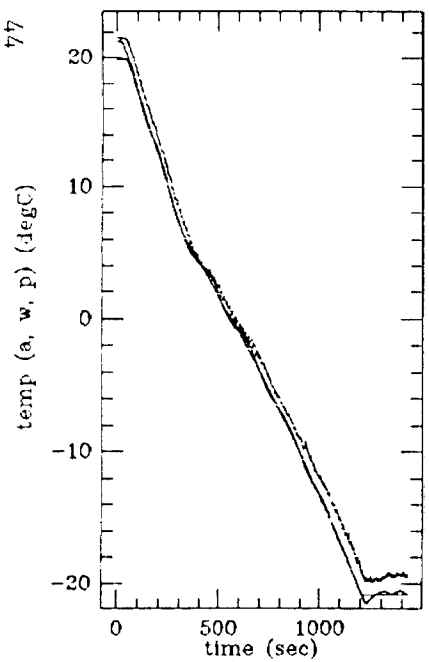


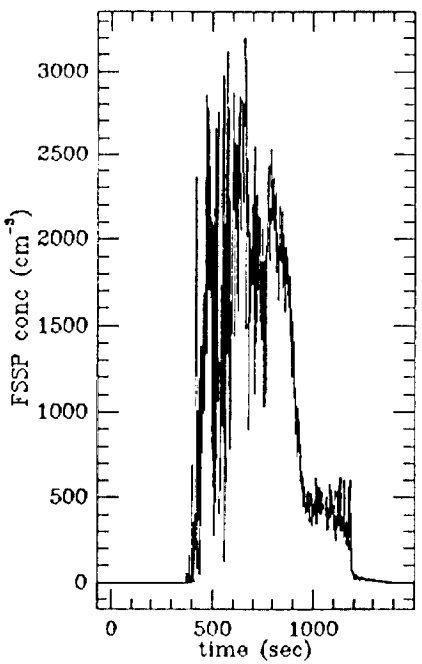


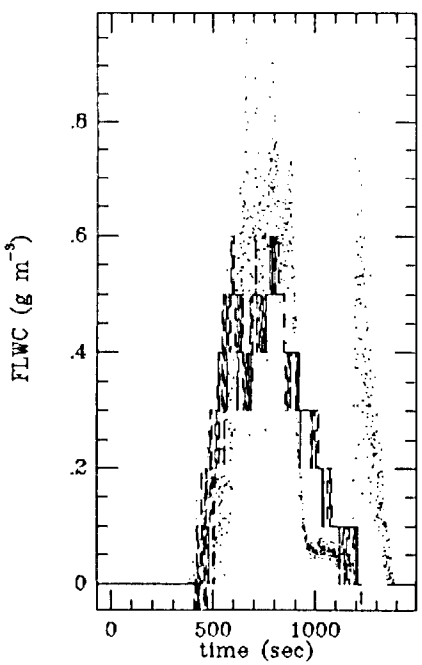


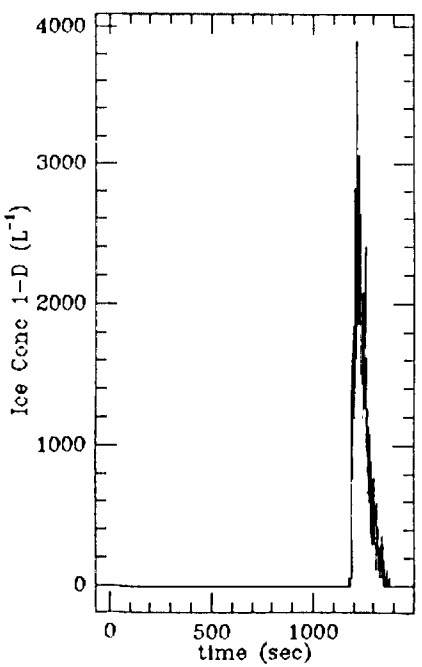

# EXPERIMENT 10

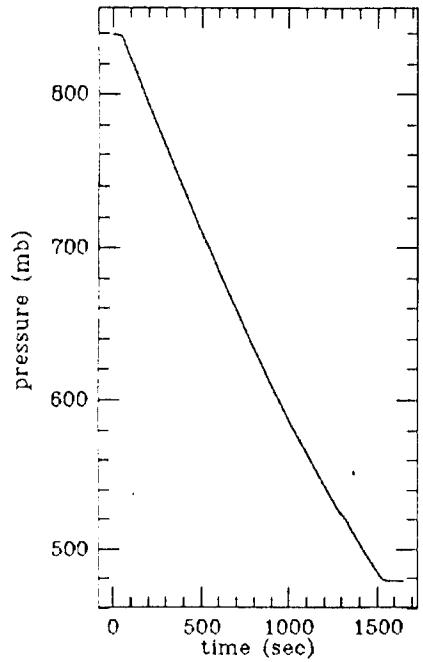


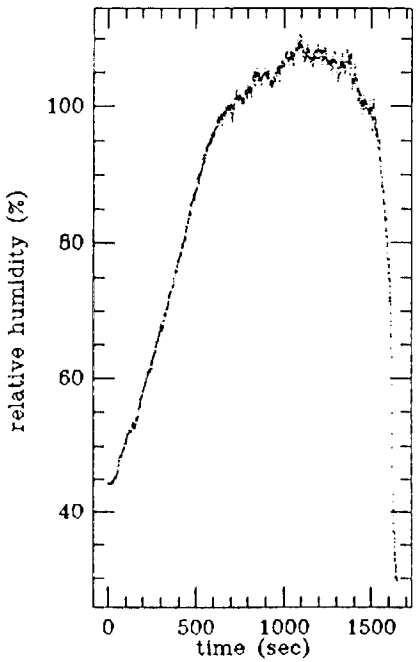


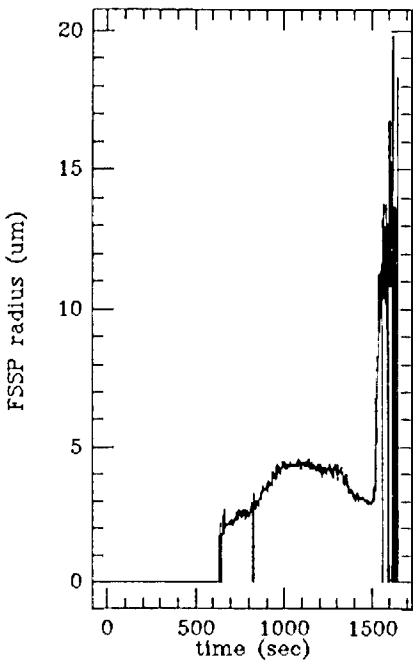


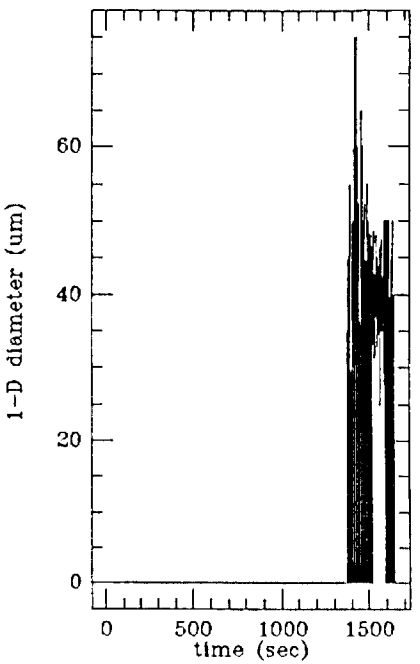


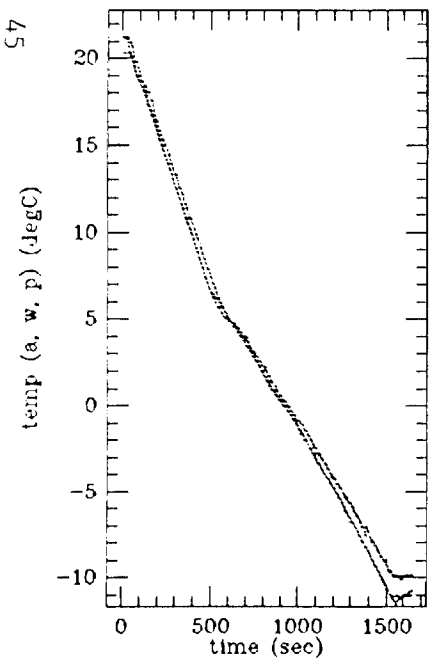


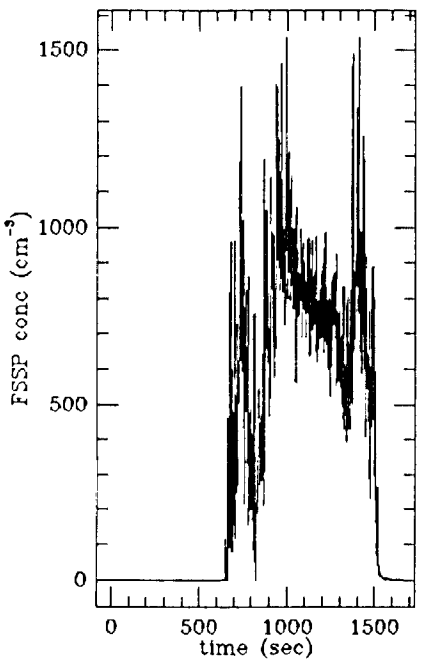


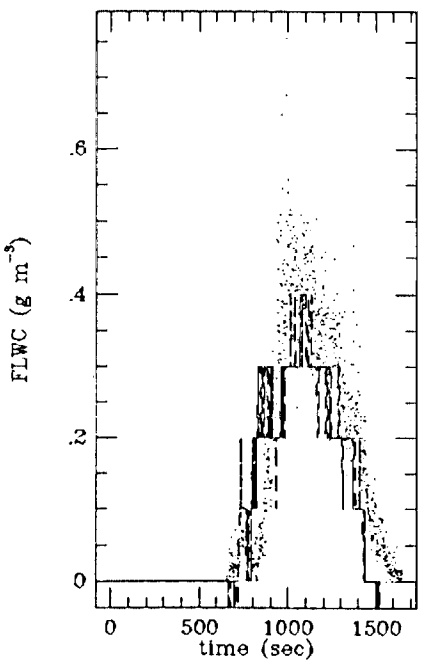


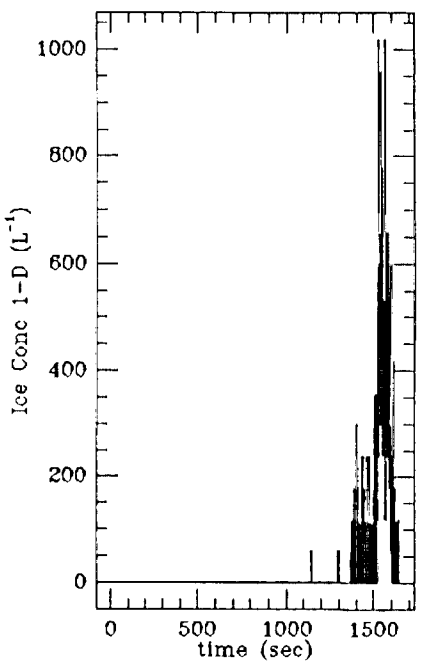

# EXPERIMENT 11

# EXPERIMENT 12

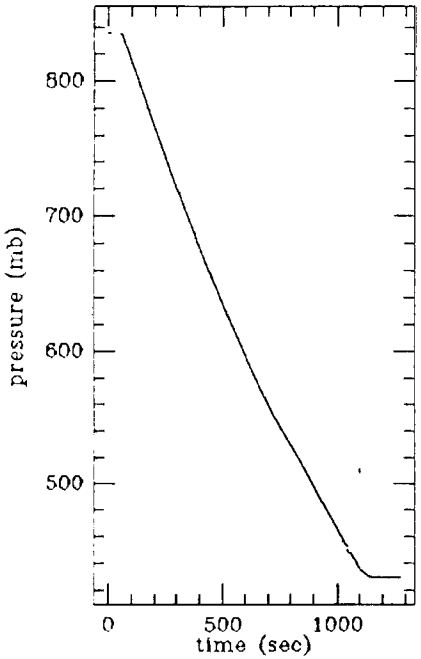


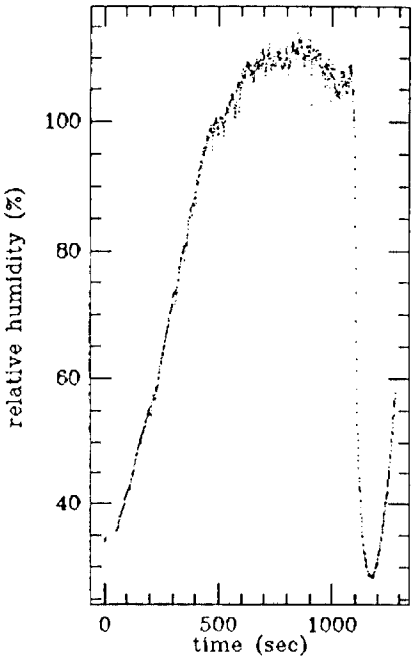


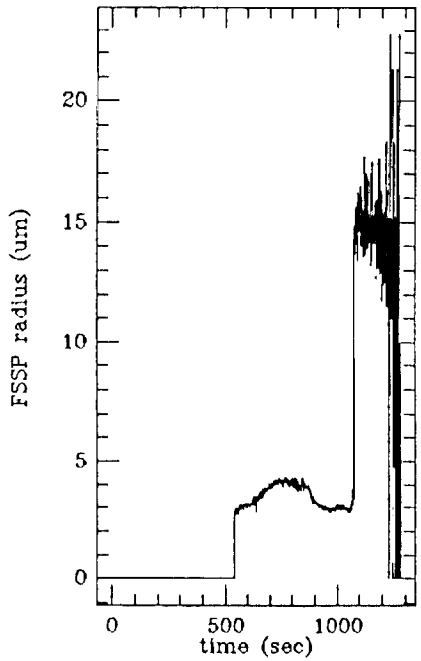


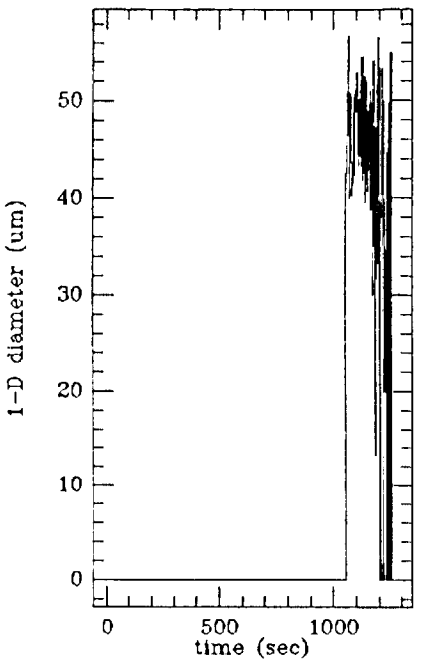


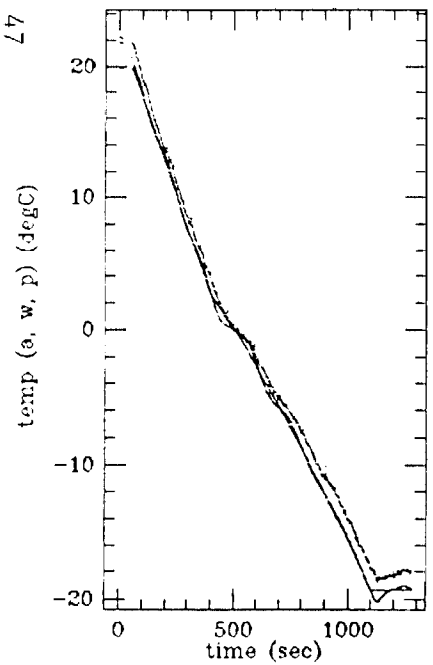


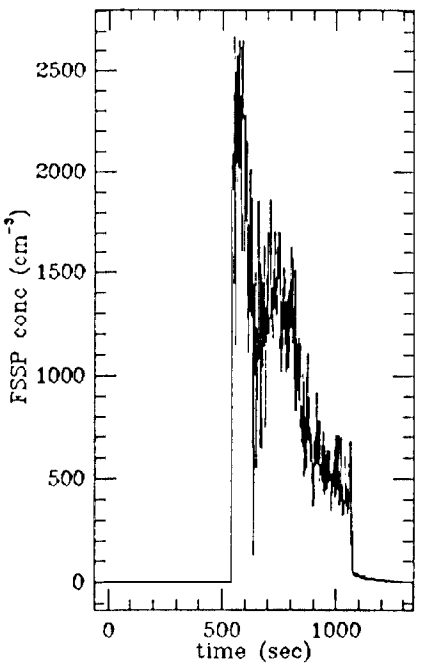


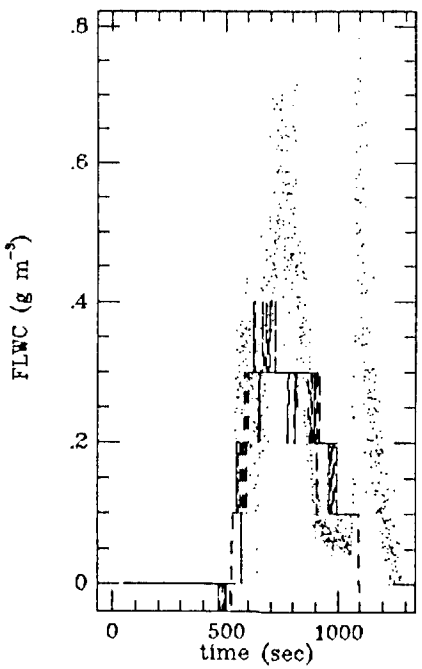


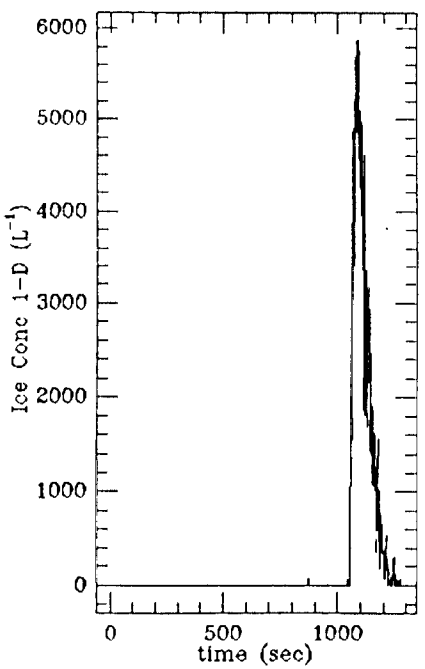

EXPERIMENT 13
pressure (mb)
temp (a, w, p) (degC)
relative humidity (%)
FSSP conc (cm⁻³)
FSSP radius (um)
FLWC (g m⁻³)
1-D diameter (um)
Ice Conc 1-D (L⁻¹)
time (sec)

# EXPERIMENT 14

# EXPERIMENT 15

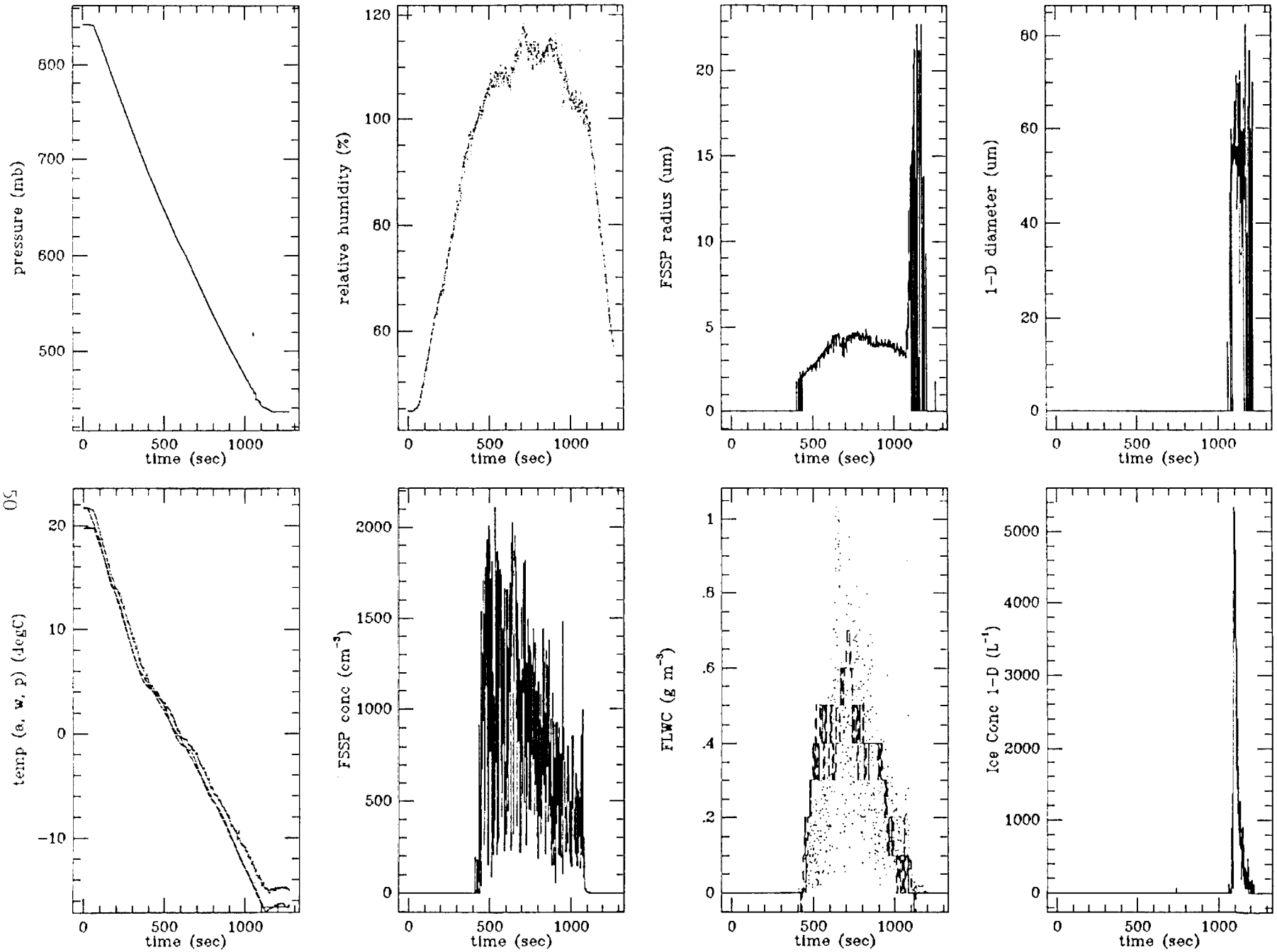

EXPERIMENT 16
pressure (mb)
temp (a, w, p) (degC)
relative humidity (%)
FSSP cone (cm⁻³)
FSSP radius (um)
FLWC (g m⁻³)
Ice Cone 1-D (L⁻¹)
1-D diameter (um)
time (sec)

# EXPERIMENT 17

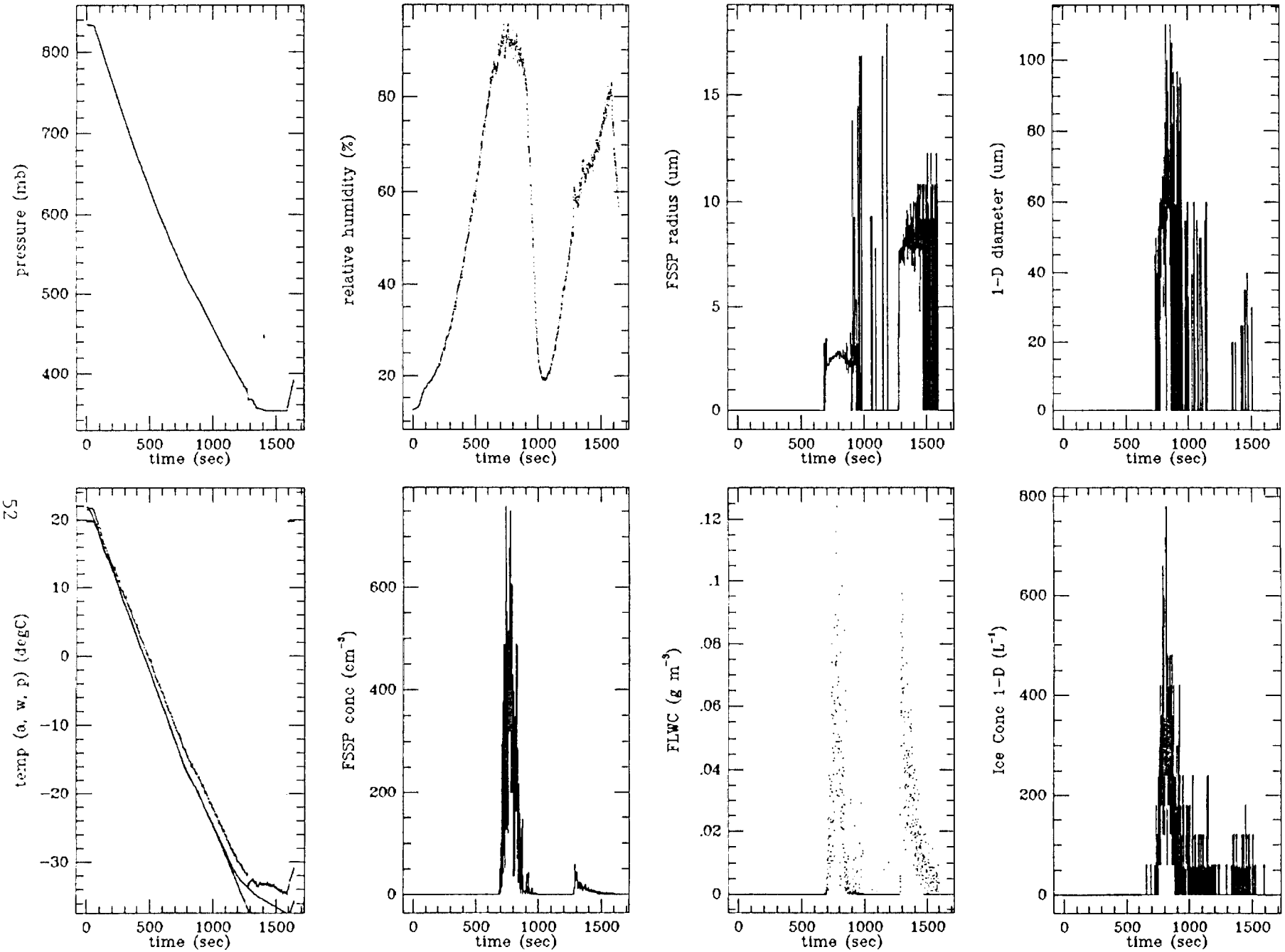

# EXPERIMENT 18

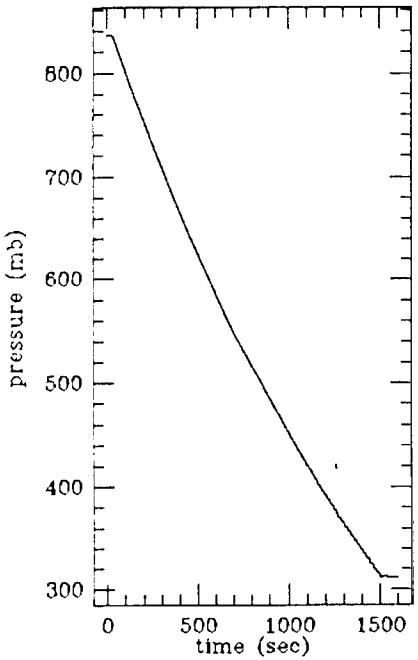


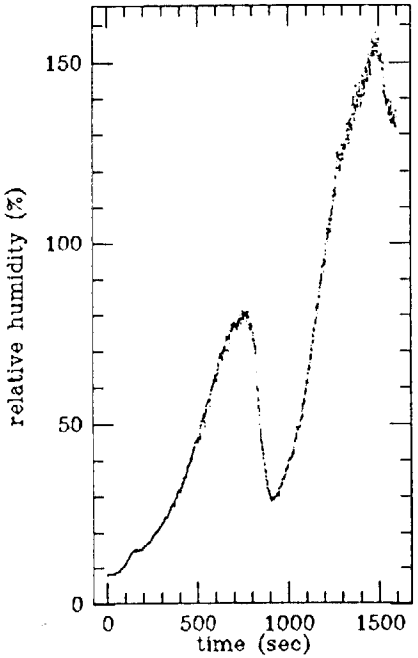


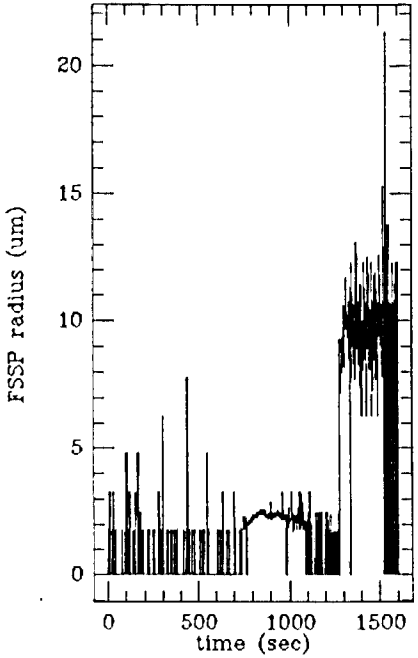


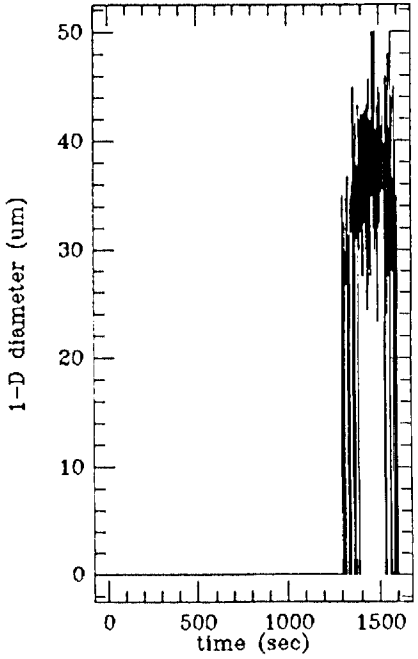


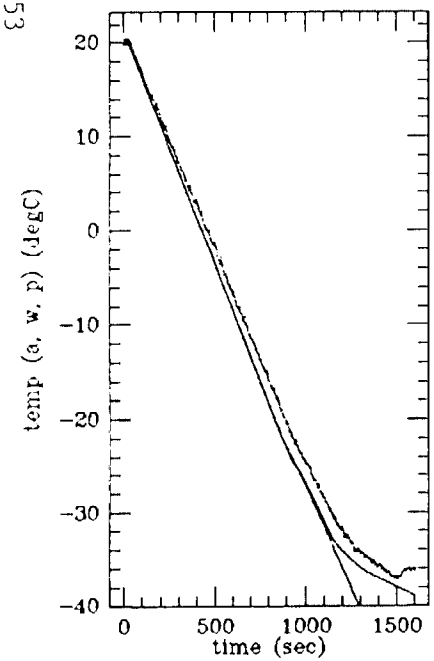


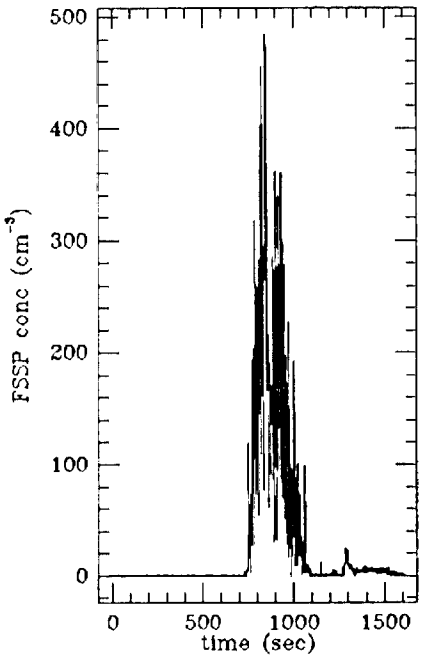


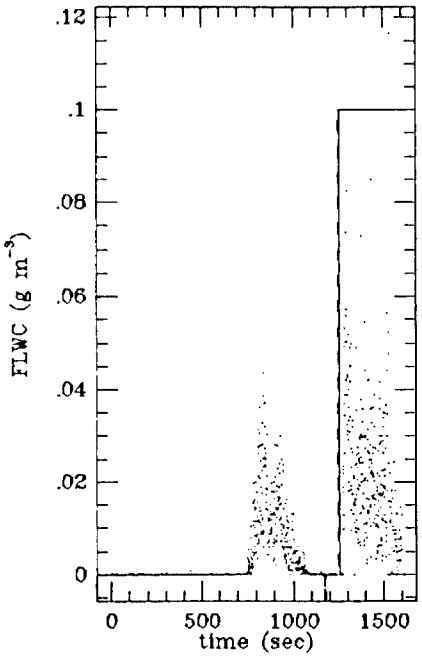


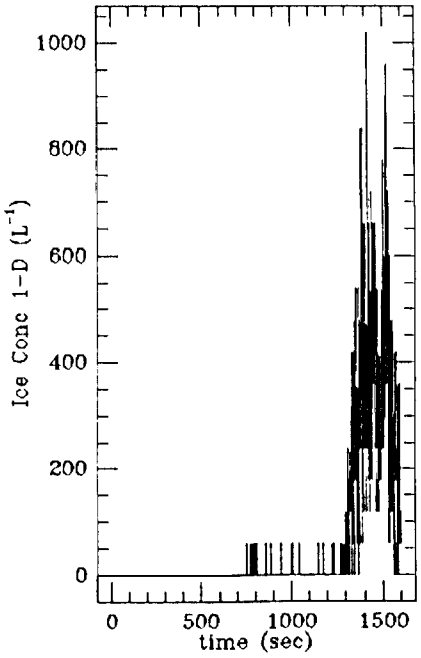

# APPENDIX C

## Raw Data Produced by the PVM for all Experiments

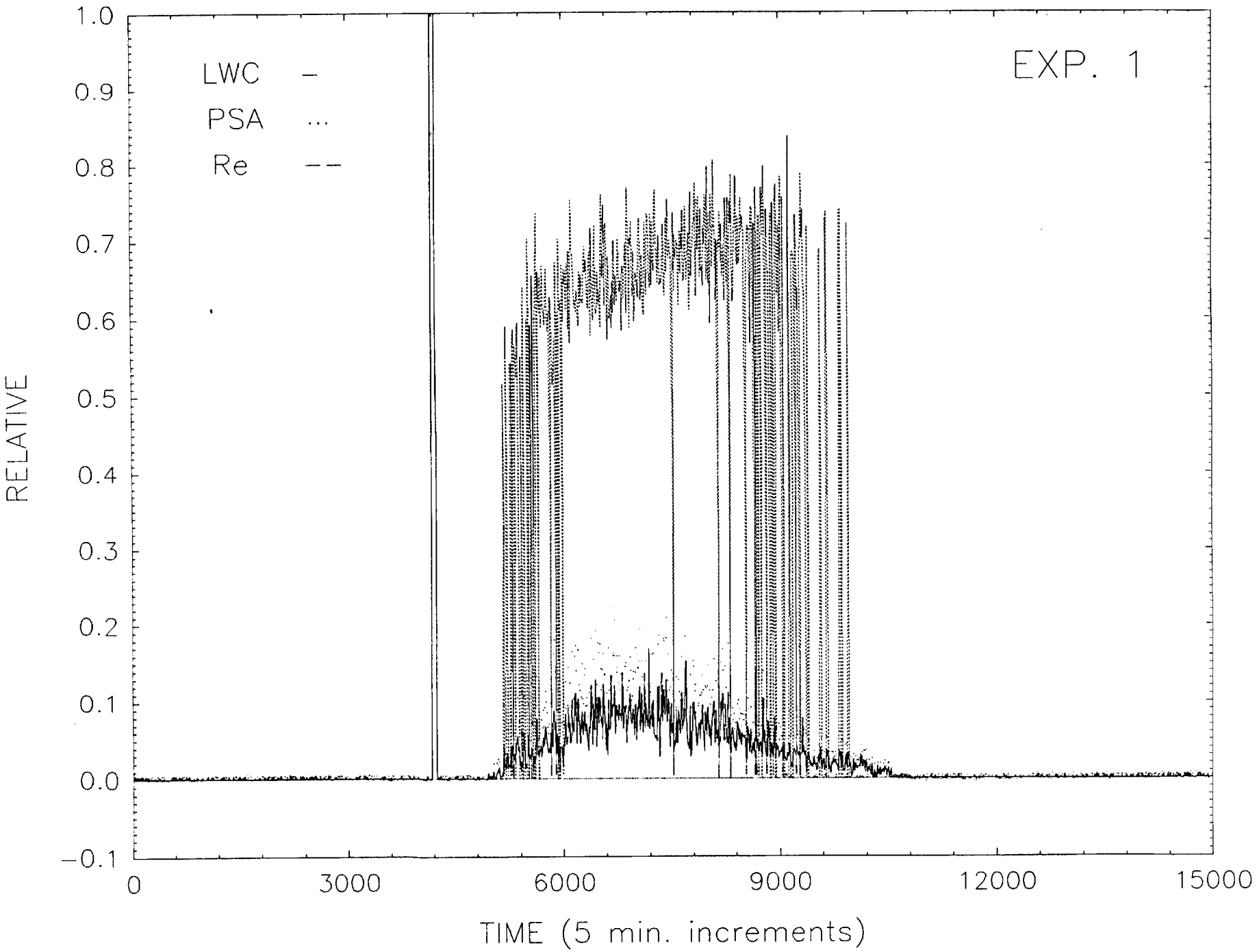
LWC –
PSA ...
Re – –
EXP. 1
RELATIVE
1.0
0.9
0.8
0.7
0.6
0.5
0.4
0.3
0.2
0.1
0.0
−0.1
0
3000
6000
9000
12000
15000
TIME (5 min. increments)

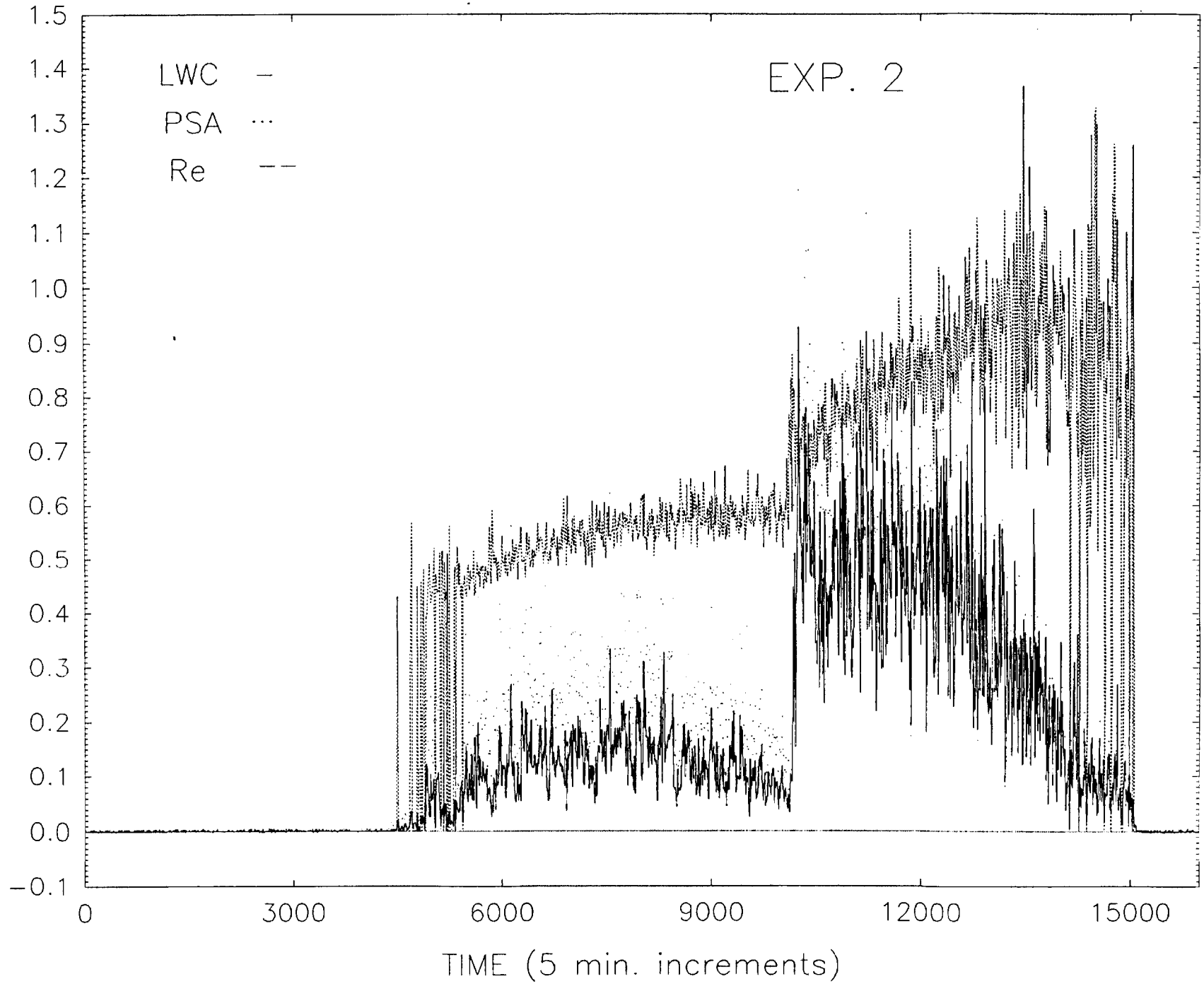
LWC –
PSA ···
Re – –
EXP. 2
RELATIVE
1.5
1.4
1.3
1.2
1.1
1.0
0.9
0.8
0.7
0.6
0.5
0.4
0.3
0.2
0.1
0.0
−0.1
0
3000
6000
9000
12000
15000
TIME (5 min. increments)

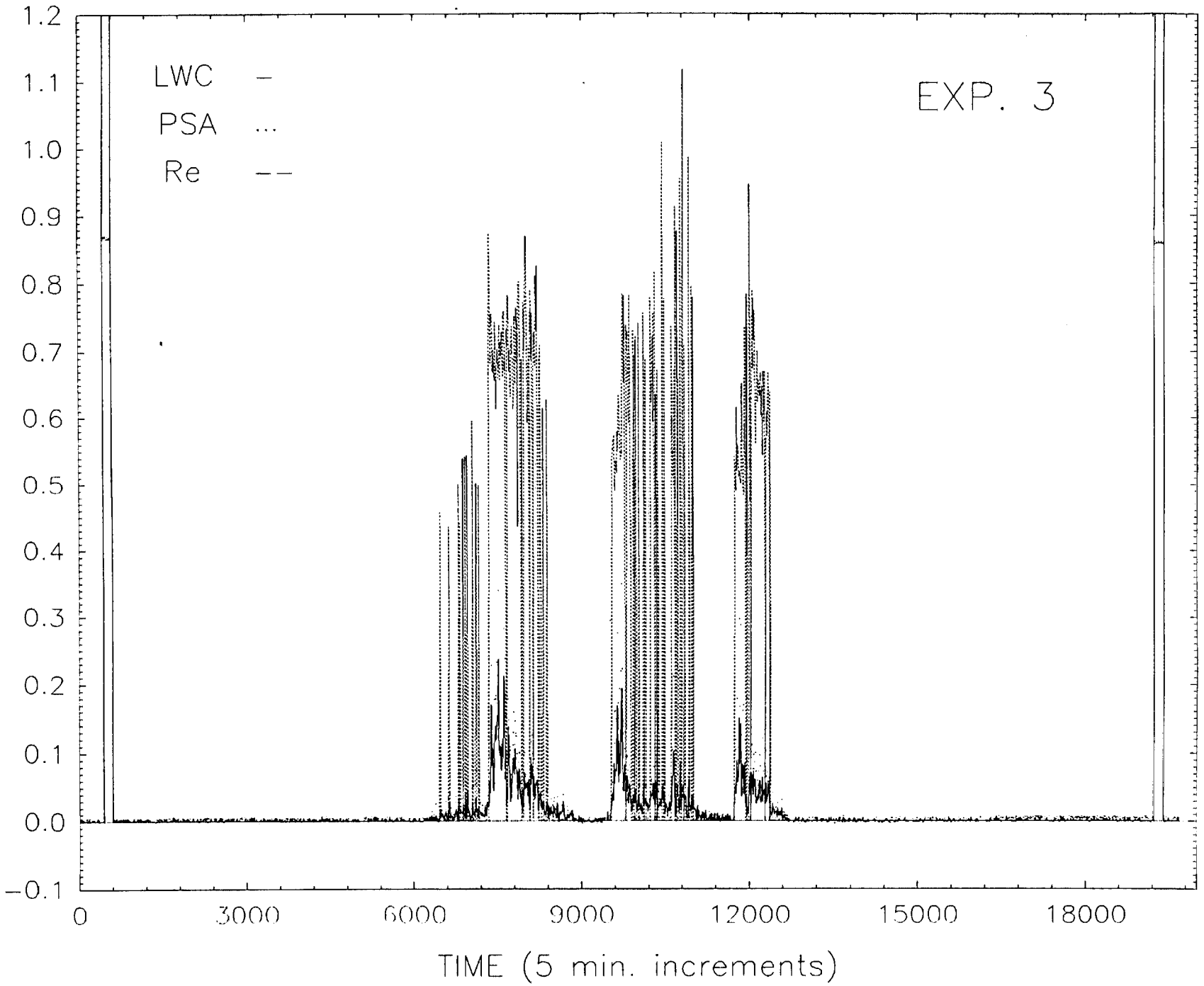
LWC —
PSA ...
Re --
EXP. 3
RELATIVE
1.2
1.1
1.0
0.9
0.8
0.7
0.6
0.5
0.4
0.3
0.2
0.1
0.0
-0.1
0
3000
6000
9000
12000
15000
18000
TIME (5 min. increments)

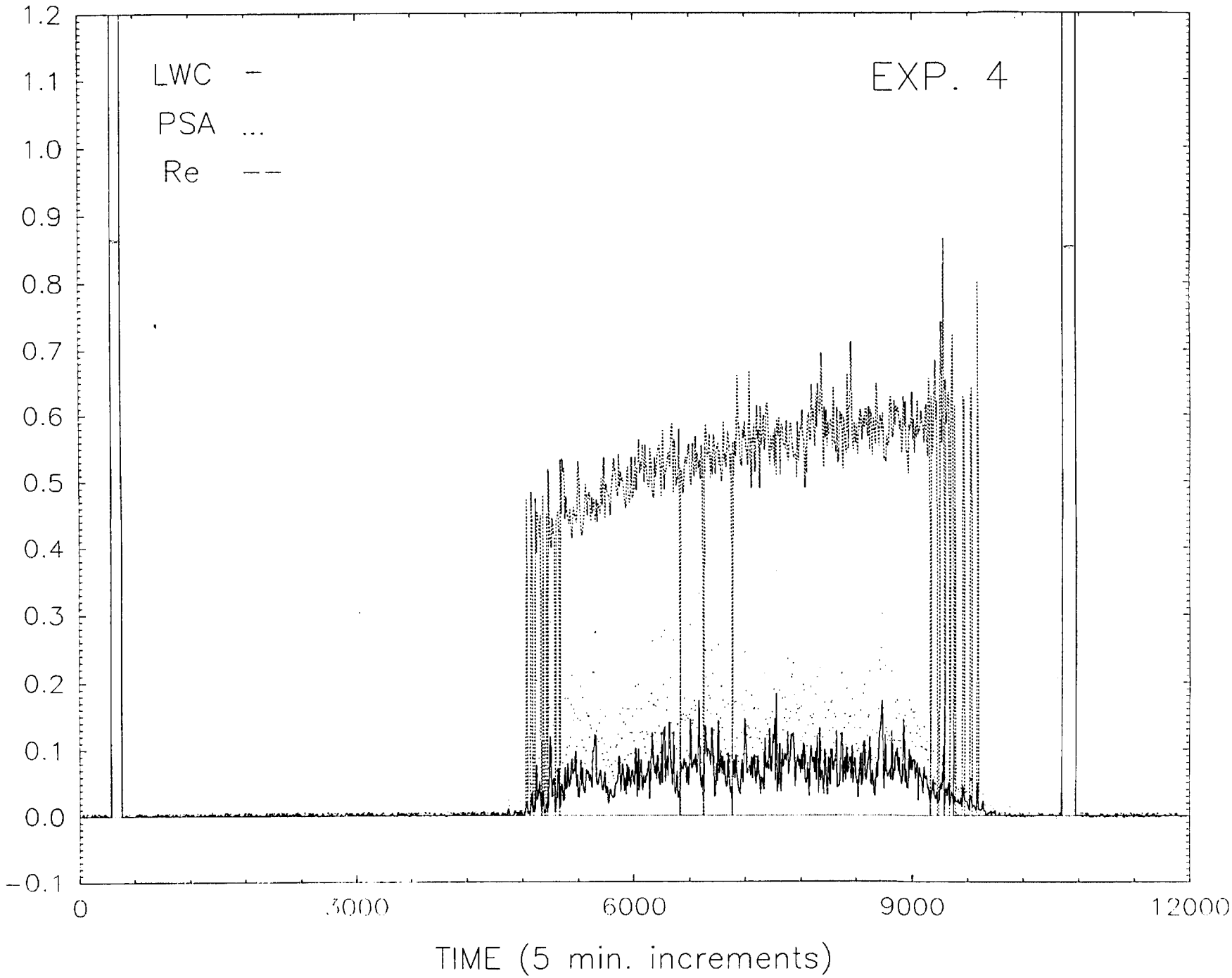
LWC –
PSA ...
Re – –
EXP. 4
RELATIVE
1.2
1.1
1.0
0.9
0.8
0.7
0.6
0.5
0.4
0.3
0.2
0.1
0.0
−0.1
0
3000
6000
9000
12000
TIME (5 min. increments)

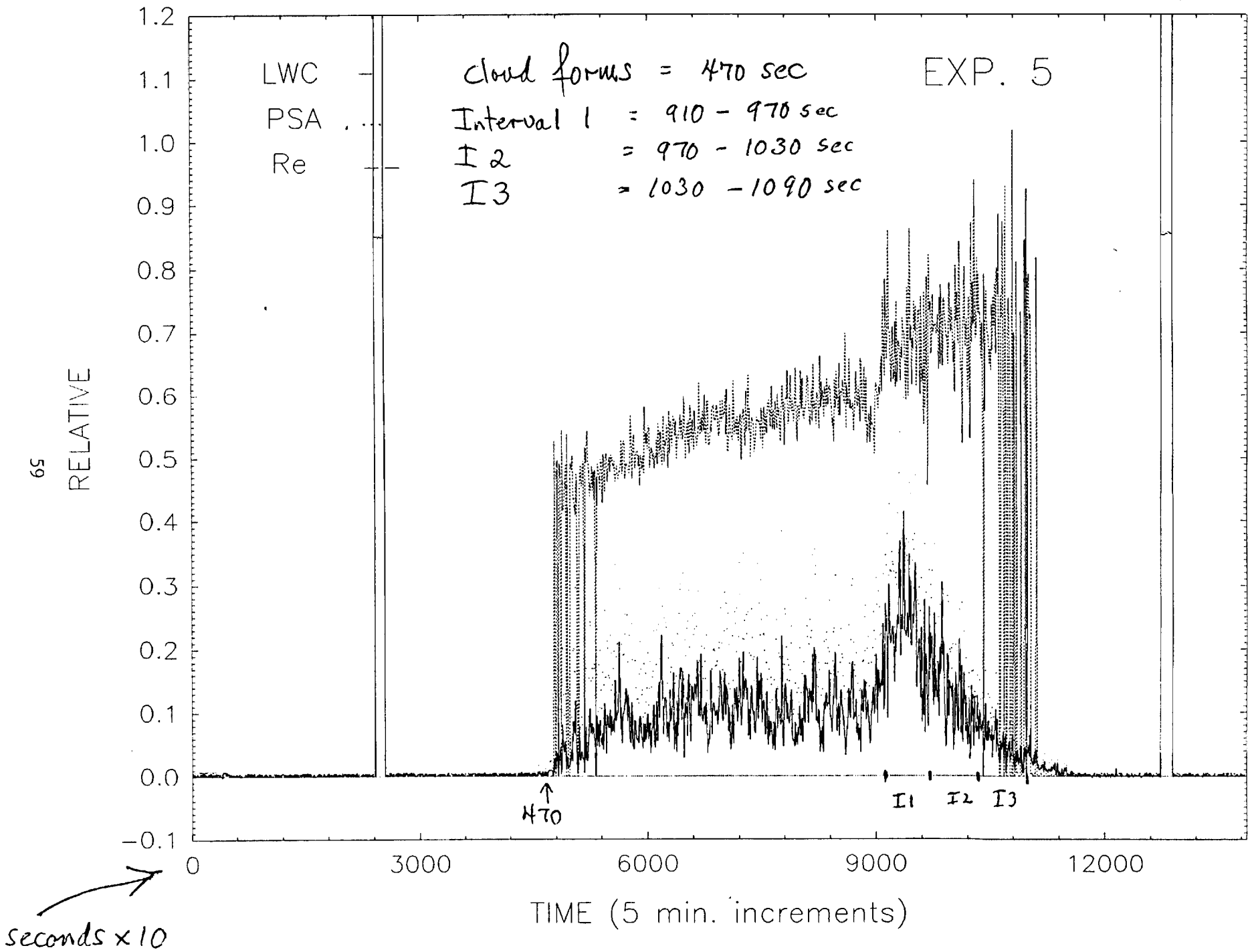
LWC
PSA
Re
cloud forms = 470 sec
Interval 1 = 910 - 970 sec
I 2 = 970 - 1030 sec
I3 = 1030 - 1090 sec
EXP. 5
RELATIVE
59
1.2
1.1
1.0
0.9
0.8
0.7
0.6
0.5
0.4
0.3
0.2
0.1
0.0
-0.1
0
3000
6000
9000
12000
H70
I1
I2
I3
TIME (5 min. increments)
seconds x 10

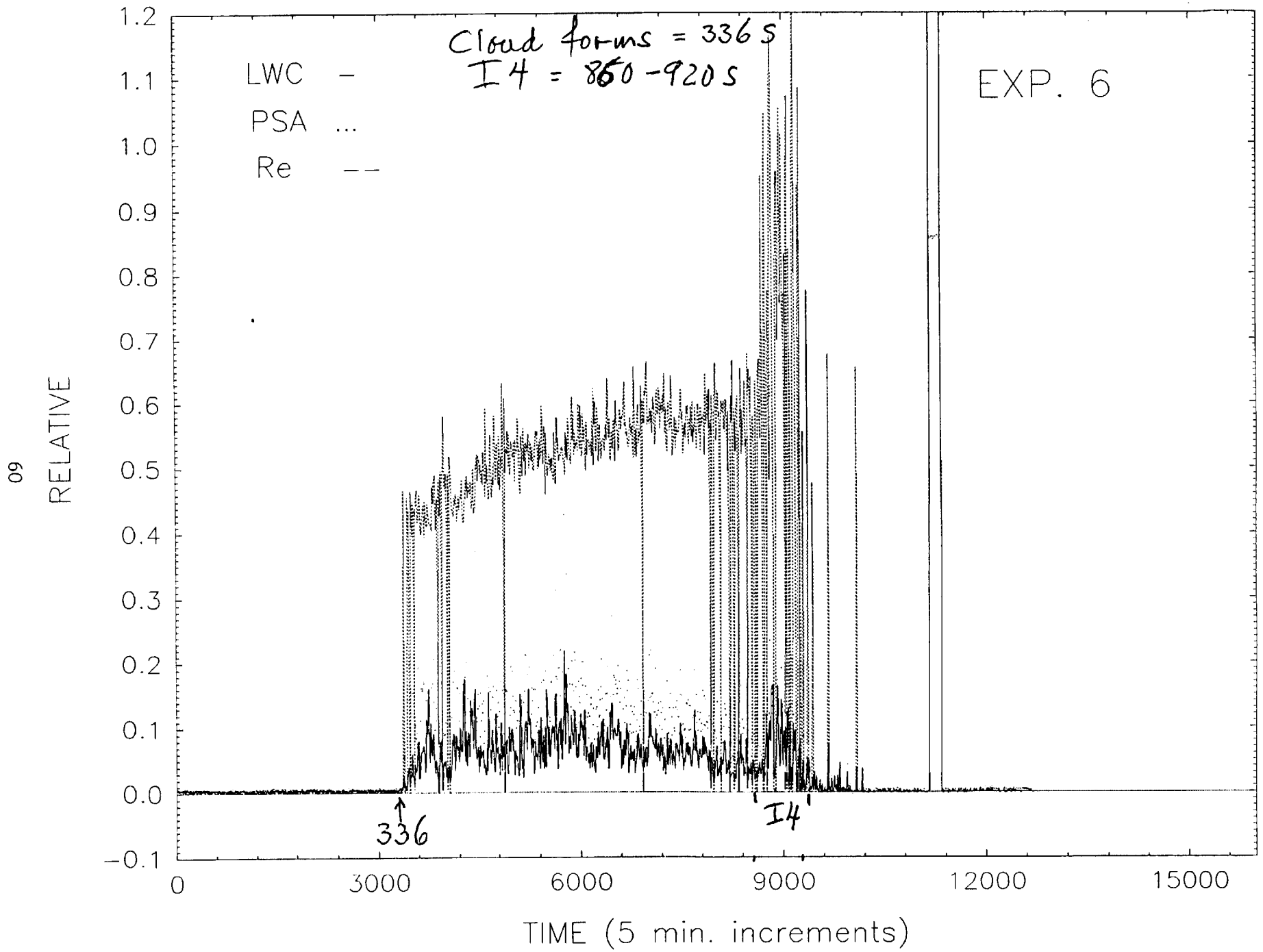
Cloud forms = 336 s
I4 = 860-920 s
LWC –
PSA ...
Re --
EXP. 6
RELATIVE
1.2
1.1
1.0
0.9
0.8
0.7
0.6
0.5
0.4
0.3
0.2
0.1
0.0
−0.1
336
I4
0
3000
6000
9000
12000
15000
TIME (5 min. increments)

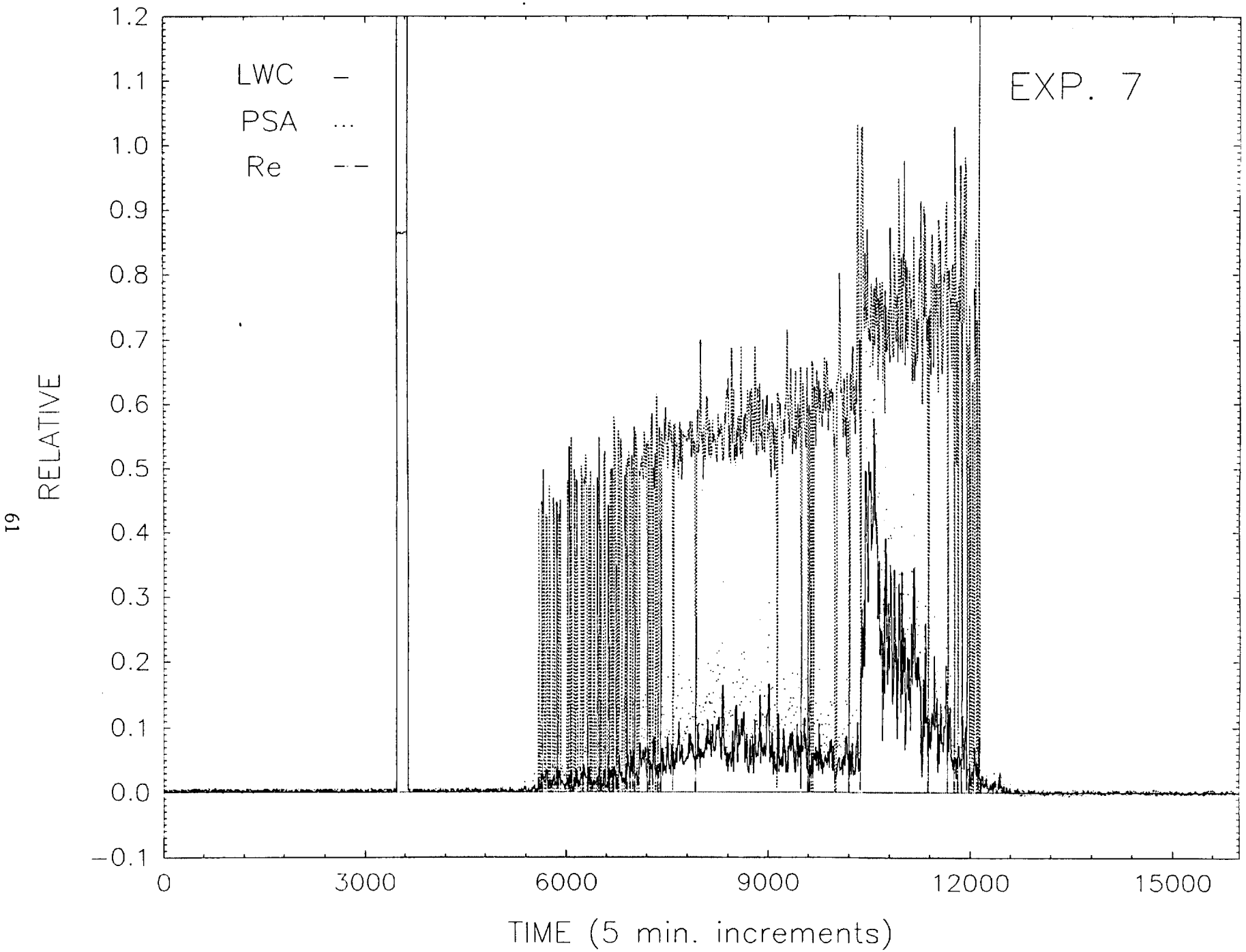
LWC —
PSA ...
Re - -
EXP. 7
RELATIVE
1.2
1.1
1.0
0.9
0.8
0.7
0.6
0.5
0.4
0.3
0.2
0.1
0.0
-0.1
0
3000
6000
9000
12000
15000
TIME (5 min. increments)

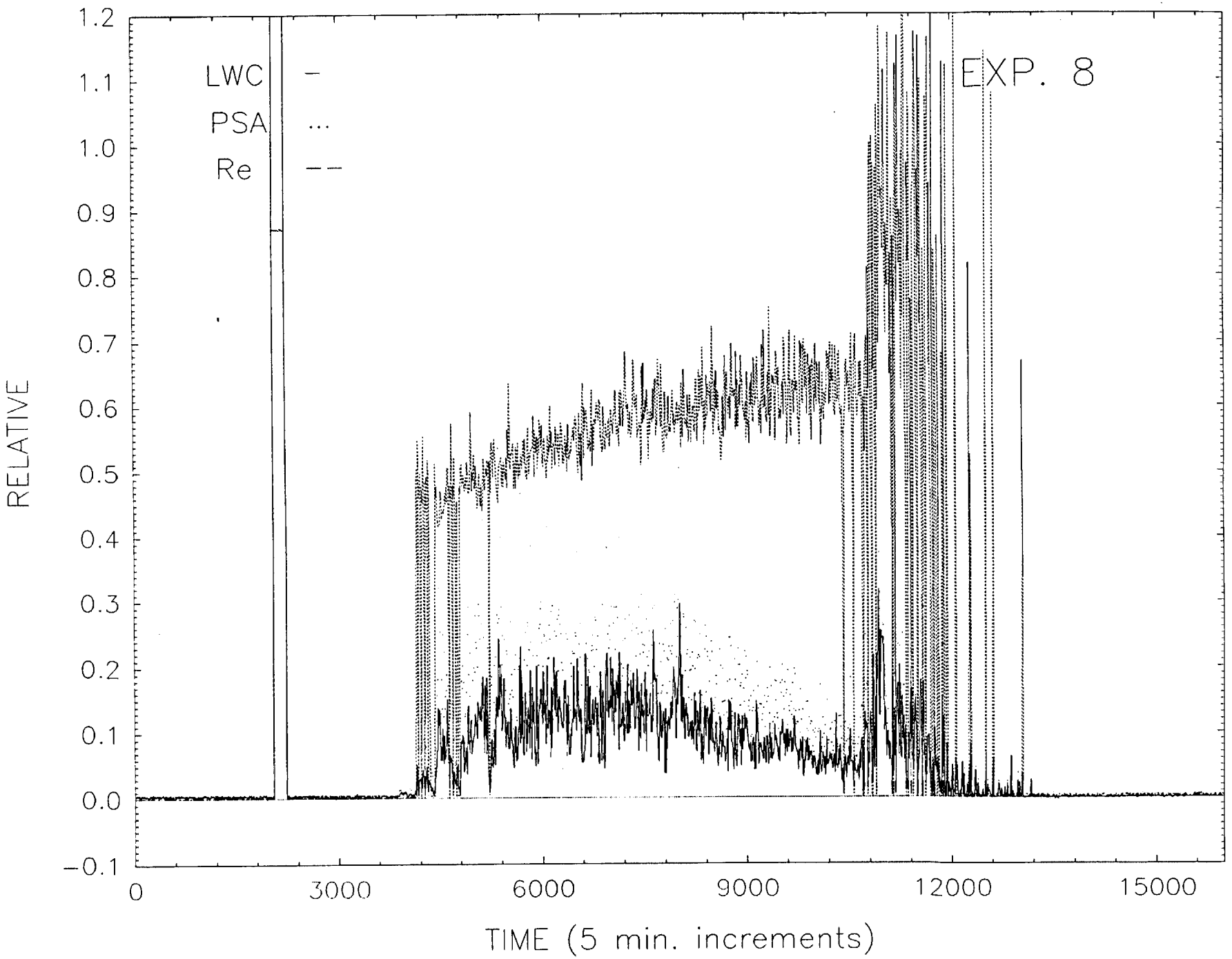
LWC
PSA
Re
EXP. 8
RELATIVE
TIME (5 min. increments)
1.2
1.1
1.0
0.9
0.8
0.7
0.6
0.5
0.4
0.3
0.2
0.1
0.0
−0.1
0
3000
6000
9000
12000
15000

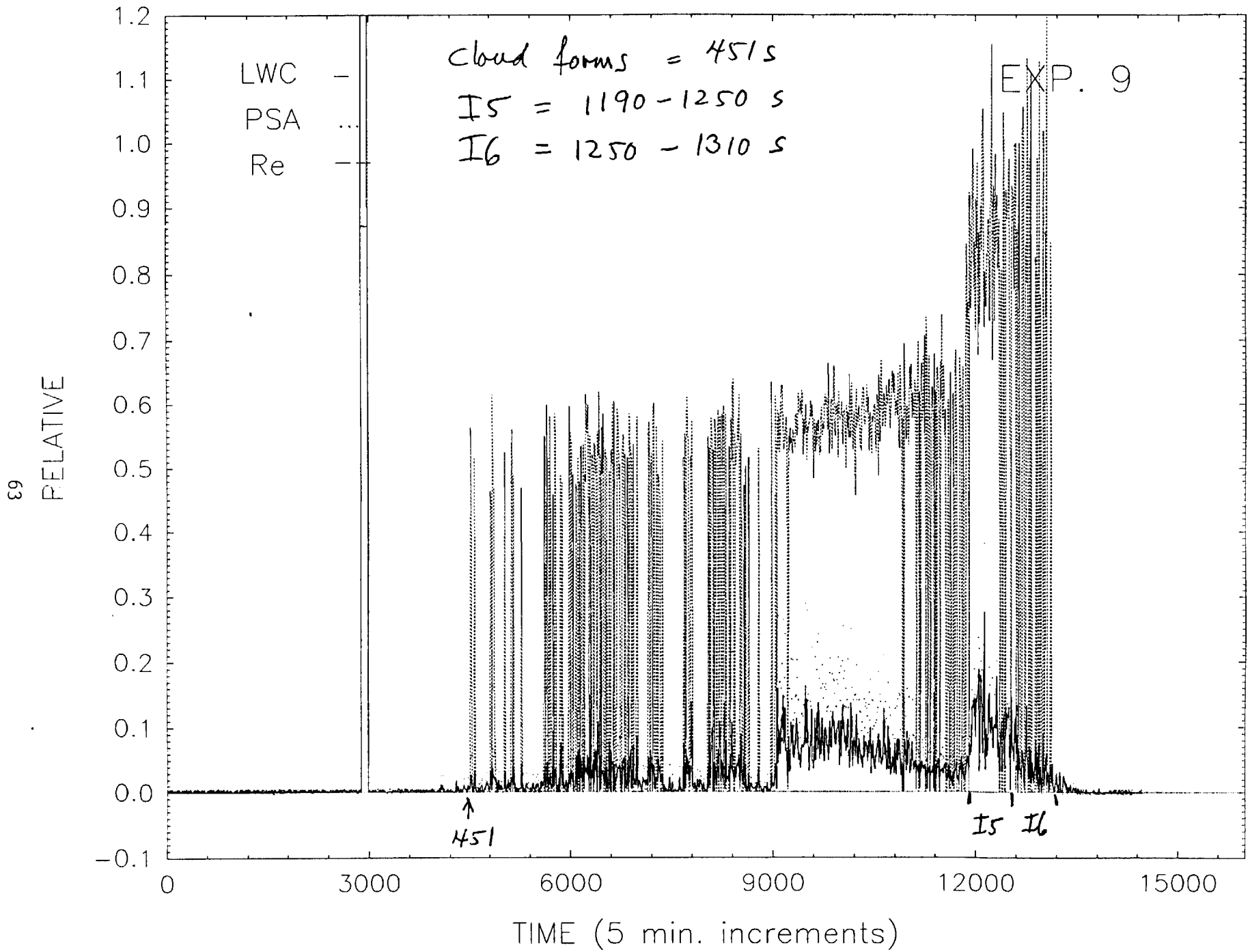
LWC
PSA
Re
Cloud forms = 451 s
I5 = 1190 - 1250 s
I6 = 1250 - 1310 s
EXP. 9
RELATIVE
1.2
1.1
1.0
0.9
0.8
0.7
0.6
0.5
0.4
0.3
0.2
0.1
0.0
-0.1
0
3000
6000
9000
12000
15000
451
I5
I6
TIME (5 min. increments)

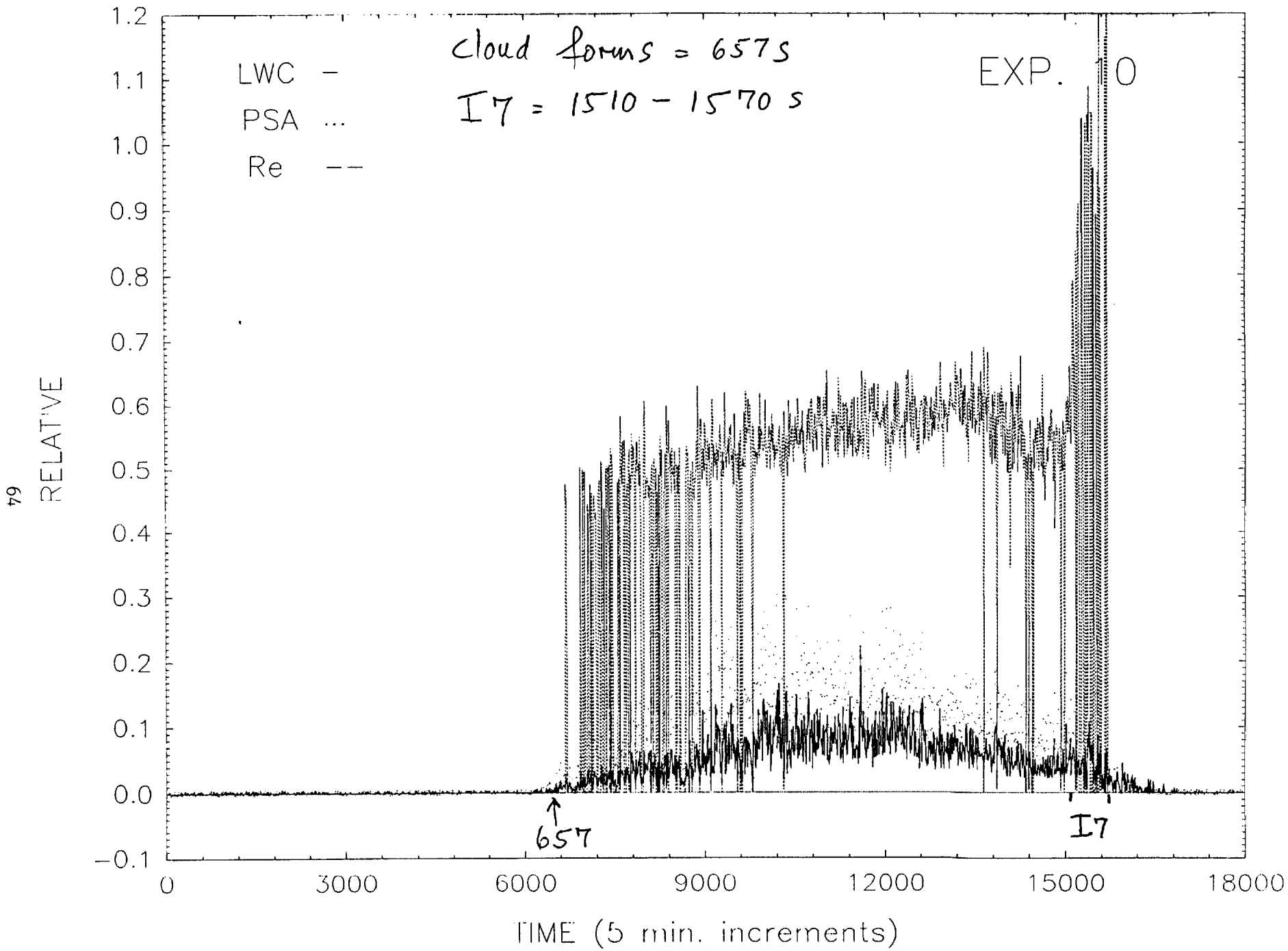
cloud forms = 657s
I7 = 1510 - 1570 s
EXP. 10
LWC –
PSA ...
Re --
RELATIVE
1.2
1.1
1.0
0.9
0.8
0.7
0.6
0.5
0.4
0.3
0.2
0.1
0.0
−0.1
657
I7
0
3000
6000
9000
12000
15000
18000
TIME (5 min. increments)

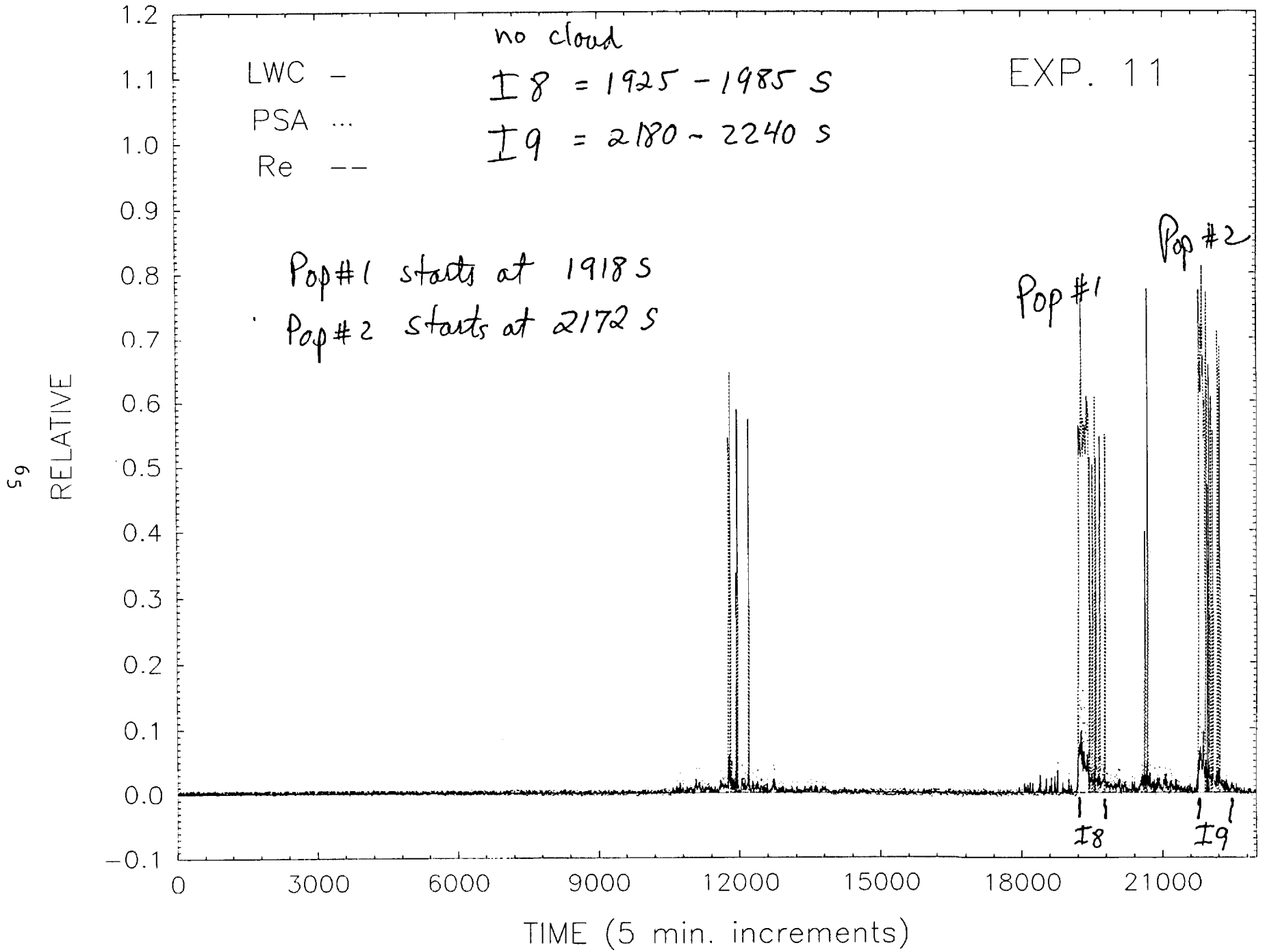
no cloud
LWC –
PSA ...
Re --
I8 = 1925 - 1985 s
I9 = 2180 - 2240 s
EXP. 11
Pop#1 starts at 1918 s
Pop#2 starts at 2172 s
Pop #1
Pop #2
I8
I9
RELATIVE
$S_9$
TIME (5 min. increments)
1.2
1.1
1.0
0.9
0.8
0.7
0.6
0.5
0.4
0.3
0.2
0.1
0.0
−0.1
0
3000
6000
9000
12000
15000
18000
21000

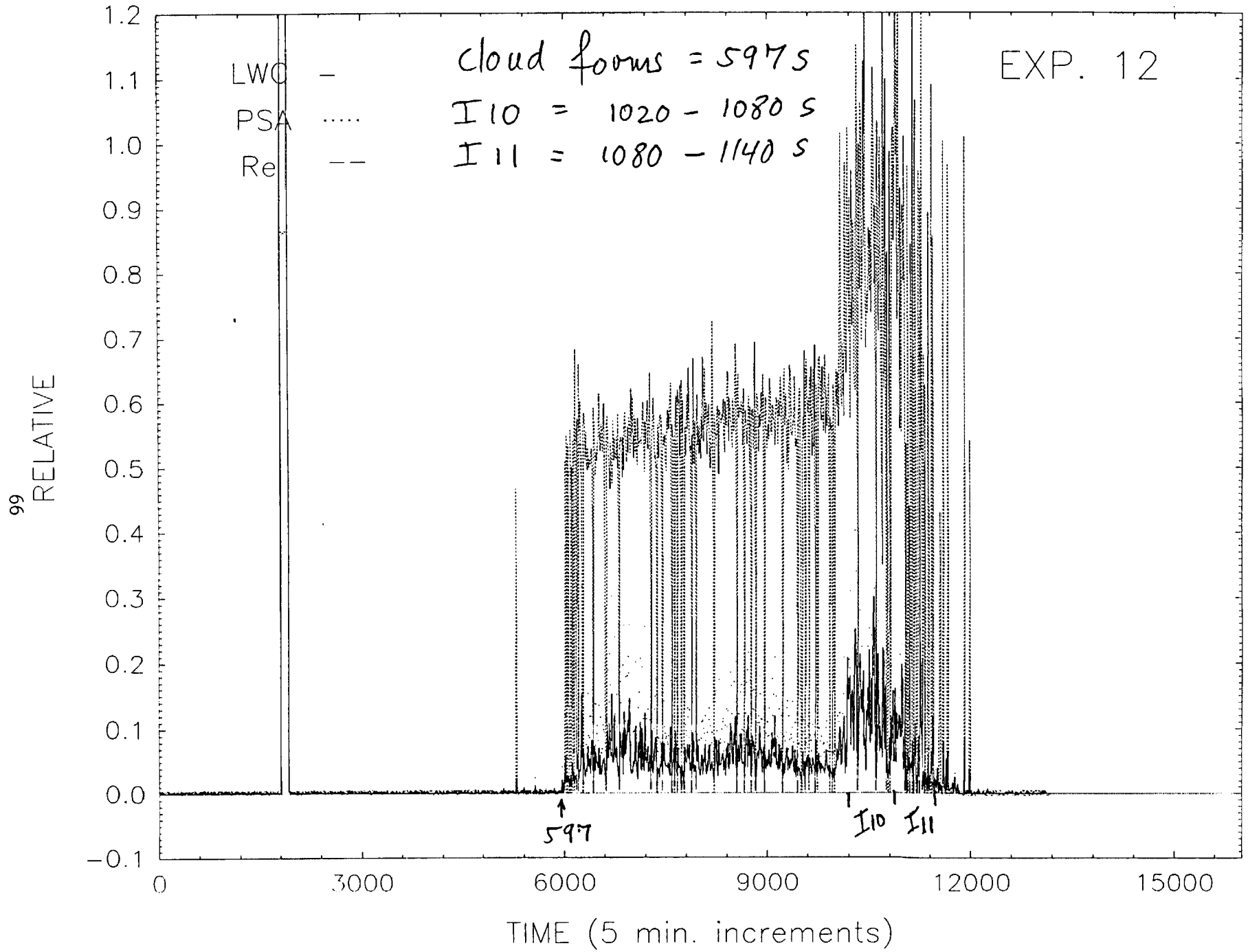
LWC –
PSA .....
Re --
cloud forms = 597 s
I10 = 1020 – 1080 s
I11 = 1080 – 1140 s
EXP. 12
99 RELATIVE
1.2
1.1
1.0
0.9
0.8
0.7
0.6
0.5
0.4
0.3
0.2
0.1
0.0
−0.1
0
3000
6000
9000
12000
15000
TIME (5 min. increments)
597
I10
I11

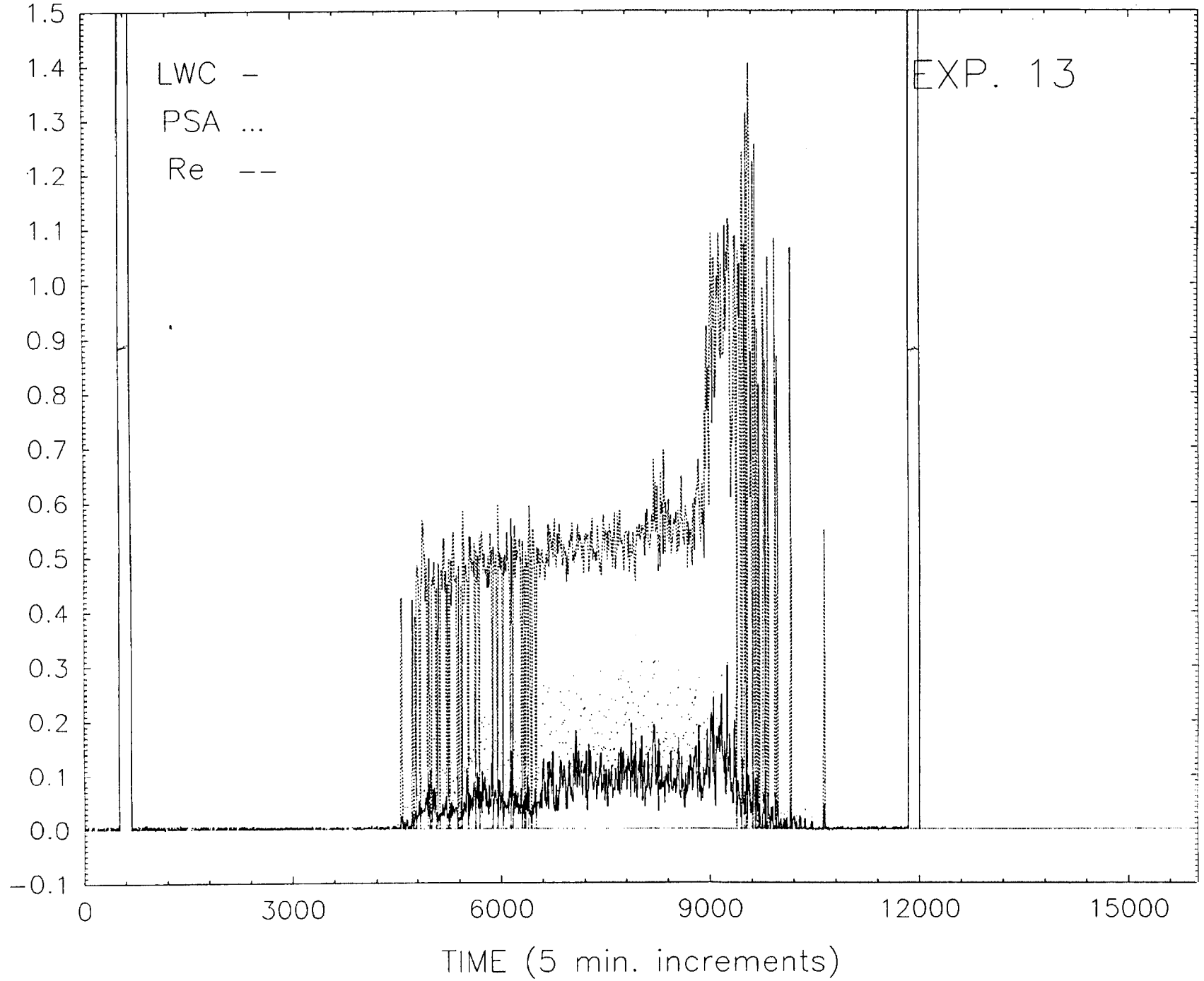
LWC –
PSA ...
Re --
EXP. 13
RELATIVE
1.5
1.4
1.3
1.2
1.1
1.0
0.9
0.8
0.7
0.6
0.5
0.4
0.3
0.2
0.1
0.0
−0.1
0
3000
6000
9000
12000
15000
TIME (5 min. increments)

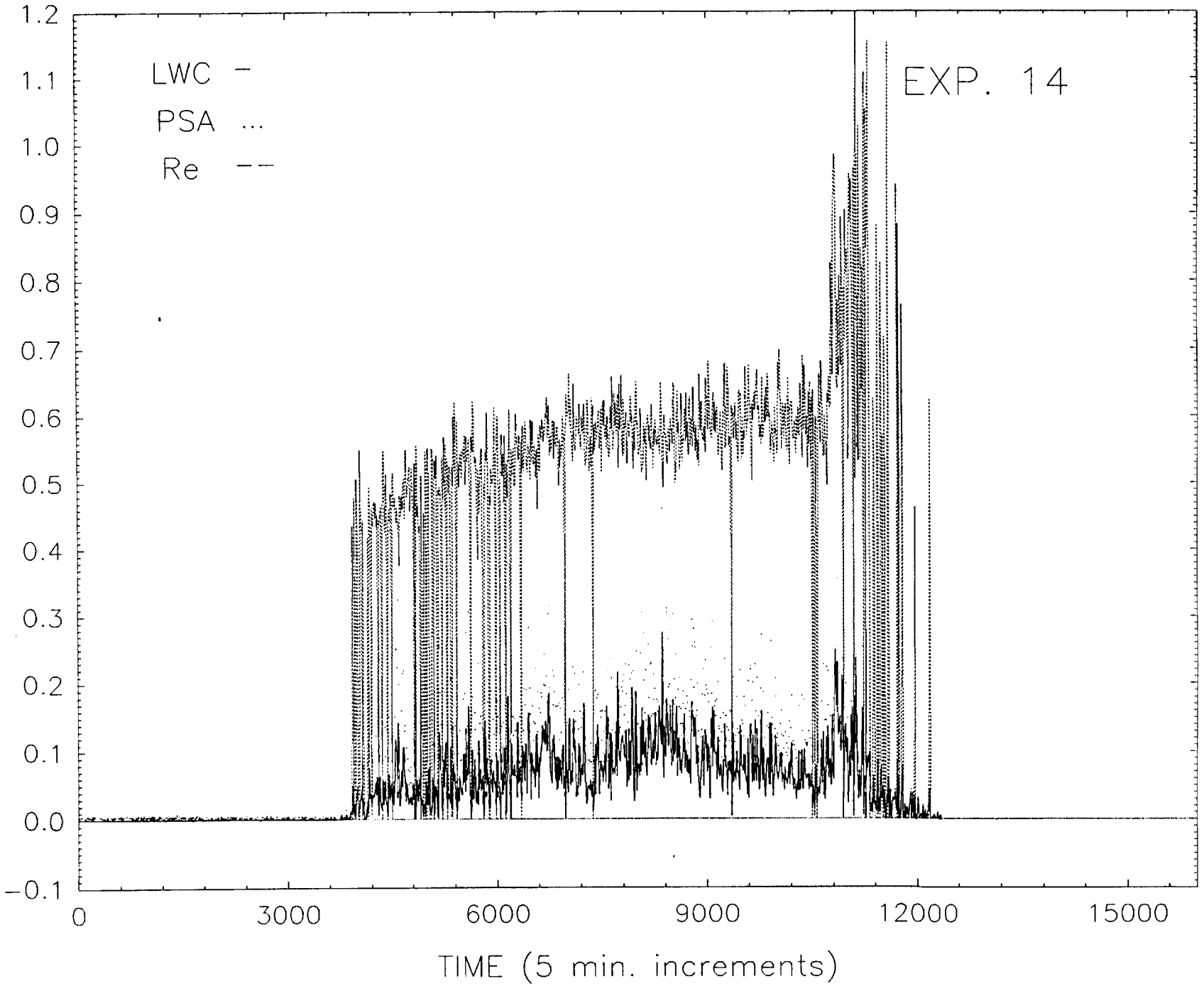
LWC –
PSA ...
Re --
EXP. 14
RELATIVE
TIME (5 min. increments)
1.2
1.1
1.0
0.9
0.8
0.7
0.6
0.5
0.4
0.3
0.2
0.1
0.0
−0.1
0
3000
6000
9000
12000
15000

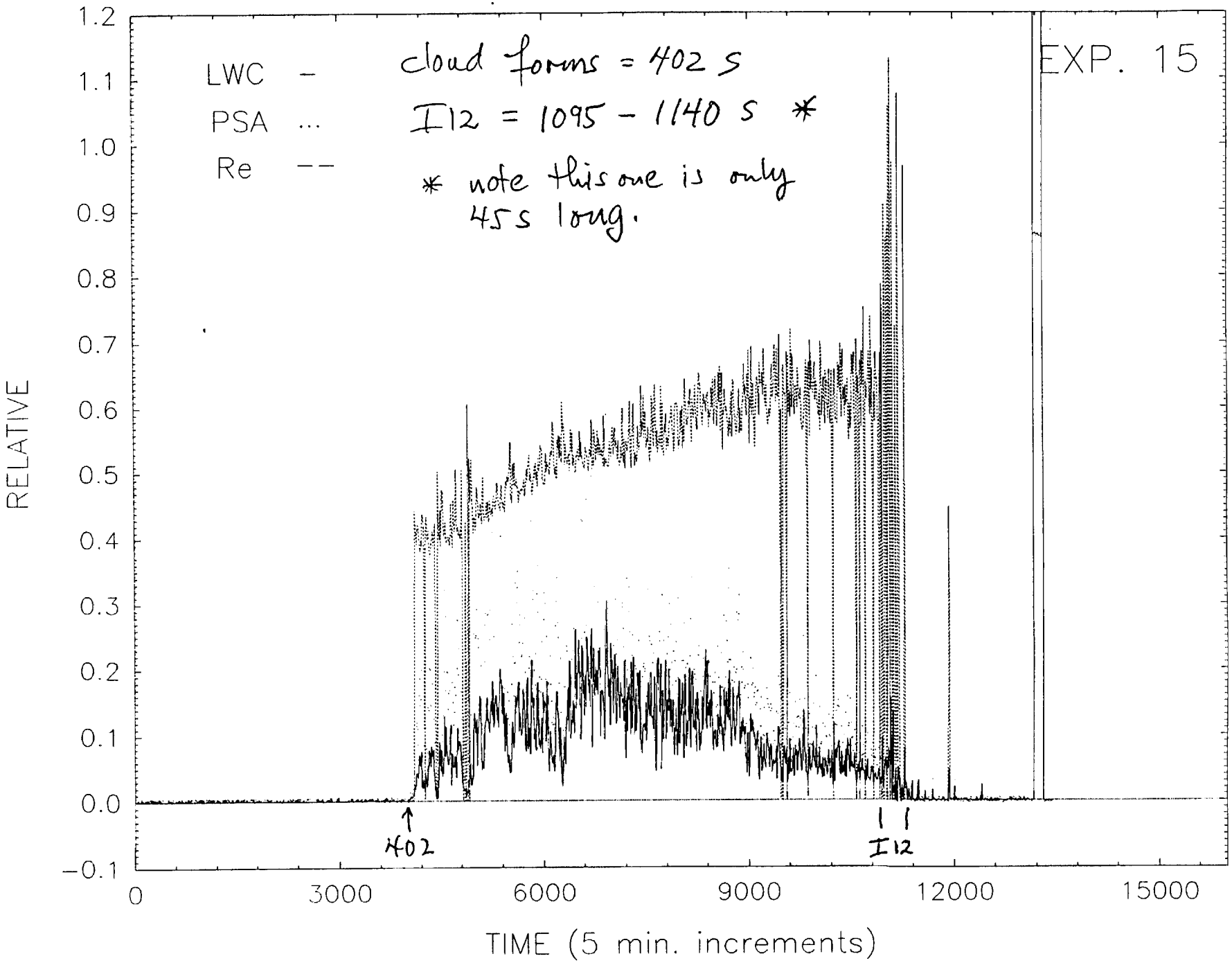
EXP. 15
LWC –
PSA ...
Re --
cloud forms = 402 s
I12 = 1095 – 1140 s *
* note this one is only 45 s long.
RELATIVE
TIME (5 min. increments)
1.2
1.1
1.0
0.9
0.8
0.7
0.6
0.5
0.4
0.3
0.2
0.1
0.0
−0.1
0
3000
6000
9000
12000
15000
402
I12

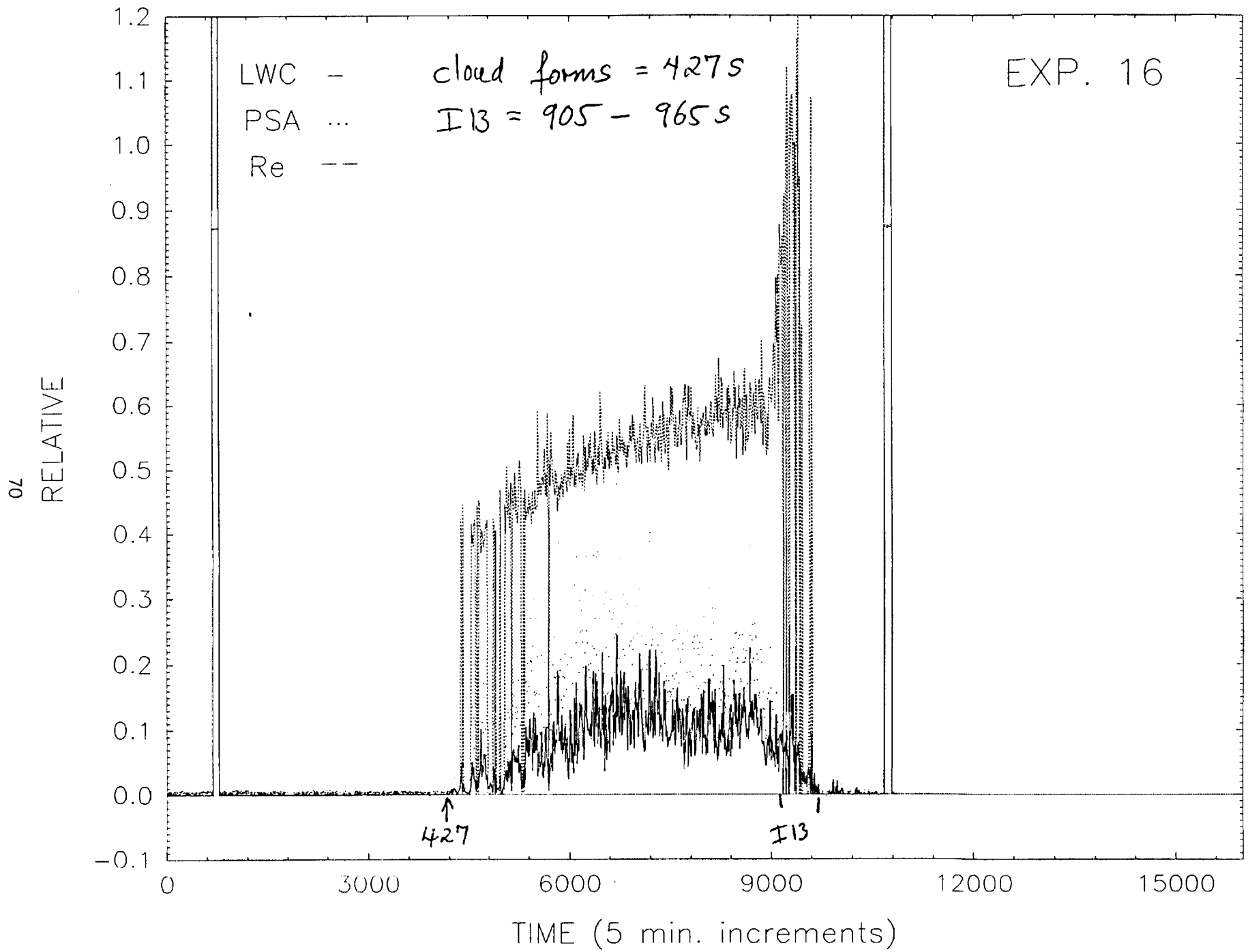
LWC –
PSA ...
Re --
cloud forms = 427 s
I13 = 905 – 965 s
EXP. 16
RELATIVE
TIME (5 min. increments)
427
I13
1.2
1.1
1.0
0.9
0.8
0.7
0.6
0.5
0.4
0.3
0.2
0.1
0.0
−0.1
0
3000
6000
9000
12000
15000

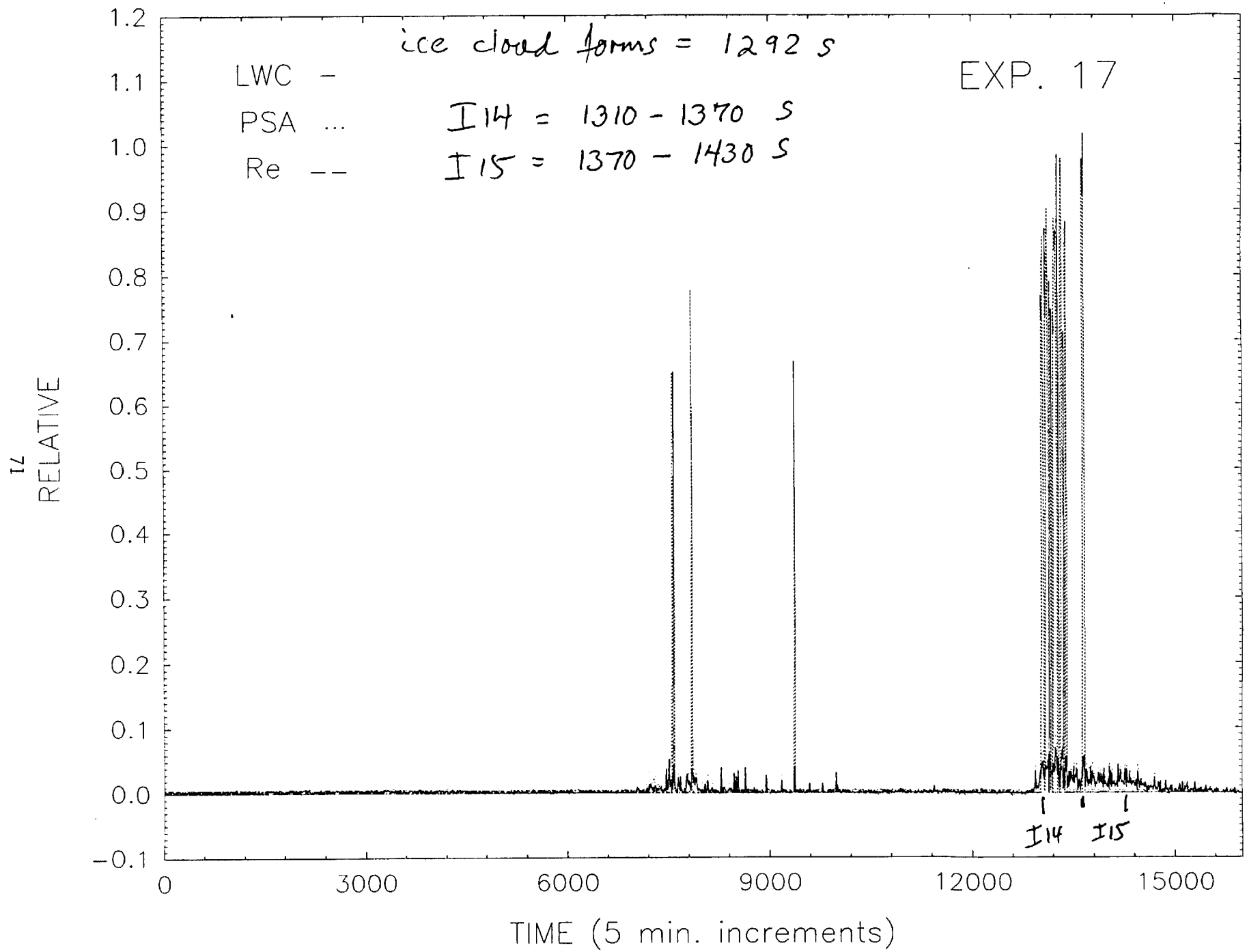
ice cloud forms = 1292 s
LWC –
PSA ...
Re --
I14 = 1310 - 1370 s
I15 = 1370 - 1430 s
EXP. 17
RELATIVE
TIME (5 min. increments)
I14
I15
1.2
1.1
1.0
0.9
0.8
0.7
0.6
0.5
0.4
0.3
0.2
0.1
0.0
-0.1
0
3000
6000
9000
12000
15000

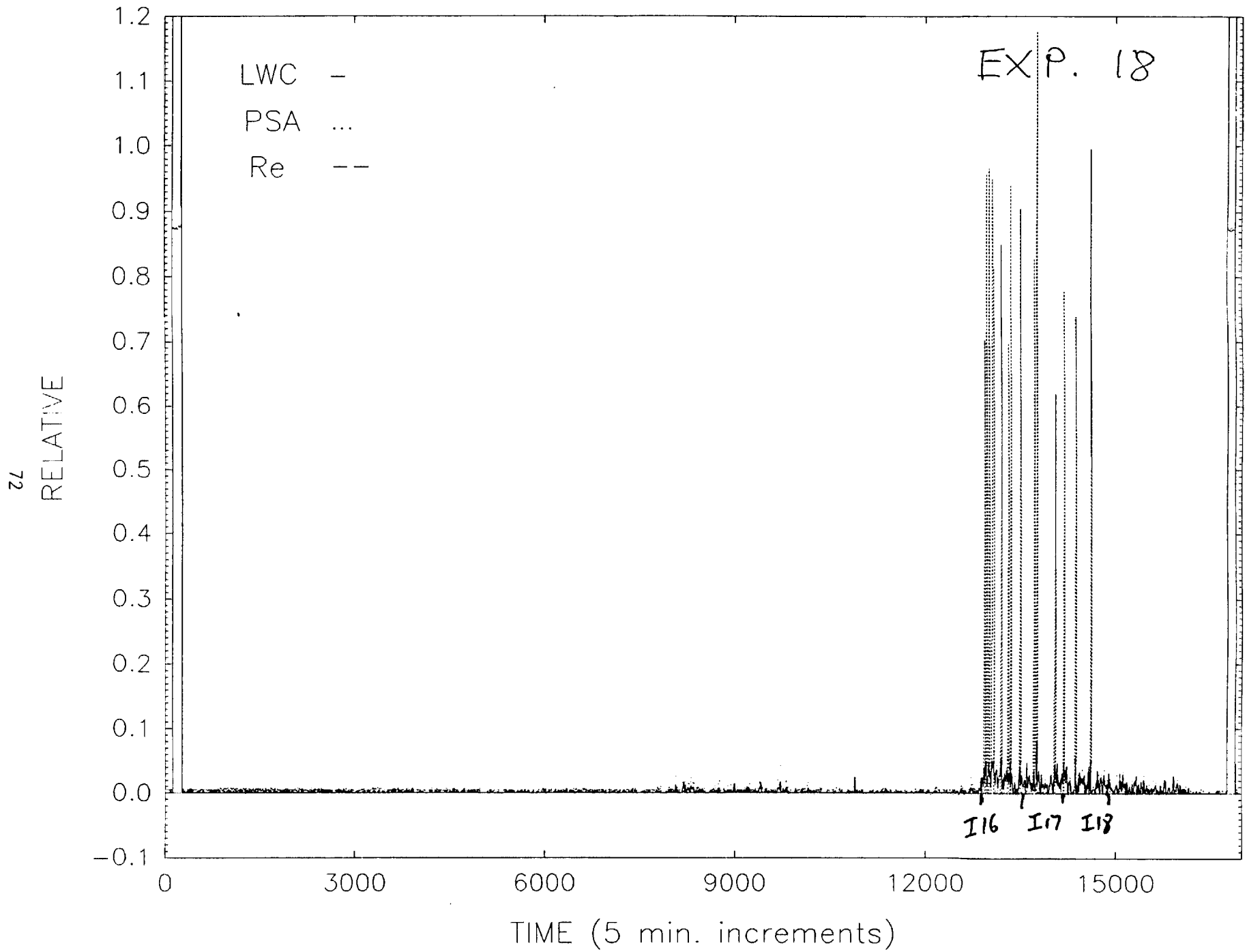
EXP. 18
LWC –
PSA ...
Re --
RELATIVE
1.2
1.1
1.0
0.9
0.8
0.7
0.6
0.5
0.4
0.3
0.2
0.1
0.0
−0.1
I16
I17
I18
0
3000
6000
9000
12000
15000
TIME (5 min. increments)

# APPENDIX D

## Analyzed Data

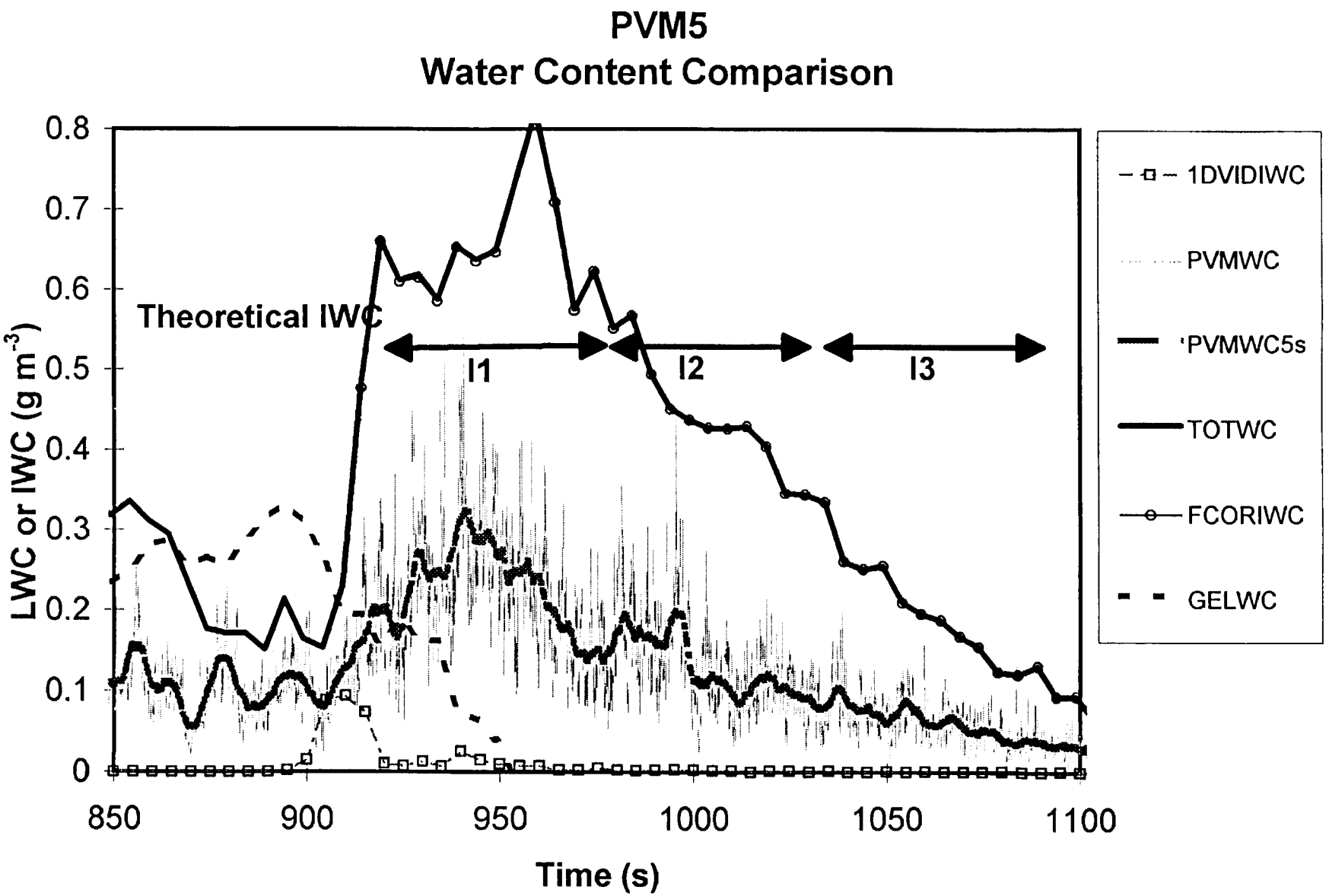
PVM5
Water Content Comparison
LWC or IWC (g m-3)
Time (s)
Theoretical IWC
I1
I2
I3
1DVIDIWC
PVMWC
PVMWC5s
TOTWC
FCORIWC
GELWC
0
0.1
0.2
0.3
0.4
0.5
0.6
0.7
0.8
850
900
950
1000
1050
1100

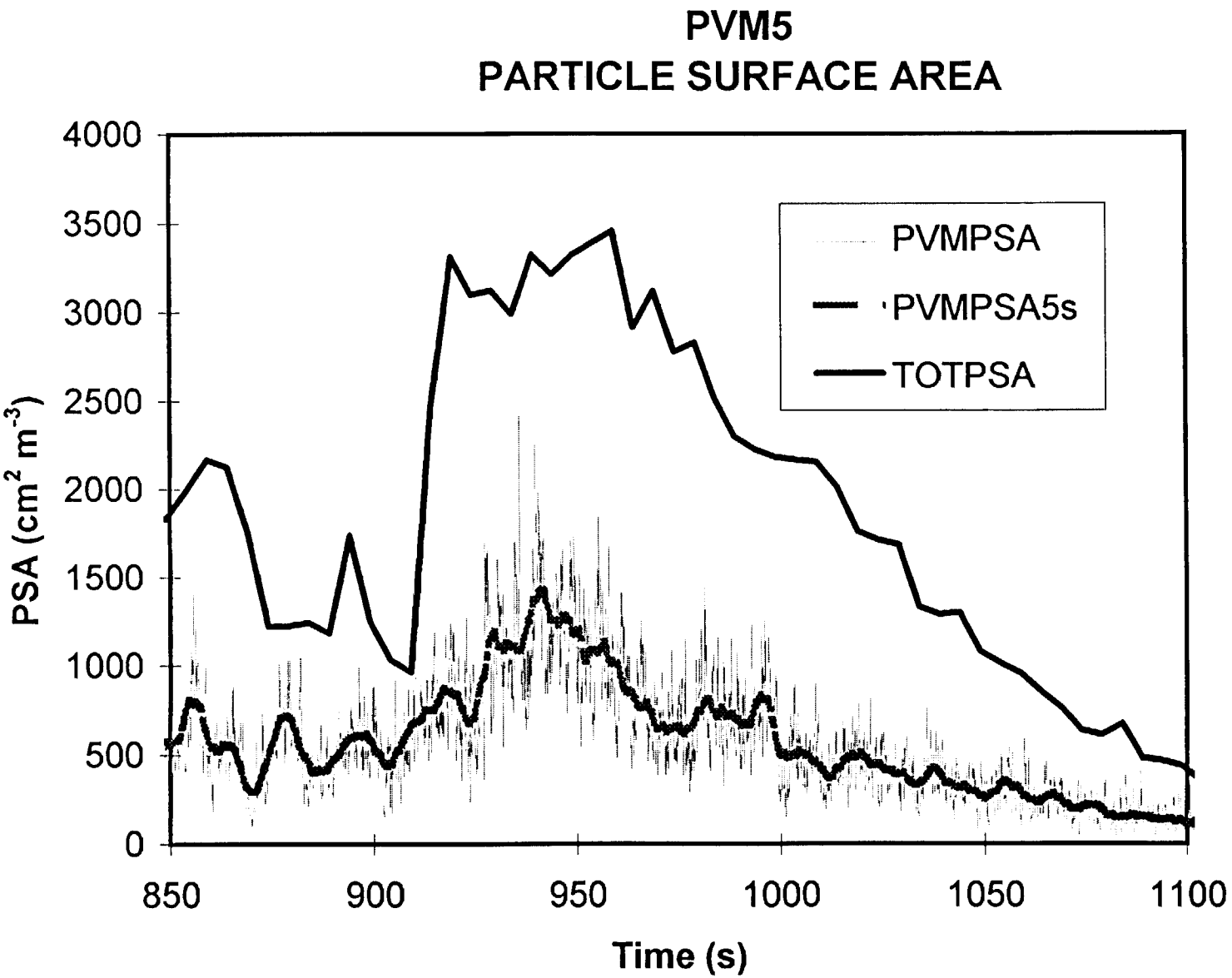
PVM5
PARTICLE SURFACE AREA
PSA (cm2 m-3)
4000
3500
3000
2500
2000
1500
1000
500
0
850
900
950
1000
1050
1100
Time (s)
PVMPSA
PVMPSA5s
TOTPSA

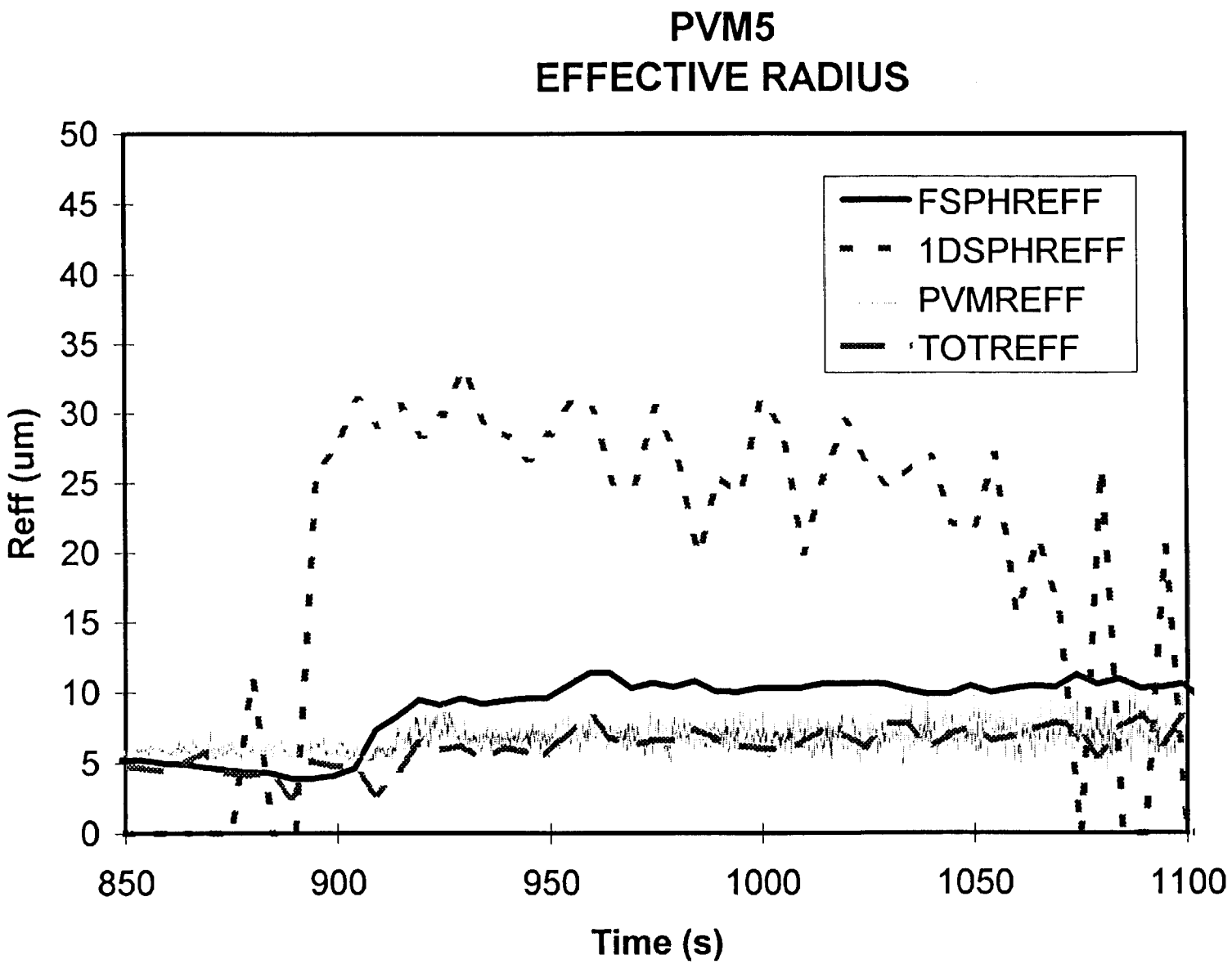
PVM5
EFFECTIVE RADIUS
FSPHREFF
1DSPHREFF
PVMREFF
TOTREFF
Reff (um)
Time (s)
0
5
10
15
20
25
30
35
40
45
50
850
900
950
1000
1050
1100

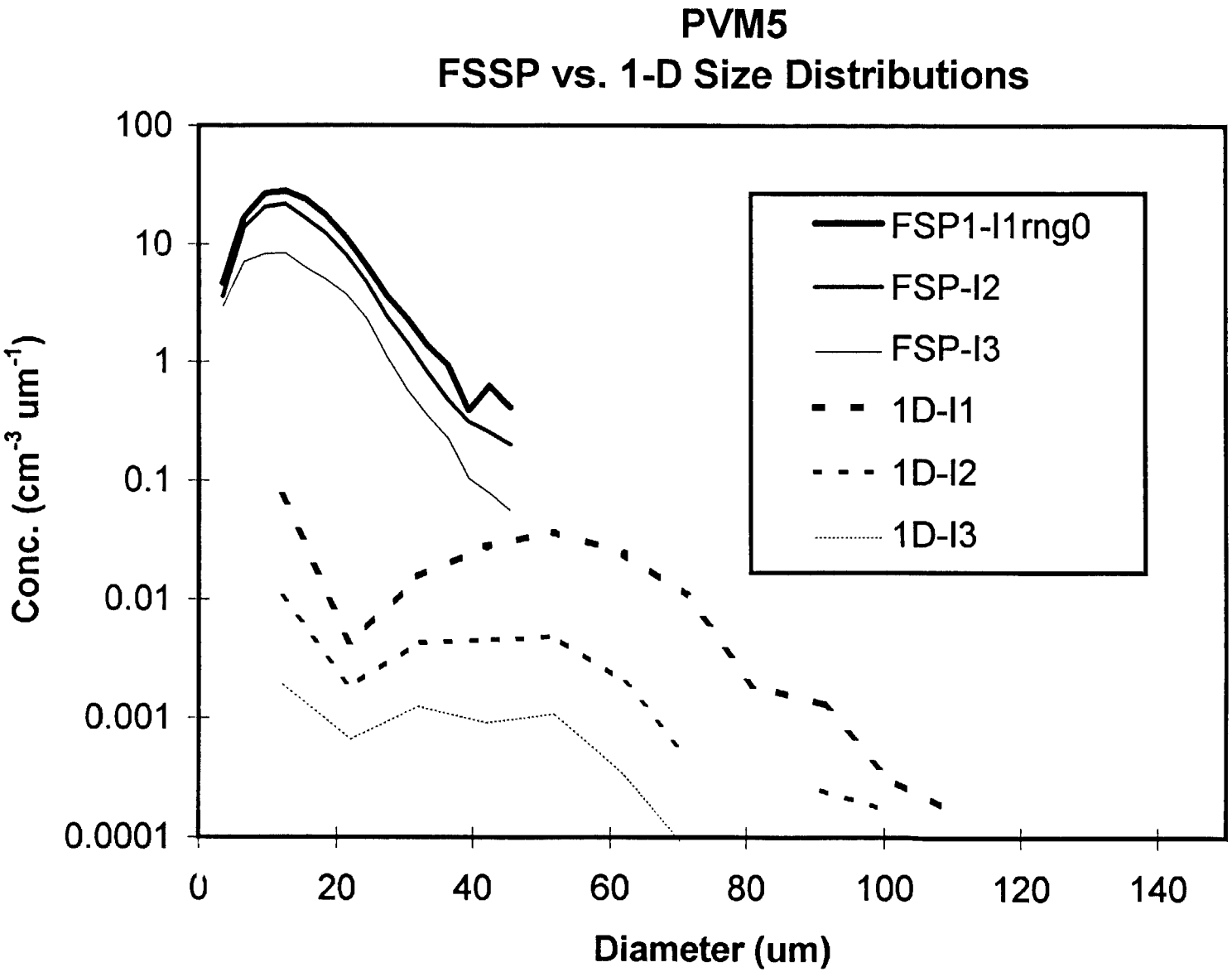
PVM5
FSSP vs. 1-D Size Distributions
Conc. (cm-3 um-1)
100
10
1
0.1
0.01
0.001
0.0001
0
20
40
60
80
100
120
140
Diameter (um)
FSP1-I1rng0
FSP-I2
FSP-I3
1D-I1
1D-I2
1D-I3

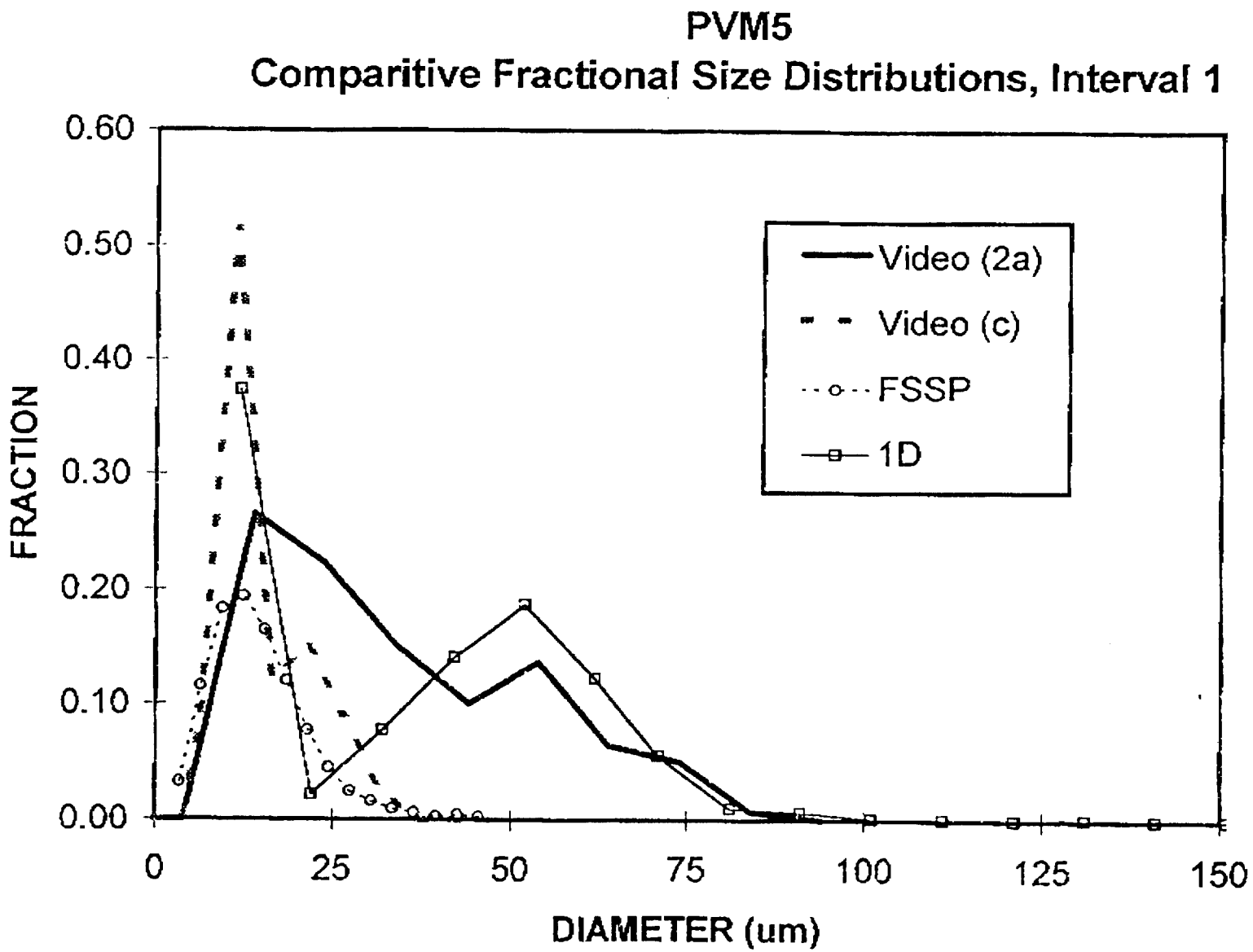
PVM5
Comparitive Fractional Size Distributions, Interval 1
FRACTION
0.60
0.50
0.40
0.30
0.20
0.10
0.00
0
25
50
75
100
125
150
DIAMETER (um)
Video (2a)
Video (c)
FSSP
1D

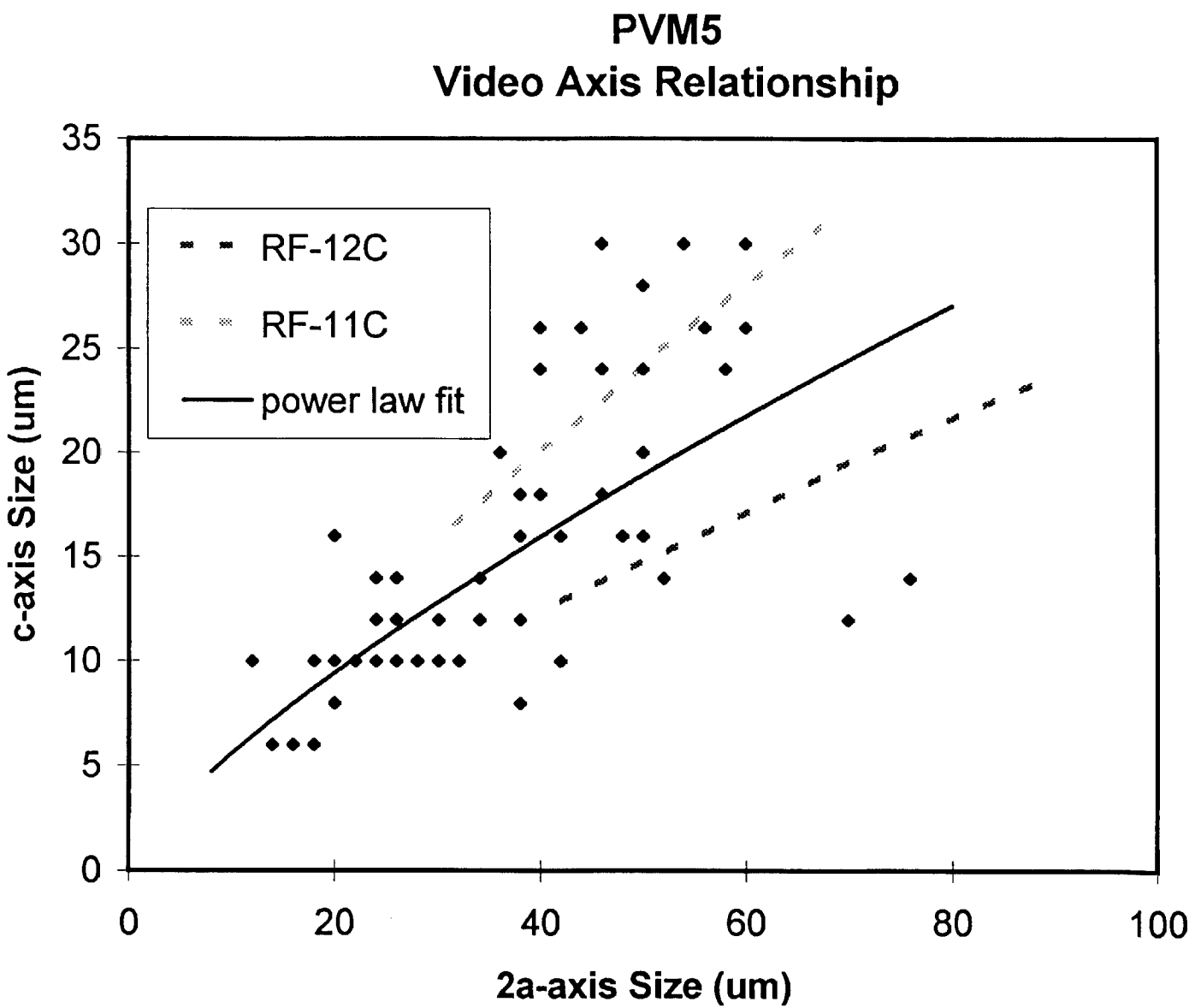
PVM5
Video Axis Relationship
RF-12C
RF-11C
power law fit
c-axis Size (um)
2a-axis Size (um)
0
5
10
15
20
25
30
35
0
20
40
60
80
100

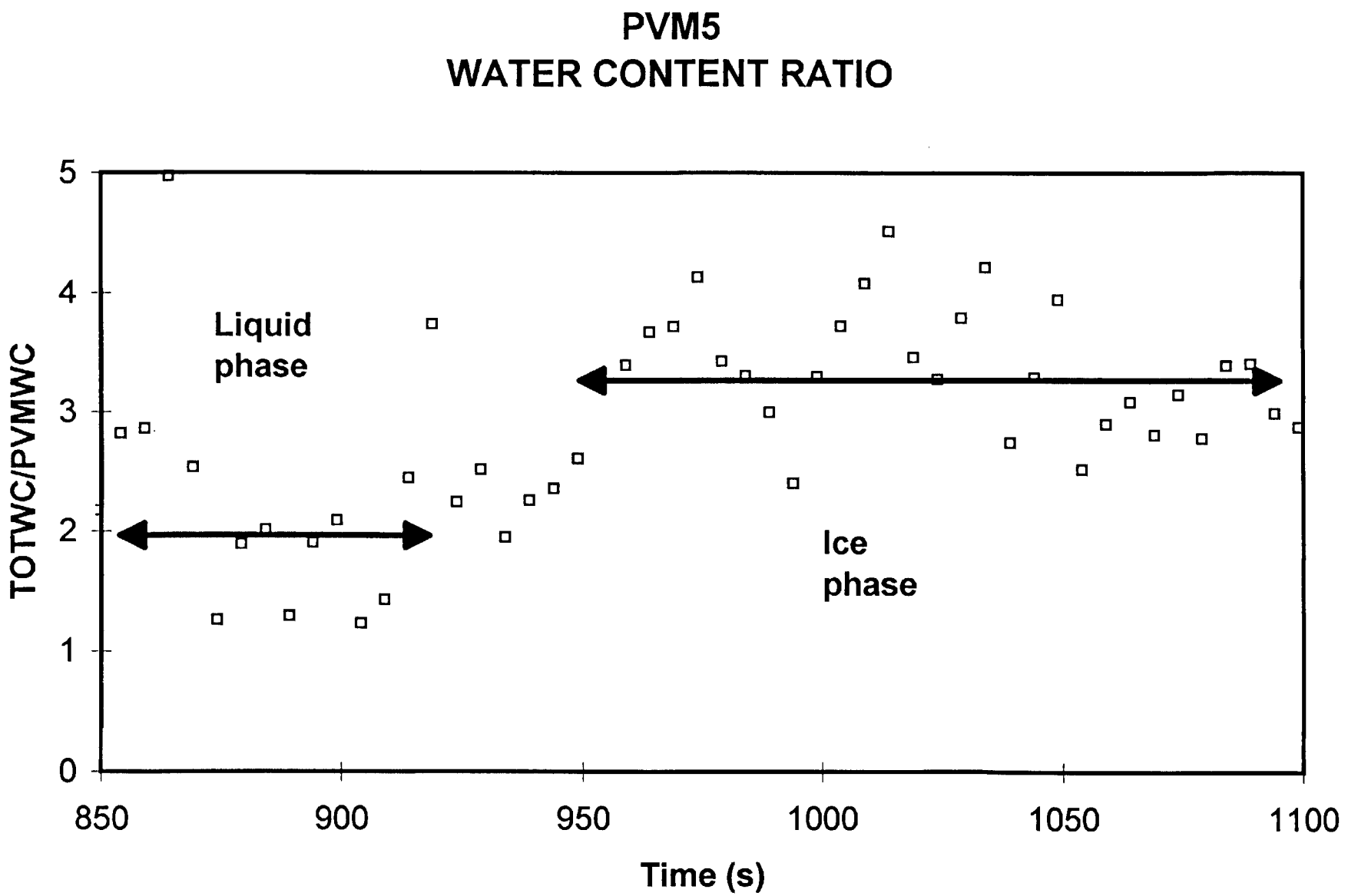
PVM5
WATER CONTENT RATIO
TOTWC/PVMWC
Liquid phase
Ice phase
Time (s)
0
1
2
3
4
5
850
900
950
1000
1050
1100

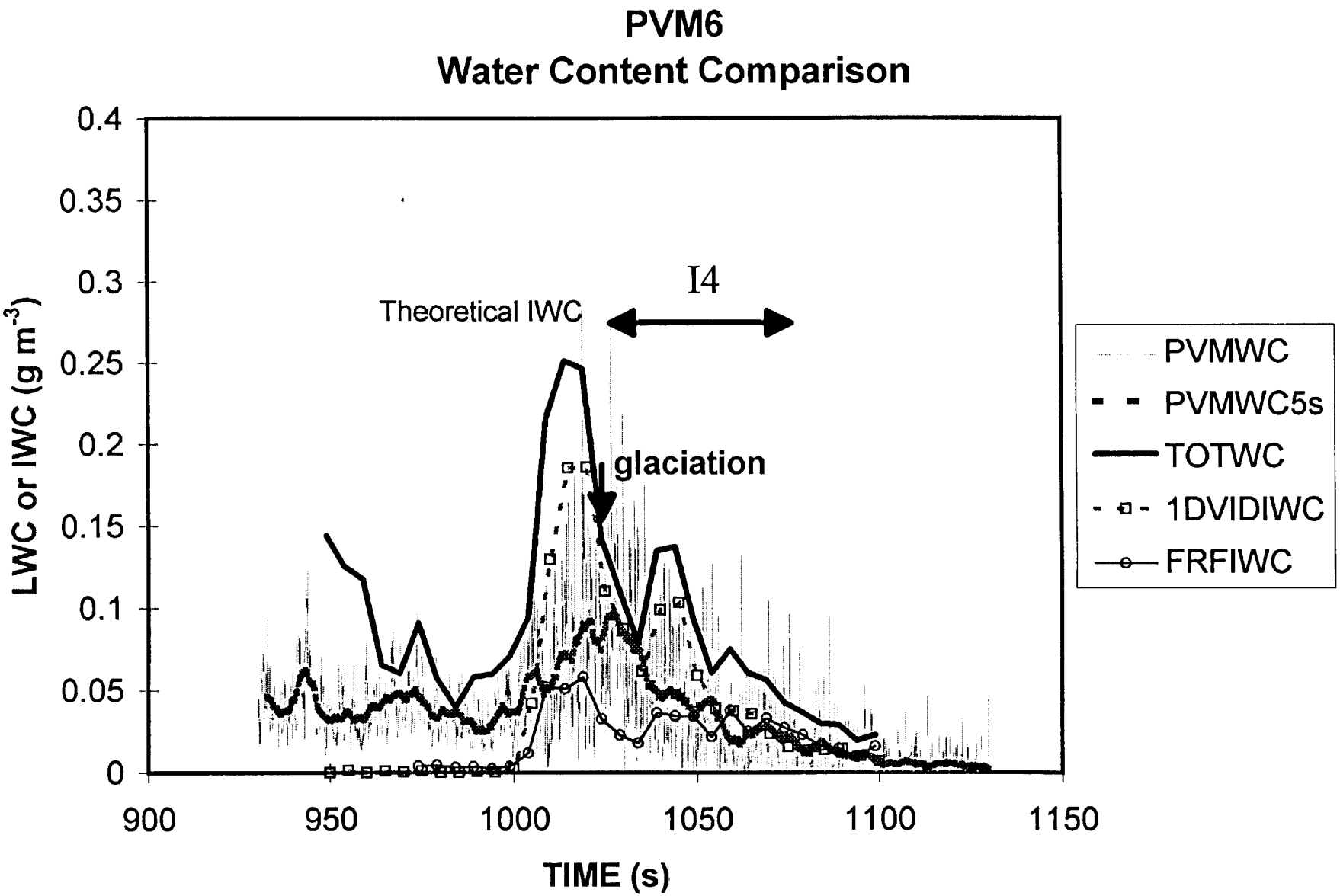
PVM6
Water Content Comparison
LWC or IWC (g m-3)
0.4
0.35
0.3
0.25
0.2
0.15
0.1
0.05
0
900
950
1000
1050
1100
1150
TIME (s)
I4
Theoretical IWC
glaciation
PVMWC
PVMWC5s
TOTWC
1DVIDIWC
FRFIWC

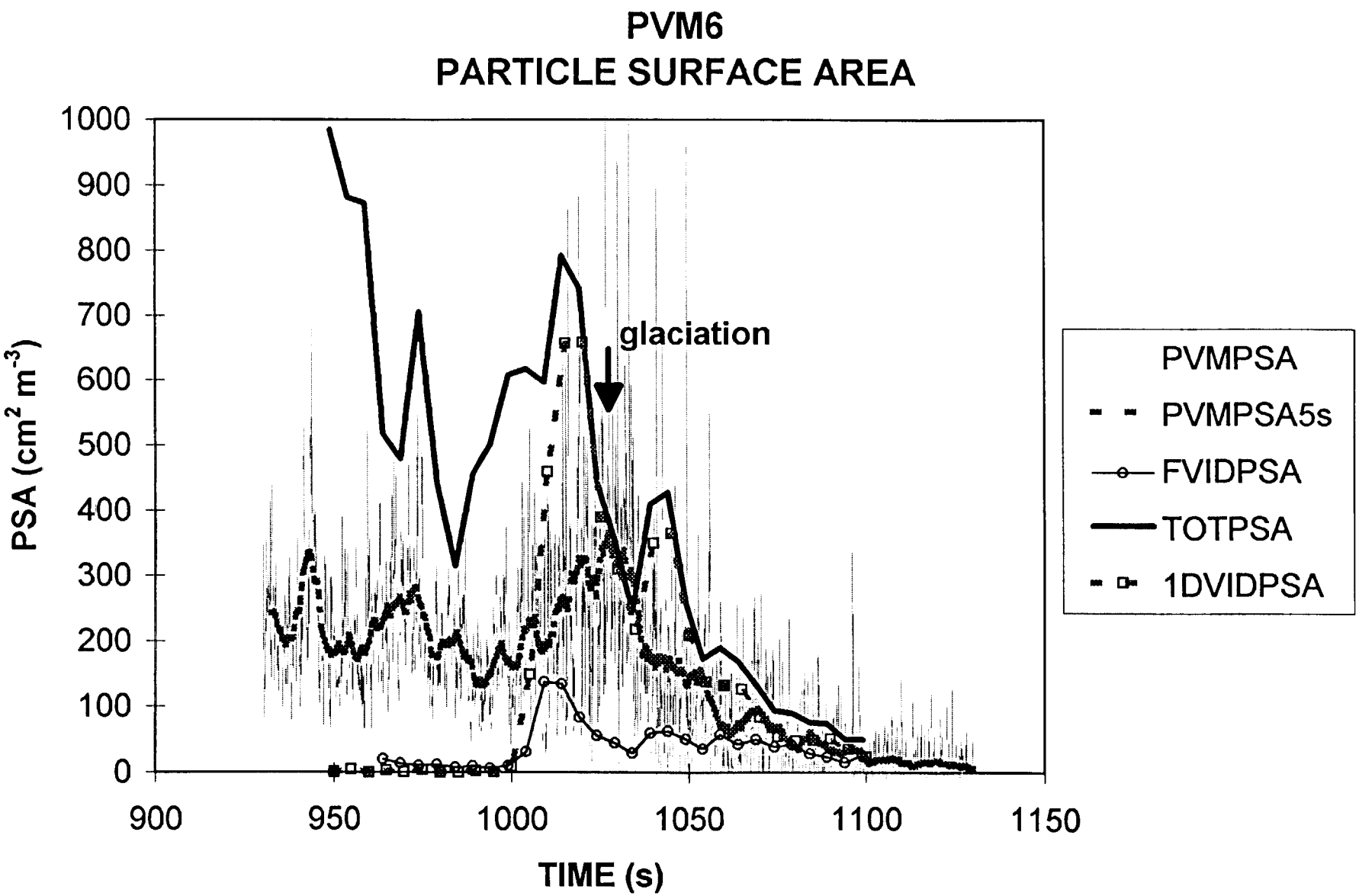
PVM6
PARTICLE SURFACE AREA
PSA (cm$^2$ m$^{-3}$)
TIME (s)
glaciation
PVMPSA
PVMPSA5s
FVIDPSA
TOTPSA
1DVIDPSA
0
100
200
300
400
500
600
700
800
900
1000
900
950
1000
1050
1100
1150

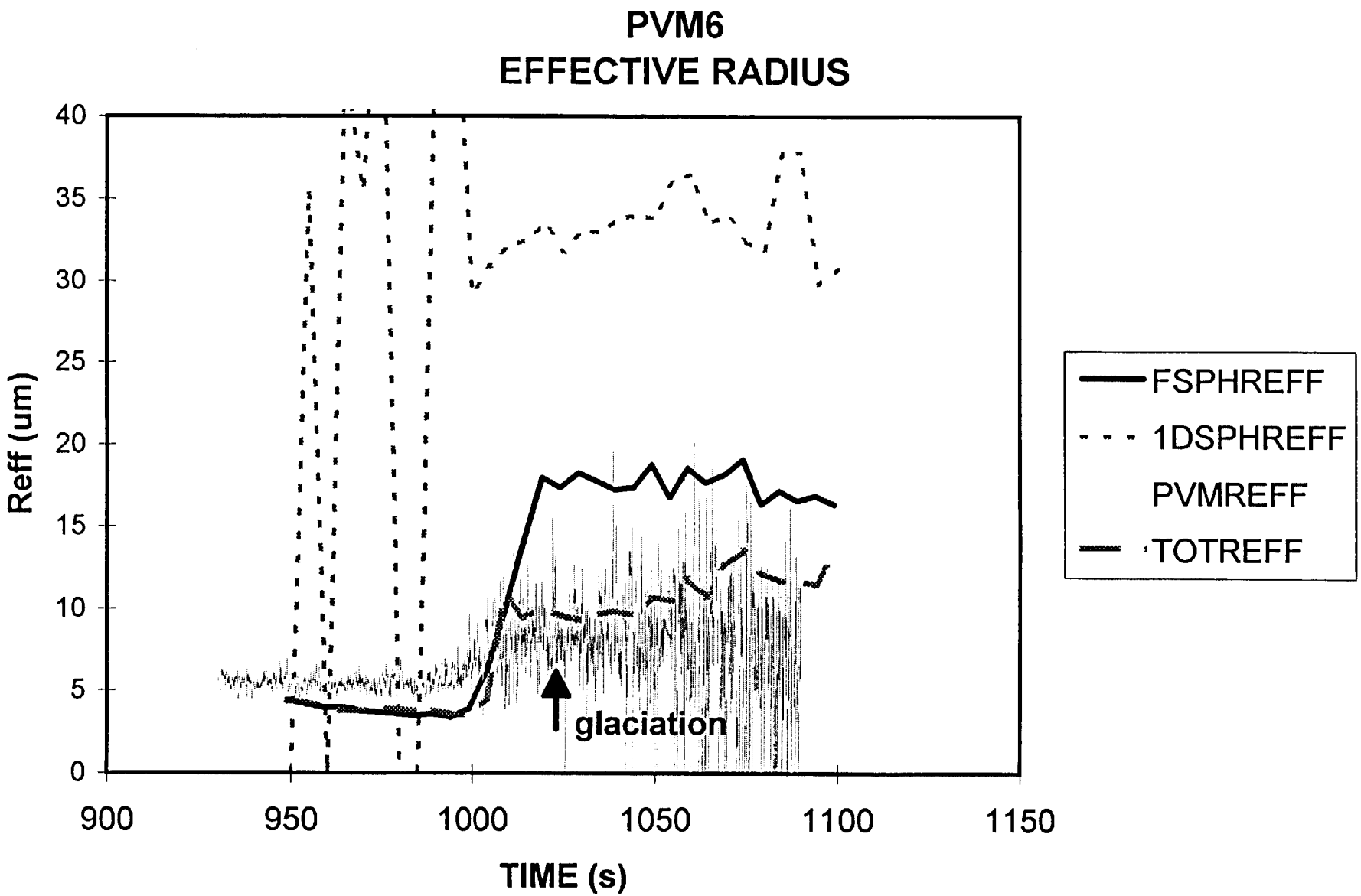
PVM6
EFFECTIVE RADIUS
Reff (um)
40
35
30
25
20
15
10
5
0
900
950
1000
1050
1100
1150
TIME (s)
glaciation
FSPHREFF
1DSPHREFF
PVMREFF
TOTREFF

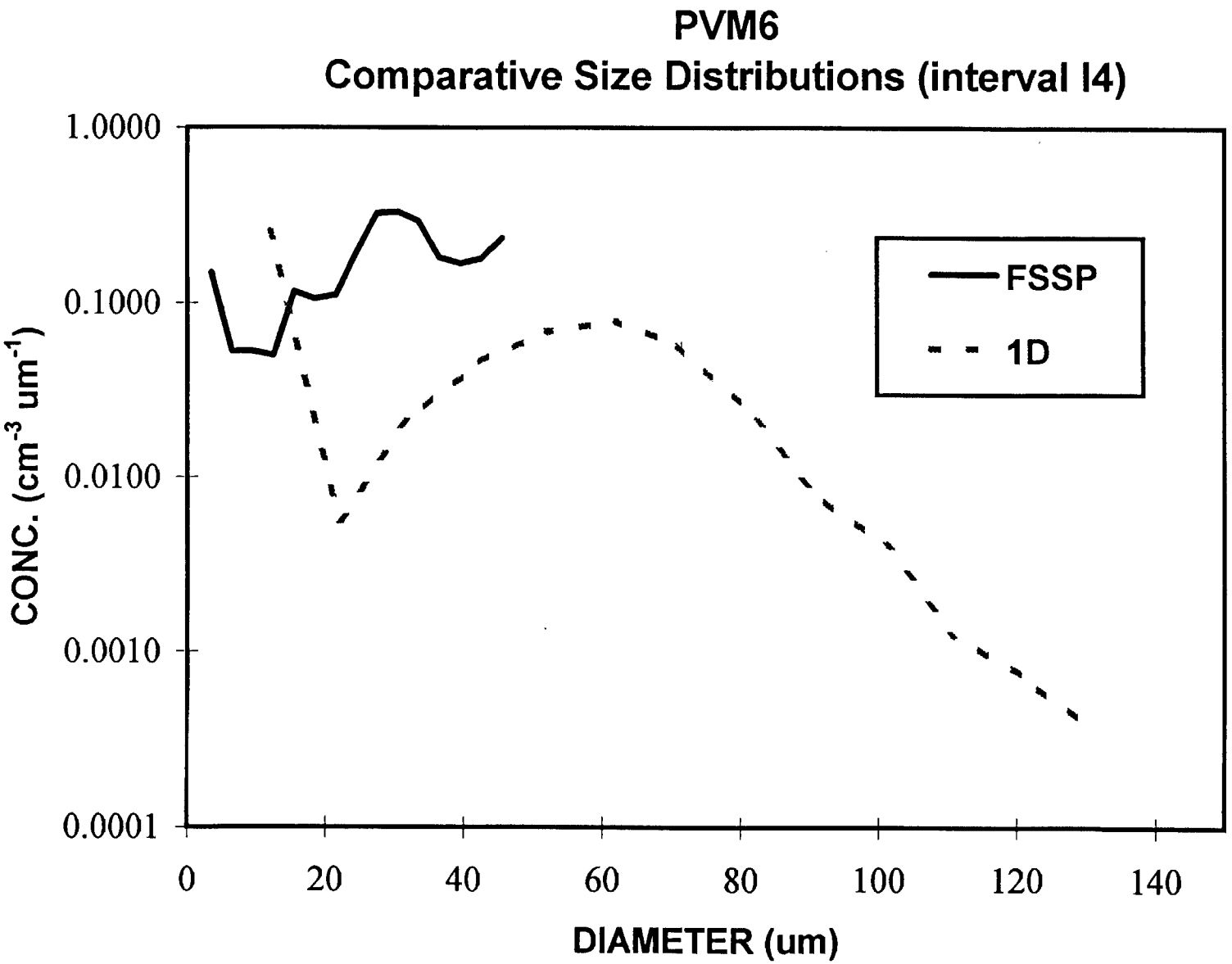
PVM6
Comparative Size Distributions (interval I4)
1.0000
0.1000
0.0100
0.0010
0.0001
CONC. (cm-3 um-1)
FSSP
1D
0
20
40
60
80
100
120
140
DIAMETER (um)

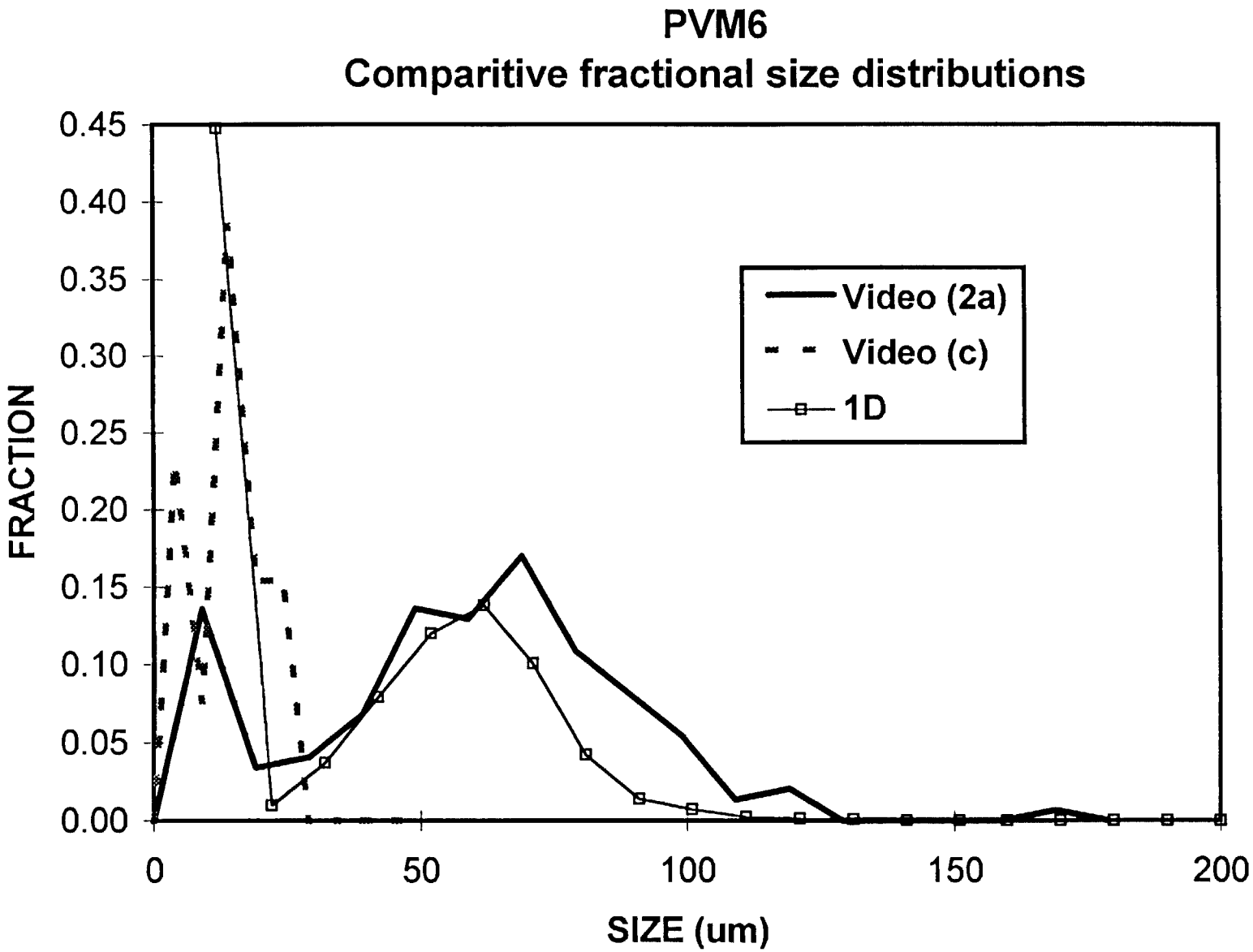
PVM6
Comparitive fractional size distributions
FRACTION
0.45
0.40
0.35
0.30
0.25
0.20
0.15
0.10
0.05
0.00
0
50
100
150
200
SIZE (um)
Video (2a)
Video (c)
1D

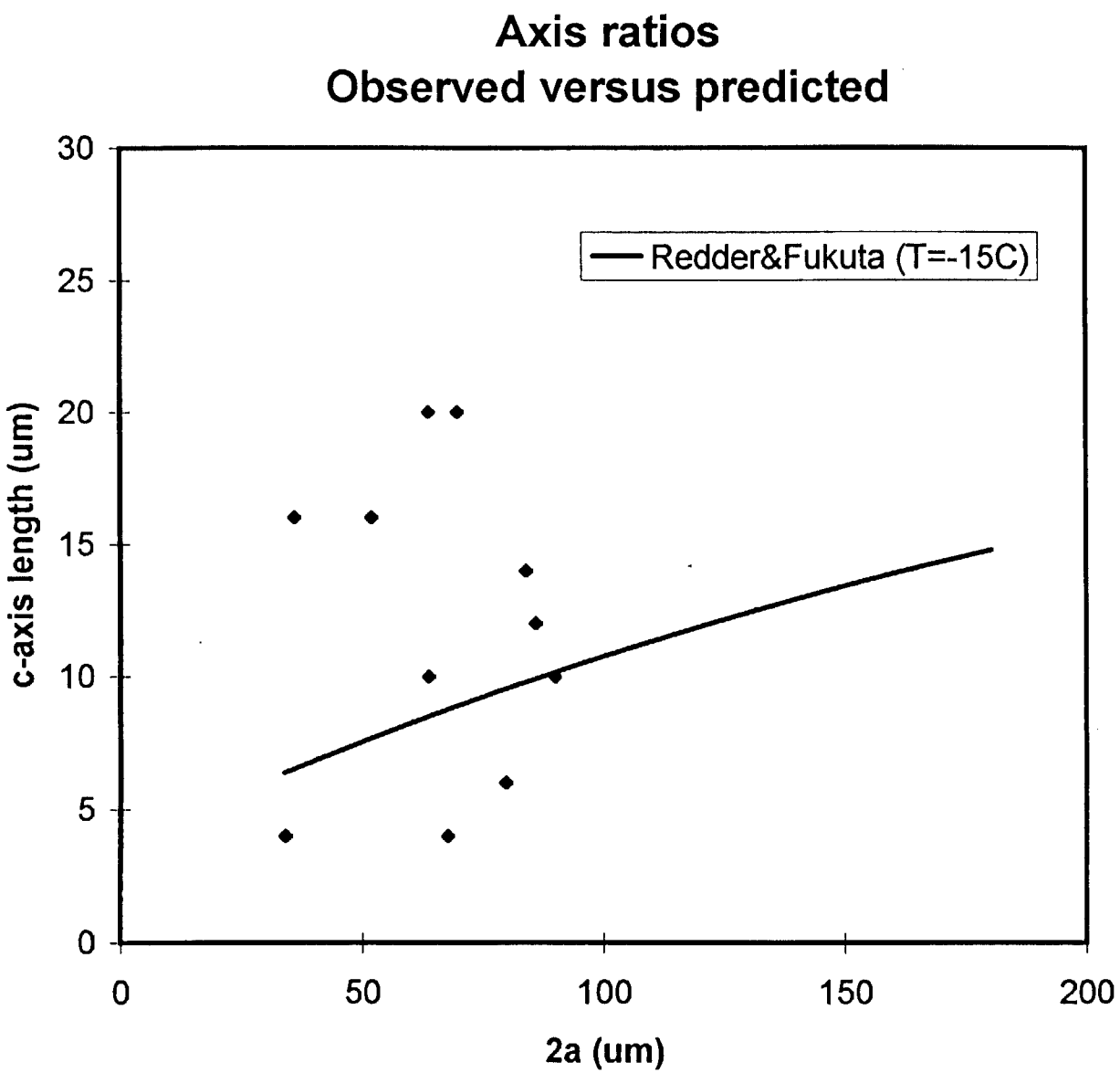
Axis ratios
Observed versus predicted
Redder&Fukuta (T=-15C)
c-axis length (um)
2a (um)
0
5
10
15
20
25
30
0
50
100
150
200

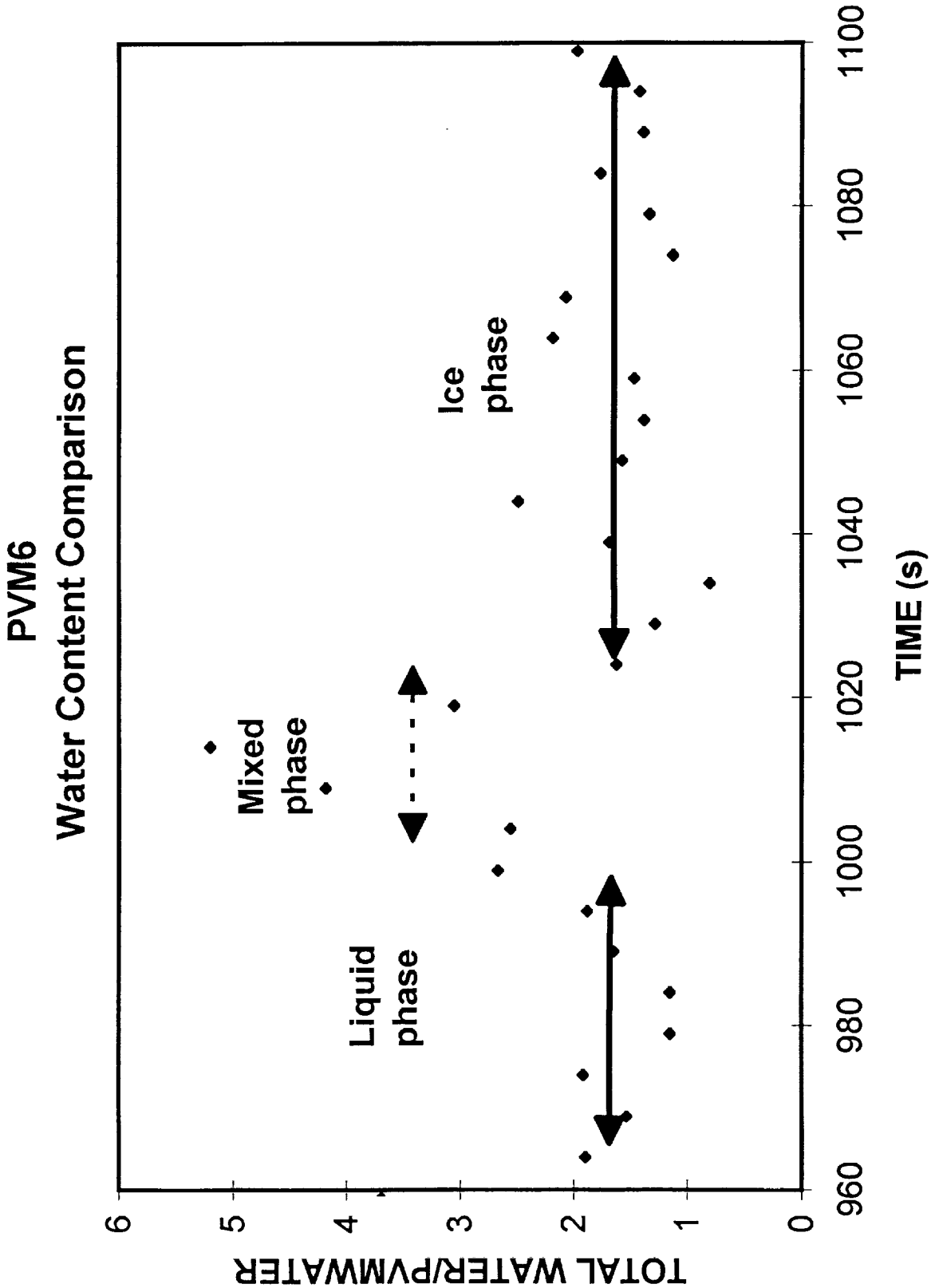
PVM6
Water Content Comparison
Mixed phase
Liquid phase
Ice phase
TOTAL WATER/PVMWATER
TIME (s)
0
1
2
3
4
5
6
960
980
1000
1020
1040
1060
1080
1100

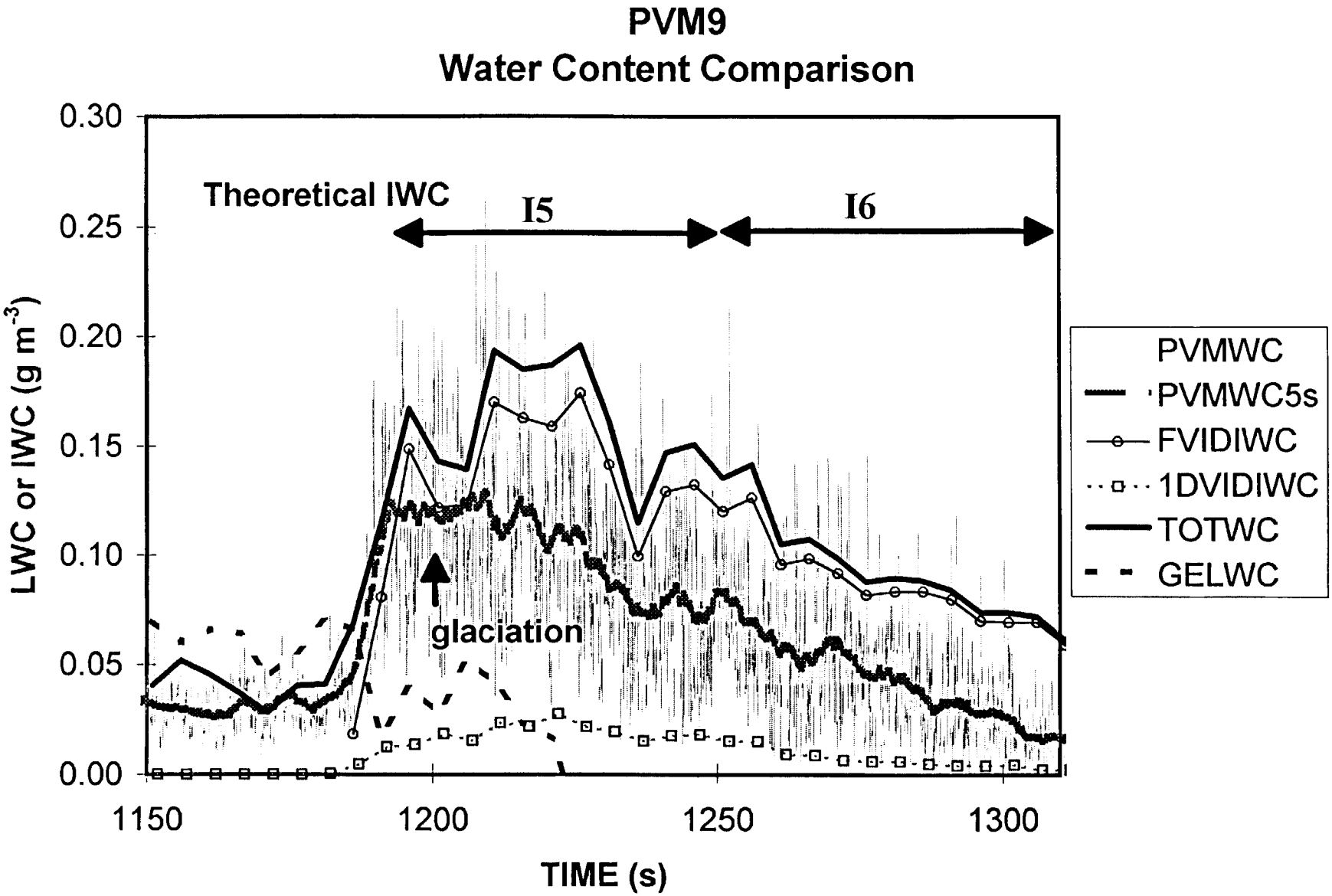
PVM9
Water Content Comparison
Theoretical IWC
I5
I6
glaciation
LWC or IWC (g m-3)
TIME (s)
0.30
0.25
0.20
0.15
0.10
0.05
0.00
1150
1200
1250
1300
PVMWC
PVMWC5s
FVIDIWC
1DVIDIWC
TOTWC
GELWC

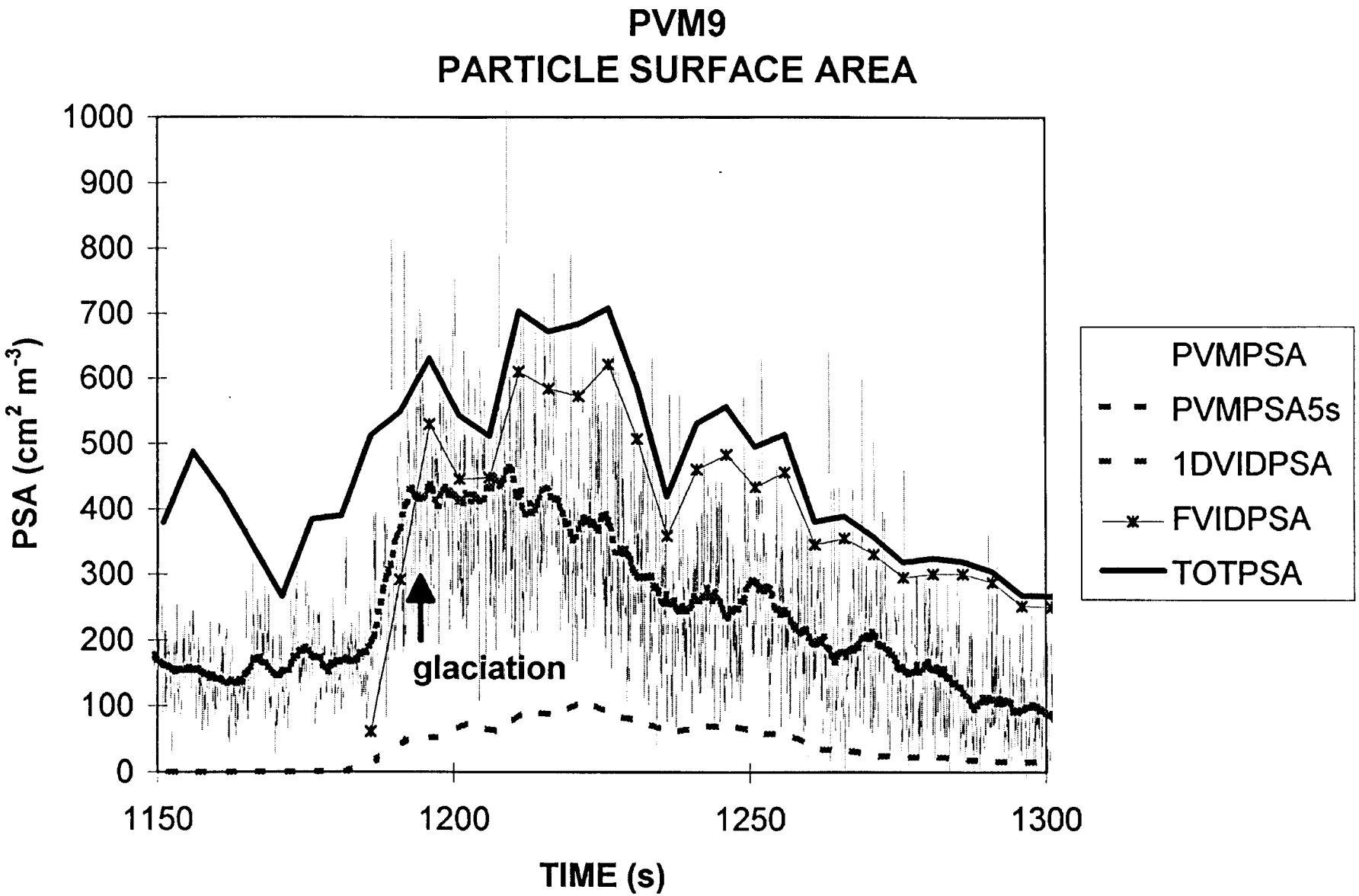
PVM9
PARTICLE SURFACE AREA
PSA (cm$^2$ m$^{-3}$)
1000
900
800
700
600
500
400
300
200
100
0
1150
1200
1250
1300
TIME (s)
glaciation
PVMPSA
PVMPSA5s
1DVIDPSA
FVIDPSA
TOTPSA

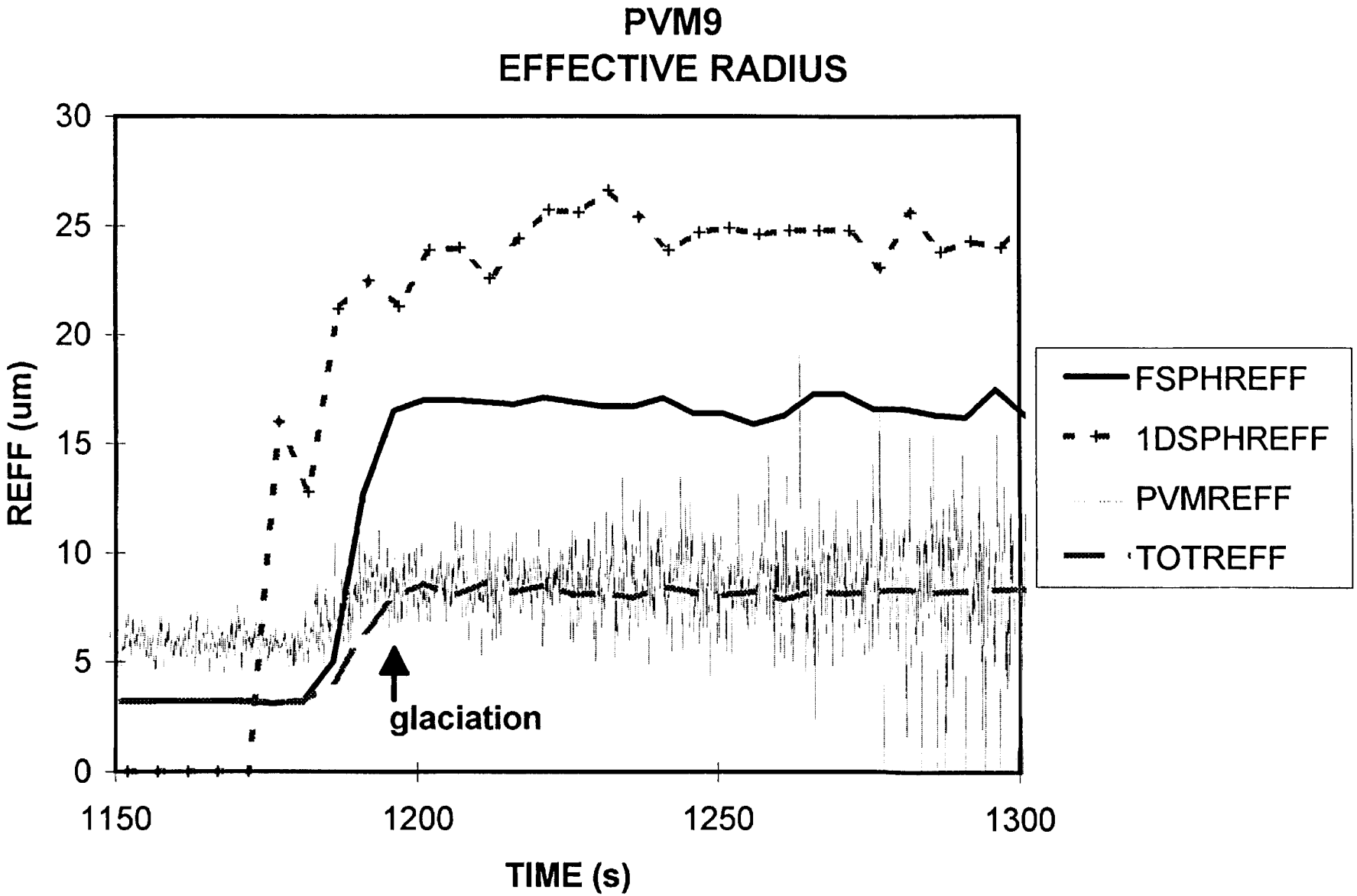
PVM9
EFFECTIVE RADIUS
REFF (um)
30
25
20
15
10
5
0
1150
1200
1250
1300
TIME (s)
glaciation
FSPHREFF
1DSPHREFF
PVMREFF
TOTREFF

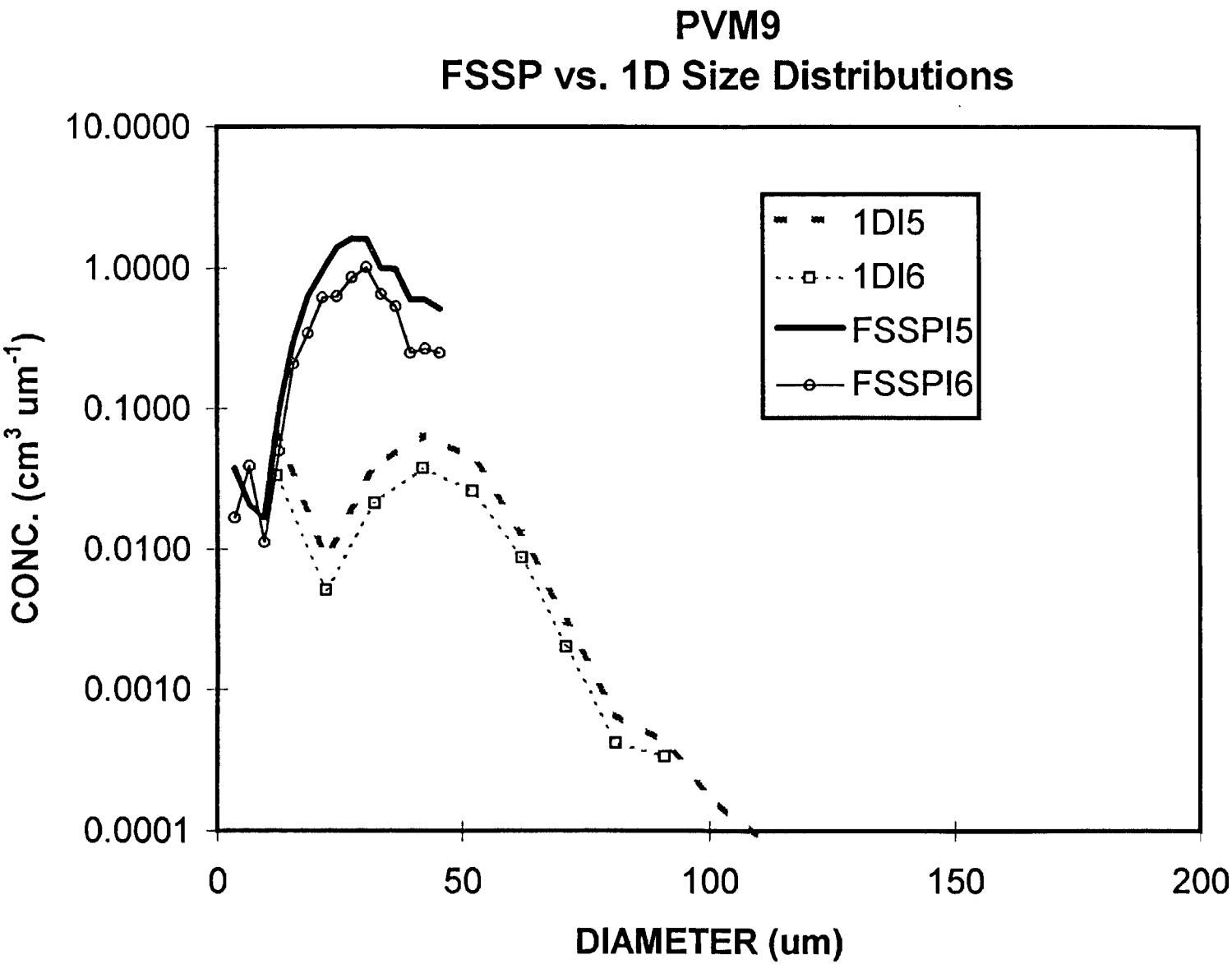
PVM9
FSSP vs. 1D Size Distributions
10.0000
1.0000
0.1000
0.0100
0.0010
0.0001
CONC. (cm3 um-1)
0
50
100
150
200
DIAMETER (um)
1DI5
1DI6
FSSPI5
FSSPI6

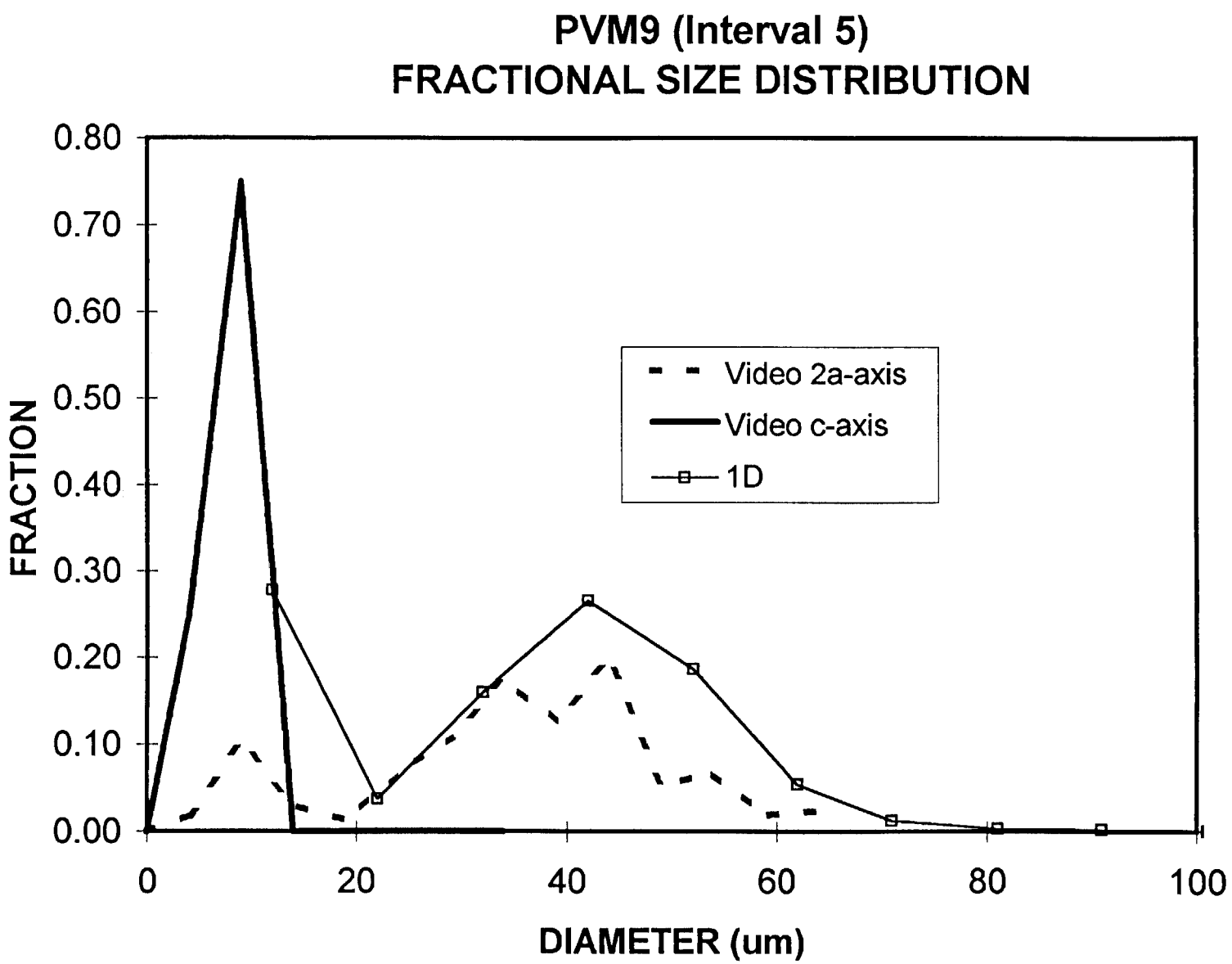
PVM9 (Interval 5)
FRACTIONAL SIZE DISTRIBUTION
FRACTION
0.80
0.70
0.60
0.50
0.40
0.30
0.20
0.10
0.00
0
20
40
60
80
100
DIAMETER (um)
Video 2a-axis
Video c-axis
1D

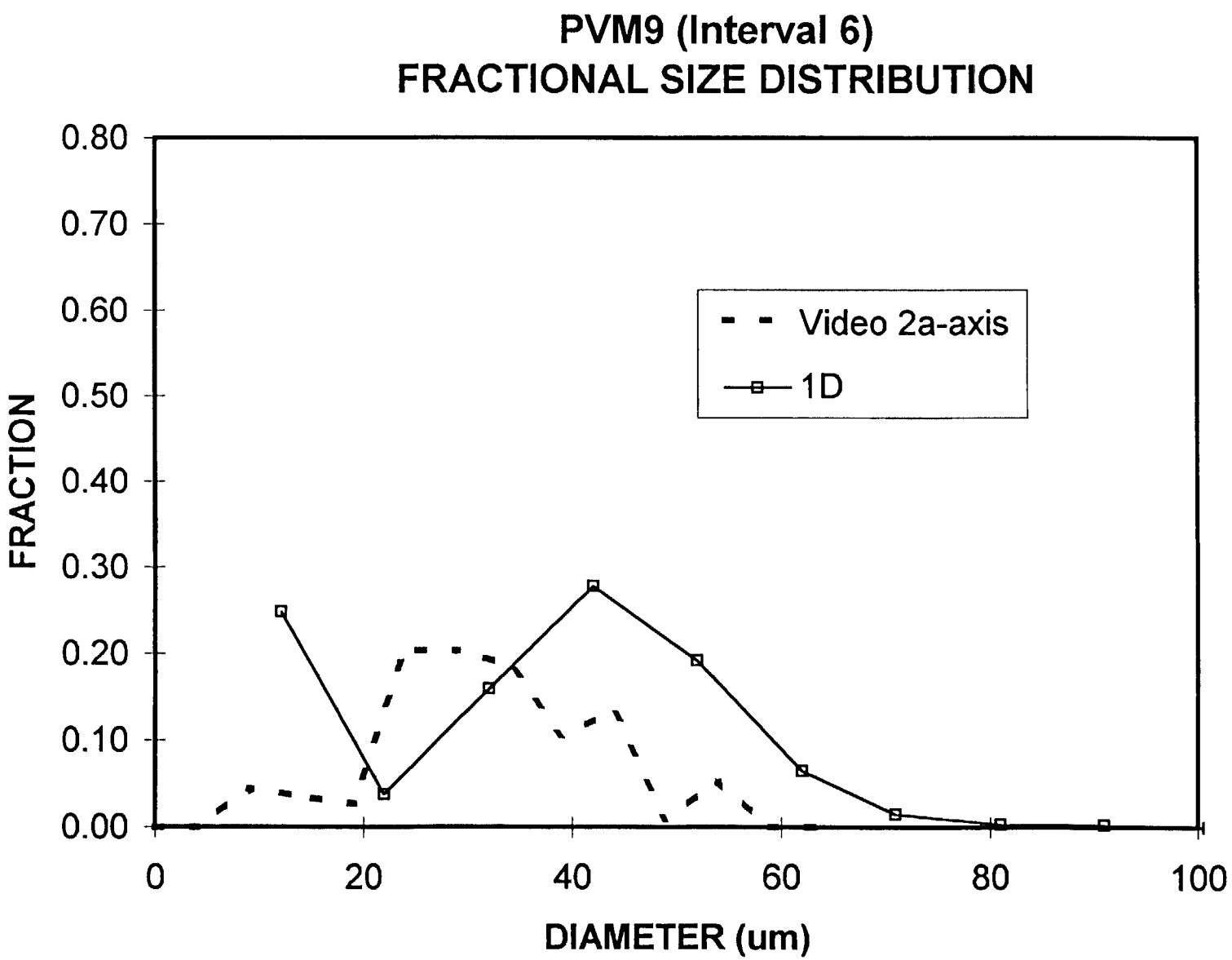
PVM9 (Interval 6)
FRACTIONAL SIZE DISTRIBUTION
FRACTION
0.80
0.70
0.60
0.50
0.40
0.30
0.20
0.10
0.00
0
20
40
60
80
100
DIAMETER (um)
Video 2a-axis
1D

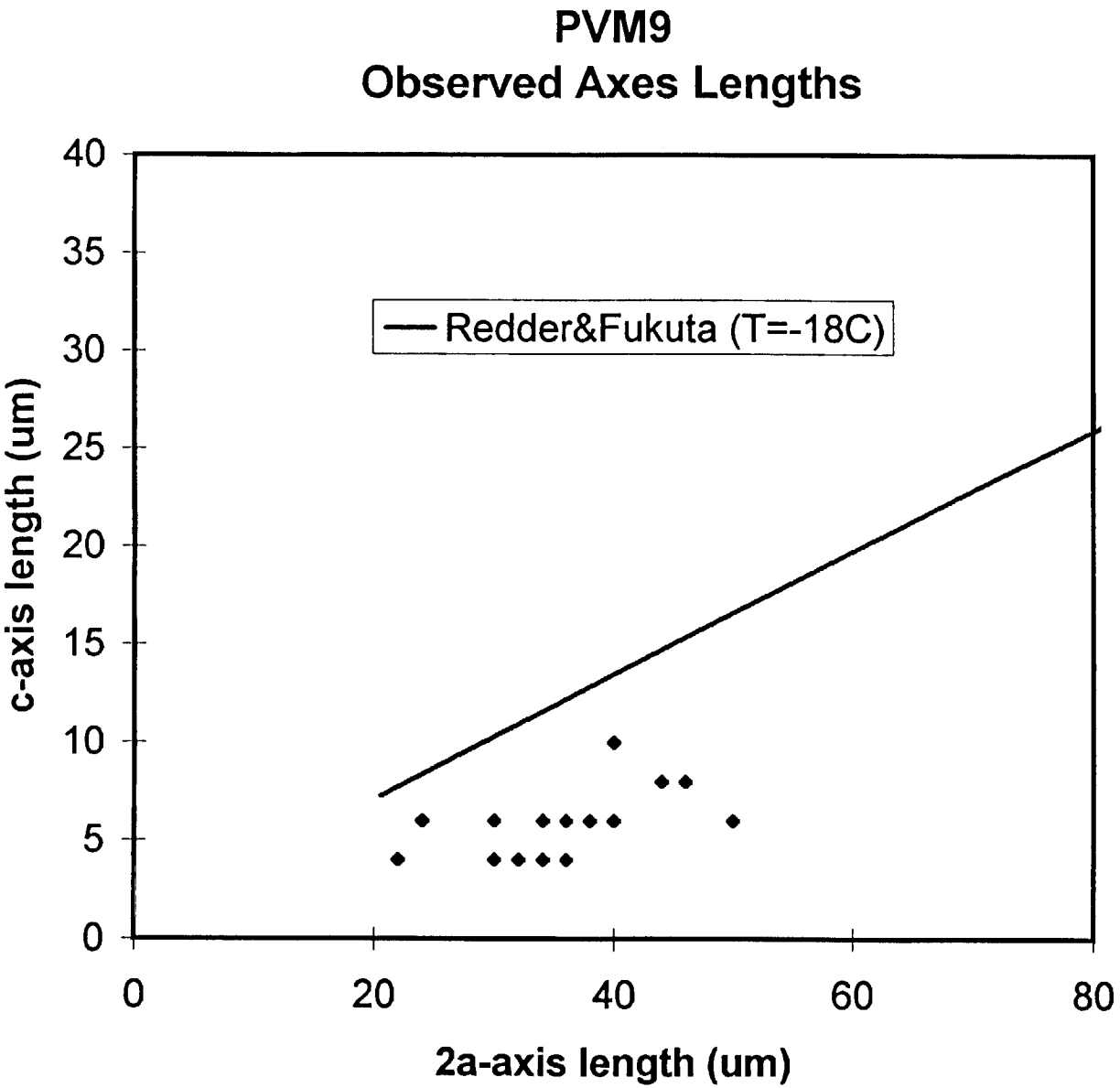
PVM9
Observed Axes Lengths
Redder&Fukuta (T=-18C)
c-axis length (um)
2a-axis length (um)
0
5
10
15
20
25
30
35
40
0
20
40
60
80

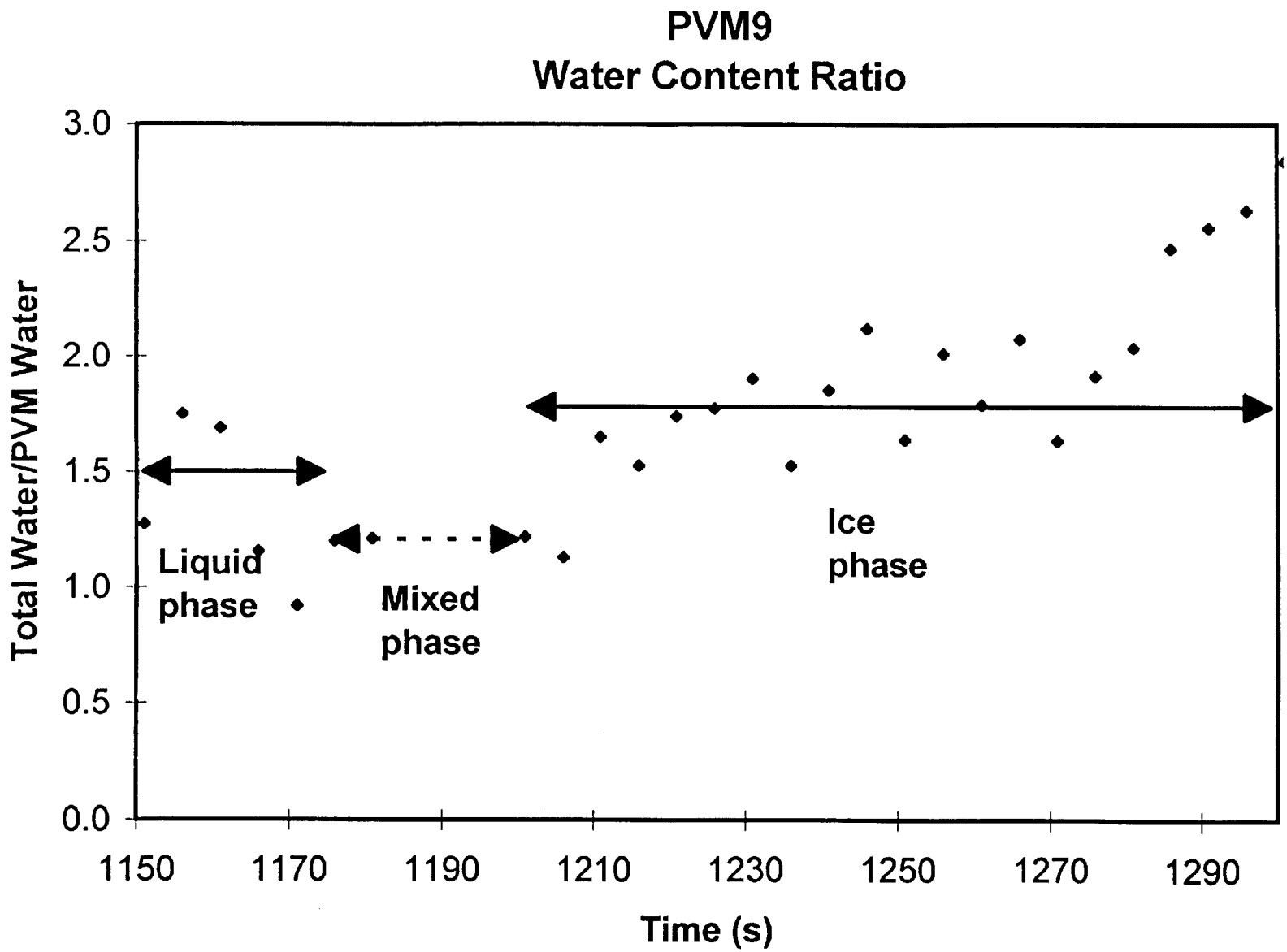
PVM9
Water Content Ratio
Total Water/PVM Water
3.0
2.5
2.0
1.5
1.0
0.5
0.0
1150
1170
1190
1210
1230
1250
1270
1290
Time (s)
Liquid phase
Mixed phase
Ice phase

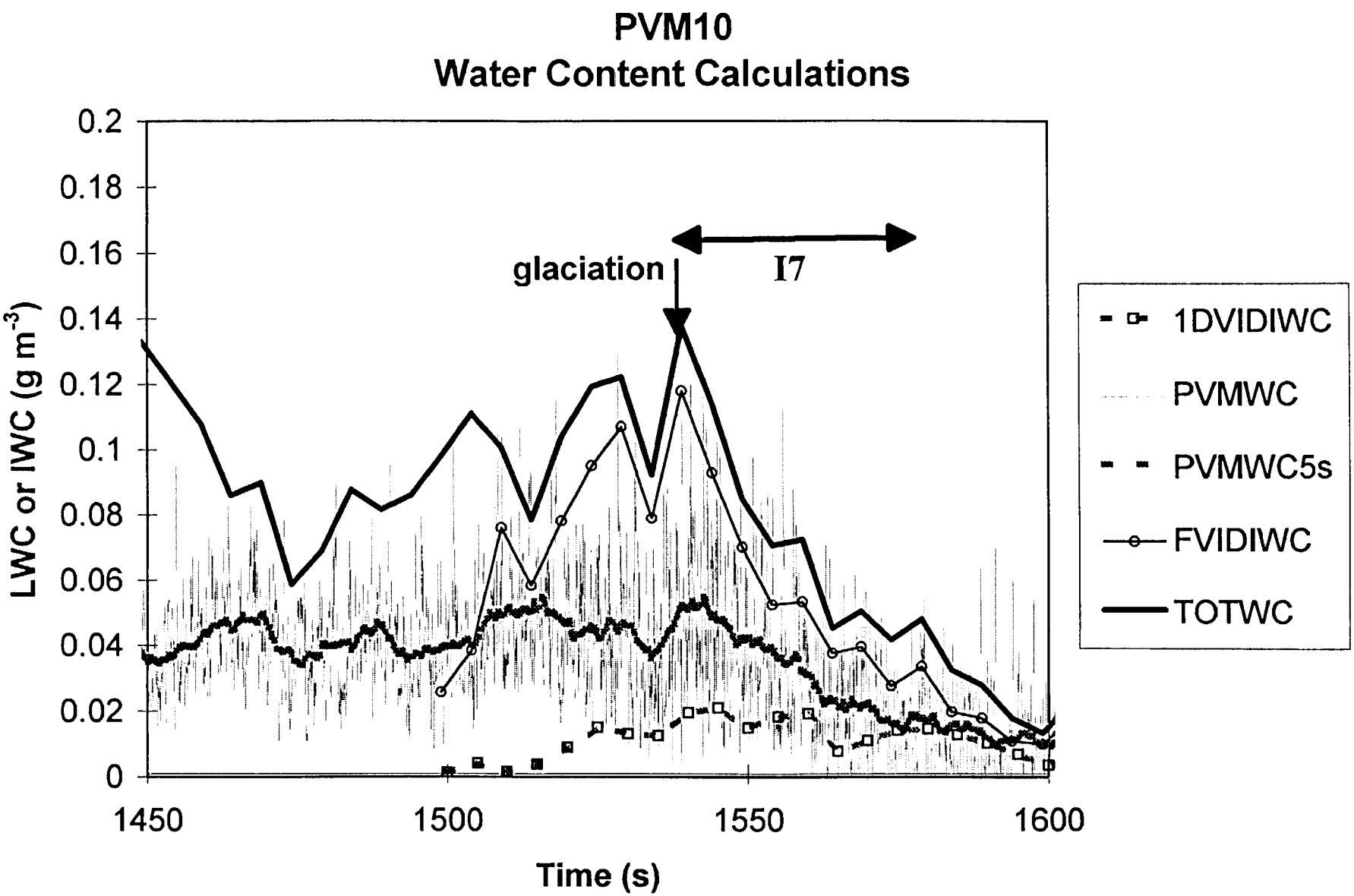
PVM10
Water Content Calculations
LWC or IWC (g m-3)
0.2
0.18
0.16
0.14
0.12
0.1
0.08
0.06
0.04
0.02
0
1450
1500
1550
1600
Time (s)
glaciation
I7
1DVIDIWC
PVMWC
PVMWC5s
FVIDIWC
TOTWC

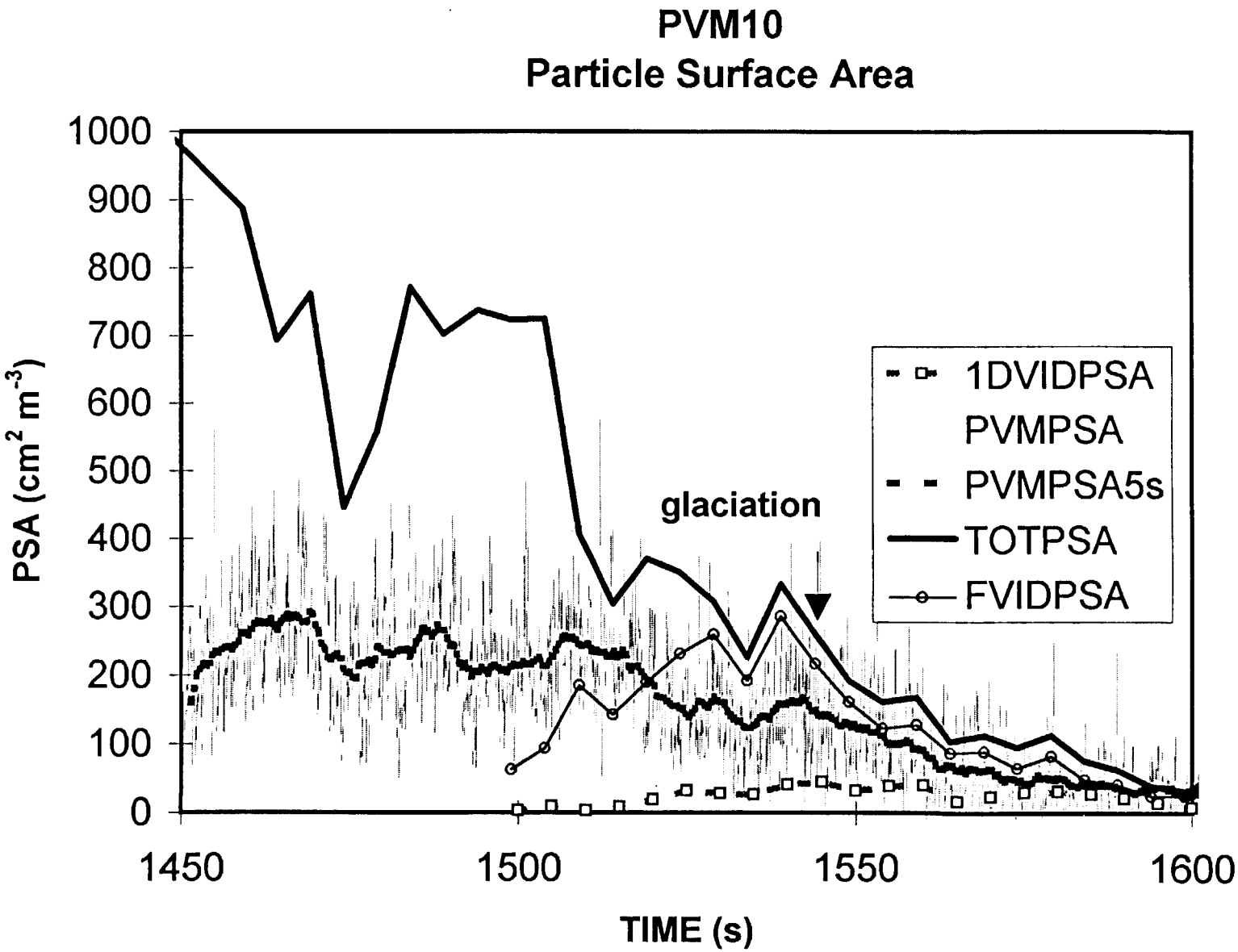
PVM10
Particle Surface Area
PSA (cm$^2$ m$^{-3}$)
1000
900
800
700
600
500
400
300
200
100
0
1450
1500
1550
1600
TIME (s)
glaciation
1DVIDPSA
PVMPSA
PVMPSA5s
TOTPSA
FVIDPSA

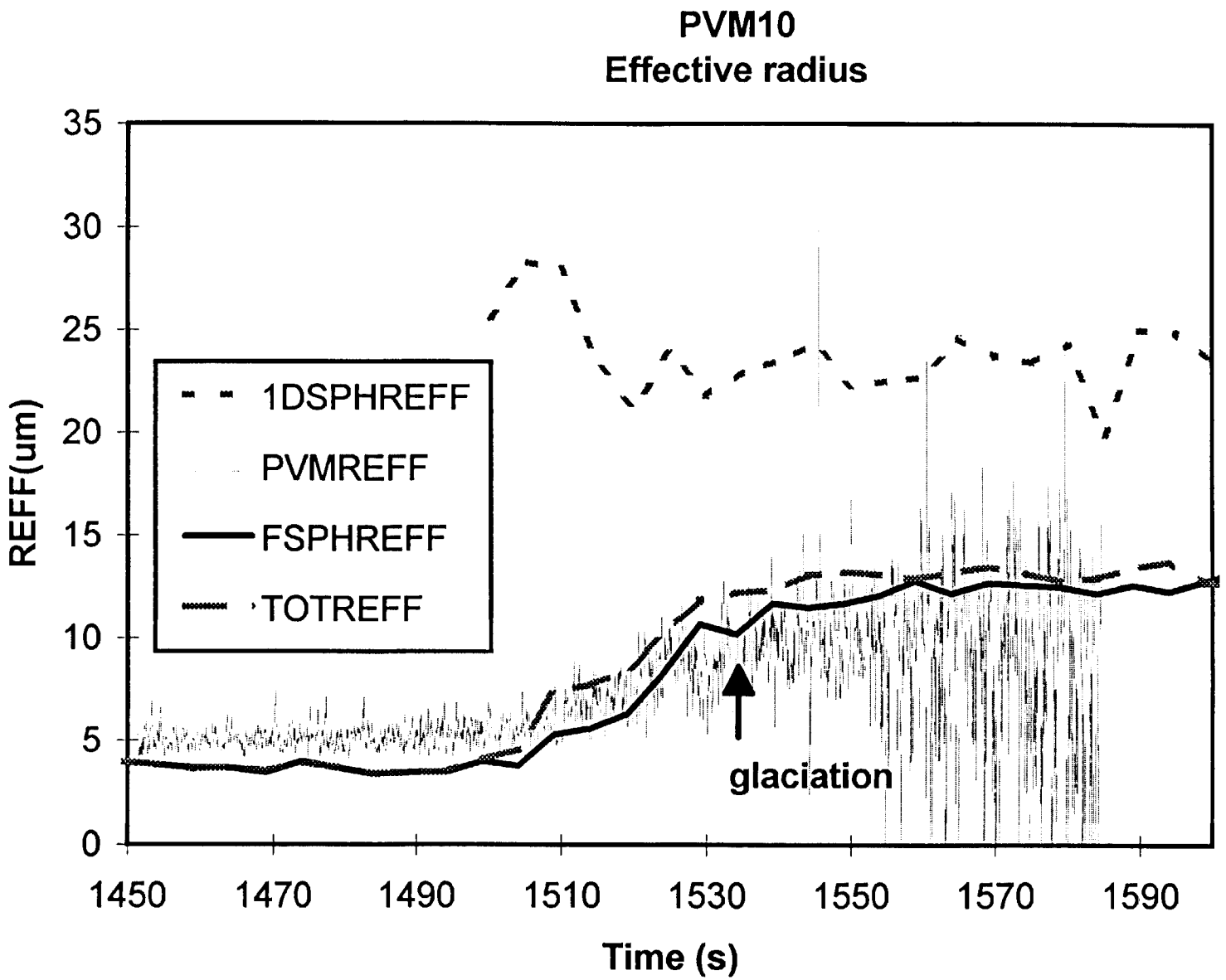
PVM10
Effective radius
REFF(um)
35
30
25
20
15
10
5
0
1DSPHREFF
PVMREFF
FSPHREFF
TOTREFF
glaciation
1450
1470
1490
1510
1530
1550
1570
1590
Time (s)

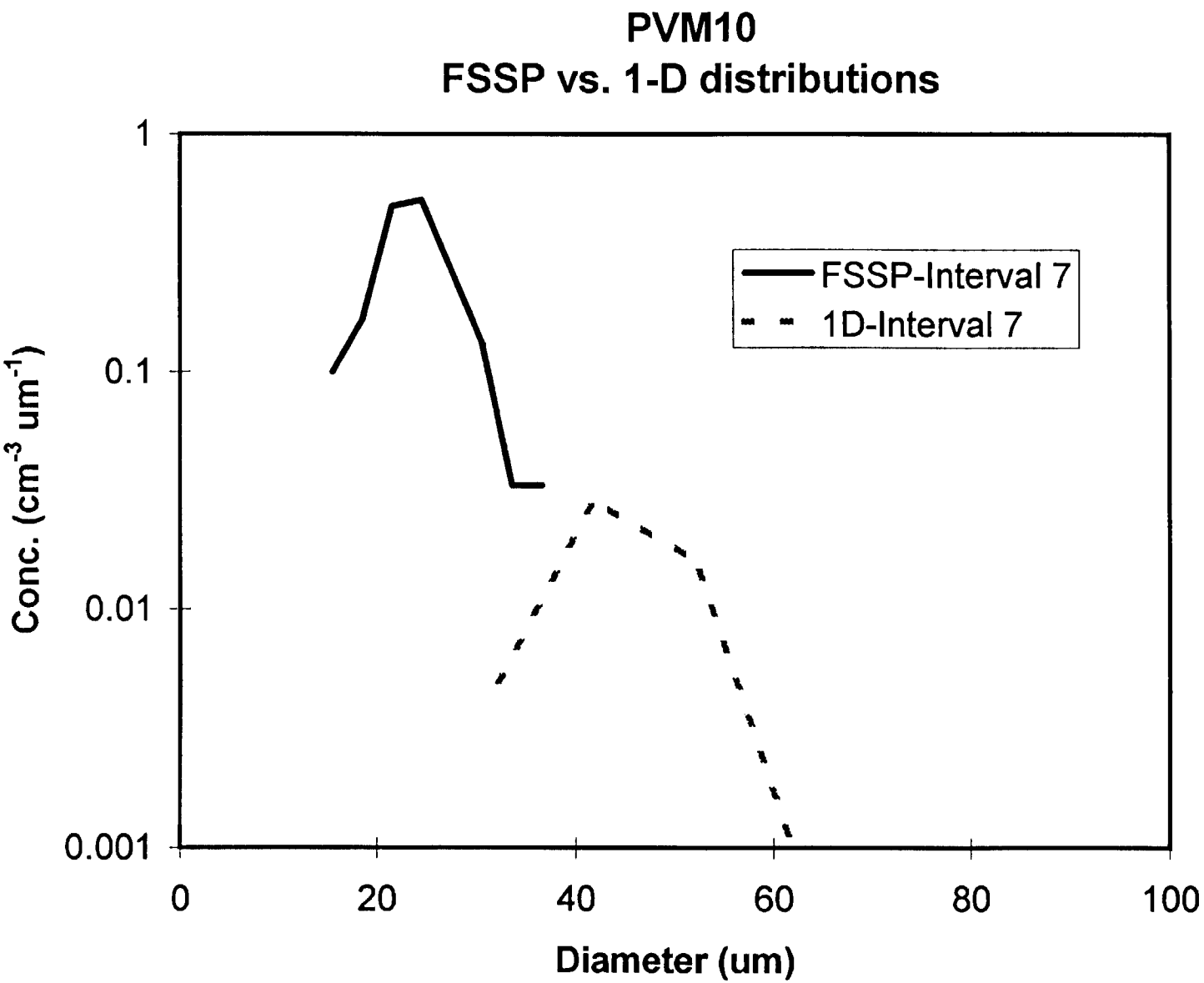
PVM10
FSSP vs. 1-D distributions
FSSP-Interval 7
1D-Interval 7
Conc. (cm-3 um-1)
1
0.1
0.01
0.001
0
20
40
60
80
100
Diameter (um)

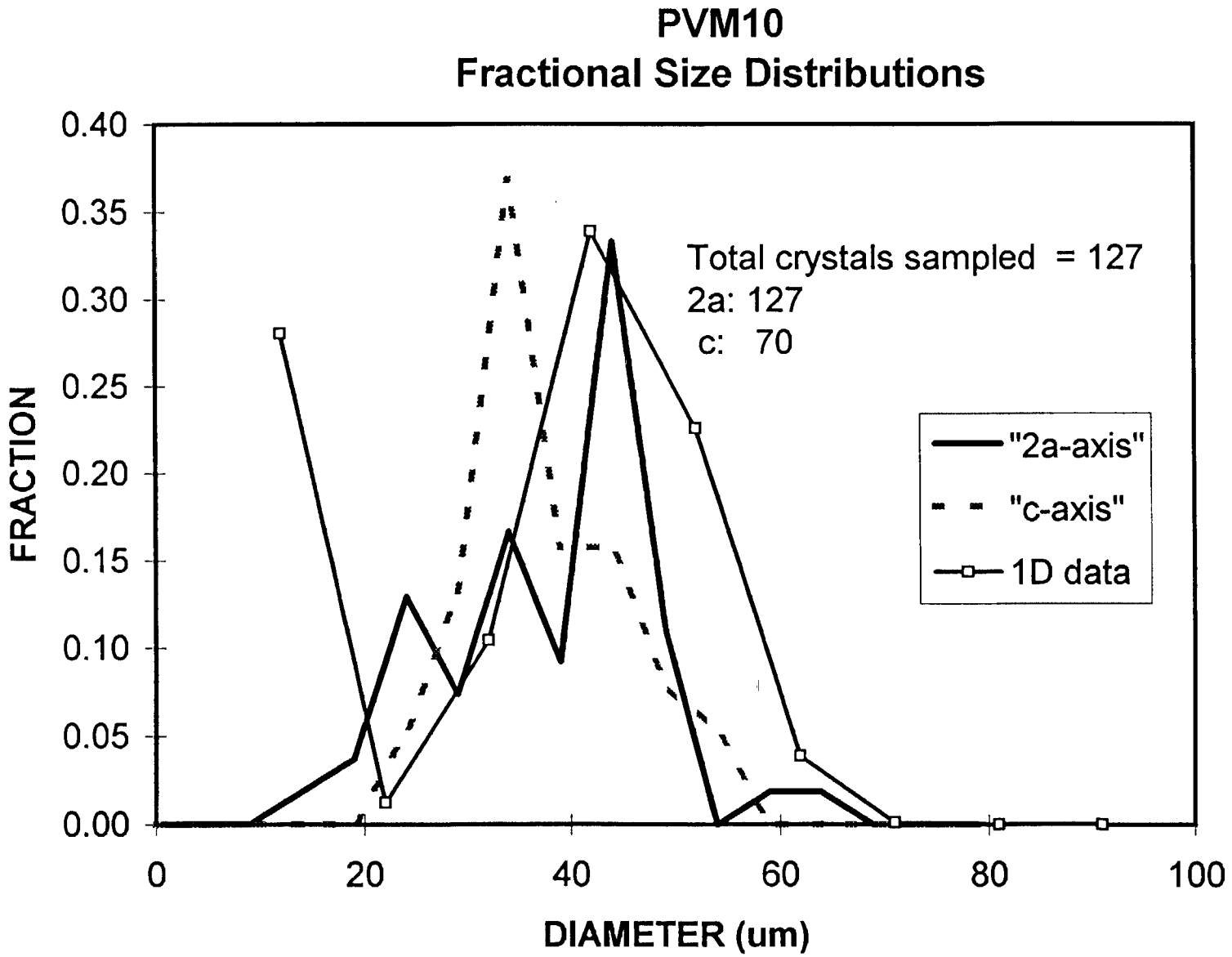
PVM10
Fractional Size Distributions
FRACTION
0.40
0.35
0.30
0.25
0.20
0.15
0.10
0.05
0.00
0
20
40
60
80
100
DIAMETER (um)
Total crystals sampled = 127
2a: 127
c: 70
"2a-axis"
"c-axis"
1D data

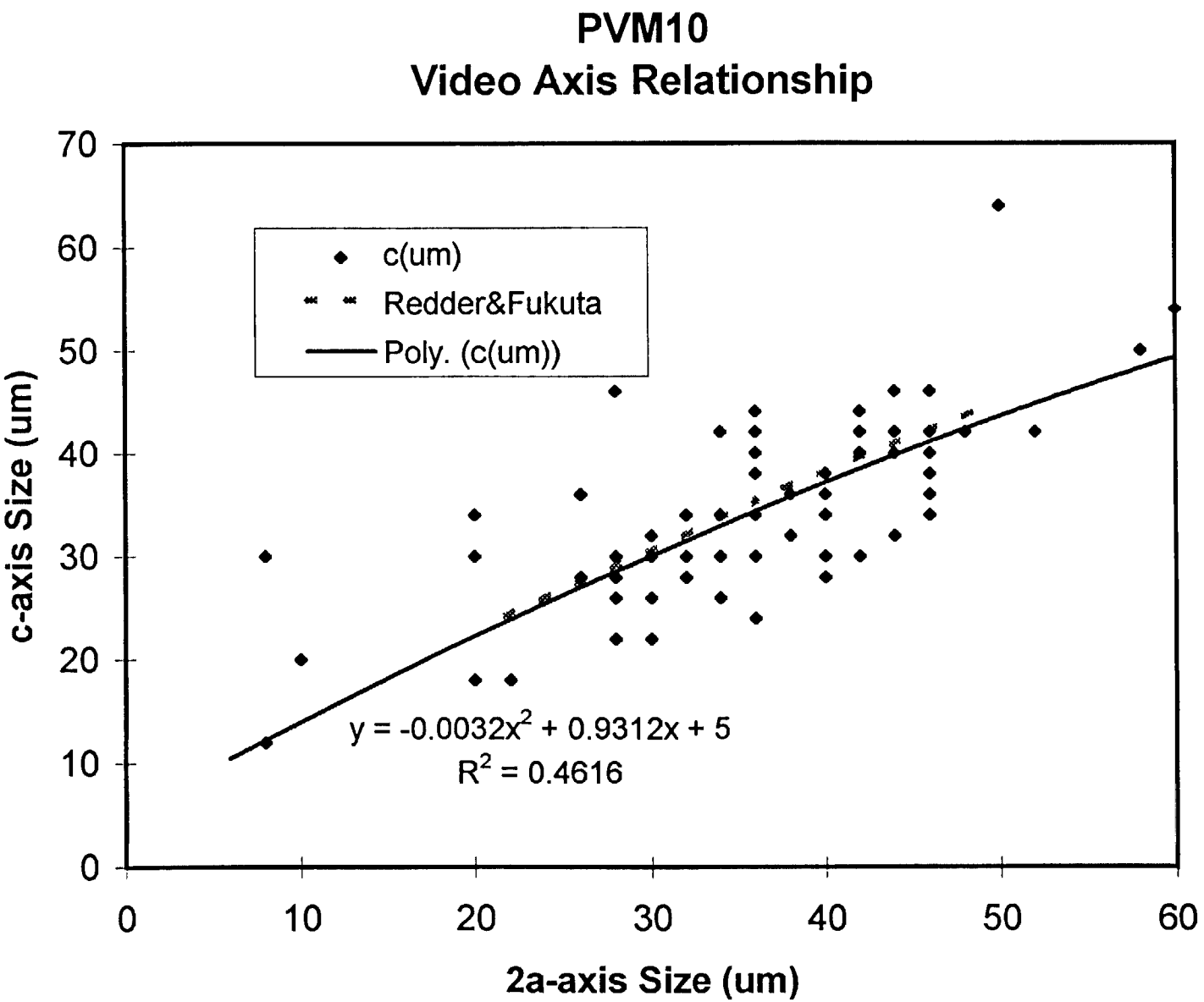
PVM10
Video Axis Relationship
c-axis Size (um)
2a-axis Size (um)
c(um)
Redder&Fukuta
Poly. (c(um))
y = -0.0032x2 + 0.9312x + 5
R2 = 0.4616
0
10
20
30
40
50
60
70

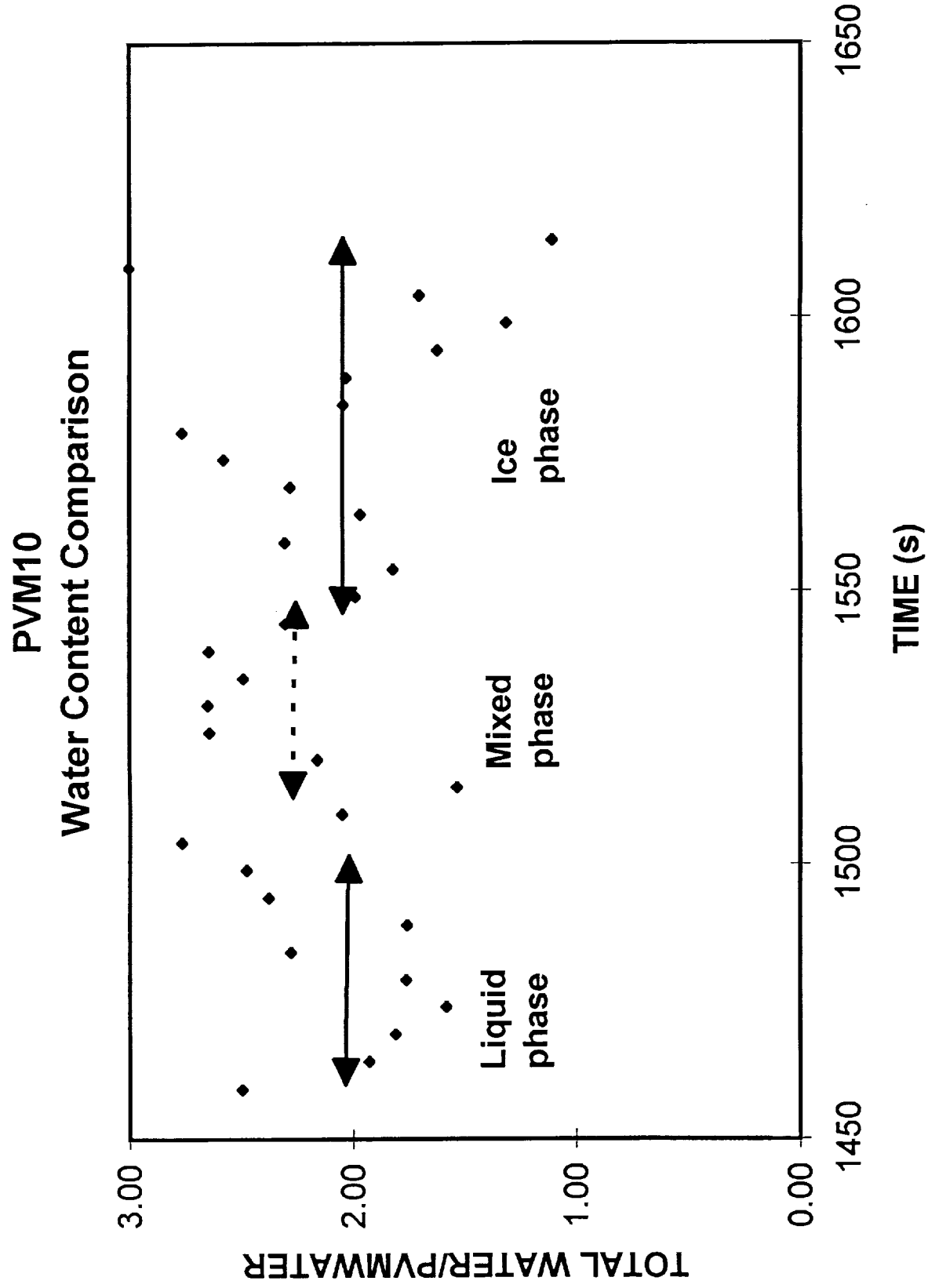
PVM10
Water Content Comparison
TOTAL WATER/PVMWATER
3.00
2.00
1.00
0.00
1450
1500
1550
1600
1650
TIME (s)
Liquid phase
Mixed phase
Ice phase

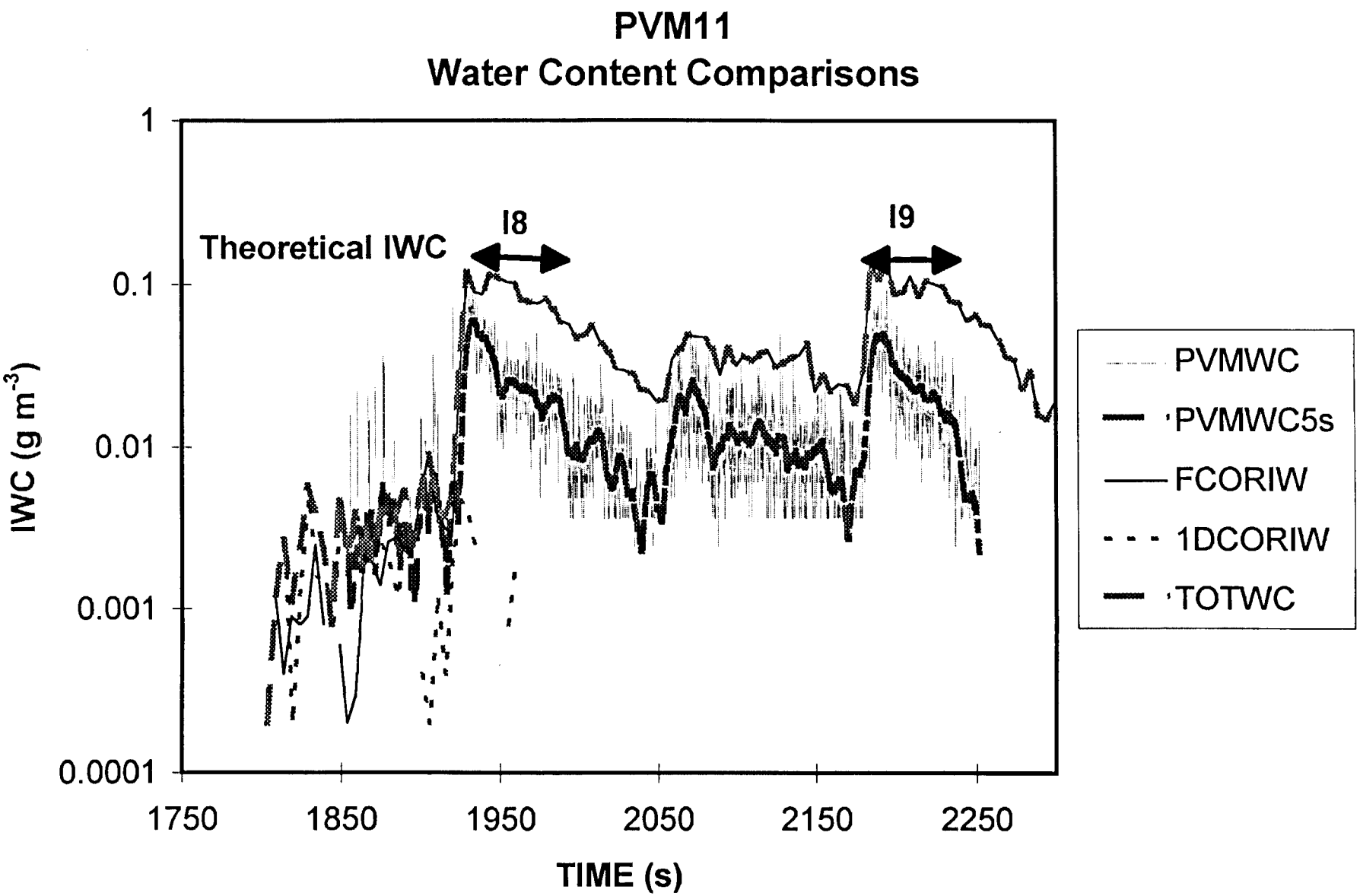
PVM11
Water Content Comparisons
Theoretical IWC
I8
I9
IWC (g m-3)
1
0.1
0.01
0.001
0.0001
1750
1850
1950
2050
2150
2250
TIME (s)
PVMWC
PVMWC5s
FCORIW
1DCORIW
TOTWC

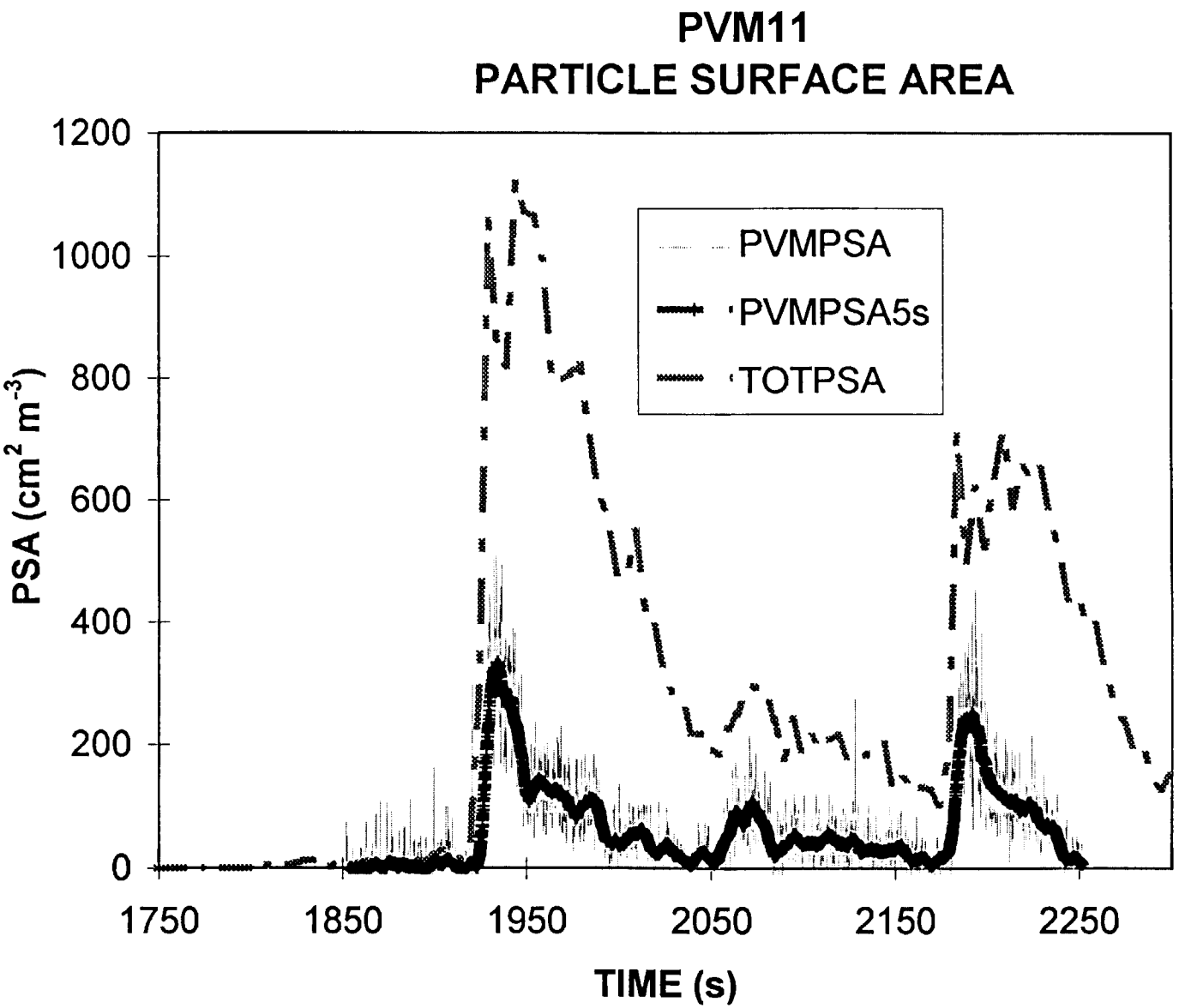
PVM11
PARTICLE SURFACE AREA
PSA (cm$^2$ m$^{-3}$)
1200
1000
800
600
400
200
0
1750
1850
1950
2050
2150
2250
TIME (s)
PVMPSA
PVMPSA5s
TOTPSA

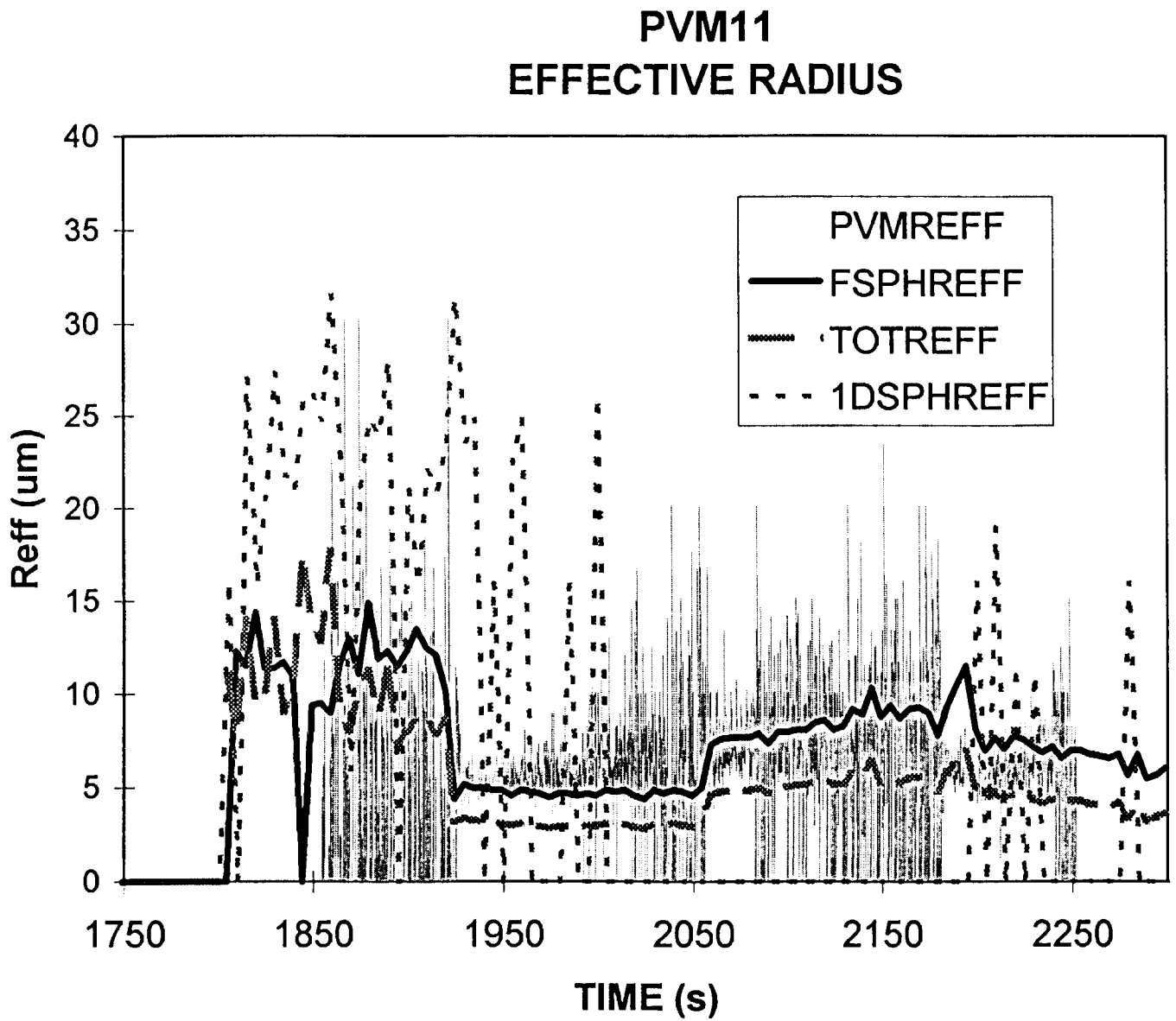
PVM11
EFFECTIVE RADIUS
PVMREFF
FSPHREFF
TOTREFF
1DSPHREFF
Reff (um)
TIME (s)
0
5
10
15
20
25
30
35
40
1750
1850
1950
2050
2150
2250

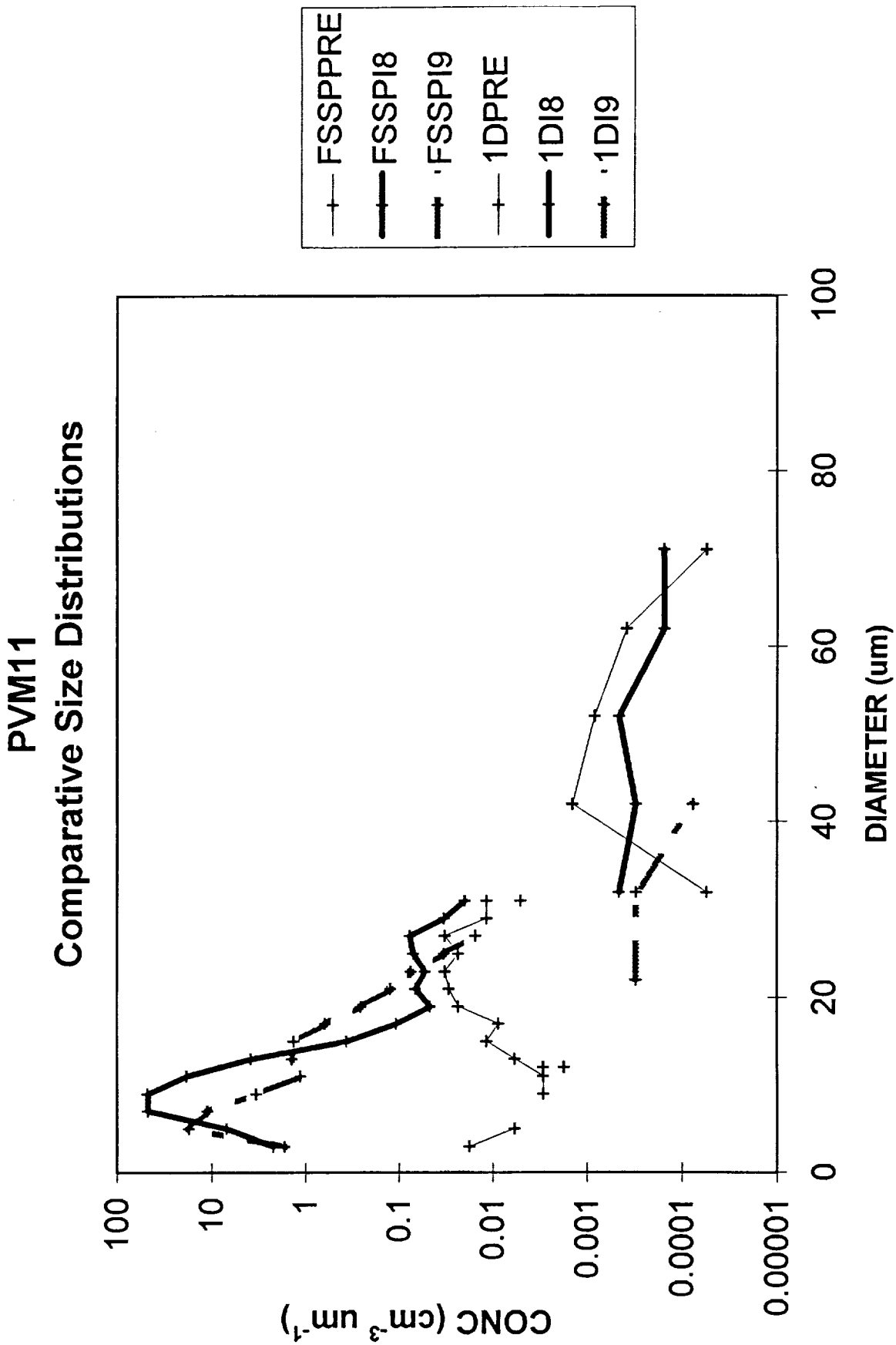
PVM11
Comparative Size Distributions
FSSPPRE
FSSPI8
FSSPI9
1DPRE
1DI8
1DI9
CONC (cm-3 um-1)
100
10
1
0.1
0.01
0.001
0.0001
0.00001
0
20
40
60
80
100
DIAMETER (um)

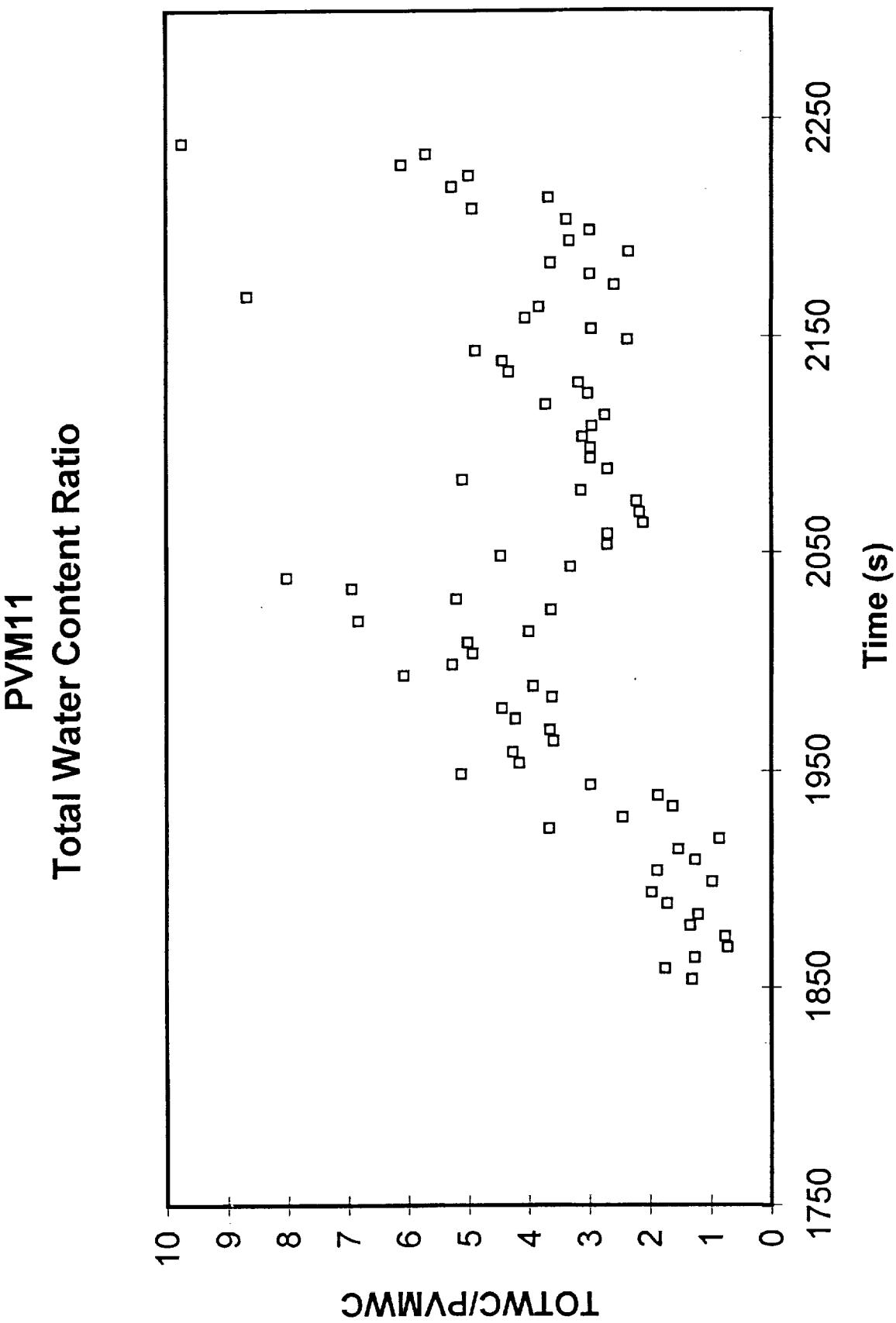
PVM11
Total Water Content Ratio
TOTWC/PVMWC
0
1
2
3
4
5
6
7
8
9
10
1750
1850
1950
2050
2150
2250
Time (s)

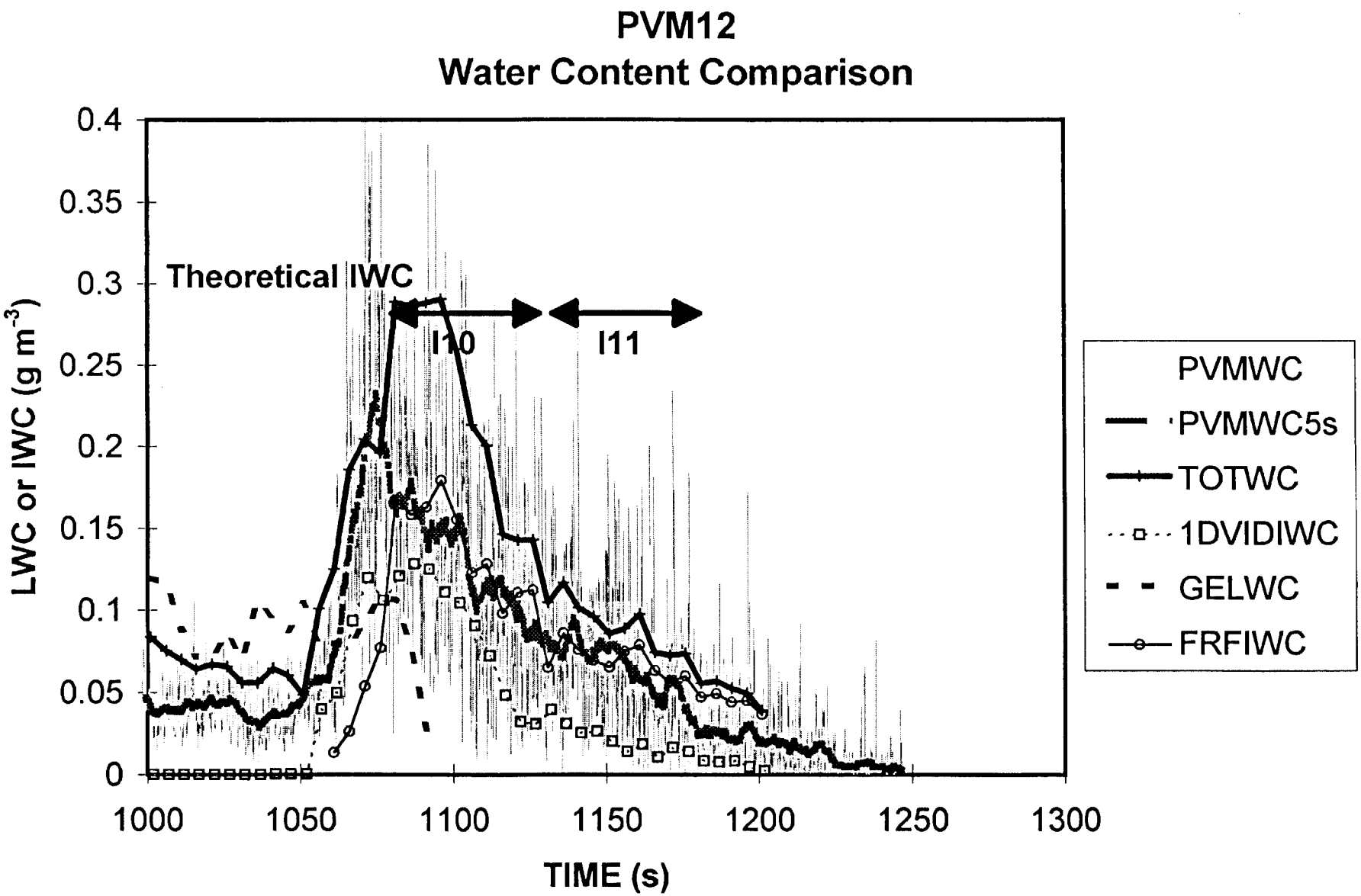
PVM12
Water Content Comparison
Theoretical IWC
I10
I11
LWC or IWC (g m-3)
TIME (s)
0.4
0.35
0.3
0.25
0.2
0.15
0.1
0.05
0
1000
1050
1100
1150
1200
1250
1300
PVMWC
PVMWC5s
TOTWC
1DVIDIWC
GELWC
FRFIWC

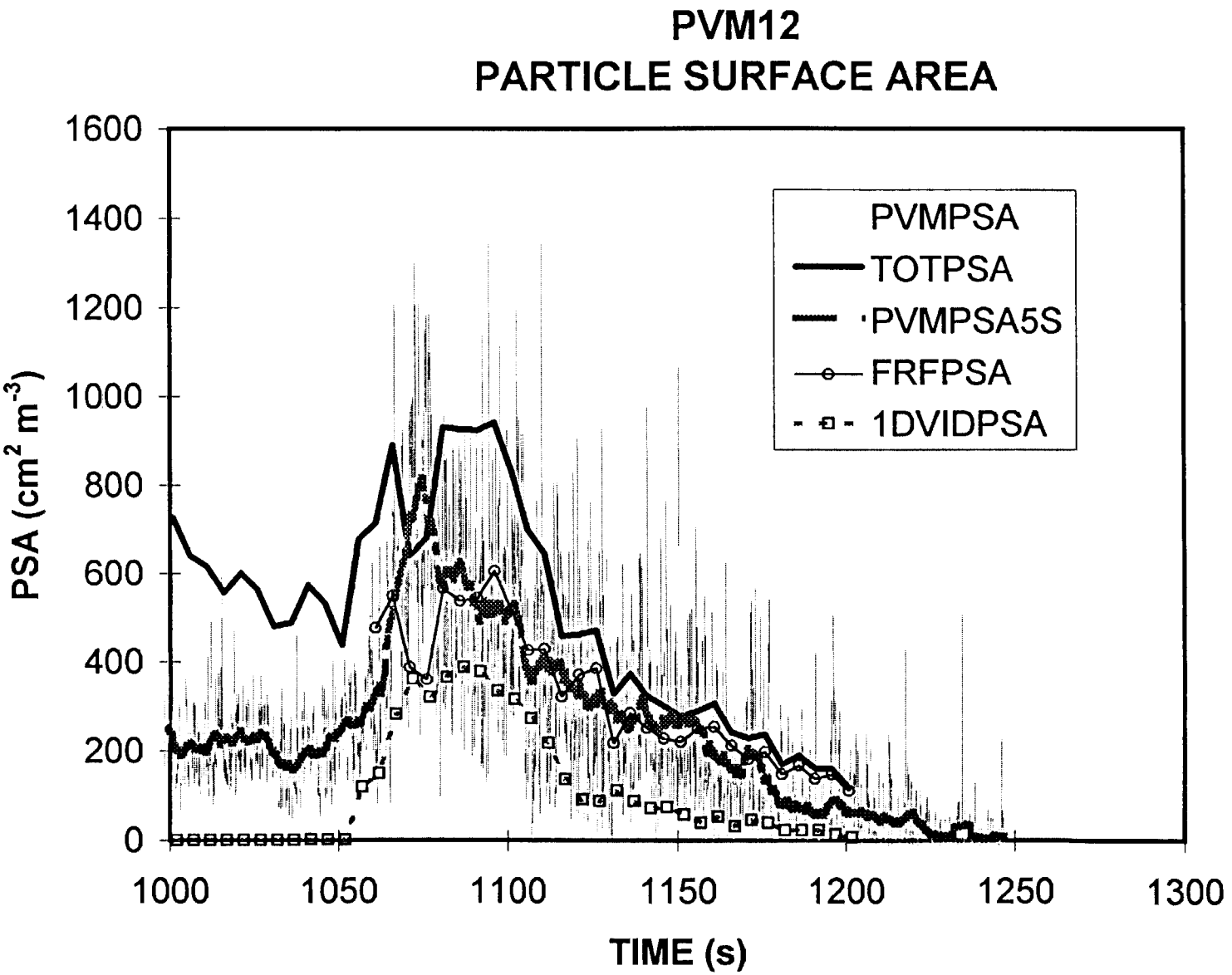
PVM12
PARTICLE SURFACE AREA
PSA (cm$^2$ m$^{-3}$)
TIME (s)
1600
1400
1200
1000
800
600
400
200
0
1000
1050
1100
1150
1200
1250
1300
PVMPSA
TOTPSA
PVMPSA5S
FRFPSA
1DVIDPSA

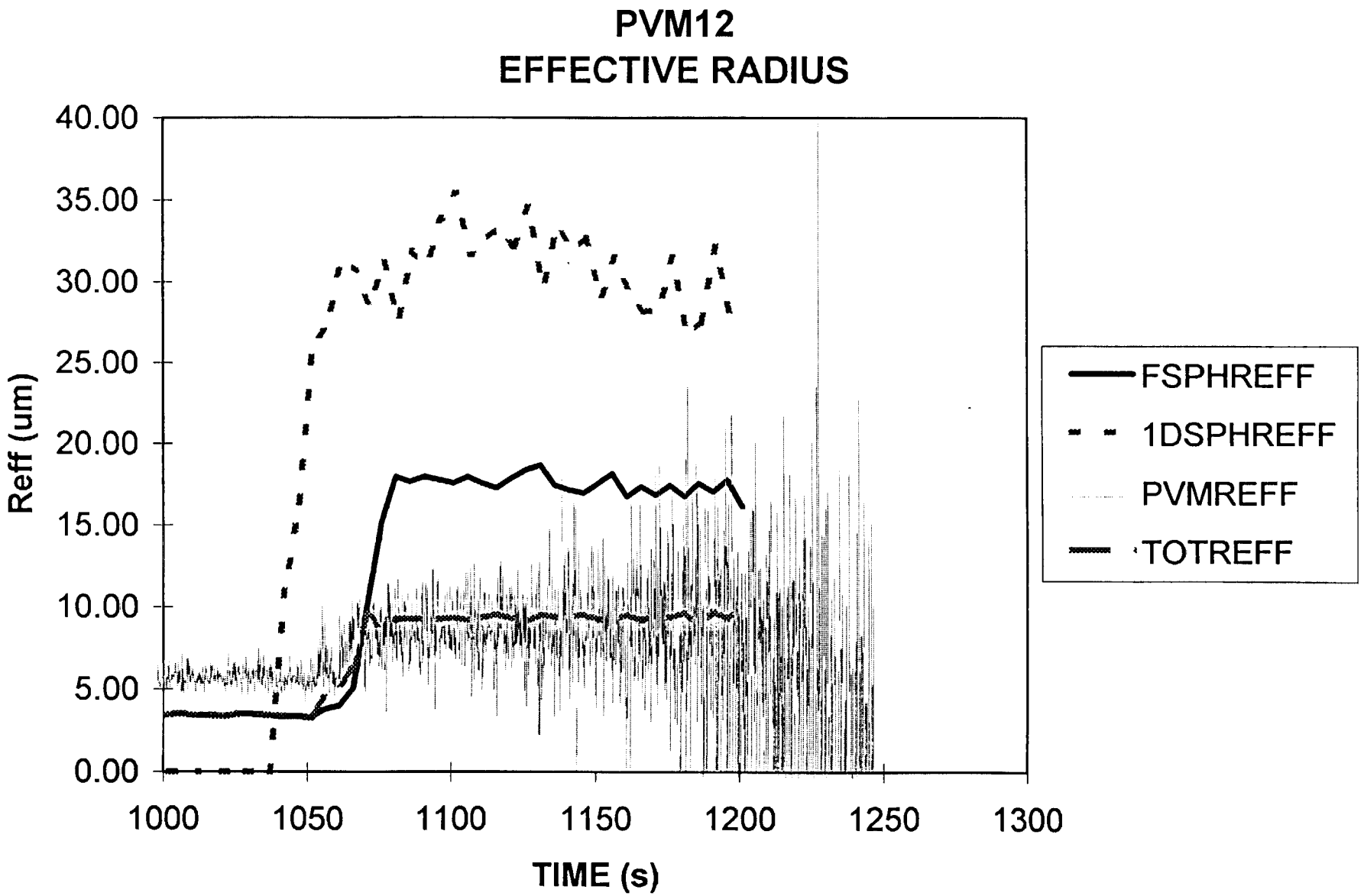
PVM12
EFFECTIVE RADIUS
Reff (um)
40.00
35.00
30.00
25.00
20.00
15.00
10.00
5.00
0.00
1000
1050
1100
1150
1200
1250
1300
TIME (s)
FSPHREFF
1DSPHREFF
PVMREFF
TOTREFF

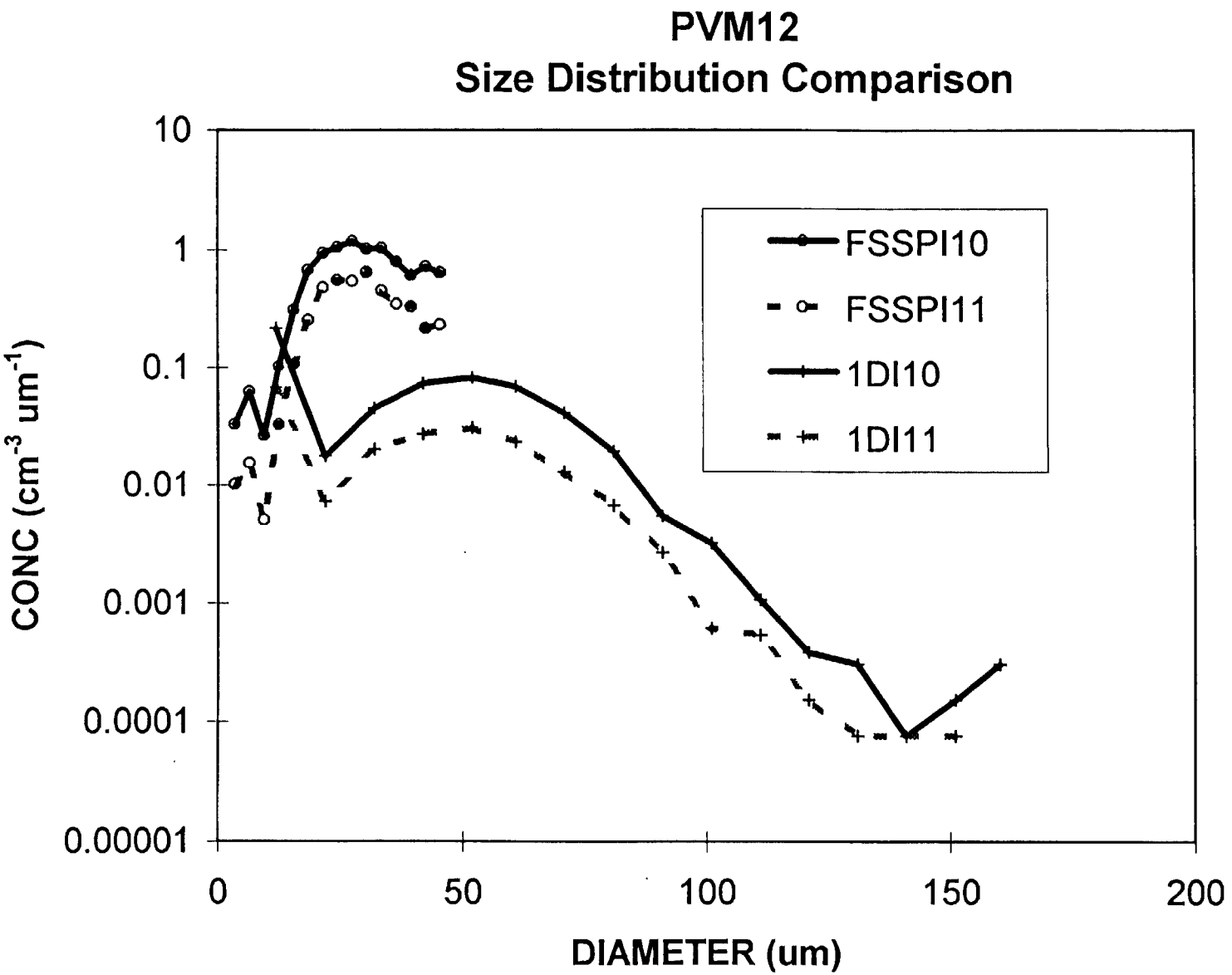
PVM12
Size Distribution Comparison
CONC (cm-3 um-1)
10
1
0.1
0.01
0.001
0.0001
0.00001
0
50
100
150
200
DIAMETER (um)
FSSPI10
FSSPI11
1DI10
1DI11

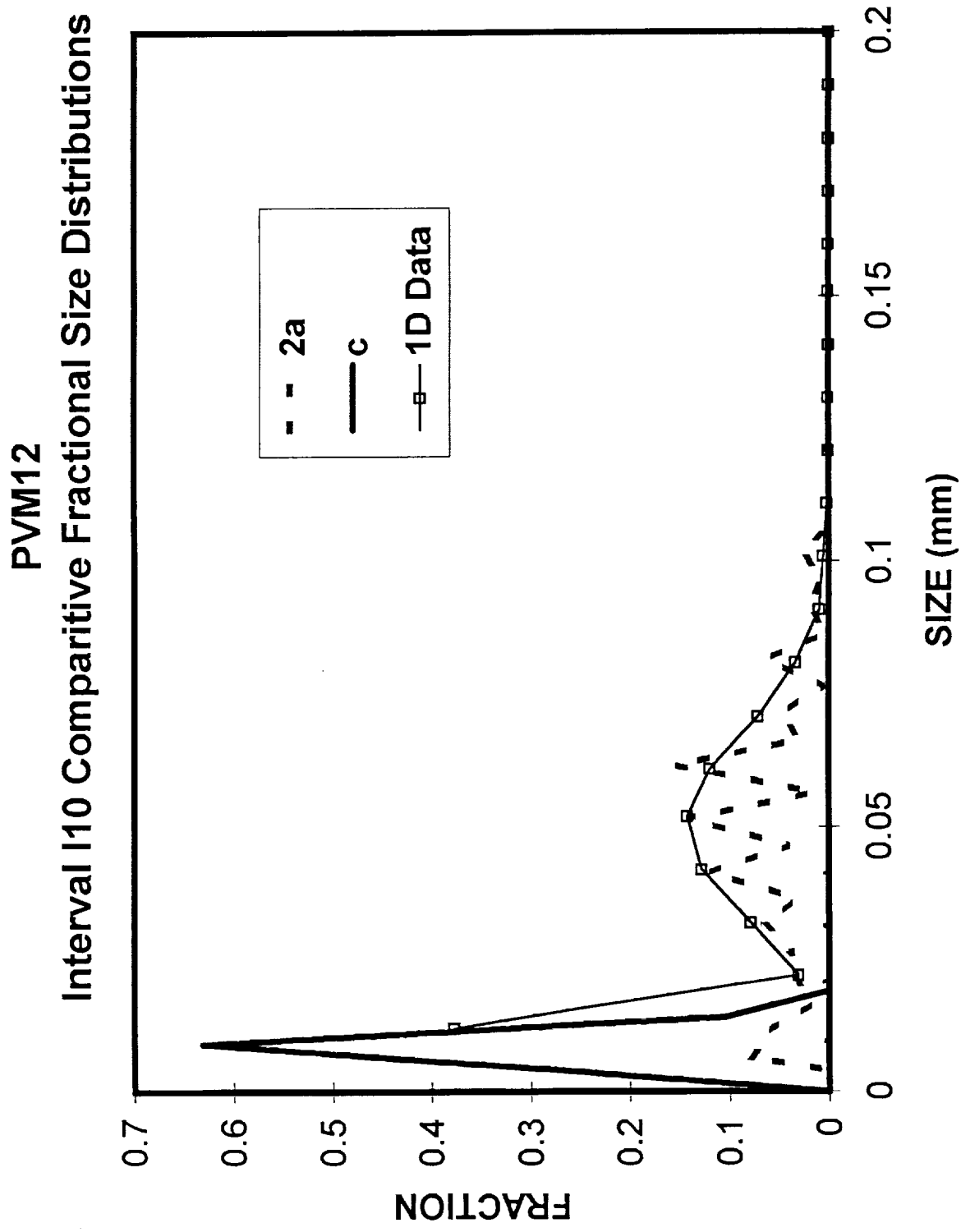
PVM12
Interval I10 Comparitive Fractional Size Distributions
2a
c
1D Data
FRACTION
0.7
0.6
0.5
0.4
0.3
0.2
0.1
0
0
0.05
0.1
0.15
0.2
SIZE (mm)

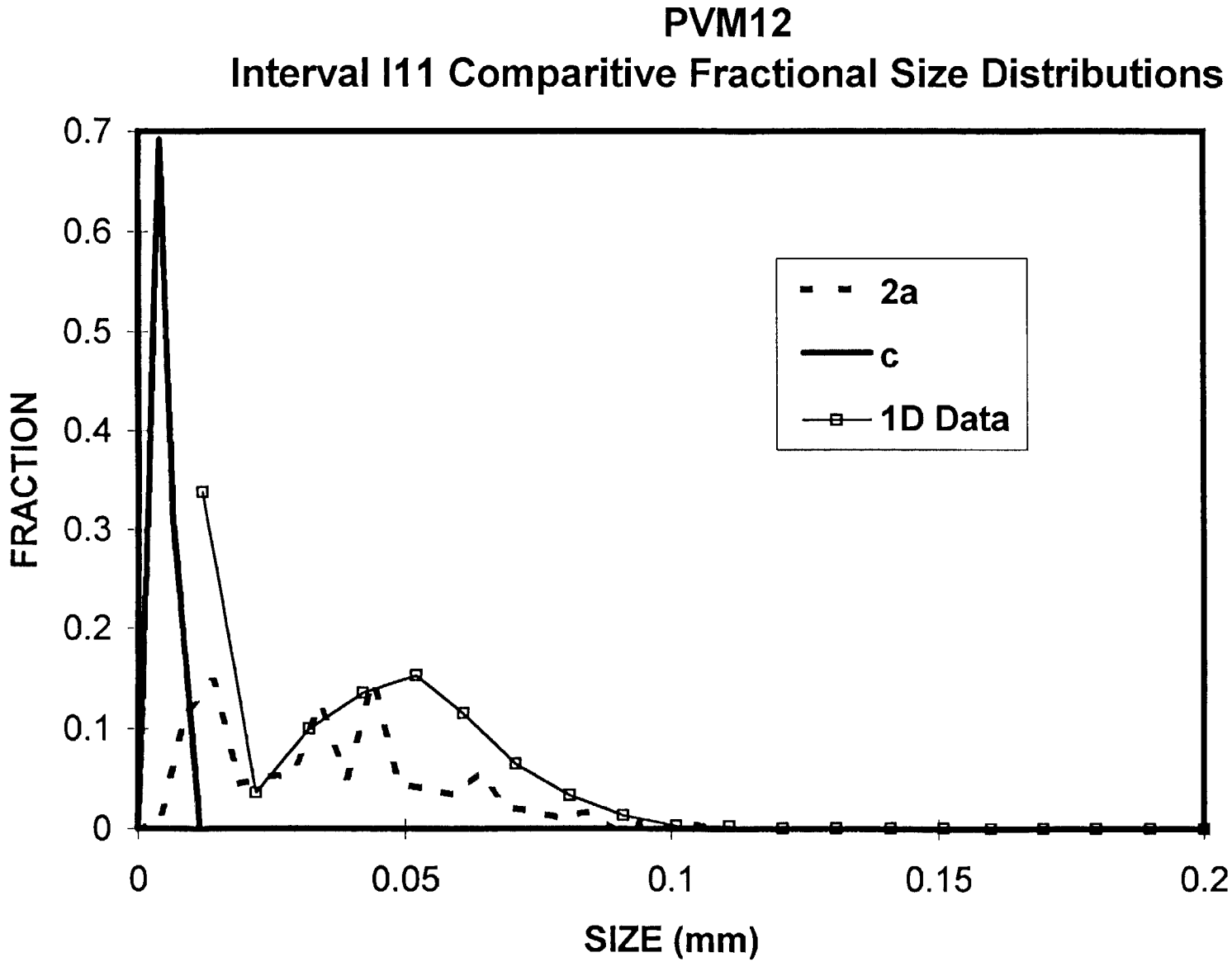
PVM12
Interval I11 Comparitive Fractional Size Distributions
FRACTION
0.7
0.6
0.5
0.4
0.3
0.2
0.1
0
0
0.05
0.1
0.15
0.2
SIZE (mm)
2a
c
1D Data

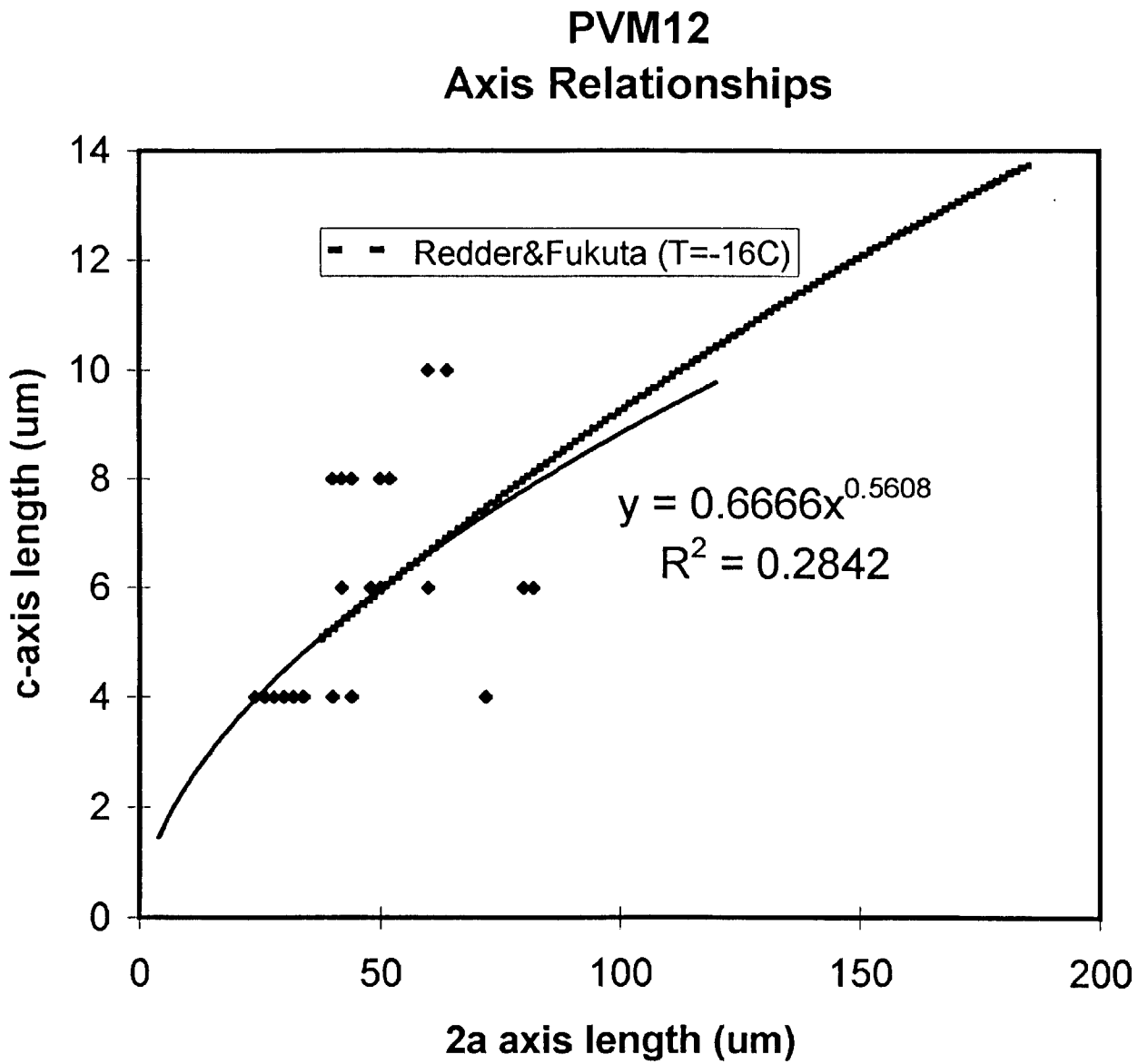
PVM12
Axis Relationships
Redder&Fukuta (T=-16C)
y = 0.6666x^0.5608
R^2 = 0.2842
c-axis length (um)
2a axis length (um)
0
2
4
6
8
10
12
14
0
50
100
150
200

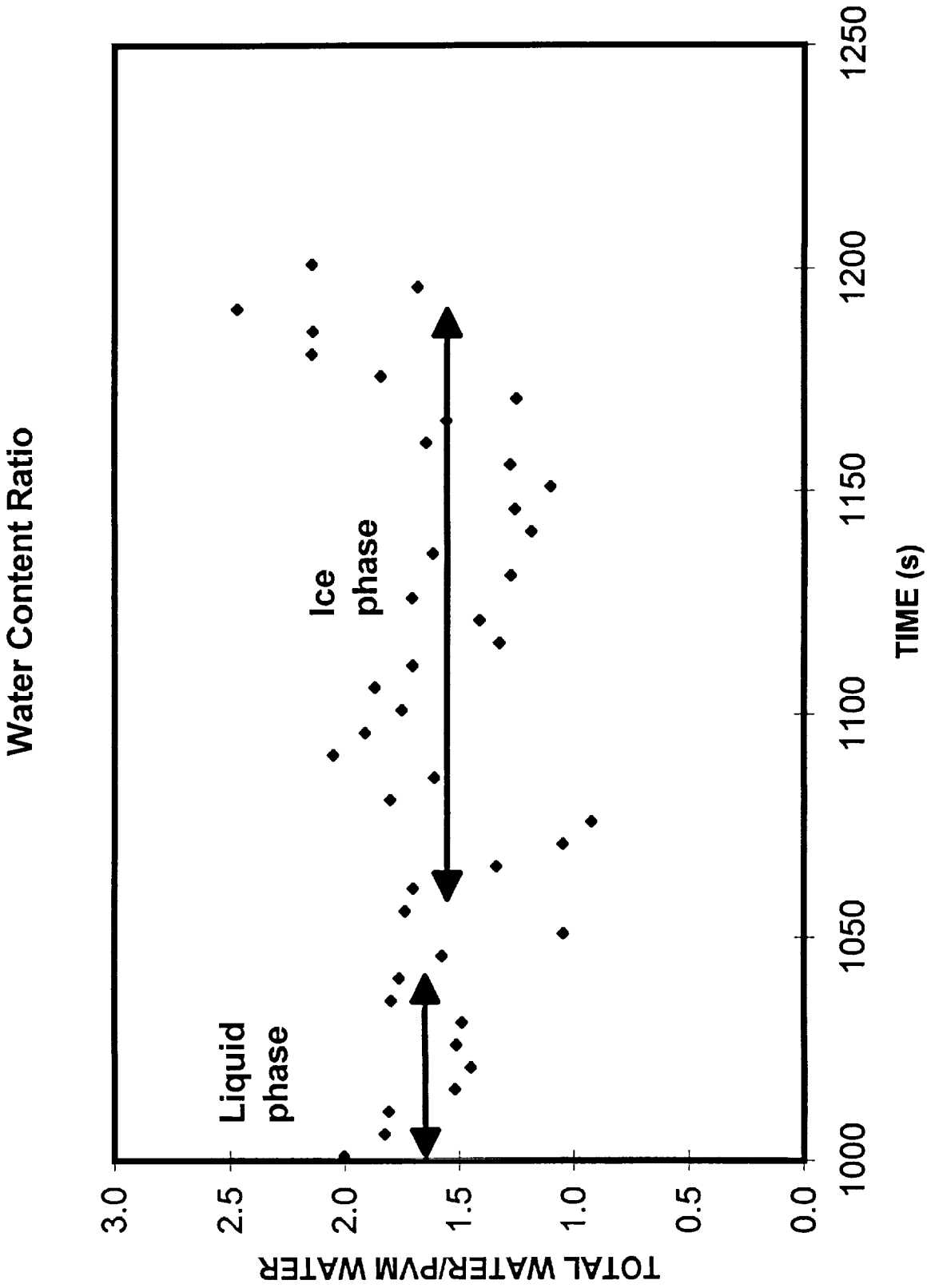
Water Content Ratio
Liquid phase
Ice phase
TOTAL WATER/PVM WATER
TIME (s)
3.0
2.5
2.0
1.5
1.0
0.5
0.0
1000
1050
1100
1150
1200
1250

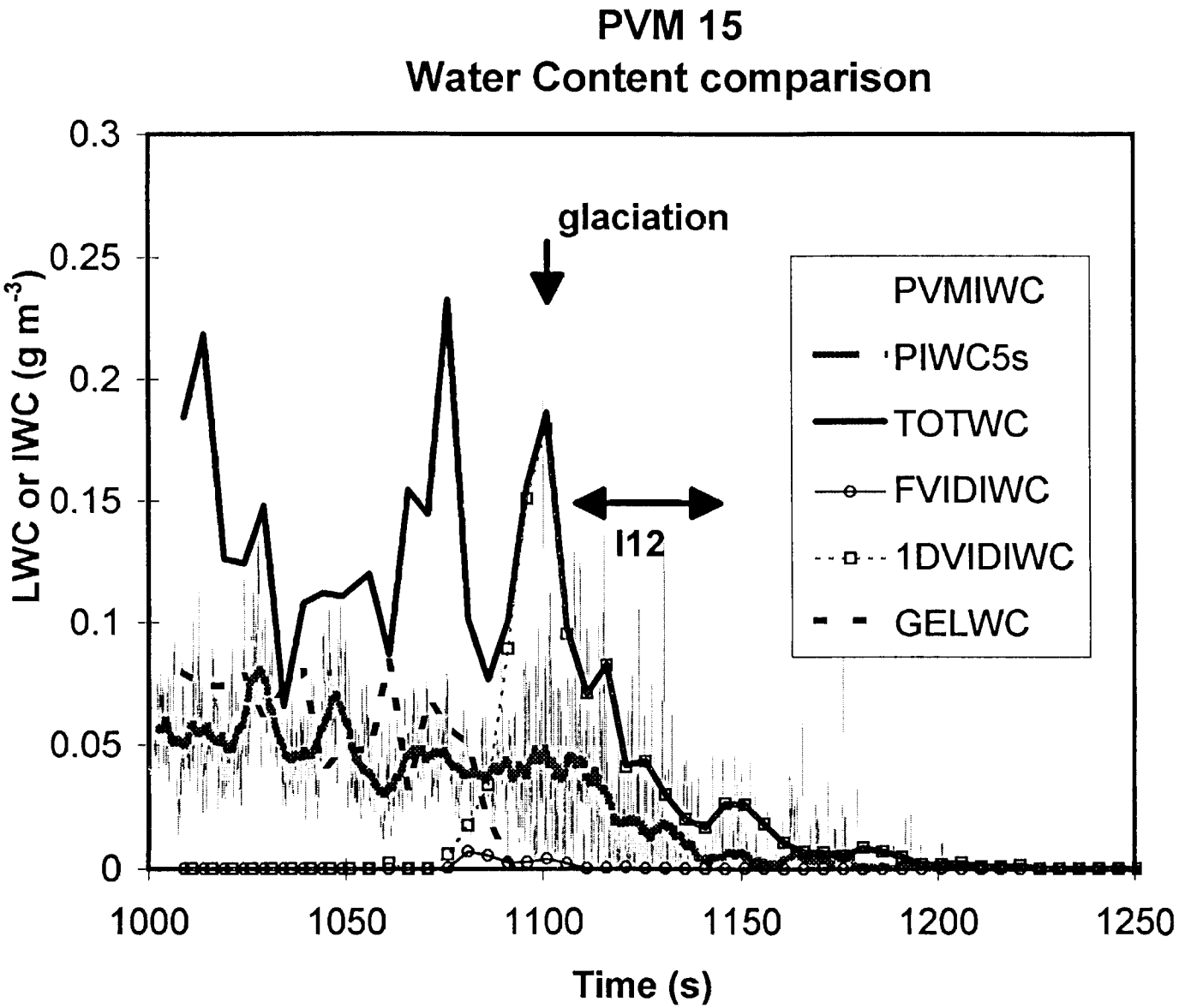
PVM 15
Water Content comparison
glaciation
I12
PVMIWC
PIWC5s
TOTWC
FVIDIWC
1DVIDIWC
GELWC
LWC or IWC (g m-3)
0.3
0.25
0.2
0.15
0.1
0.05
0
1000
1050
1100
1150
1200
1250
Time (s)

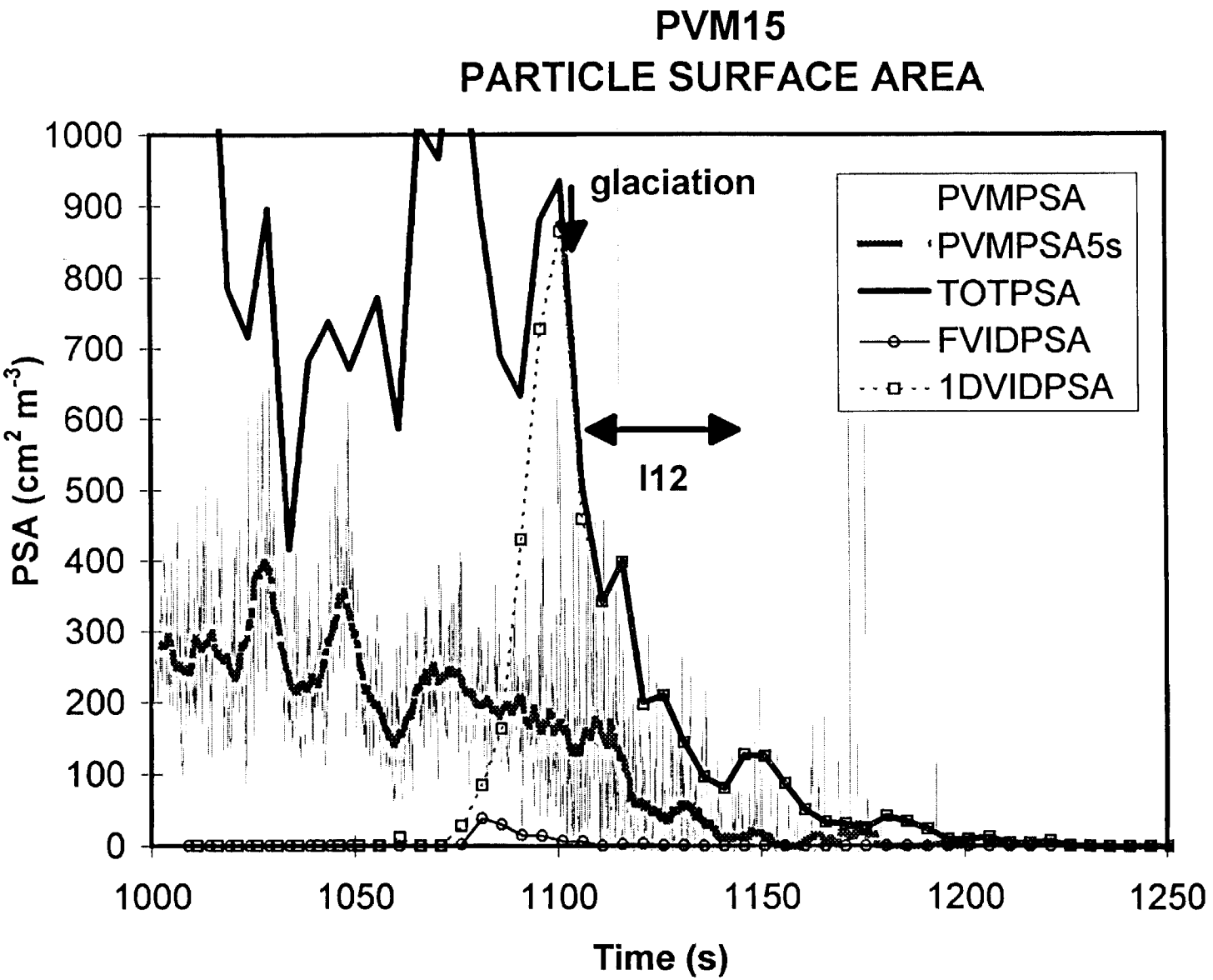
PVM15
PARTICLE SURFACE AREA
glaciation
I12
PVMPSA
PVMPSA5s
TOTPSA
FVIDPSA
1DVIDPSA
PSA (cm2 m-3)
Time (s)
0
100
200
300
400
500
600
700
800
900
1000
1000
1050
1100
1150
1200
1250

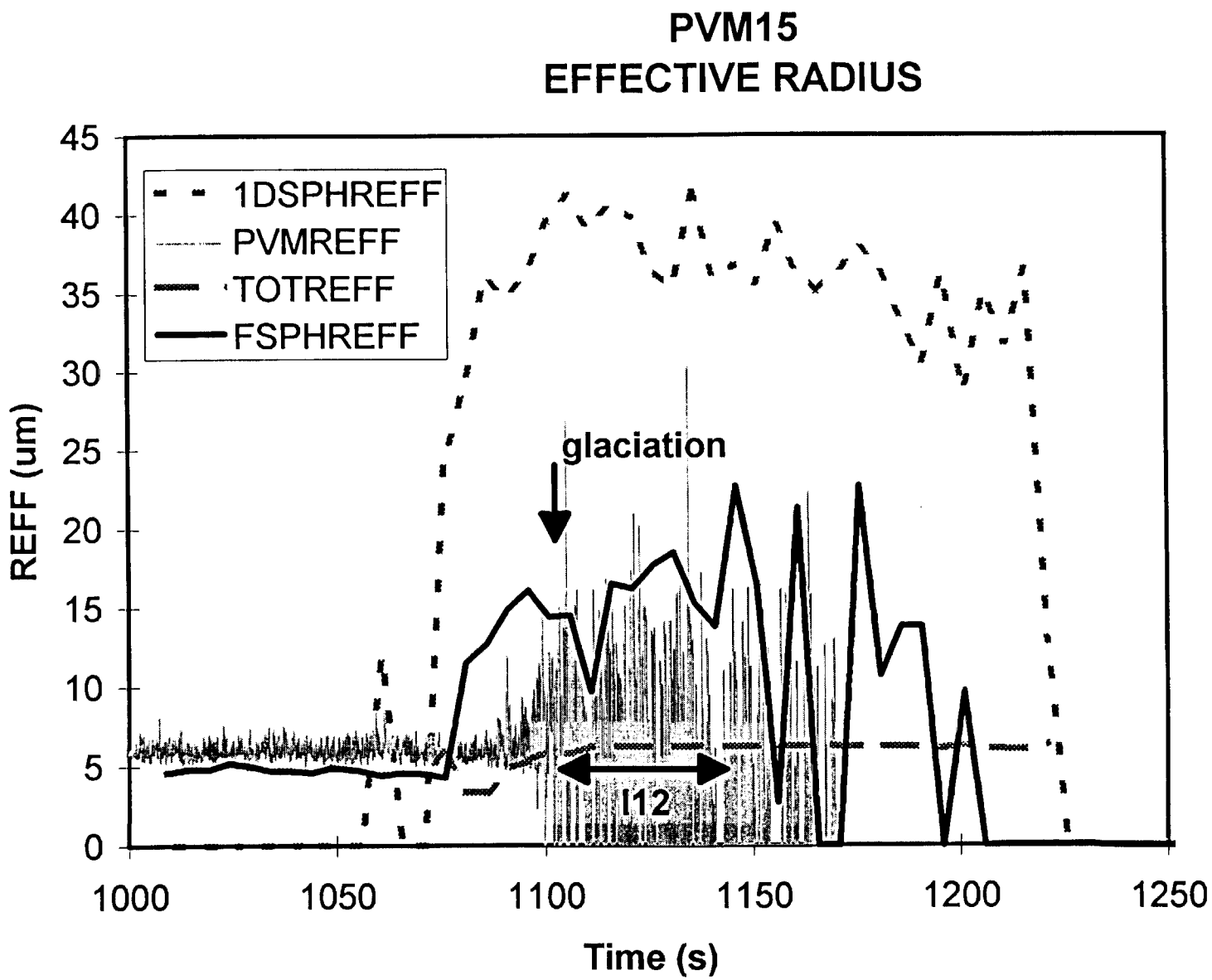
PVM15
EFFECTIVE RADIUS
1DSPHREFF
PVMREFF
TOTREFF
FSPHREFF
glaciation
I12
REFF (um)
Time (s)
0
5
10
15
20
25
30
35
40
45
1000
1050
1100
1150
1200
1250

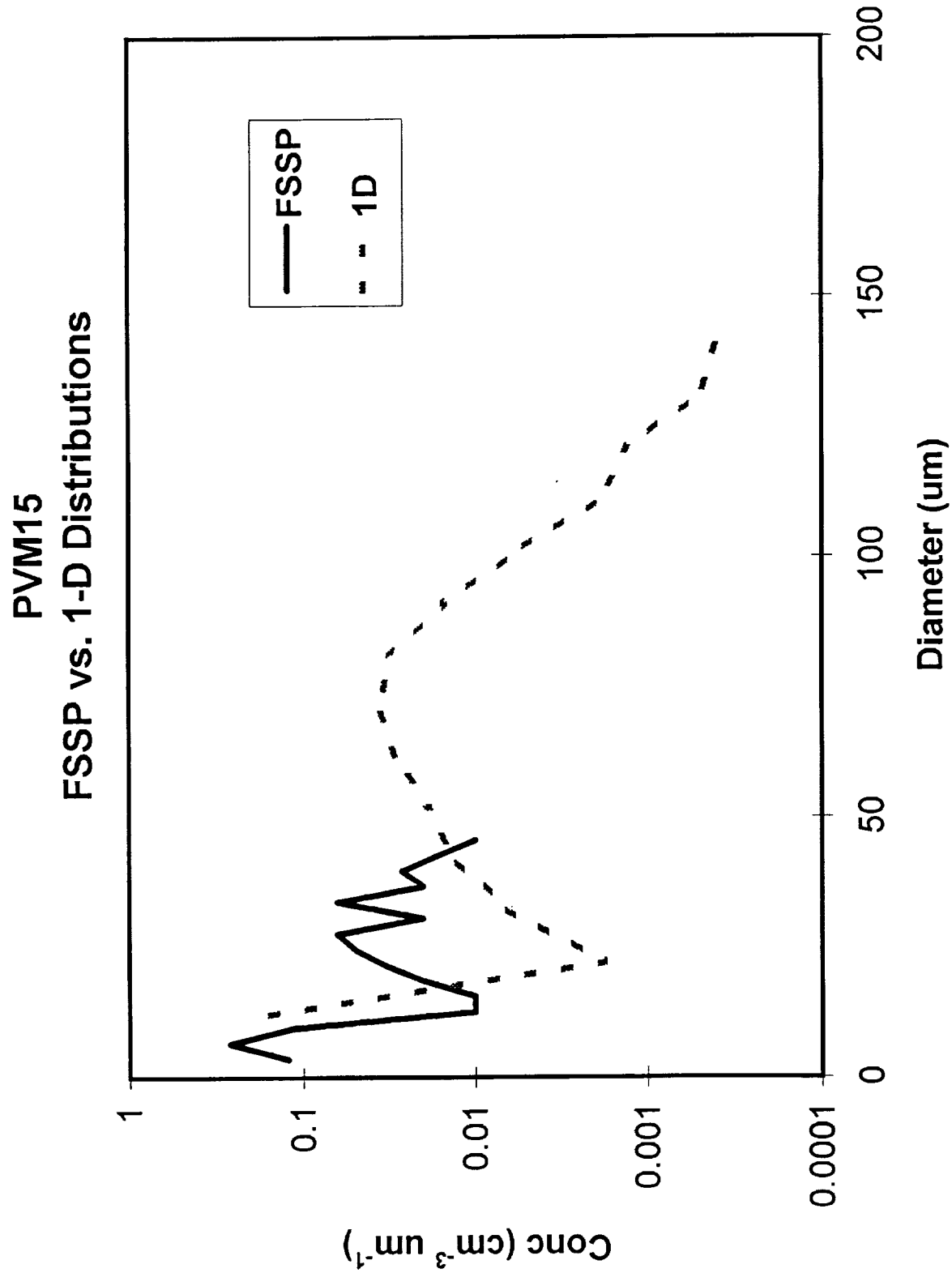
PVM15
FSSP vs. 1-D Distributions
FSSP
1D
Conc (cm-3 um-1)
1
0.1
0.01
0.001
0.0001
0
50
100
150
200
Diameter (um)

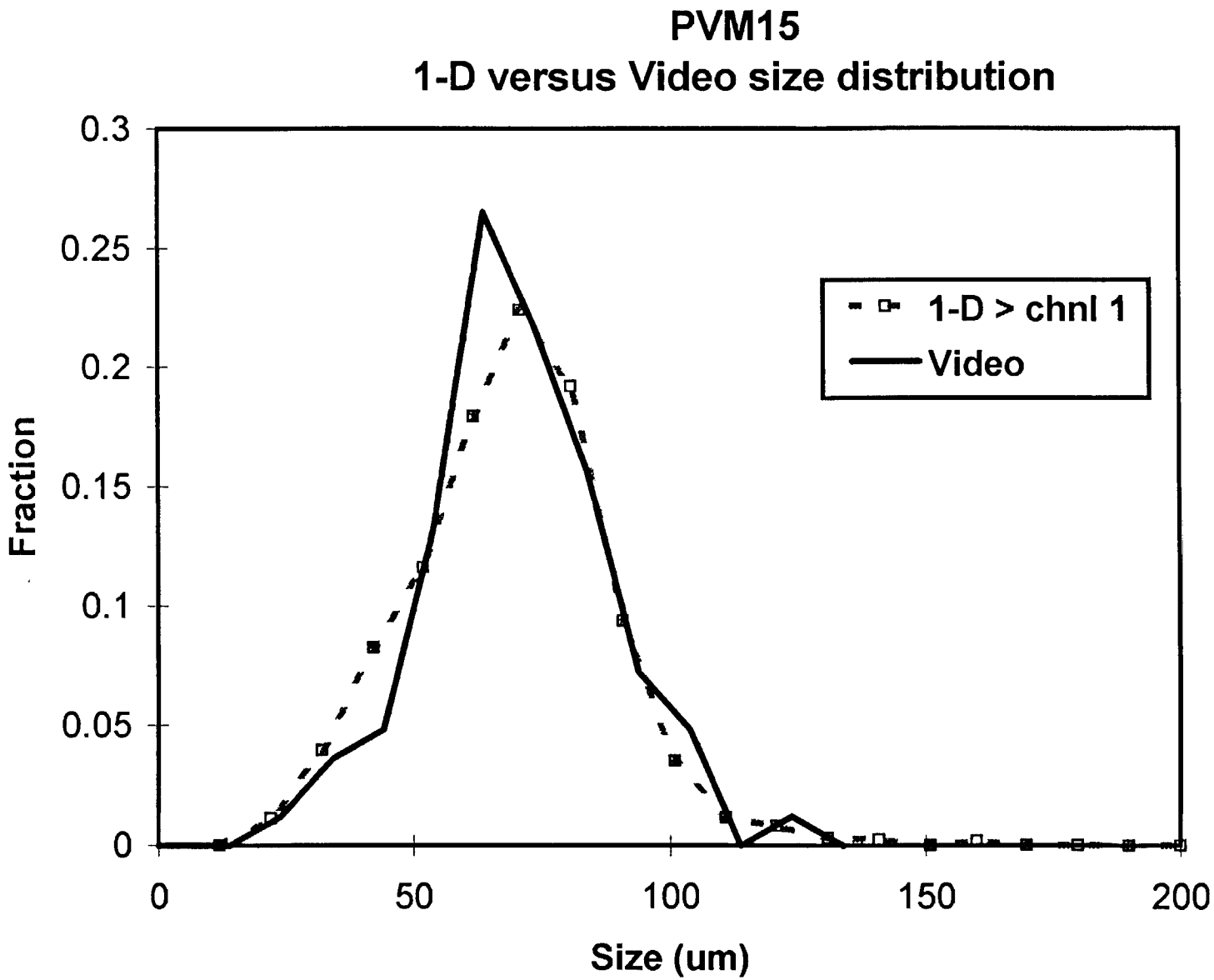
PVM15
1-D versus Video size distribution
Fraction
0.3
0.25
0.2
0.15
0.1
0.05
0
0
50
100
150
200
Size (um)
1-D > chnl 1
Video

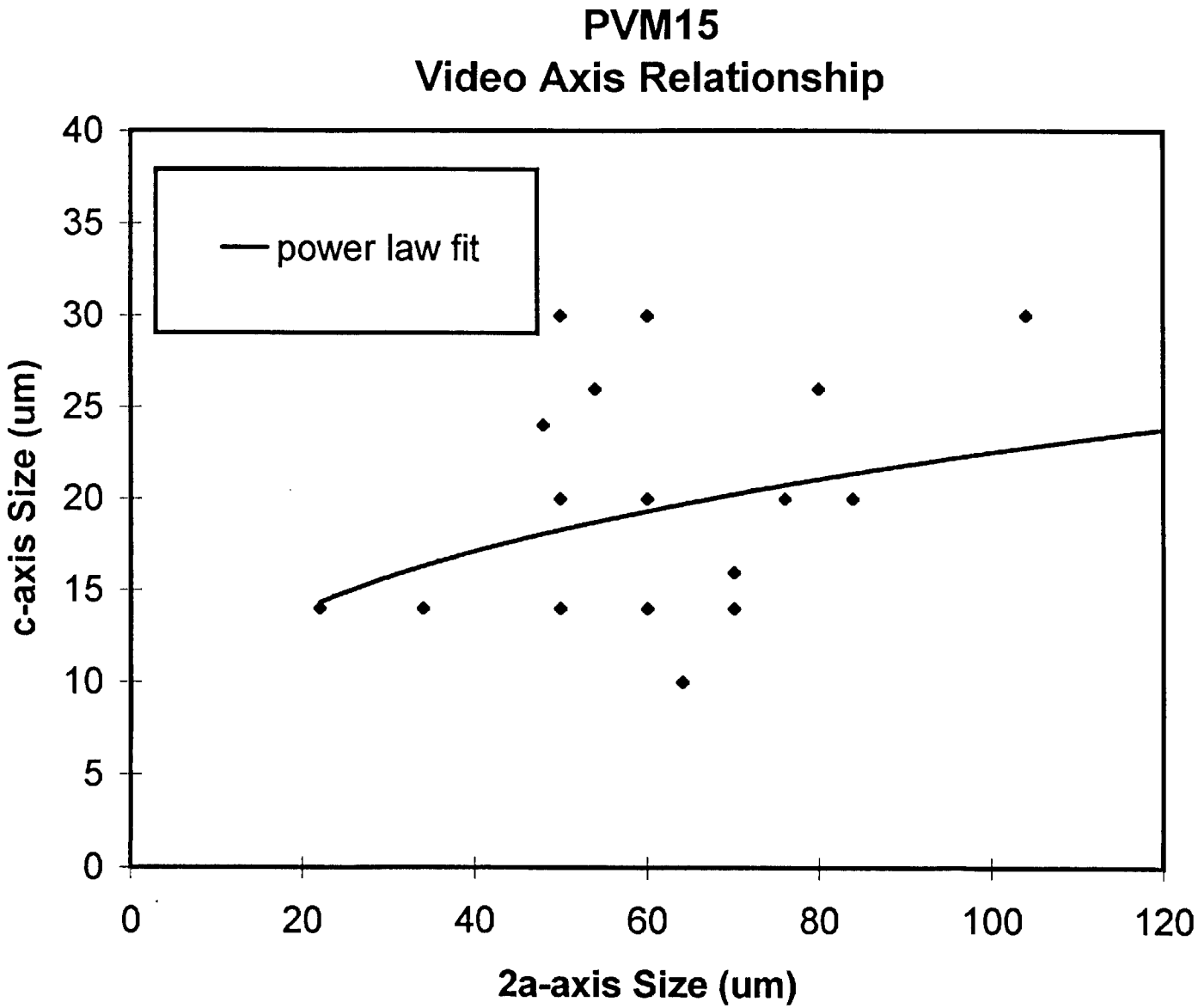
PVM15
Video Axis Relationship
power law fit
c-axis Size (um)
2a-axis Size (um)
0
5
10
15
20
25
30
35
40
0
20
40
60
80
100
120

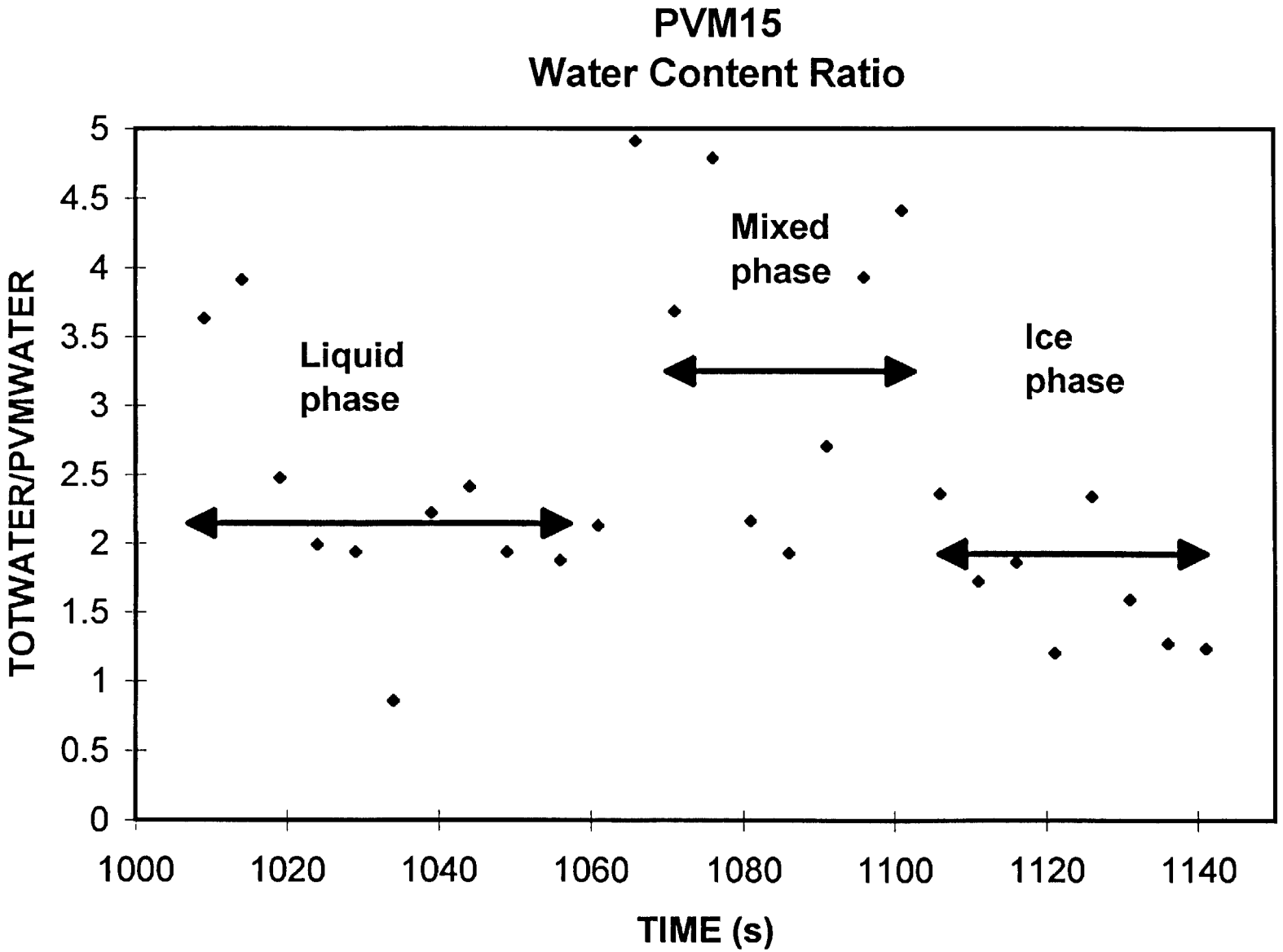
PVM15
Water Content Ratio
TOTWATER/PVMWATER
TIME (s)
Liquid phase
Mixed phase
Ice phase
0
0.5
1
1.5
2
2.5
3
3.5
4
4.5
5
1000
1020
1040
1060
1080
1100
1120
1140

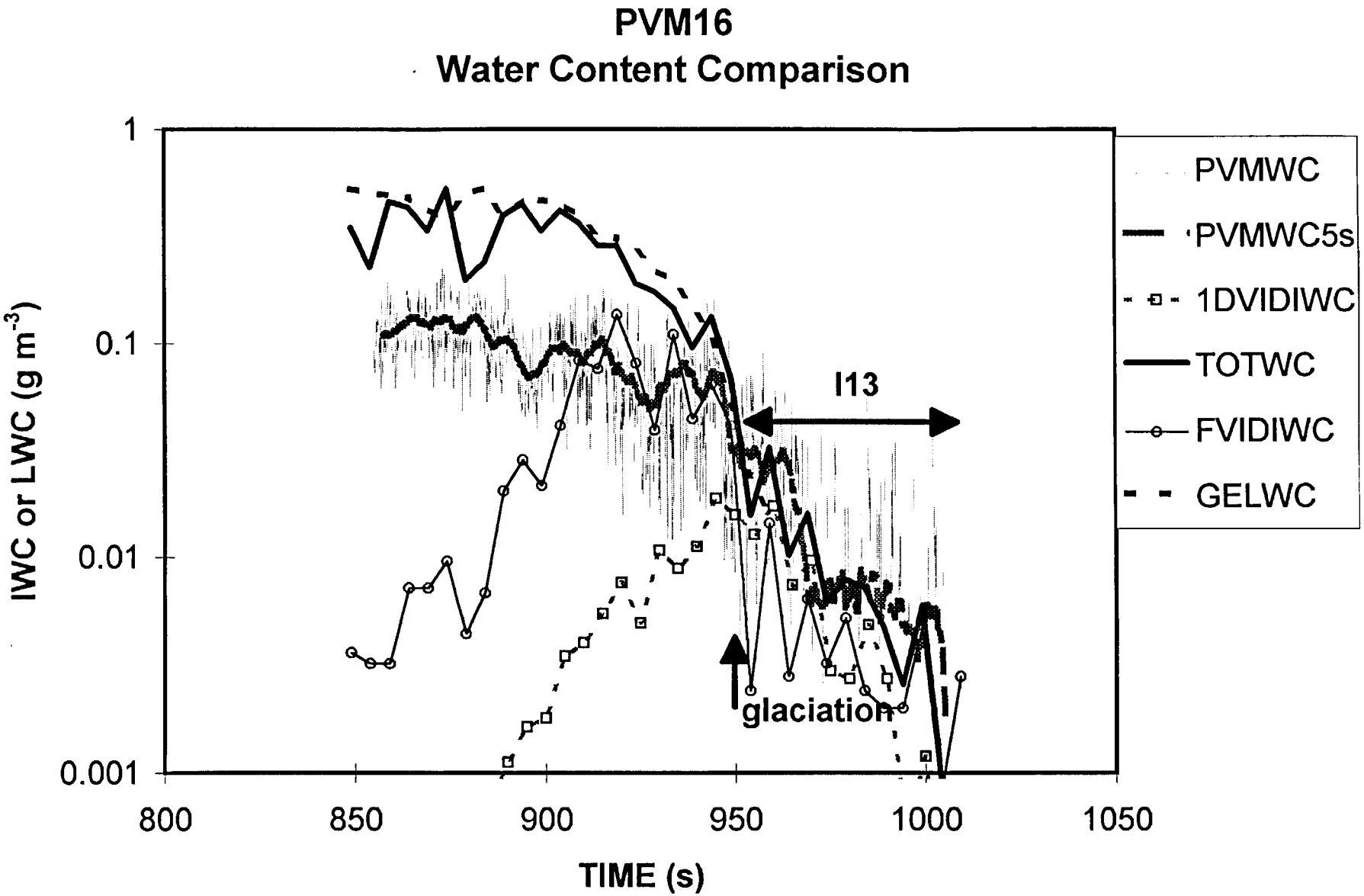
PVM16
Water Content Comparison
IWC or LWC (g m-3)
1
0.1
0.01
0.001
800
850
900
950
1000
1050
TIME (s)
PVMWC
PVMWC5s
1DVIDIWC
TOTWC
FVIDIWC
GELWC
I13
glaciation

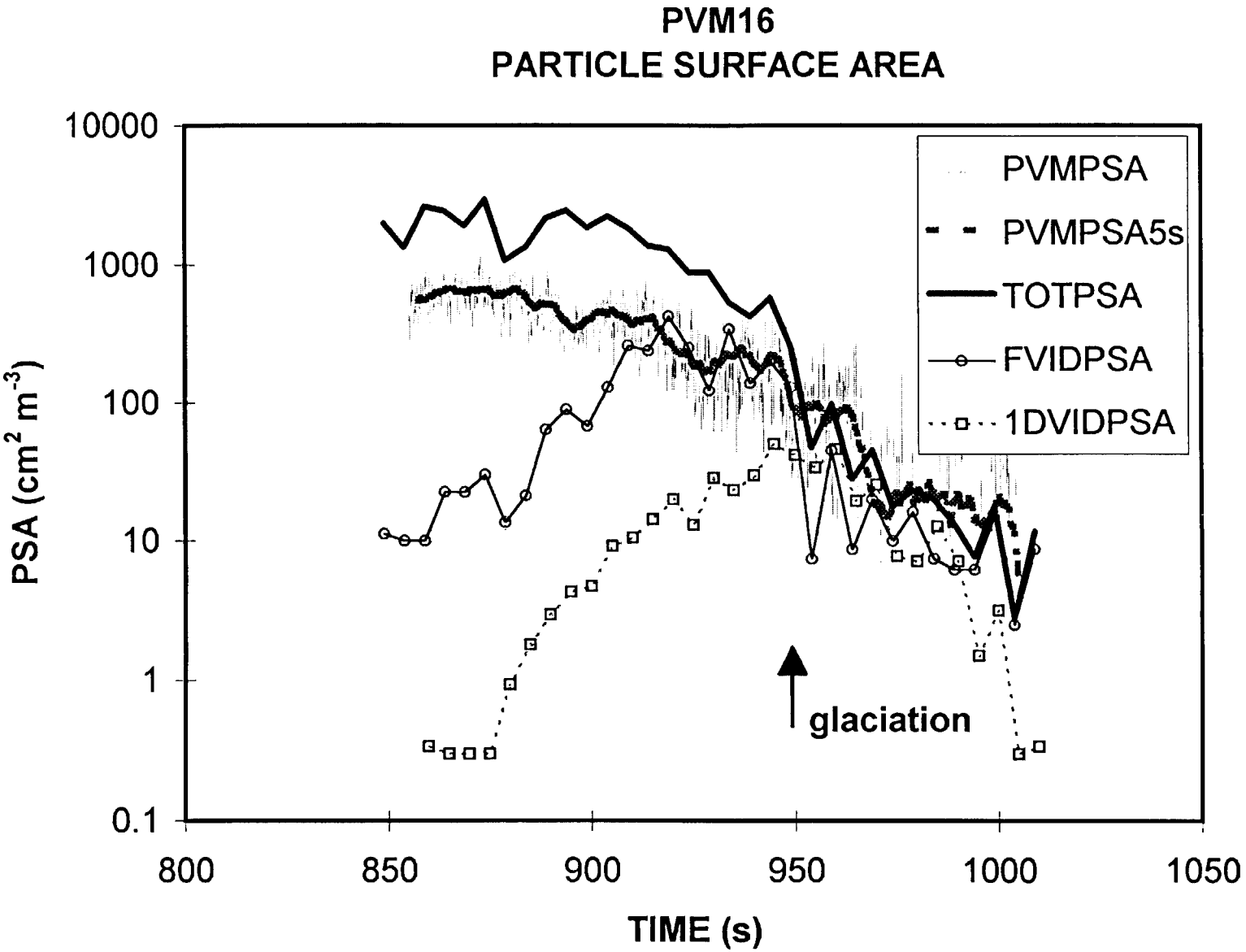
PVM16
PARTICLE SURFACE AREA
PSA (cm$^2$ m$^{-3}$)
10000
1000
100
10
1
0.1
800
850
900
950
1000
1050
TIME (s)
PVMPSA
PVMPSA5s
TOTPSA
FVIDPSA
1DVIDPSA
glaciation

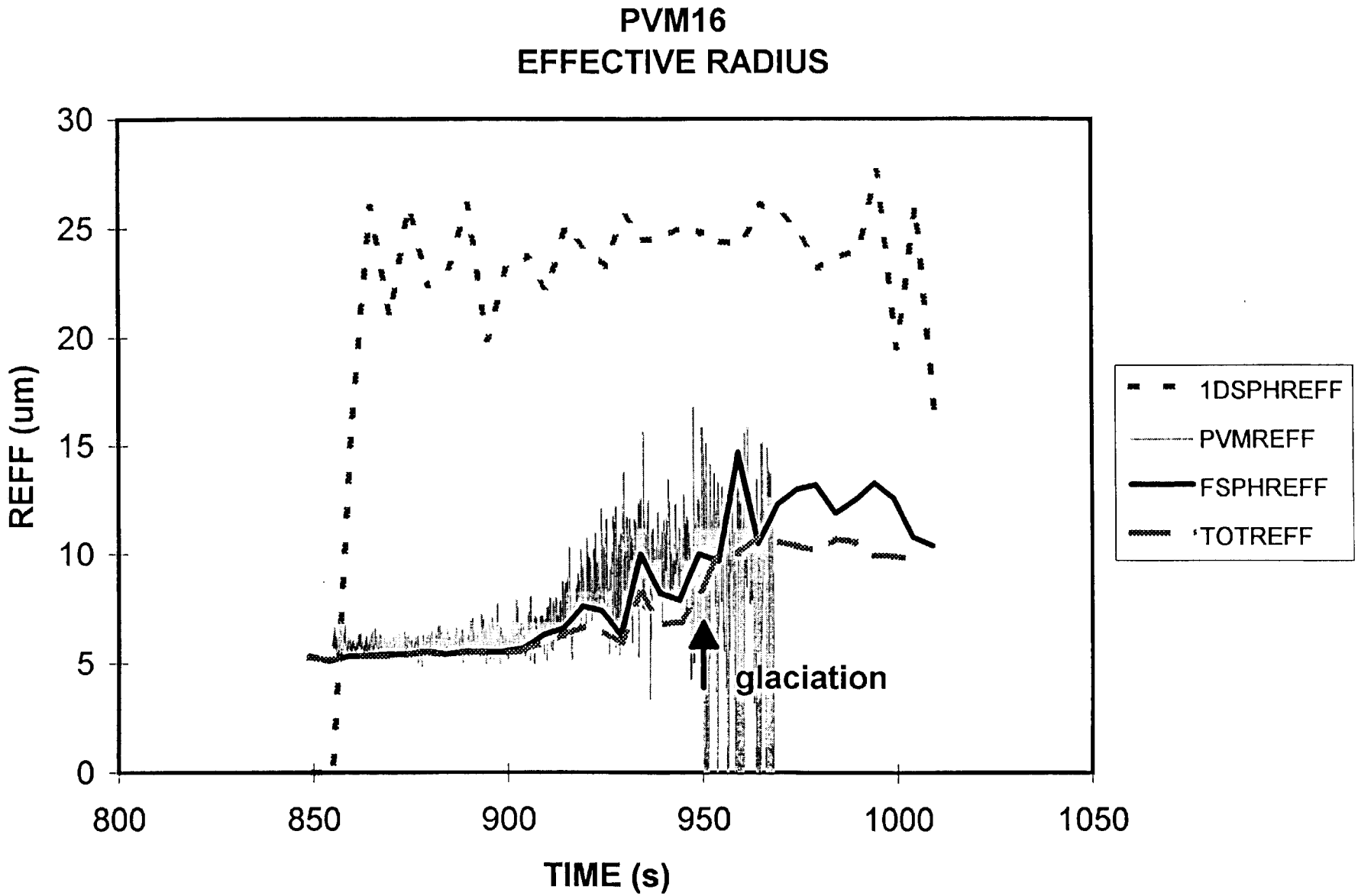
PVM16
EFFECTIVE RADIUS
REFF (um)
TIME (s)
30
25
20
15
10
5
0
800
850
900
950
1000
1050
glaciation
1DSPHREFF
PVMREFF
FSPHREFF
'TOTREFF

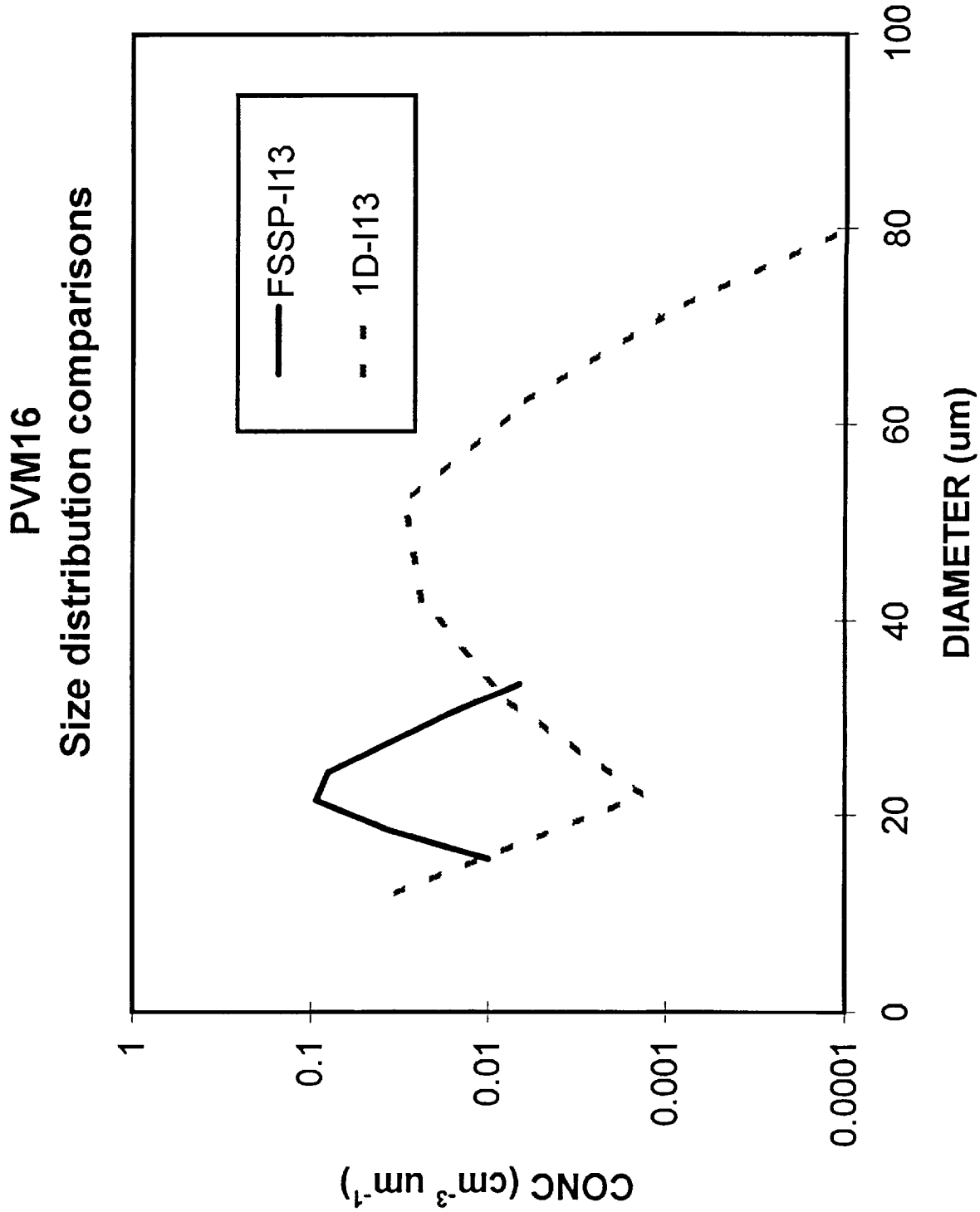
PVM16
Size distribution comparisons
FSSP-I13
1D-I13
CONC (cm-3 um-1)
1
0.1
0.01
0.001
0.0001
0
20
40
60
80
100
DIAMETER (um)

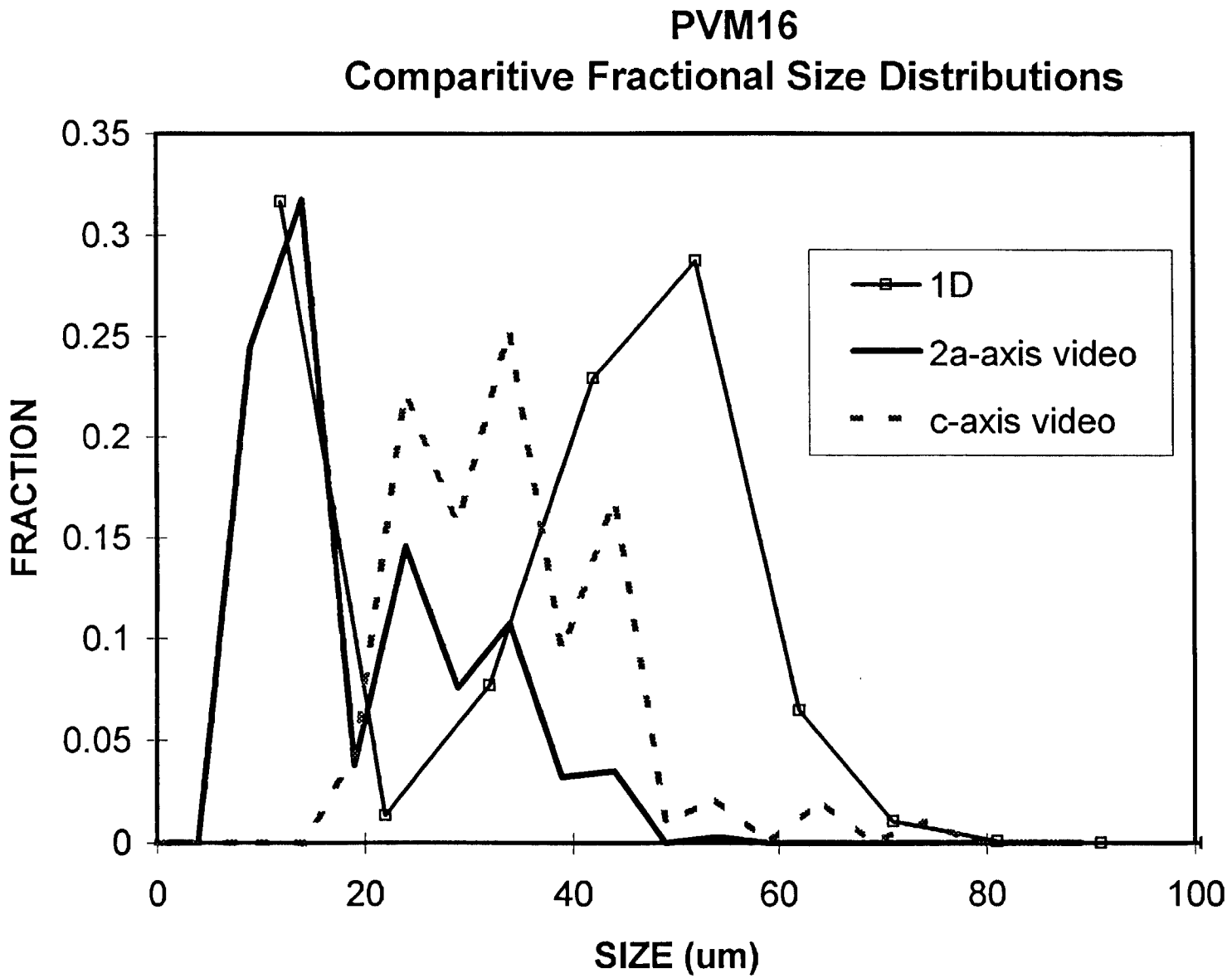
PVM16
Comparitive Fractional Size Distributions
FRACTION
0.35
0.3
0.25
0.2
0.15
0.1
0.05
0
0
20
40
60
80
100
SIZE (um)
1D
2a-axis video
c-axis video

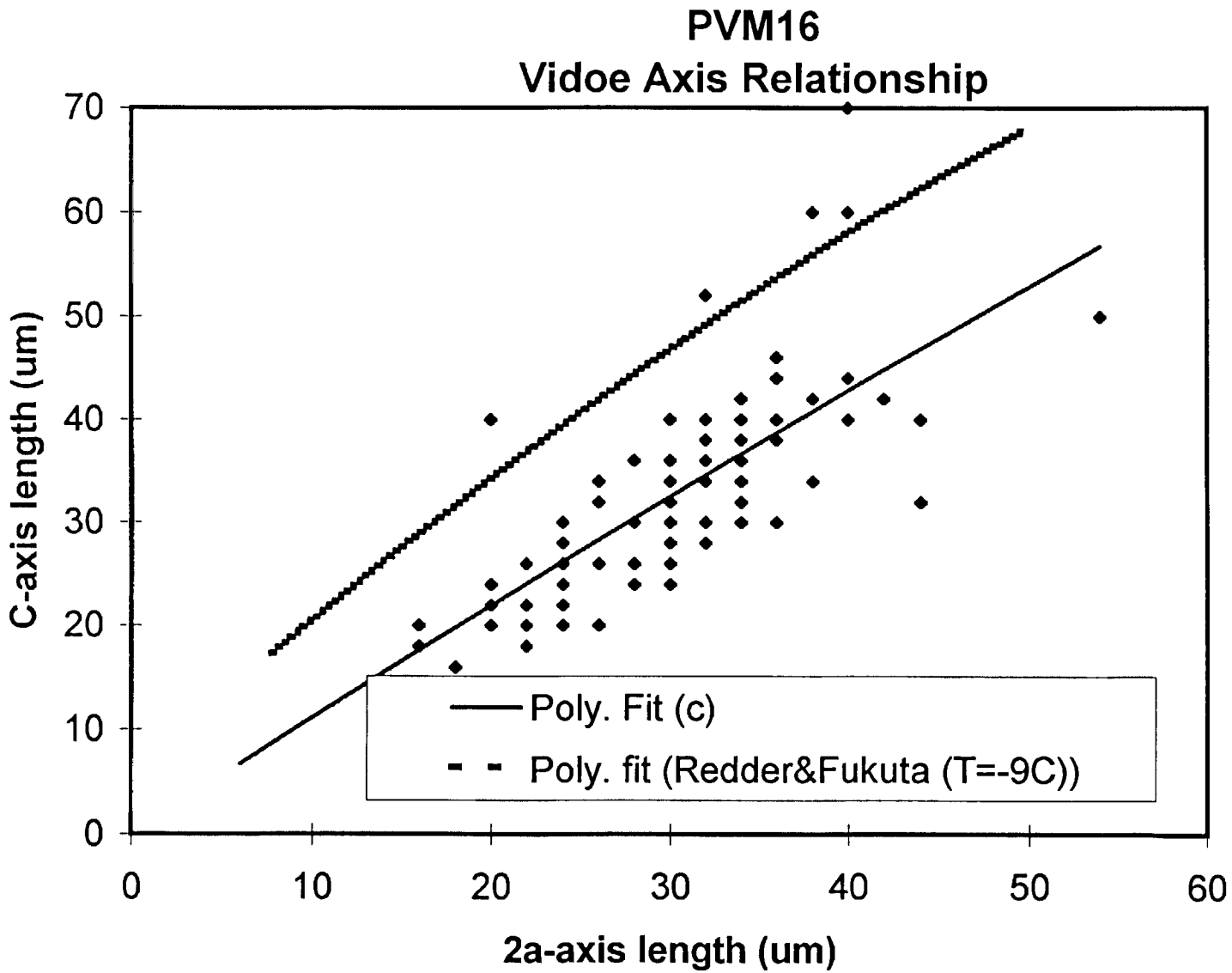
PVM16
Vidoe Axis Relationship
C-axis length (um)
2a-axis length (um)
0
10
20
30
40
50
60
70
Poly. Fit (c)
Poly. fit (Redder&Fukuta (T=-9C))

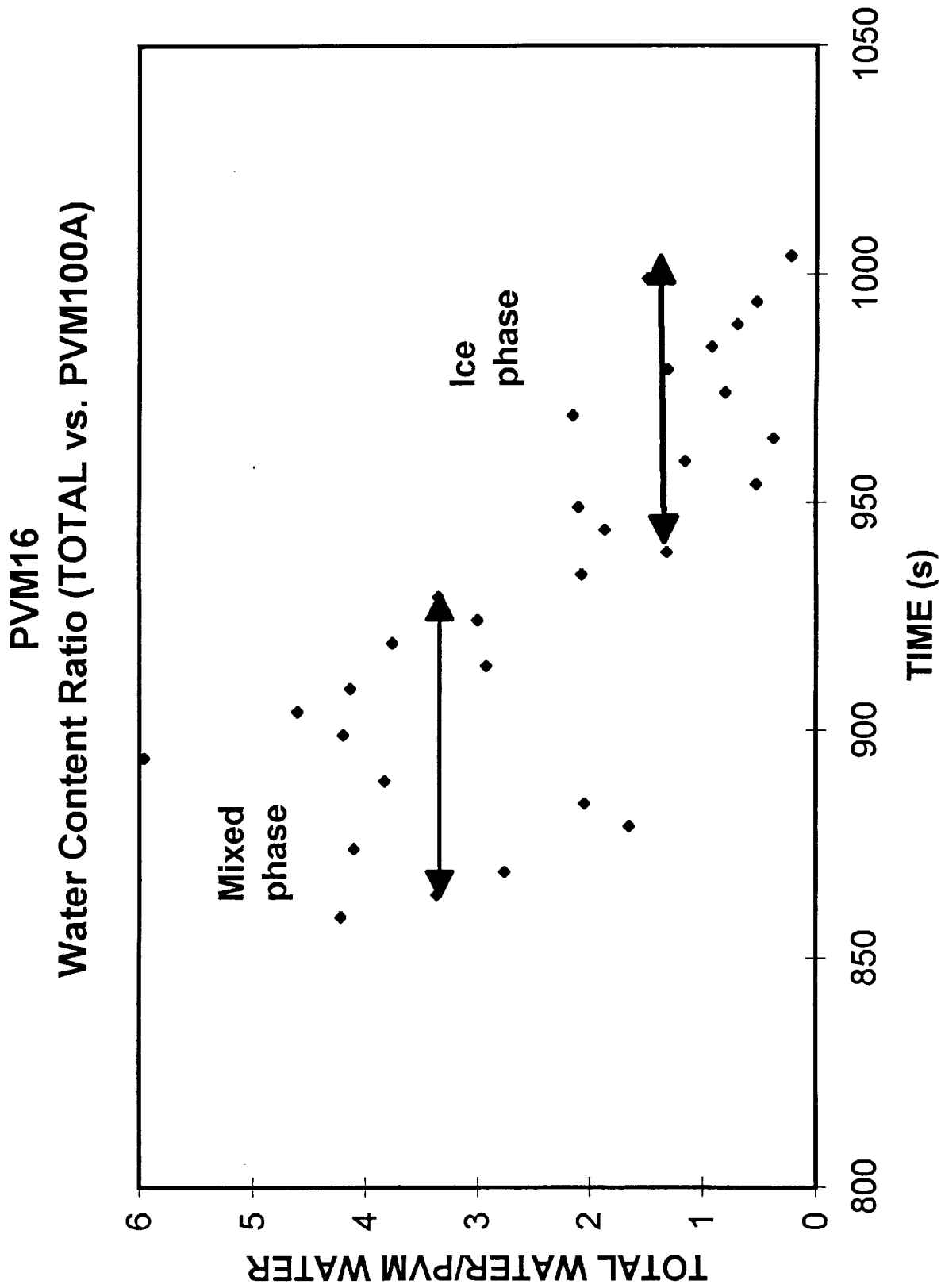
PVM16
Water Content Ratio (TOTAL vs. PVM100A)
TOTAL WATER/PVM WATER
TIME (s)
Mixed phase
Ice phase
0
1
2
3
4
5
6
800
850
900
950
1000
1050

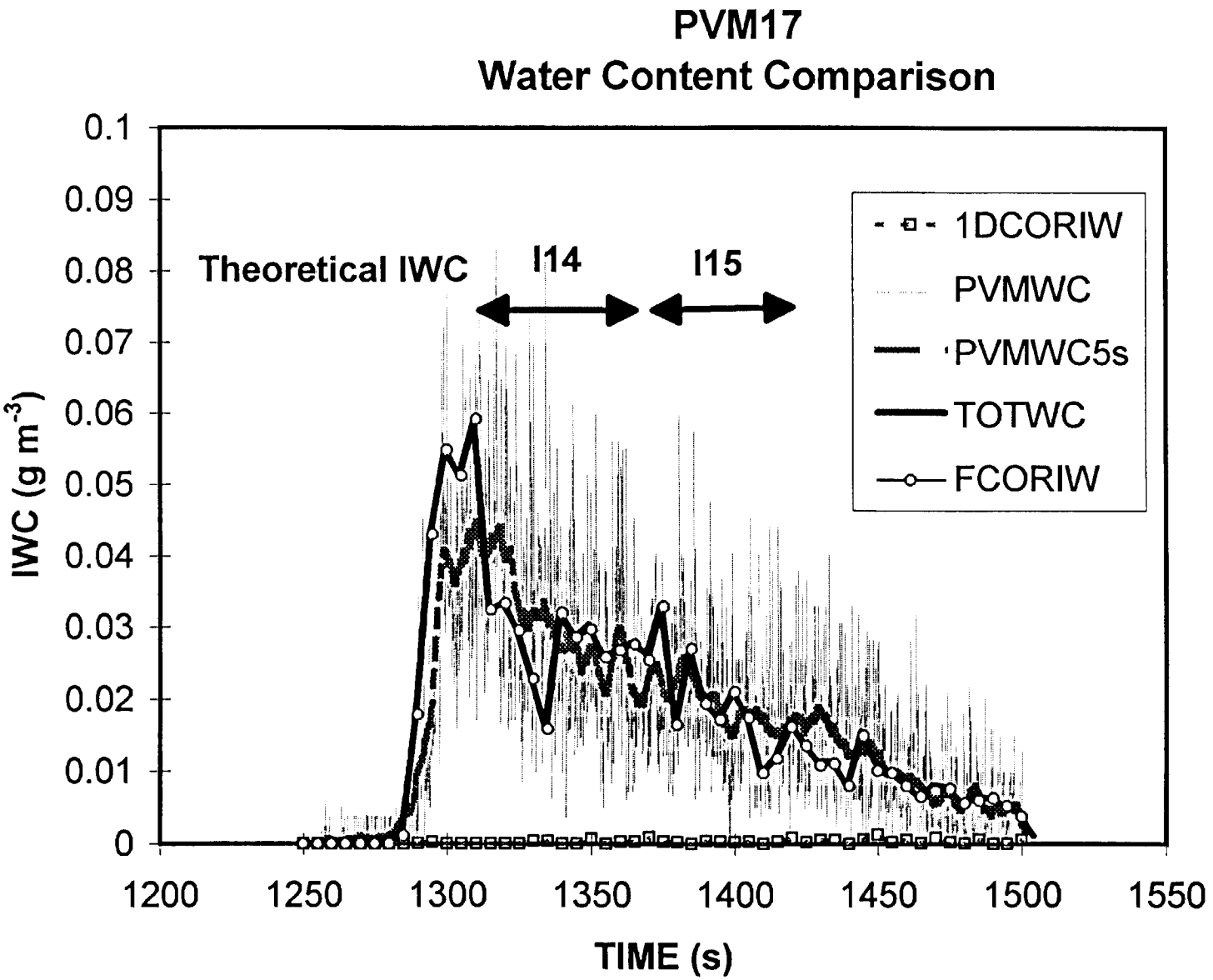
PVM17
Water Content Comparison
Theoretical IWC
I14
I15
1DCORIW
PVMWC
PVMWC5s
TOTWC
FCORIW
IWC (g m-3)
TIME (s)
0.1
0.09
0.08
0.07
0.06
0.05
0.04
0.03
0.02
0.01
0
1200
1250
1300
1350
1400
1450
1500
1550

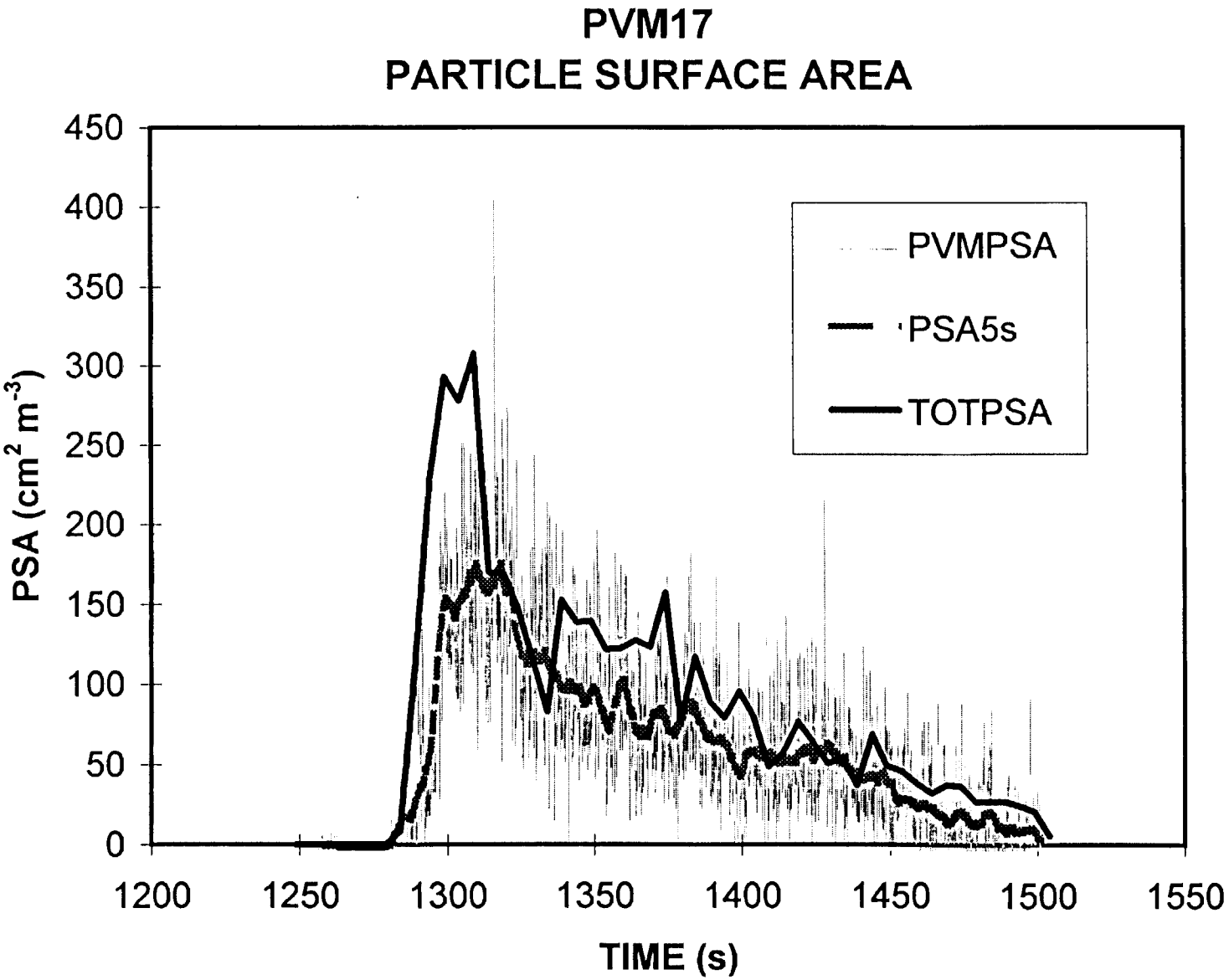
PVM17
PARTICLE SURFACE AREA
PSA (cm2 m-3)
TIME (s)
PVMPSA
PSA5s
TOTPSA
0
50
100
150
200
250
300
350
400
450
1200
1250
1300
1350
1400
1450
1500
1550

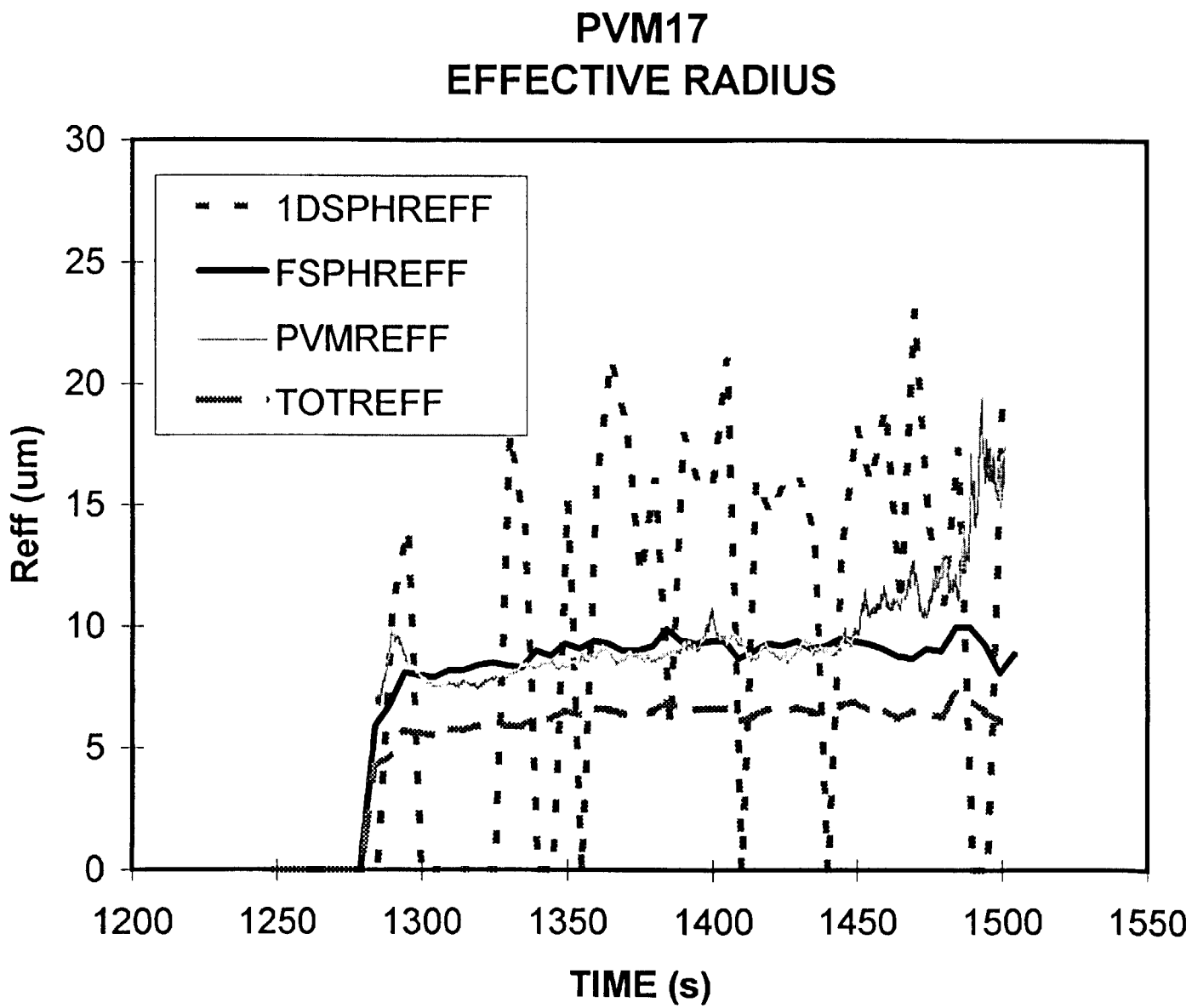
PVM17
EFFECTIVE RADIUS
1DSPHREFF
FSPHREFF
PVMREFF
TOTREFF
Reff (um)
TIME (s)
0
5
10
15
20
25
30
1200
1250
1300
1350
1400
1450
1500
1550

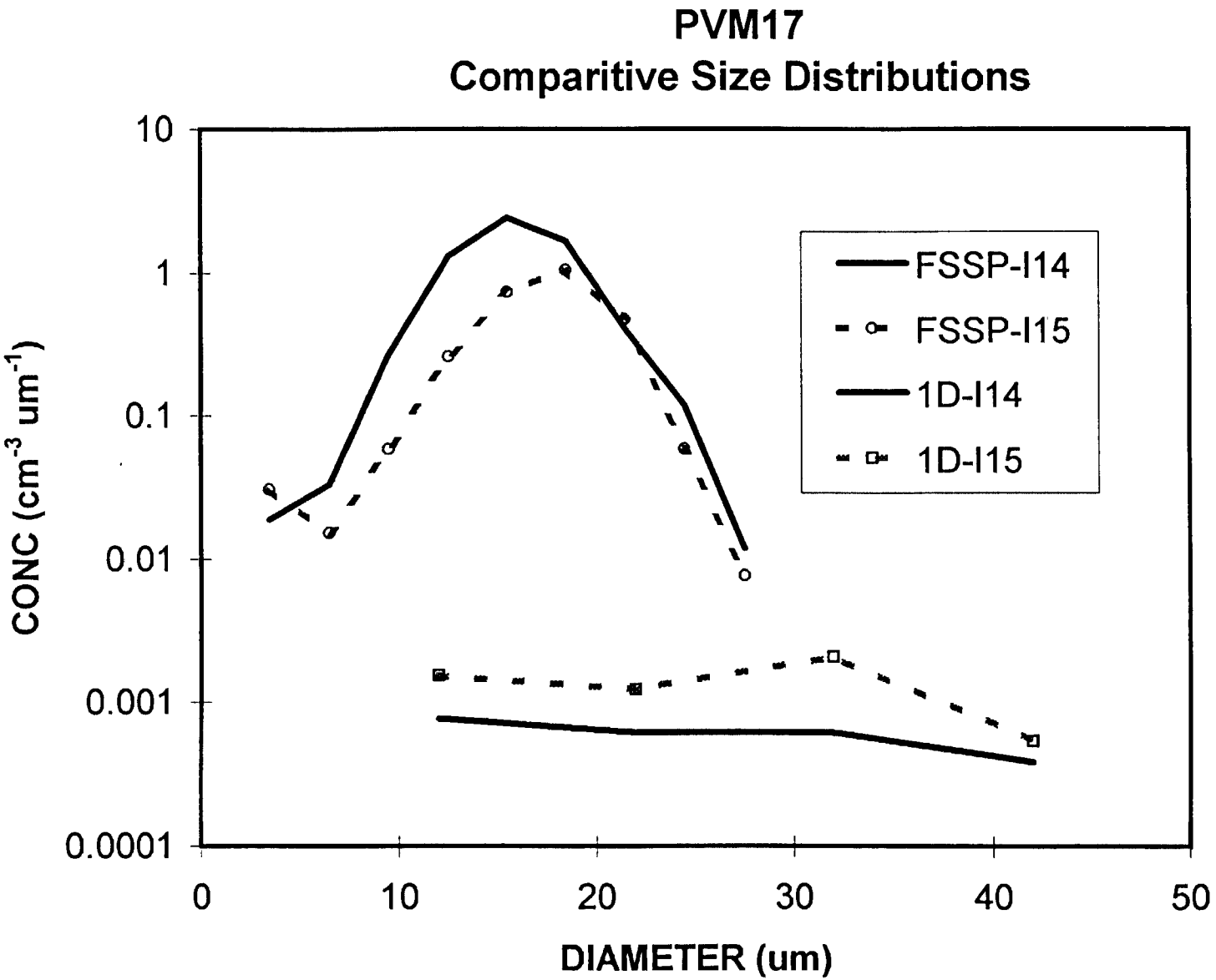
PVM17
Comparitive Size Distributions
CONC (cm-3 um-1)
10
1
0.1
0.01
0.001
0.0001
0
10
20
30
40
50
DIAMETER (um)
FSSP-I14
FSSP-I15
1D-I14
1D-I15

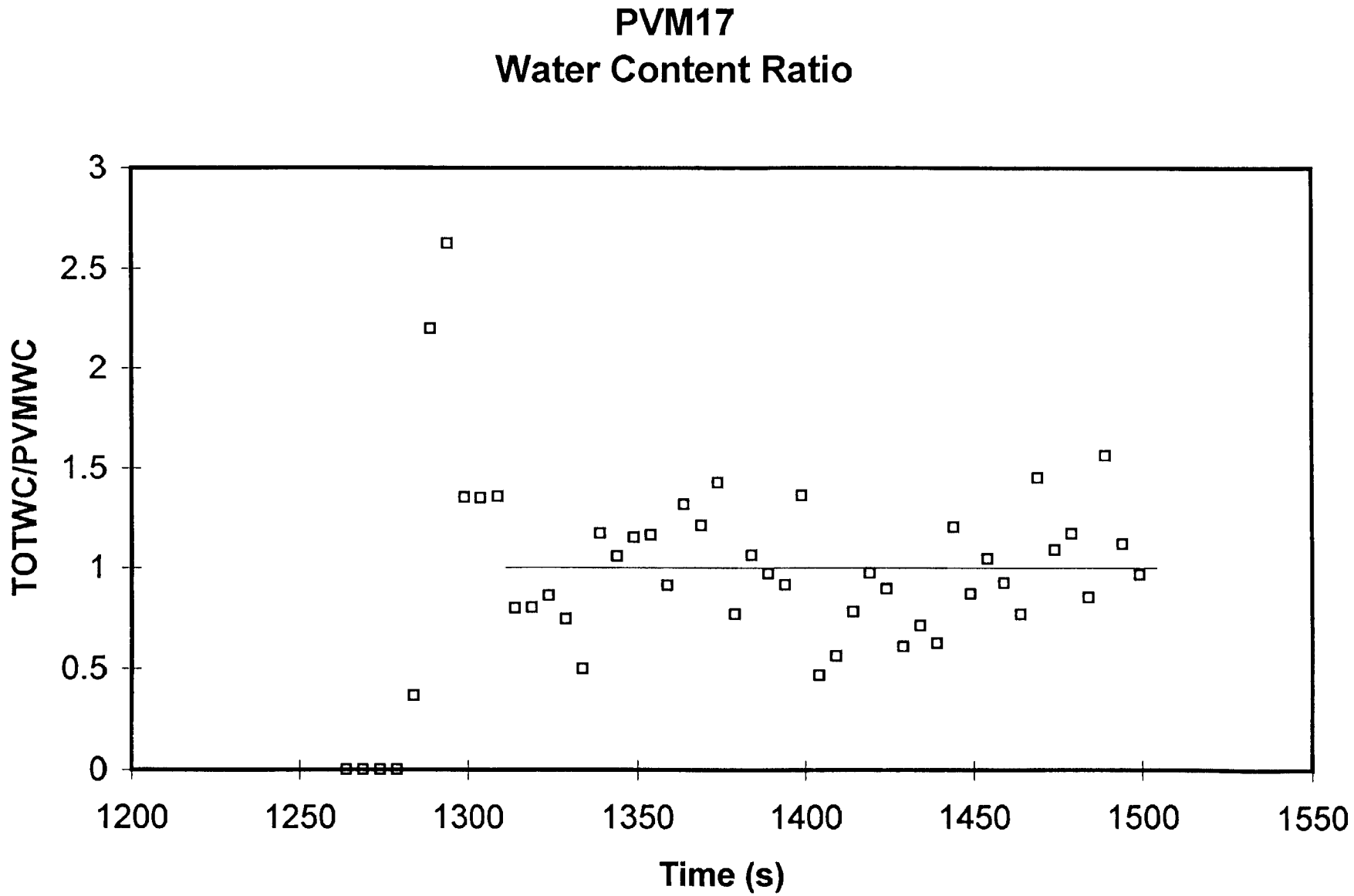
PVM17
Water Content Ratio
TOTWC/PVMWC
3
2.5
2
1.5
1
0.5
0
1200
1250
1300
1350
1400
1450
1500
1550
Time (s)

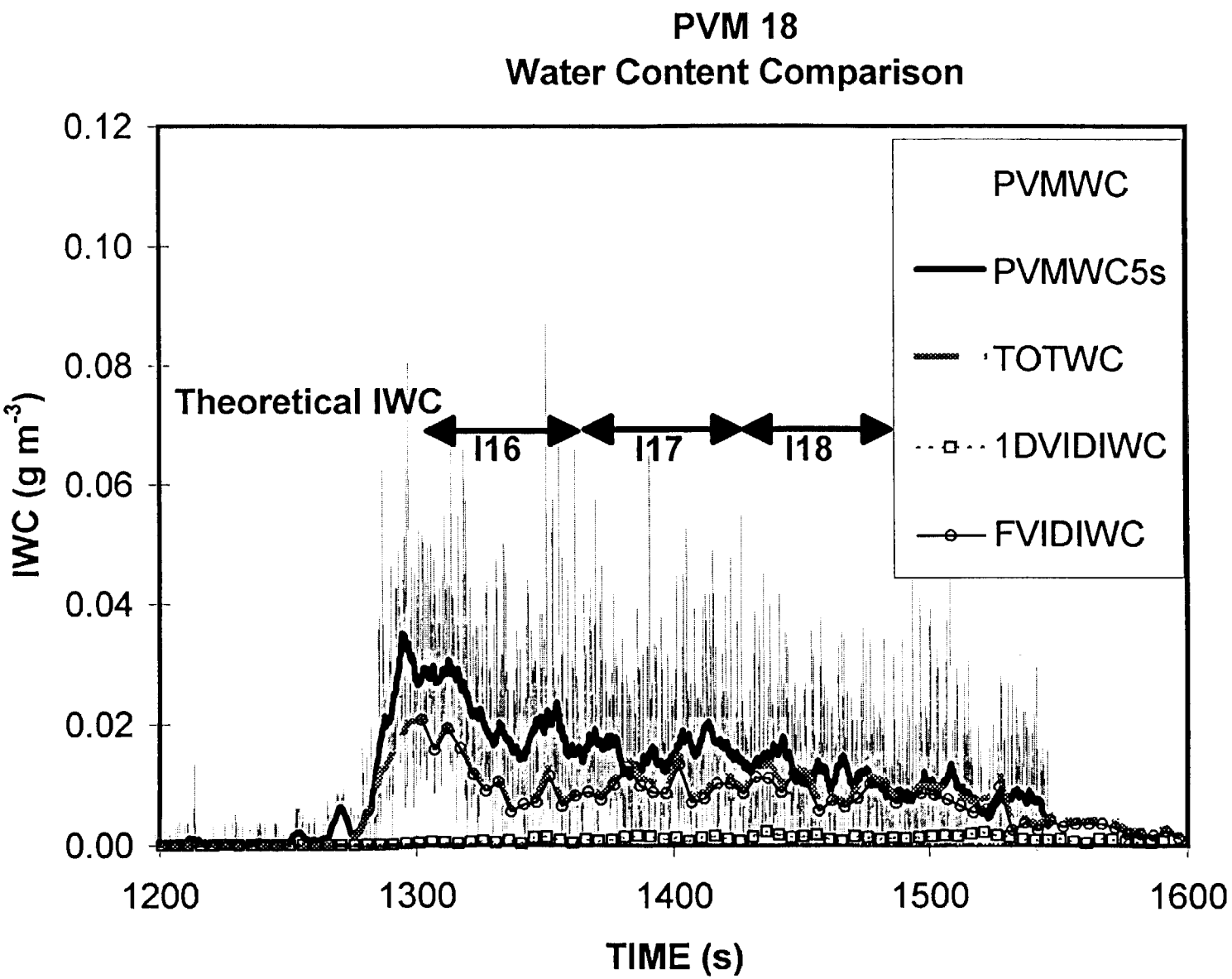
PVM 18
Water Content Comparison
0.12
0.10
0.08
0.06
0.04
0.02
0.00
IWC (g m-3)
Theoretical IWC
I16
I17
I18
PVMWC
PVMWC5s
TOTWC
1DVIDIWC
FVIDIWC
1200
1300
1400
1500
1600
TIME (s)

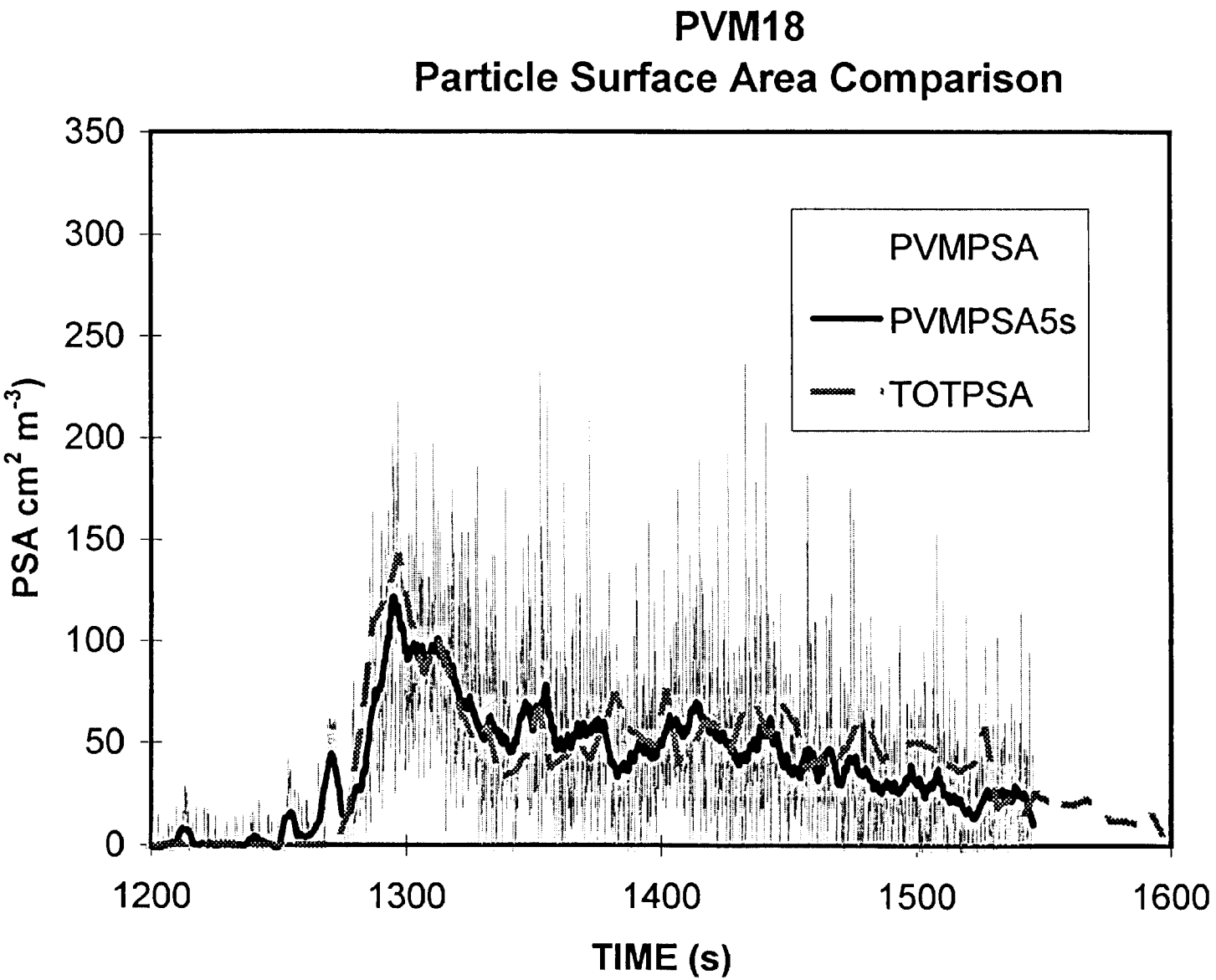
PVM18
Particle Surface Area Comparison
PSA cm$^2$ m$^{-3}$)
350
300
250
200
150
100
50
0
1200
1300
1400
1500
1600
TIME (s)
PVMPSA
PVMPSA5s
TOTPSA

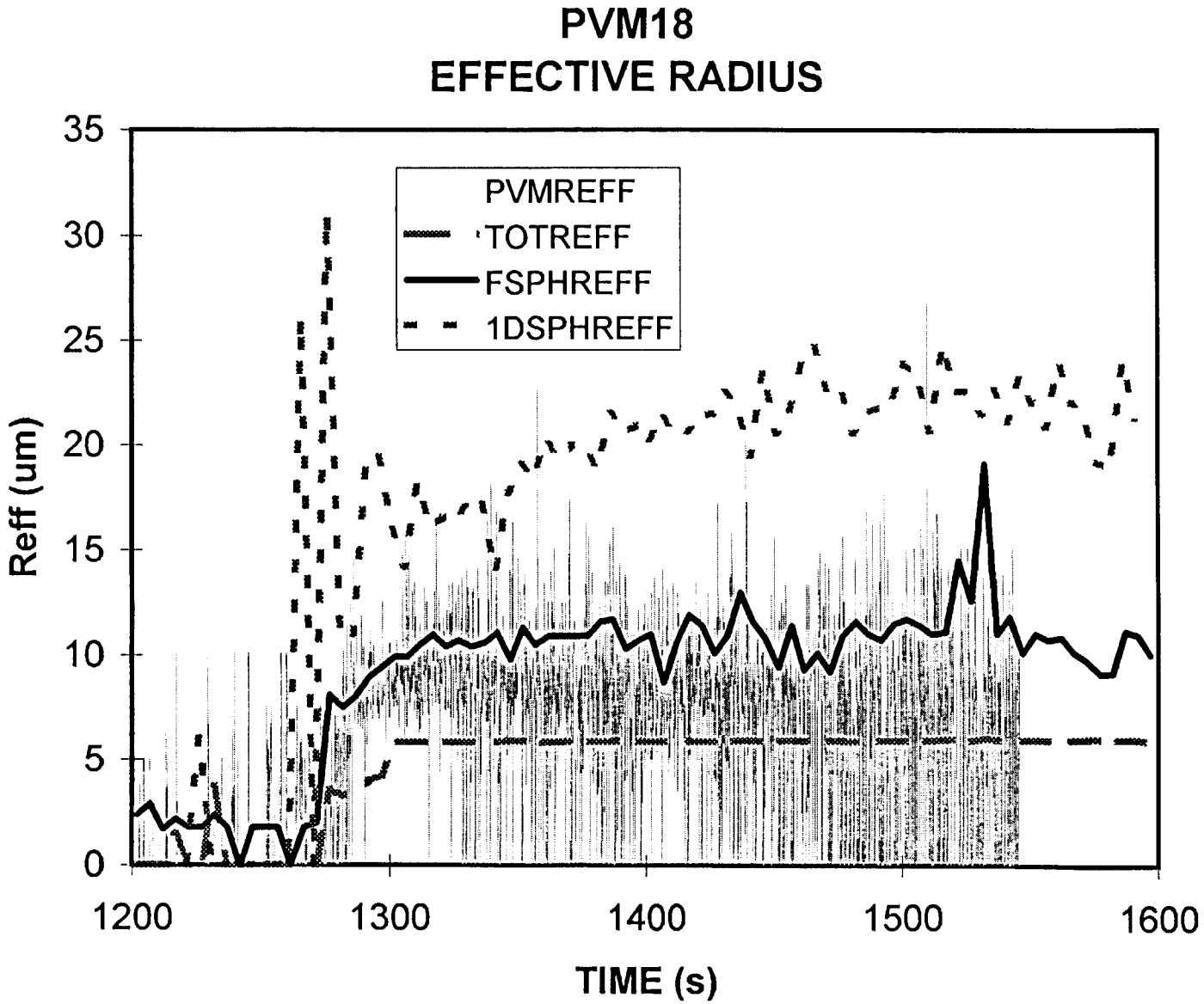
PVM18
EFFECTIVE RADIUS
PVMREFF
TOTREFF
FSPHREFF
1DSPHREFF
Reff (um)
TIME (s)
0
5
10
15
20
25
30
35
1200
1300
1400
1500
1600

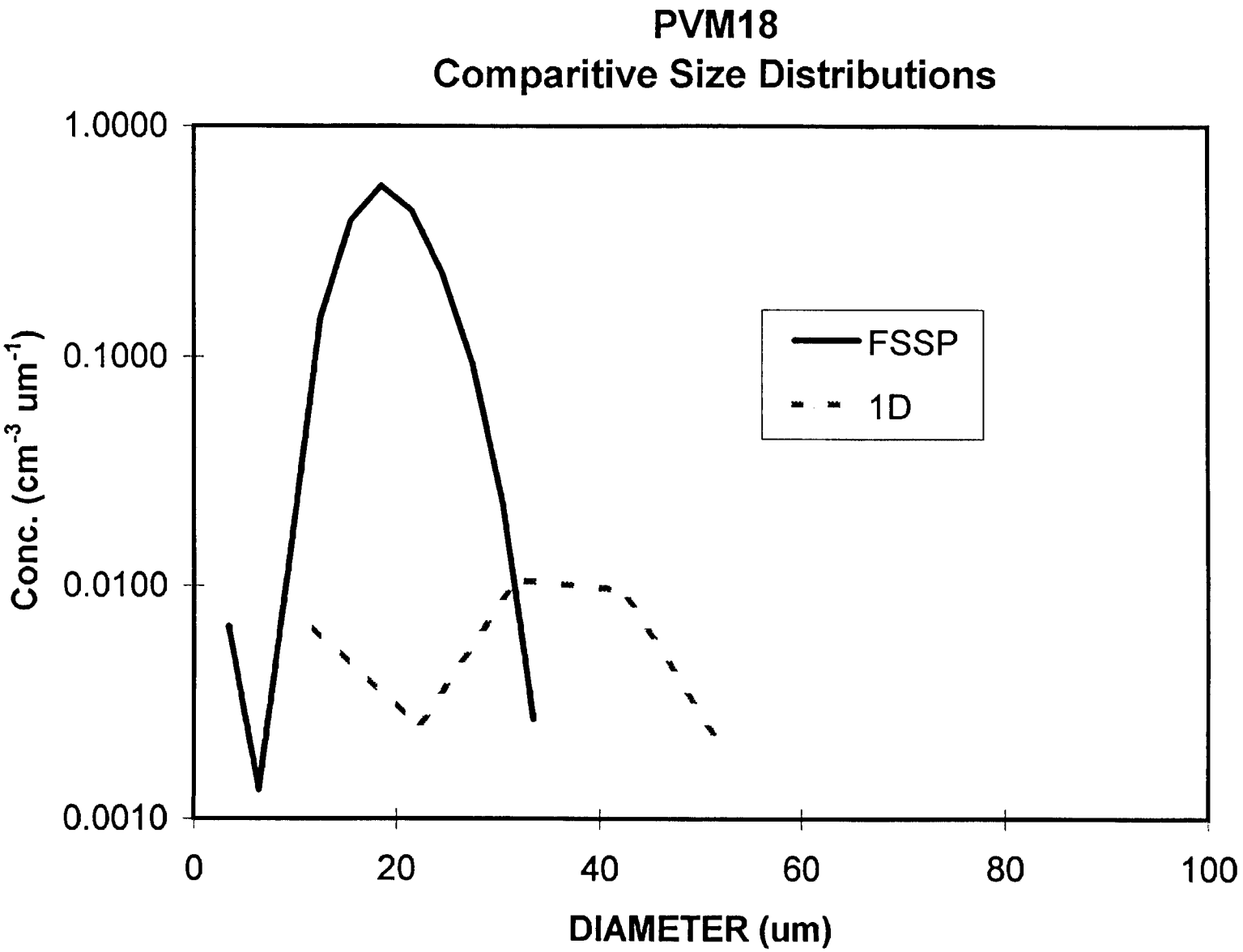
PVM18
Comparitive Size Distributions
1.0000
0.1000
0.0100
0.0010
Conc. (cm-3 um-1)
FSSP
1D
0
20
40
60
80
100
DIAMETER (um)

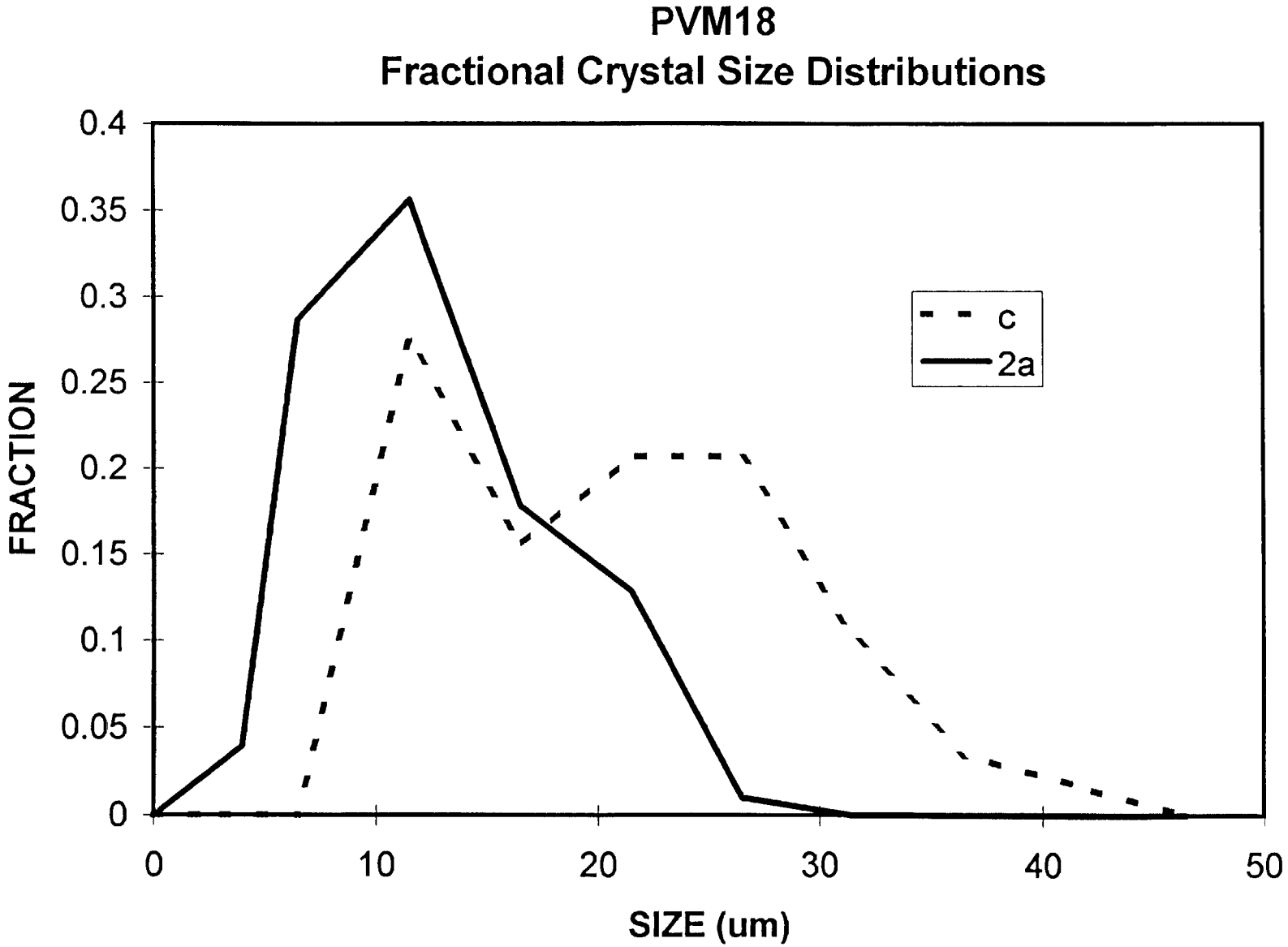
PVM18
Fractional Crystal Size Distributions
FRACTION
0.4
0.35
0.3
0.25
0.2
0.15
0.1
0.05
0
0
10
20
30
40
50
SIZE (um)
c
2a

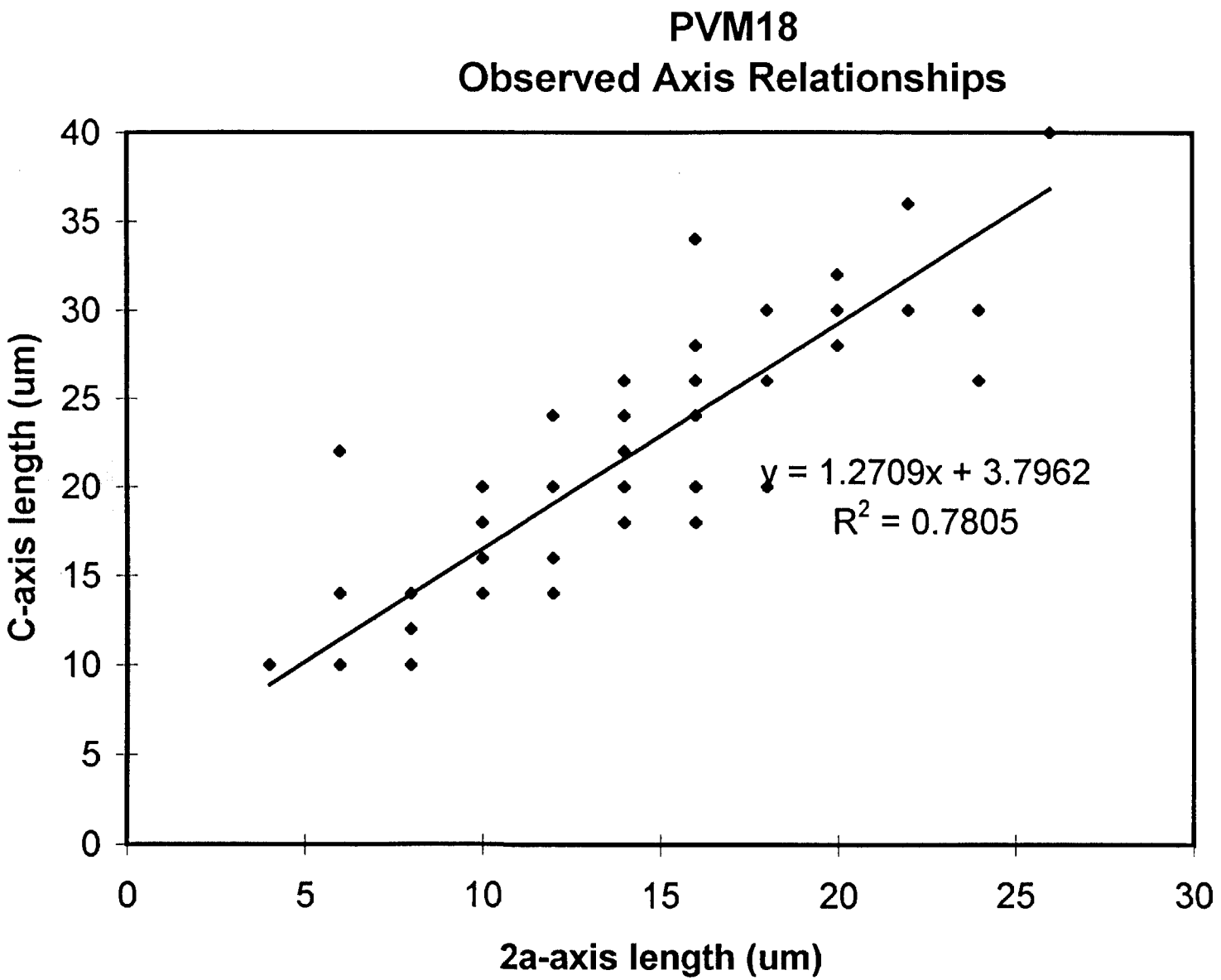
PVM18
Observed Axis Relationships
C-axis length (um)
2a-axis length (um)
y = 1.2709x + 3.7962
R2 = 0.7805
0
5
10
15
20
25
30
35
40

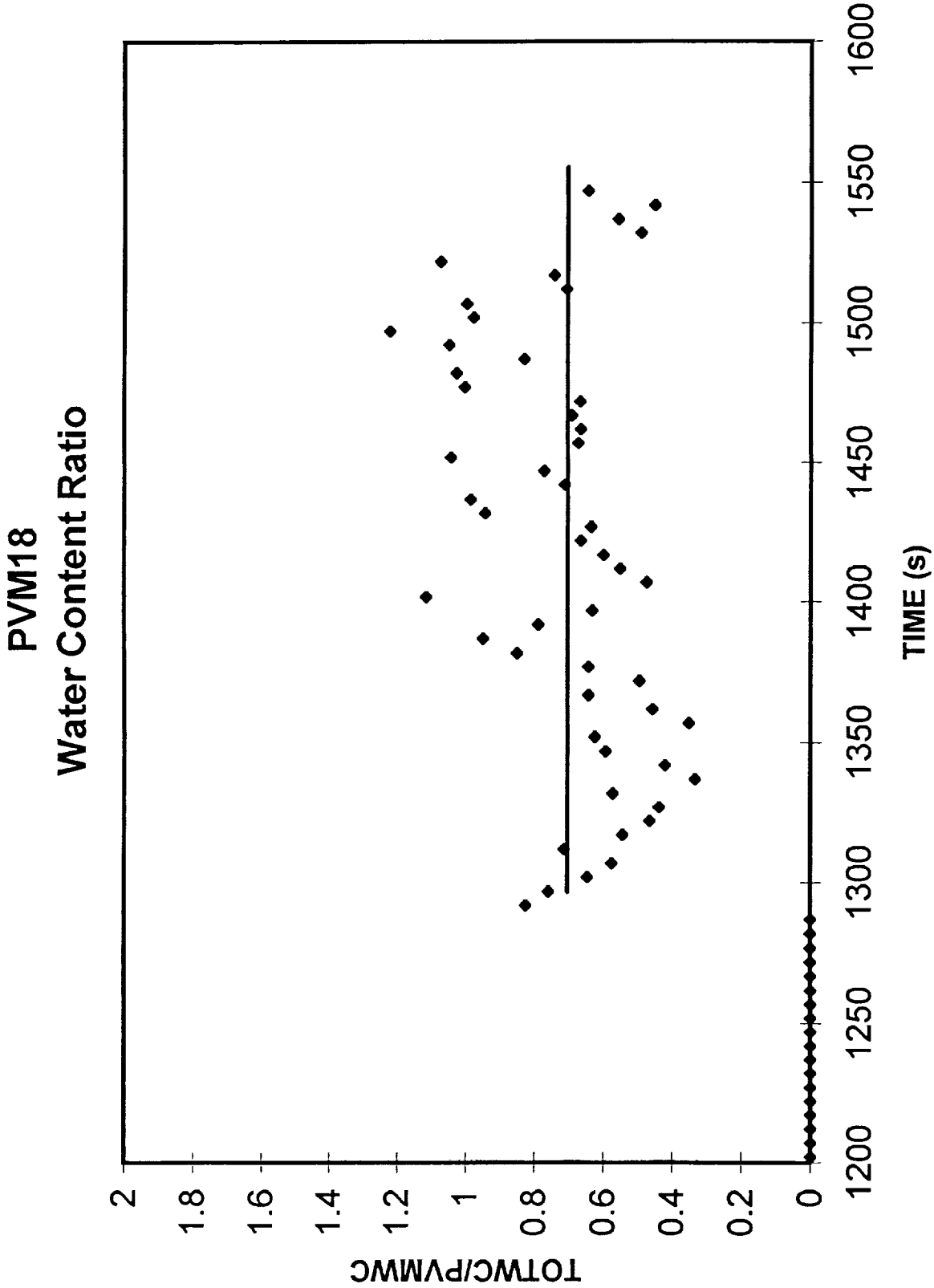
PVM18
Water Content Ratio
TOTWC/PVMWC
TIME (s)
0
0.2
0.4
0.6
0.8
1
1.2
1.4
1.6
1.8
2
1200
1250
1300
1350
1400
1450
1500
1550
1600

# REPORT DOCUMENTATION PAGE

Form Approved
OMB No. 0704-0188



| 1. AGENCY USE ONLY (Leave blank) | 2. REPORT DATE | 3. REPORT TYPE AND DATES COVERED |
|---|---|---|
| | 28 Dec., 1995 | 15 May 1995 to 31 Oct., 1995; Final Report |

**4. TITLE AND SUBTITLE**
Laboratory Investigation of Direct Measurement of Ice Water Content, Ice Surface Area, and Effective Radius of Ice Crystals Using a Laser-Diffraction Instrument

**5. FUNDING NUMBERS**
C
NAS2-1426

**6. AUTHOR(S)**
H. Gerber
P.J. DeMott
D.C. Rogers

**7. PERFORMING ORGANIZATION NAME(S) AND ADDRESS(ES)**
Gerber Scientific Inc.
1643 Bentana Way
Reston, VA 22090

Colorado State University
Dept. Atmospheric Science
Ft. Collins, CO 80523

**8. PERFORMING ORGANIZATION REPORT NUMBER**
Final Report
No. 1

**9. SPONSORING/MONITORING AGENCY NAME(S) AND ADDRESS(ES)**
NASA Ames Research Center
Moffett Field, CA 94035

**10. SPONSORING/MONITORING AGENCY REPORT NUMBER**

**11. SUPPLEMENTARY NOTES**

**12a. DISTRIBUTION/AVAILABILITY STATEMENT**
Unlimited

**12b. DISTRIBUTION CODE**

**13. ABSTRACT**

The aircraft microphysics probe, PVM-100A, was tested in the Colorado State University dynamic cloud chamber to establish its ability to measure ice water content (IWC), PSA, and Re in ice clouds. Its response was compared to other means of measuring those ice-cloud parameters that included using FSSP-100 and 230-X 1-D optical probes for ice-crystal concentrations, a film-loop microscope for ice-crystal habits and dimensions, and an in-situ microscope for determining ice-crystal orientation. Intercomparisons were made in ice clouds containing ice crystals ranging in size from about 10 um to 150 um diameter, and ice crystals with plate, columnar, dendritic, and spherical shapes.

It was not possible to determine conclusively that the PVM accurately measures IWC, PSA, and Re of ice crystals, because heat from the PVM evaporated in part the crystals in its vicinity in the chamber thus affecting its measurements. Similarities in the operating principle of the FSSP and PVM, and a comparison between Re measured by both instruments, suggest, however, that the PVM can make those measurements. The resolution limit of the PVM for IWC measurements was found to be on the order of 0.001 g/m$^3$. Algorithms for correcting IWC measured by FSSP and PVM were developed.

| 14. SUBJECT TERMS | 15. NUMBER OF PAGES |
|---|---|
| ice crystal, ice water content, effective radius, cirrus clouds | 142 |
| | 16. PRICE CODE |

| 17. SECURITY CLASSIFICATION OF REPORT | 18. SECURITY CLASSIFICATION OF THIS PAGE | 19. SECURITY CLASSIFICATION OF ABSTRACT | 20. LIMITATION OF ABSTRACT |
|---|---|---|---|
| Unclassified | Unclassified | Unclassified | UL |